THERMAL DEGRADATION OF RESINS

This Thesis is submitted in partial fulfilment
of the requirements for the degree of Doctor of Philosophy
at the University of Aston in Birmingham.

By

GHULAM NABI

Department of Chemistry
(Polymer Technology)
The University of Aston in Birmingham.

April, 1969.

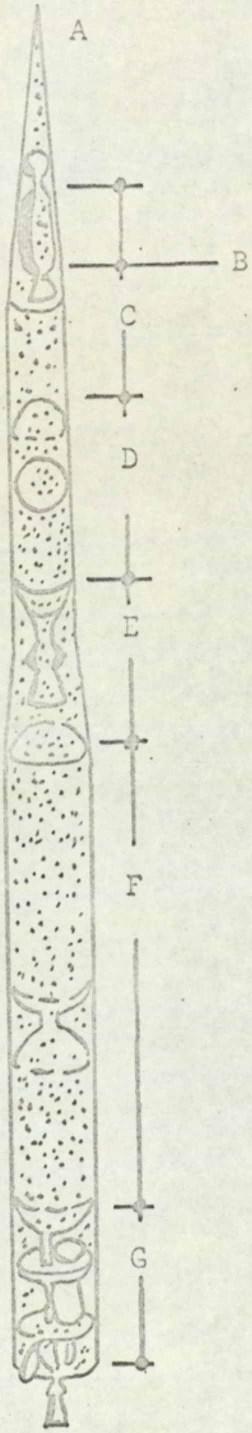

A.	Nosecone Moulded asbestos phenolic with titanium tip
B.	3rd stage bottle
C.	2nd stage skin magnesium-thorium
D.	2nd stage integral tankage stainless steel
E.	Spacer section Magnesium
F.	1st stage integral tankage Aluminium
G.	Tail can Magnesium

Fig.1. Asbestos phenolic flies high[12]

ACKNOWLEDGEMENTS

The author wishes to express his sincere thanks to Dr.G.S.Learmonth for his supervision and keen interest throughout the work.

Sincere thanks are also due to Professor W.G.S.Parker in whose department the present work was carried out.

The author would like to express his thanks to the Punjab University, Lahore, West Pakistan, for grant of four years study leave and IMperial Metal Industries, Summerfield, Kidderminster, for providing the necessary financial support for this project.

The author thanks Mrs.M.Stephenson for typing a difficult manuscript.

The author acknowledges with thanks the co-operation of the technical and library staff of the University of Aston in Birmingham.

The author thanks Professor Badar-Ud-Din of the Panjab University, Lahore,in whose department Isothermal Thermogravimetric Analysis was carried out.

FORM OF THE THESIS

The Thesis is divided into two parts. Part I deals with the programmed thermogravimetric and the differential thermal analyses, carried out at the Department of Chemistry, the University of Aston in Birmingham, U.K., and the Part II (Chapter ix) comprises of the isothermal thermogravimetric analysis done at the Institute of Chemistry, the Panjab University, Lahore, Pakistan.

The work at both the places has been done under the supervision of Dr.G.S.Learmonth (Aston).

CONTENTS

PART I

Page

CHAPTER I

CHAPTER II

CHAPTER III

CHAPTER IV - EXPERIMENTAL (DTA)

CHAPTER V

CHAPTER VI - EXPERIMENTAL (PTGA)

CHAPTER VII

CHAPTER VIII

PART II

CHAPTER IX - ISOTHERMAL THERMOGRAVIMETRIC ANALYSIS (ITGA)

PART I

CHAPTER 1

SYNOPSIS

Differential Thermal Analysis (DTA) and thermogravimetric analysis (TGA) have been used to study the pyrolysis of phenol-formaldehyde moulding compounds based on chrysotile asbestos.

A survey of the literature showed a good deal of information about the reactions involved, but it was difficult to correlate the results of different investigations.

Though the thermograms are sensitive to experimental conditions, with care, consistent and useful results could be obtained. The effect of some analytical variations is reported.

1. The peaks obtained from DTA or TGA fall into three main groups, correlated with completion of curing (i.e. postcuring), thermal reforming and carbonisation. In addition some other effects can be observed, e.g. dissociation of hexamine and dehydration of alumina or asbestos.
2. The group associated with completion of cure, showed consistent peaks, but affected by instrument variables, and partly by the composition of the system. The structure of the cured network appears remarkably independent of conditions, providing postcure is complete.

   (It was found that the novolac used gave the highest carbon yield with 10-17% hexamine. The resole used gave comparable results with 5% added hexamine.)

3. The results of TGA strongly suggest that once cure is complete, the second stage (reforming) is not affected much by any of the additives used.

4. The third group of peaks (carbonisation) is affected by various changes

   The dehydration of asbestos at ca.700°C shows a marked endotherm

   The effect of mineral oxides, powdered metals and Lewis acids are reported later. In some cases the changes in weight were marked. Added organic materials did not seem to have much effect.

5. Analysis of the kinetics of the stages of pyrolysis has been attempted. While activation energies are reported, it seemed that the sensitive technique and involved procedure needed to extract the information will give varying results, and only isothermal studies will give reliable figures. Values of activation energies from DTA indicate thermal scission, while those from TGA show oxidative degradation.

6. Suggestions are made as to modification to phenolic/asbestos compounds, which may be worth following up by empirical trials, e.g.

   Use of reducing materials - crocidolite asbestos or Mg or Al.

   Addition of mineral oxides, e.g. MnO_2 or Sb_2O_3.

   Catalysis by Lewis Acids, e.g. $FeCl_3$.

7. Suggestions are made for extension of this work in a number of fields.

   Attempt to obtain pure thermal fission by elimination of oxygen from the system during cure.

   Study of isothermal pyrolysis at high temperatures.

   Examination of the pyrolysis of phenolic resin compounds in the form of moulded surfaces in the temperature range 1000-2000°C.

   Determination of the physical and chemical nature of the carbon residue.

8. The results recorded show certain difficulties in the use of this particular equipment for thermal analysis, where pyrolysis is being studied. In particular there is a continued shift in base line and sensitivity. The results are therefore affected both by variation in the thermal transfer and variation of residual time of fragments in the pyrolysis zone, due to the geometry of the tubes used.

ABBREVIATIONS

A	Asbestos
Acet	Acetate
Acry	Acrylonitrile
Alc	Alcohol
B	Boric Acid
C	Carbon
C/A	Chromel-Alumel
Cell. Buty	Cellulose Acetate Co butyrate
CMCell	Carboxymethyl cellulose
D	Dust
E	Energy of activation
Fur	Furfuryl Alcohol
GF	Glass Fibre
Gluc	Glucose
H	Hexamethylenetetramine
K	reaction rate constant
ϕ	Heating rate °C/min
LC	Lead Chloride
n	Order of reaction
N 6:6	Nylon 6:6
PF	Phenol formaldehyde
Psty	Polystyrene
PV	Polyvinyl

Ref	Refrasil
S	Sulphur
SCFH	Standard cubic foot per hour
Si	Silica
Sm	Sodium Metaborate
SP	Sodium phosphate
Sta	Starch
Suc	Sucrose
W_o	Initial weight of material
Z	Frequency factor

<u>Example</u>

PFHASm	Phenolformaldehyde + Hexamine + Asbestos + Sodium metaborate.

Notes:

1. All the chemicals are GPR, supplied by Hopkin Williams.
2. Glass Fibre (¼" long) is ECO 115.
3. Chrysolite asbestos is
   4T·5 Lake asbestos of Quebec Ltd., Black Lake, Quebec, Canada.
4. Nylon 66 Bristles (ICI) 0·18" diameter.
5. Resins supplied by Bakelite.

Different specimens of graphite and carbon

Name	Specifications
C	Graphite
C_o	Carbon fibre cut to $\frac{1}{8}$"
No.1.	Graphite E.T.9<300 mesh. An artificial but highly perfect graphite.
No.2.	SEVAL kv Black. Heated to 2,600°C $\sim$ 3,500°A in diameter. A "low structure" carbon black.
No.3.	As No.2, except <u>not</u> heated to 2,600°C.
No.4.	Non-graphitic coke<150 mesh.
No.5.	STATEX F. 12 Black. Heated to 2,600°C. "High-structure" furnace black $\sim$ 290°A in diameter.
No.6.	As No.5, except <u>not</u> heated to 2,600°C
No.7.	Petroleum coke<36 mesh. Coked petroleum pitch giving a fairly graphitic coke.
No.8.	Non-graphitic coke<36 mesh, - as No.4, except for size grading.

Notes:

1. C - graphite (by Hopkin Williams)
2. C_o - carbon fibre (by Ministry of Technology, RACE, Farnborough).
3. Specimens Nos.1-8 were supplied by Morganite Research and Development Ltd., London.

INTRODUCTION

GENERAL

The stability of polymers, when subjected to heat has been fairly extensively investigated under laboratory conditions. This topic is of considerable industrial importance in a number of fields where plastics materials are subjected to high temperatures, and there have also been semi-empirical studies in this connection.

Of course, the effect of mild heating - (up to 150° or 200°C) on polymers is well-known, and extensive studies have been made of the second order transition (T_G) and first order transition temperatures (T_M) which occur. We are concerned here, however, with higher temperatures where energy levels, of the same order of magnitude as bond energies, are available. As a result we are involved in a discussion of chemical reactions occurring due to the heating of polymer based materials.

The polymers which are of particular interest are cross-linked thermoset materials obtained from phenolformaldehyde resins. These materials have important applications in plastics components for use in rocket motor, space technology and many other mechanical and electrical engineering fields.

The success of ablation mechanism in protecting the underlying layers of the nose cones, rocket combustion chamber, nozzles and other similar parts against thermal degradation has resulted in more systematic research for still better ablative materials. Consequently, a large amount of work has been done in U.S.A. and other research centres on the use of phenolics and other compounds. While these investigations show the effect of many variables, both in the resin itself and the other materials added to it during compounding, it is evident that in many ways the simple resins from phenol and formaldehyde are unsurpassed, and these may be reinforced by asbestos, glass, silica, magnesia, carbon and other fibrous materials. Unfortunately, although this is undoubtedly true, our knowledge of the effect of variations in resin itself and the added material is not very systematic. The object of the work described here is to gain some fundamental knowledge of thermochemistry involved in one small corner of the field - namely, resins from phenolformaldehyde and of their compounding.

The present work is directed towards the understanding of the pyrolytic decomposition of commercial phenolic resins - novolac and resole, and composite phenolics.

An understanding of the decomposition mechanism of phenolics is necessary to comprehend their molecular structure. Therefore, the immediate goal was the detailed study of phenolics by thermo-analytical (DTA and TGA) techniques.

These investigations included:-

1. Effect of thermal treatment on phenolics
2. Study of curing parameters
3. Effects of heating rates, packing density, particle size, vacuum, atmosphere of different gases, etc.

Having established curing conditions of phenolic resins for maximum stability, it was hoped:-

(a) to improve *thermostability*,

(b) increase proportion of *residual char*,

(c) to suppress *exothermic reactions*, and

(d) to *modify the structure of the char*.

The following substances were added to that effect:

(1) Carbon

(2) Powdered metals

(3) Metallic oxides

(4) Lewis Acids

(5) Magnesia fibre, asbestos and other inorganic compounds

(6) Carbohydrates

(7) Organic polymeric materials

ROCKET MOTOR

It is well-known in ancient technology how to obtain propulsive force by burning a fuel and an oxidizing agent together in a specially constructed chamber, often fitted with a venturi (or nozzle) to obtain a jet of exhaust gases. The reaction of the system to the loss of mass/energy into the jet, of course, provides the propulsion. The combustion vessel and nozzle are subjected to intense heat and a high velocity gas stream, which may contain quite abrasive solid particles. Since very few construction materials can withstand these severe conditions, ablative material must be used.

Plastics[1] have been used for re-entry nose cones and structural parts of rockets. However, rigorous conditions for long range rockets require that the efficiency of the plastics under these ambient conditions, must be increased. This can be achieved by empirical and theoretical investigations, which help in better understanding the problems of rocketry.

It is very difficult to separate the effects of high pressure and the momentum of the gas stream from chemical reactivity of the extremely hot products from the reaction of the propellant, with the plastic insulation of the rocket motor.

There is a complex interaction which occurs between the competing rate processes because surface ablation and resin pyrolysis take place at an increasing rate with increasing temperature.

The main reason for using plastics to work under such degradative conditions lies in a unique combination of properties which reinforced plastics possess. Thermal and mechanical shock resistance, low thermal conductivity, high endothermic heats of transformation, and slow uniform surface ablation contribute most significantly to successful insulation performance.

Structure of Rocket[2]

Reinforced phenolic resins have been used in space and rocket technology for the following distinct applications:

(a) Nose cones and other items subject to reacting conditions, i.e. which will enter the earth's atmosphere from the stratosphere regions at high velocities and develop temperatures as high as 10-15,000°C during aerodynamic heating.

(b) Nozzles and similar parts exposed to the flame from a rocket powered by solid or liquid fuel systems, where the temperature is of the order of 2,000-4,000°C.

(c) Thermal insulation parts for rocket motors under conditions similar to (b).

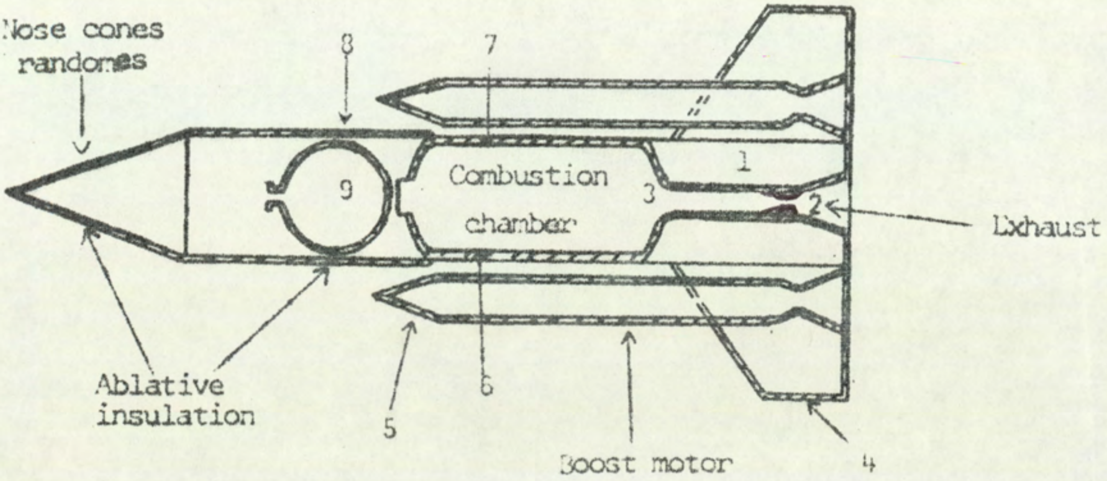

Fig.2. A simplified sketch of a rocket, lists the chief components made in reinforced plastics.

1. Blast pipe
2. Choke
3. Venturi
4. Fins
5. Boost Nose Cone
6. Insulation
7. Inhibitor
8. Missile bodies
9. Gas pressure storage vessel.

The Ablative Process

Ablation (or sacrificial loss of material) in high-temperature environments is a subject of great complexity. To date certain physical and chemical aspects of this process have been identified.

A simplified ablation theory is given here. Ablation of plastic material is a heat and mass transfer in which a large amount of heat energy is consumed by sacrificial loss of material, thus limiting high environmental temperatures to the surface region. The thermal flux from the environment is absorbed or dissipated by numerous mechanisms[3]. These are grouped into two main classes, physical and chemical.

(A) Physical

These are:

(i) Heat conduction into the material substrate and storage by its effective heat capacity.

(ii) Material phase changes.

(iii) Heat absorption by gaseous products of decomposition as they percolate the material to the surface.

(iv) Transpiration of gases from the ablating surface into the boundary layer.

(v) Convection of heat in a surface fluid layer.

(vi) Surface bulk radiation.

(vii) Maximum [4] cooling effect is also obtained when the gaseous products of ablation are of low molecular weight.

(B) Chemical

This method involves all endothermic chemical reactions.

In its simplest form, the energy balance at the ablating surface is

$$H_i = h_{cond} + h_{vap} + h_{trans} + h_{rad} \; ^{*}$$

The amount of energy consumed by each mechanism is variable depending upon the particular materials and environmental parameters involved.

The resin matrix and the reinforcement and filler components absorb large quantities of heat energy during pyrolysis, which acts as a barrier to heat transmission, hence lowering the rate of interior deterioration[5,6]. The gaseous products[7] of decomposition, such as H_2O, CO_2, CO, H_2, CH_4, and other hydrocarbon fragments transpire through the adjacent hot boundary layer and scavenge additional heat by:

(a) endothermic decomposition,

(b) by flow of the cool gas directly opposed to the flow of heat, and

(c) by lowering the enthalpy of the environment.

Other decomposition products are tars and carbonaceous residue.

* Where,

cond	conduction
vap	vaporisation
trans	transition
rad	radiation

The formation of hard carbonaceous surface during pyrolysis is vital because of its resistance to thermal and mechanical ablation and chemical attack. As the organic resin or its residual char is removed by the environment, the reinforcing fibres are left exposed and unsupported. The vitreous fibres then undergo melting, with the molten material covering the surface as liquid droplets, irregular globules, or a thin film. With the continued addition of heat to the surface the melt is vaporized. These phase changes are further responsible for the removal of energy[8]. However, chemical interaction of the propellant combustion products with the residue of pyrolysed insulation, e.g. oxidation of the carbonaceous char by CO_2 and H_2O, is manifested by drastic changes in the rate of surface ablation. This exothermic reaction is detrimental to residual char even in absence of O_2.

$$CO_2 + C \longrightarrow 2CO$$

$$C + H_2O \longrightarrow CO + H_2$$

$$C + 2H_2O \longrightarrow CO_2 + 2H_2$$

The mechanism of ablative degradation of a fibre glass reinforced phenolic resin is illustrated pictorially in Fig.3, page 8 b.

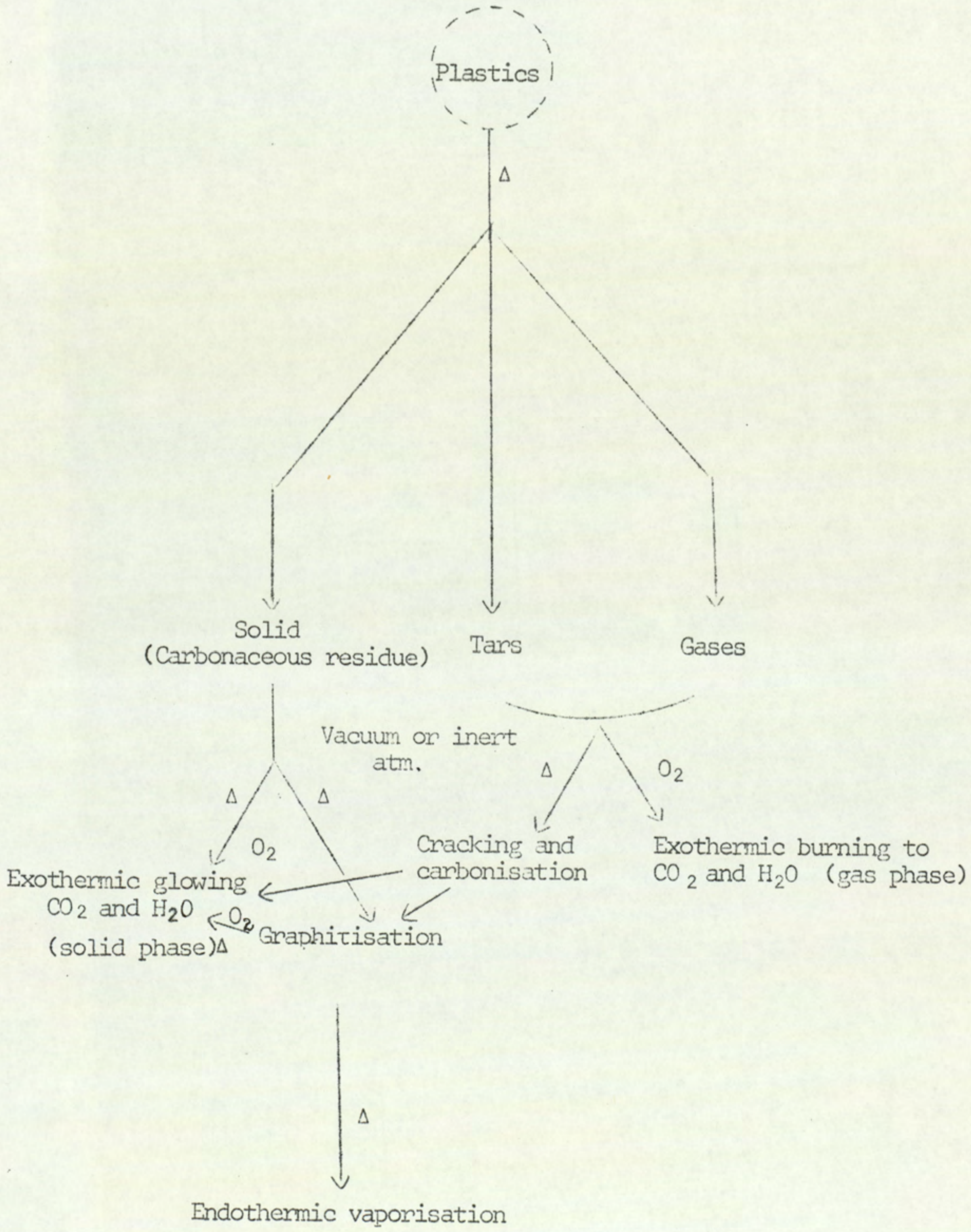

<u>Pyrolysis of plastics is outlined above</u>

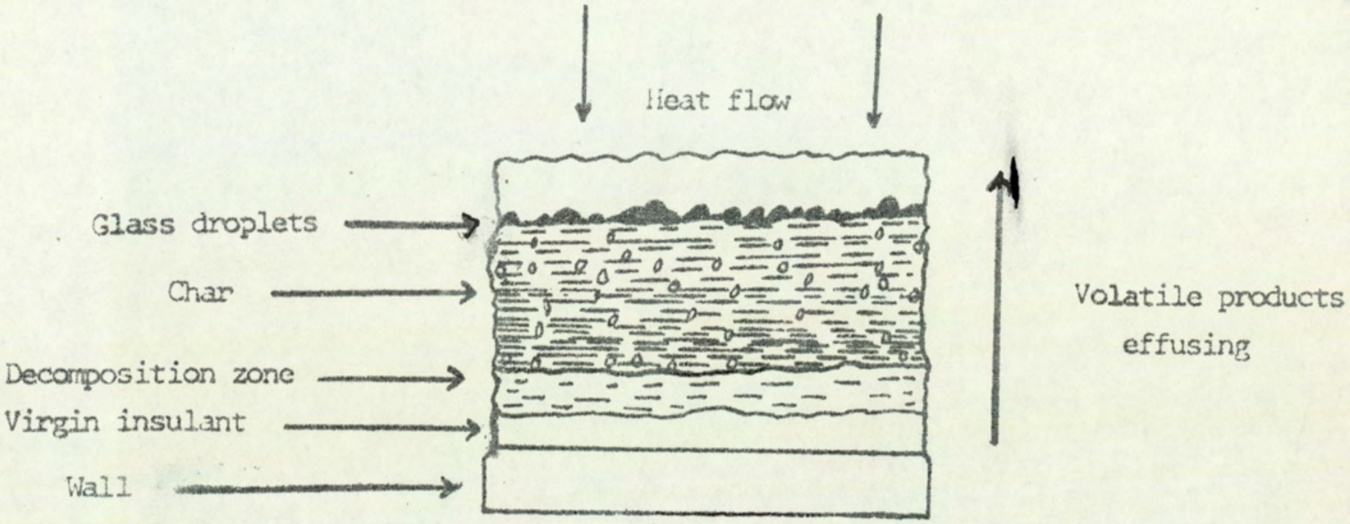

Fig.3. The mechanism of ablative degradation of a fibre glass reinforced phenolic resin.

Damage to the material is seen in four separate layers:

1. The surface material has been removed by the combined action of thermal, chemical and mechanical effects. On the ablated surface are a thin film and an army of molten glass droplets.
2. Below the top surface layer, a porous carbonized material reinforced with residual glass fibre is present.
3. The volatilization zone is adjacent to the char layer, where the slight loss of organic resin occurs.
4. The virgin material lies under these damaged zones and has experienced little or no rise in temperature,

Materials used[2]

Exact details of materials used in some missile applications are subject to security regulations. However, some of the information available from the U.S.A. sources is summarised here. Among the materials evaluated are:

Reinforcements: glass fibres, silica fibres (Refrasil and quartz), asbestos fibres, carbon fibre, magnesia fibre, refractory fibres, nylon, terylene and other miscellaneous solid fillers.

Impregnating resins: Phenolic, epoxide, silicone, melamine and phosphorus modified phenolic.

Many combinations and permutations can be made with two or more types of fillers and/or resin.

Materials for Nozzle Insulation

The classification of materials for rockets appears to vary with conditions and quite contradictory results are reported using empirical methods such as firing tests of various kinds.

Phenolics having different inorganic fillers have been tested at the Rocket Engineering Department, Utah Division, Thiokol Chemical Corporation. Gilchrist[9] has classified the materials by the type of fillers.

1. Glass: Erosion was quite high.
2. Quartz: Erosion was quite severe.
3. Asbestos: Asbestos-filled phenolics are good heat insulators, but they proved to have poor erosion resistance.
4. Graphite: This material proved to have excellent erosion resistance, but its heat conductivity was so high that it charred through.
5. Refrasil: It is shown that the Refrasil-filled systems were the best materials for the exit cone applications. Oriented fabrics were good in erosion resistance as slong as they are held together, but delamination frequently occurred.

Graphite in Rocket Technology

Theoretical analysis and rocket motor studies show the essential properties for plastic insulators. High temperature degradation must yield a carbonaceous stable residue[10]. This char must be hard and strong to resist erosion caused by the gas flow stresses. It must be porous to allow percolation of the products of substrate decomposition, and it should form a heat-transfer medium for "cracking" reactions. The carbonaceous char should be amorphous rather than graphitic to achieve lowest heat conductivity. The reinforcement should hold the char layer to the substrate and undergo endothermic changes. Endothermic reactions and transpiration of gaseous products should be increased to obtain maximum absorption of heat. Materials of poor heat conductivity must be used to maintain high insulation quality in the substrate insulation layers.

High-yield char-forming plastics are generally highly cross-linked thermoset resins of the phenolic, epoxy-anhydride, polyter-vinylbenzene, and polyacrylonitrile type. Microporous char structures may be achieved by introducing decomposable fillers that have high energy of decomposition or vaporisation and react in the right temperature range during the carbonisation process.

For every advanced project[11], involving hot spots of 2,000-3,000°C graphite is an apparently outstanding choice. In spite of its virtues, it possesses a number of weak points. The awkward limitations are:

1. At room temperature it has zero ductility and only 5% extensibility at 2,500°C.
2. It does not resist oxidation or <u>erosion to hot gases</u>
3. It has high thermal conductivity.

However, as some compensation for these shortcomings, it absorbs a great deal of heat when vaporised at high temperature.

Improvements of Graphite

Conventional graphite needs improvement in respect of density, porosity and protection from oxidation. Porosity has a very pronounced effect on graphite strength as is seen from the exponential type formula[12].

$$S = S_o e^{-7\rho}$$

where S = actual strength,

S_o = strength of non-porous body, and

ρ = fractional porosity.

Hence increase in density will improve graphite. (This may block the percolation of volatile products, which remove excess of heat during ablation.) A double furfuryl alcohol impregnation of an already reasonably dense graphite, followed by baking and graphitising showed improvements in density, transverse bending strength, compressive strength and Young's modulus.

The low-temperature oxidation resistance can be improved by the densification and removal of impurities. Pyrolytic-graphite coatings appear to increase the oxidation resistance of graphite to high-temperature gases. Complete oxidation protection of graphite at temperatures up to 2,100°C through the use of iridium coatings has been reported recently[13].

Effect of Moulding and Postcuring

Hourt (loc cit) has reported in tabular form, effect of moulding variables, particularly temperature, pressure and time on reinforced phenolic resin. Results of a number of SPAR nozzle tests indicate that the performance of phenolic-Refrasil based nozzles may improve asymptotically with increasing moulding pressure. It is believed that thicker the nozzle wall, the greater will be the benefit of higher moulding pressures. Postcuring appears to have only a little effect on performance so long as the unit is mechanically sound and compact.

PYROLYSIS OF ORGANIC POLYMERS

The recent advances in rocketry and space technology have demanded to increase the thermal resistance of ablative polymeric materials. Hence, studies on the thermal behaviour of polymers are important from the scientific and practical view points. Naturally the fundamental information about the mechanisms of changes in polymer under the influence of heat and other degradative agencies (light, U.V.rays, γ-rays, X-rays, oxidation, hydrolysis etc.) is essential to construct the molecular structure resistant to attack by these enemies. In consequence the research work which followed has revealed a great deal of information regarding the relationship between polymer structure and stability. The wealth of such data finds application in the problems of flameproofing textiles and building materials, structural parts of rocket motor, nose cones of space vehicles and host of other daily uses.

Theories of Polymer Degradation

There are a number of postulates as to how a macromolecular structure can be ruptured into fragments.

According to Winslow et al[14] polymer pyrolysis consists of two competitive processes:

1. Scission reaction to form low molecular weight fragments and volatile products.
2. Condensation reactions resulting in the formation of polymer carbon.

According to Grassie[15] one can distinguish between three different mechanisms of depolymerisation reactions:

1. Random Degradation

Random degradation is seen when chain rupture occurs at random points along the chain as each bond being of equal strength and accessibility. This leaves comparatively large fragments. Appreciable quantity of monomer will not make appearance before the fragment size has been reduced considerably.

2. Stepwise Depolymerisation

Stepwise depolymerisation occurs when an unzipping reaction starts from the chain end, producing monomer exclusively.

3. Reverse Polymerisation

Reverse polymerisation begins with chain scission at random points over the chain, or at weak links, forming free radicals, which immediately lose monomer or small polymer fragments until they are completely degraded, provided the depolymerisation reaction is not interrupted by chain transfer. After the chain rupture at the weak links has occurred, the reverse polymerisation process is similar to the stepwise depolymerisation process.

Determination of molecular weight of the residue and of the rate of monomer formation gives an indication of which process prevails. During random degradation the molecular weight reduces considerably before any monomer appears. In stepwise depolymerisation the decrease in molecular weight and monomer production are proportional, while reverse polymerisation gives monomer without appreciable loss in molecular weight of the remaining product.

Plastic materials prepared by condensation polymerisation generally decompose according to a random degradation mechanism, rarely forming true monomers. However, addition type polymers usually decompose according to a reverse polymerisation mechanism. According to Simha et al[16a b] degradation of vinyl and other polymers involves a mechanism shown below:

1. Initiation. This is a unimolecular reaction consisting of the scission of carbon-carbon bonds of the chain to produce free radicals.

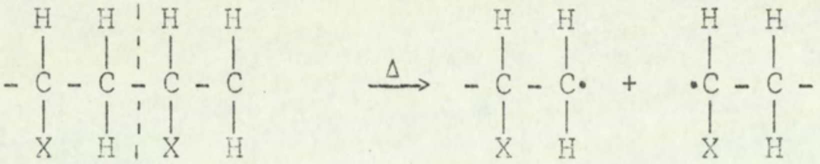

$$-\mathrm{CH(X)}-\mathrm{CH_2}-\mathrm{CH(X)}-\mathrm{CH_2} \xrightarrow{\Delta} -\mathrm{CH(X)}-\dot{\mathrm{C}}\mathrm{H_2} + \cdot\mathrm{CH(X)}-\mathrm{CH_2}-$$

2. Propagation. This step is reverse of the propagation step in addition polymerisation and results in the formation of monomers and the primary free radical ends of chains.

$$-\mathrm{CH_2}-\mathrm{CH(X)}-\mathrm{CH_2}-\dot{\mathrm{C}}\mathrm{H(X)} \longrightarrow -\mathrm{CH_2}-\dot{\mathrm{C}}\mathrm{H(X)} + \mathrm{CH_2}=\mathrm{CH(X)}$$

3. Free Radical Transfer

This step is of two kinds:

(a) Intermolecular transfer, in which a free radical abstracts hydrogen from another chain.

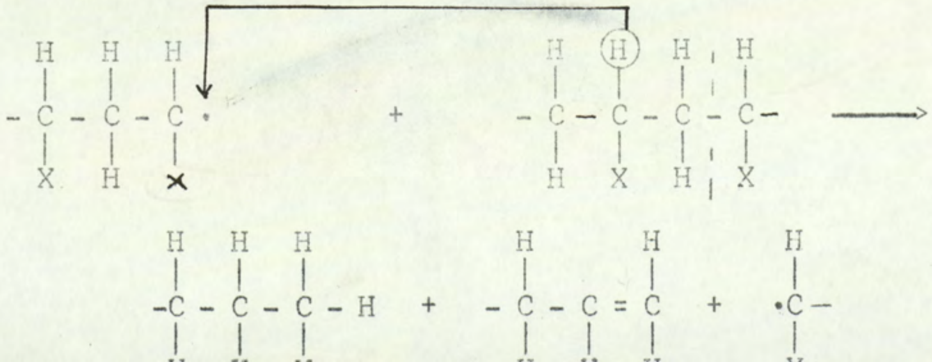

(b) Intramolecular transfer, in which a free radical abstracts a hydrogen from its own chain.

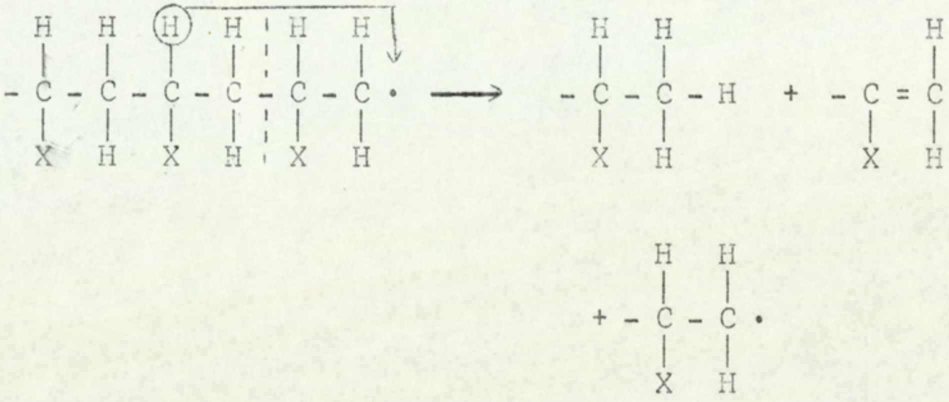

The result in either case consists in the formation of one saturated end, one unsaturated end, and probably a new free radical.

4. Termination. This occurs when two free radicals combine to form one polymer chain or by disproportionation (hydrogen abstraction).

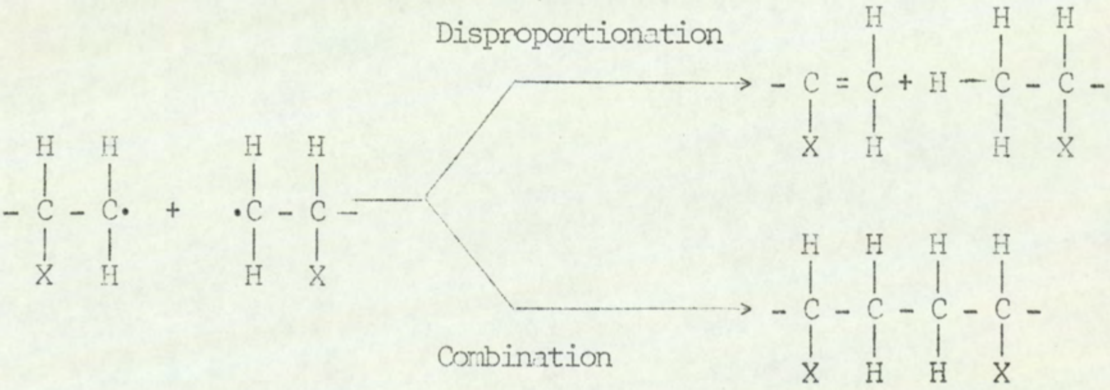

Free radical formed in steps (2) and (3) is probably involved in two competing reactions:

(a) Propagation (unzipping) to yield monomers.

(b) Free radical transfer involving an abstraction of hydrogen (disproportionation) from a polymer chain.

The amount of hydrogen present on the chain determines the course of reaction either way. Thus for polyethylene or polymethylene, the transfer reaction will be a predominant one, and as a result the degradation products will consist of chain fractions of various sizes, and very few monomers.

However, when some of the hydrogen atoms on the chain are replaced with methyl or other small groups, e.g. polyisobutylene, hydrogen transfer becomes restricted. This results in the formation of free radicals that propagate to yield monomers.

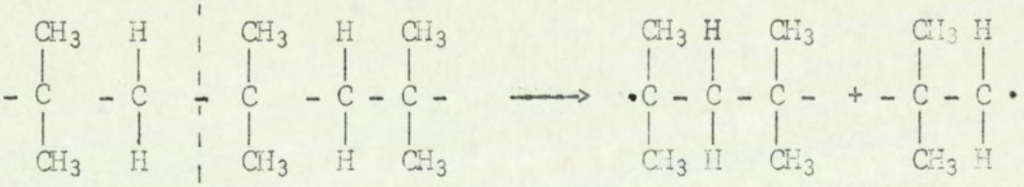

$$-\underset{\mathrm{CH_3}}{\overset{\mathrm{CH_3}}{\mathrm{C}}}-\underset{\mathrm{H}}{\overset{\mathrm{H}}{\mathrm{C}}}-\underset{\mathrm{CH_3}}{\overset{\mathrm{CH_3}}{\mathrm{C}}}-\underset{\mathrm{H}}{\overset{\mathrm{H}}{\mathrm{C}}}-\underset{\mathrm{CH_3}}{\overset{\mathrm{CH_3}}{\mathrm{C}}}- \longrightarrow \cdot\underset{\mathrm{CH_3}}{\overset{\mathrm{CH_3}}{\mathrm{C}}}-\underset{\mathrm{H}}{\overset{\mathrm{H}}{\mathrm{C}}}-\underset{\mathrm{CH_3}}{\overset{\mathrm{CH_3}}{\mathrm{C}}}- + -\underset{\mathrm{CH_3}}{\overset{\mathrm{CH_3}}{\mathrm{C}}}-\underset{\mathrm{H}}{\overset{\mathrm{H}}{\mathrm{C}}}\cdot$$

and

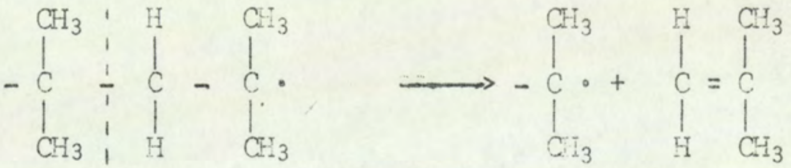

$$-\underset{\mathrm{CH_3}}{\overset{\mathrm{CH_3}}{\mathrm{C}}}-\underset{\mathrm{H}}{\overset{\mathrm{H}}{\mathrm{C}}}-\underset{\mathrm{CH_3}}{\overset{\mathrm{CH_3}}{\mathrm{C}}}\cdot \longrightarrow -\underset{\mathrm{CH_3}}{\overset{\mathrm{CH_3}}{\mathrm{C}}}\cdot + \underset{\mathrm{H}}{\overset{\mathrm{H}}{\mathrm{C}}}=\underset{\mathrm{CH_3}}{\overset{\mathrm{CH_3}}{\mathrm{C}}}$$

etc.

Thermal Scission

Thermal scissions can be imagined as follows. When ordinary hydrocarbon compounds (paraffins) in the liquid or solid state are heated, thermal energy manifests itself in the form of vibrational, rotational and translational motions of the molecules. Each individual molecule acts more or less as a unit in response to the heat input. Hence some of the parts receive more energy than others. The kinetic motions are hindered at the same time, because of the big size of the molecules. As a result strains are created at various points, causing ruptures.

At sufficiently high temperature some of the molecules (not too large) will vaporise without decomposition. If the pyrolysis is carried out in a closed system, these gaseous molecules will react to form different compounds until equilibrium sets in. Free radical transfer and hydrogen abstraction may be involved in these reactions. If there is an excess of hydrogen on carbon atoms of the main chains (polymethylene) these chain scissions are accompanied by an abstraction of hydrogen from a carbon adjacent to the broken C-C bond. However, if the main chain is poor in hydrogen (polypropylene or polyisobutylene) some of the scissions are not accompanied by a hydrogen transfer. As a consequence free radicals are formed which propagate to yield monomers.

METHODS OF STUDYING DEGRADATION

1. Differential Thermal Analysis

Measuring difference in energies during physical or chemical transformations. Inert (reference) material and the test sample are heated in a rising temperature programme. The changes in energy of the test sample, cause changes in relative temperature which are recorded.

2. Thermogravimetric Analysis

Measuring the rate of weight loss of the polymer during isothermal or linear heating rate in standard conditions.

3. Pressure Method

The rate of increase of pressure of pyrolysis gaseous products is followed.

4. Viscosity Method

This technique consists of studying the rate of change of viscosity of the residue as a function of conversion.

5. End-group Analysis

The measurement of the rate of formation of molecules with a specific end group, which can be identified by titration or other means.

6. Spectrometric Method

The rate of formation or disappearance of functional groups is followed spectrometrically.

7. Light-scattering Method

This method consists of measuring light scattered by solution at different angles. The intensity of the scattered light is related to molecular weight of the polymer.

8. Dilatometric Method

This method consists of measuring the rate of change of volume as a function of degradation.

DEGRADATION OF RESINS

Pyrolysis of organic materials result in the series of reactions discussed above. In most cases, even where "unzipping" or depolymerisation occurs, part of the product is a solid residue. This is interesting because it is often graphitic in nature. Thus at some stage even aliphatic materials must undergo ring closure to give the aromatic structure characteristic of graphite. (Mechanism of char formation will be discussed later.)

Graphite possesses higher thermal stability because of loss in mobility and increase in concentration of stable aromatic rings. The graphite may be turbostratic or polycrystalline depending upon the heat treatment.

Some examples of the work done on the pyrolyses of polymers follow :

Polyvinyl acetate

Grassie[17] found that polyvinyl acetate decomposes into acetic acid and polyacetylene above 190 °C in a vacuum, thus

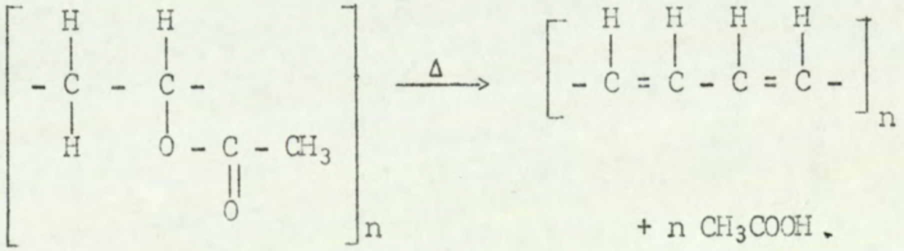

$$\left[-\overset{H}{\underset{H}{C}}-\overset{H}{\underset{O-\underset{\overset{\|}{O}}{C}-CH_3}{C}}-\right]_n \xrightarrow{\Delta} \left[-\overset{H}{C}=\overset{H}{C}-\overset{H}{C}=\overset{H}{C}-\right]_n + n\,CH_3COOH .$$

The C - O bonds are weaker than the C - C bonds and therefore break first on heating the polymer. A break of a C - O bond is accompanied by an abstraction of hydrogen from an adjacent carbon to form CH_3COOH. The C - O bond in the β-position to a double bond in the chain breaks more easily than the other bonds on the chain and the formation of CH_3COOH thus proceeds by an "unzipping" reaction.

Polyvinyl Alcohol[18]

Thermal degradation of polyvinyl alcohol at low temperatures results in the formation of H_2O. The degradation of this polymer probably proceeds by the same chain reaction mechanism as in the case of polyvinyl acetate. After a double bond has formed in the chain in the initiation step, it tends to weaken the C - OH bonds in the β-position to it.

Polyvinyl Chloride

Gilbert et al[19] showed that thermal degradation of PVC occurs in two readily distinguishable stages. The first, which is complete at about 250°C, consists of dehydrochlorination ("unzipping" reaction), and can be represented formally as:

$$(- CH_2 - CHCl -)_n \rightarrow (- CH = CH -)_n + nHCl .$$

The second stage, which occurs mainly between 300° and 500°C, is similar to the carbonisation of coal. Tar and simple gases (H_2, CH_4) are evolved, and a carbon remains which loses very little weight between 500° and 900°C.

Polytetrafluoroethylene[20]

Pyrolysis of PTFE in vacuo at 423°-513°C yields almost 100% of monomer, $CF_2 : CF_2$. The chain rupture occurs on thermal degradation of PTFE, but the strength of the C - F bond prevents shift of a fluorine atom. (The order of the bond dissociation energies is C - F > C - H > C - Cl > C - C.) The two radicals, therefore, lose tetrafluoroethylene units by a reverse polymerisation mechanism (i.e. reverse of addition polymerisation) :-

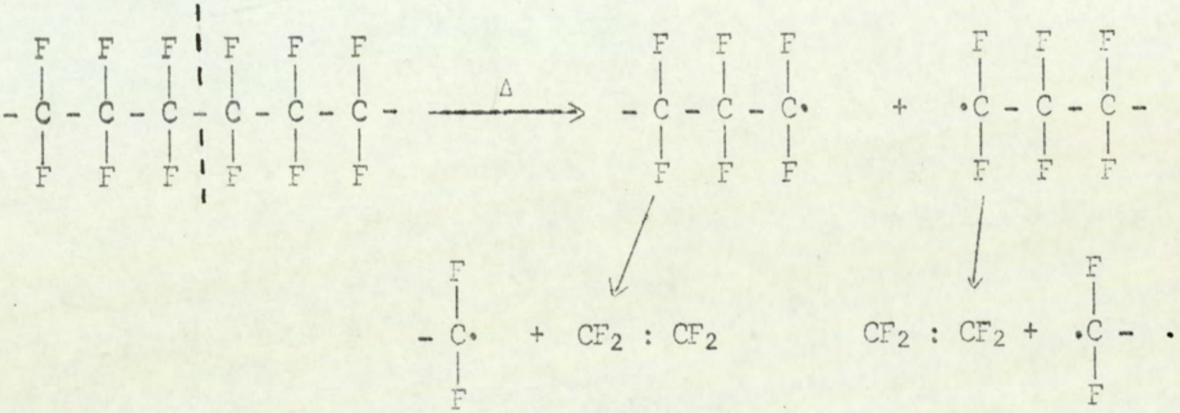

Cellulose [21-23]

The thermal degradation of cellulose produces a minimum of 18 identifiable products (H_2O, CO_2, CO, H_2, CH_4, C_2H_4, acetic acid, formic acid, lactic acid, acetone, formaldehyde, levoglucosan, etc.) and an unidentified char.

The mechanism of thermal degradation of cellulose may be assumed to include two main reactions. One reaction consists of dehydration, and the other of scissions of C - O bonds in the chain, either in the rings or between the rings. The C - O bonds are weaker than the C - C bonds and so are more likely to be broken. Ruptures of C - O bonds in the rings; designated in the structural formula of cellulose by the letters a and b, result in the disintegration of the ring to give CO_2, CO, and H_2O. Scissions of external C - O bonds (i.e. c and d) result in the formation of one levoglucosan end and one hydroxyl end, thus:

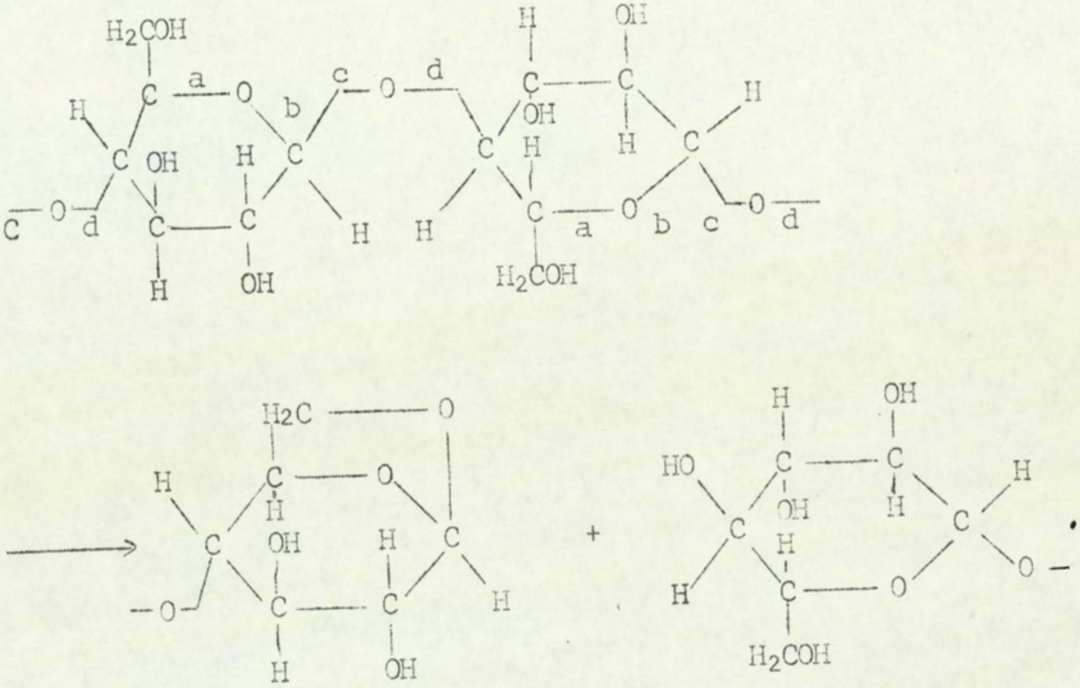

Thus in the thermal degradation of cellulose, the rate controlling step is believed to be formation of levoglucosan and subsequent intramolecular rearrangement of fragments. Some of the levoglucosan, in turn, is thought to undergo dehydration and polymerisation to form char, while some is believed to undergo destructive distillation to form volatile organics, H_2O and gases.

Polystyrene[23]

The degradation products from polystyrene consist primarily of monomer, dimer, and trimer. These fragments break off at free radical chain ends resulting from thermal or other types of scission. However, not all the scissions result in free radicals. According to Staudinger et al the pure thermal scission of C - C bonds results in one saturated and one unsaturated end, due to a hydrogen transfer, thus

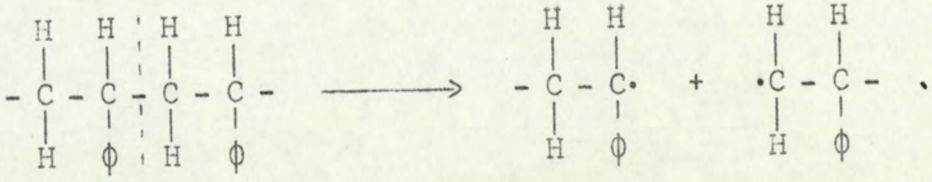

Each one of the two free radicals may then remove hydrogen intermolecularly or intramolecularly to cause new scissions (free radical transfer), or each one of the free radicals will undergo reverse depolymerisation to yield monomers.

Polyolefins [23]

Madorsky has modified Staudinger's mechanism (given above) and applied it to show the presence or absence of monomers in the pyrolysis of polyolefins and related polymers. According to this mechanism thermal agitation introduces strains in the molecule which lead to C - C scission. In those polymers where the main chain is rich in hydrogen such scissions are mainly accompanied by intramolecular hydrogen shift at the locality of sicssion. In this type of scission no free radicals are formed and, therefore there is no propagation into monomers. Polyethylene and polymethylene scissions are examples of this type, thus

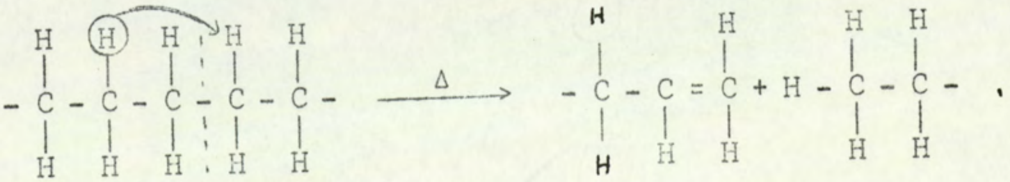

Phenolic Resins

With the advent of space and rocket technology phenolics have once again regained the top position amongst industrial plastics, as ablative materials. Researches for moon flights and other outer space programmes have greatly stimulated an interest in understanding the complex chemistry of the formation of phenolics and their degradation. Very recently an extensive survey of the existing literature was made by Learmonth and Nabi.[24] Therefore only a partial review of the work on phenolics will be given in the following pages.

Phenolformaldehyde resin is usually regarded as an extremely highly cross-linked three-dimensional polymer, since phenol can react with H_2CO at positions ortho and para to $-OH$. The results of pyrolysis in a vacuum carried out at 360°, 500°, 800° and 1200°C by Madorsky and Strauss[25] suggest the following mechanism for the thermal degradation of phenolic resin. Pure thermal scissions occur primarily at the methylene and benzene C - C bonds.

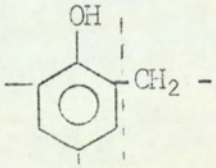

During pyrolysis at 360°C the main volatile constituents are acetone, Propylene, propanol and butanol, with no CH_4, CO, and hardly any CO_2 at 800° and 1200°C. The last three compounds, specially CO and CO_2 are formed through a complete rupture of the benzene ring. It is a process of cracking, where small fragments split off as free radicals.

The free radicals either recombine or abstract hydrogen or oxygen from the cross-linked residue. As a consequence the residue becomes progressively carbonised. Such a mechanism could account for the presence of CO, CO_2, H_2 and CH_4 among the degradation products. In this respect the thermal behaviour of phenolic resin is similar to that of polyter_vinylbenzene[23]- another highly cross-linked polymer.

Bender[26](1939) reported irregularities in the behaviour of phenolformaldehyde resins during viscometric molecular weight determinations. He explained this phenomenon using the concept of cybotaxis (special arrangement of molecules in a liquid with crystal-like orientation but lacking stability at any point).

Hall[27] observed changes in the viscosity of phenolformaldehyde novolac resins. He showed that the alterations were due to spontaneous oxidation of resins in the solid state. According to him the mode of breakdown is not simple. It is probable that both peroxide and quinone structures are formed during oxidation with consequent free radicals. The latter are responsible for the progressive discoloration of the novolac powders from white to dark red. Nearly 30% of the total oxygen absorbed appeared to form peroxidic groups. Infra-red examination of the oxidised material has revealed the presence of benzophenone-type linkages, indicating oxidation of methylene groups.

Hawkins [28](1956) made an attempt to determine the structure of novolac resins by controlled degradation of phenolics. In his study, the steps involved bromination, methylation of the phenolic-OH groups, oxidation to polyketones, cleavage of polyketones to bromoacids and bromoanisoles, demethylation and analysis of the products.

Conley and workers[29-32] have published a series of papers, in the last few years, on more systematic and controlled study of phenolics oxidation, mechanisms of char formation, and decomposition in general. Decomposition is a highly complex process involving a sequence of consecutive and competitive reactions. This complexity is indicated, partly, by the isolation of over four dozen reaction products from the decomposition of phenolics.

Chromatography and mass spectroscopy were used by Conley et al., Heron[33] and other workers[34-39] to identify the pyrolysis products of phenolics. Brauer[40], in a review article on pyrolytic techniques, has referred to the technical bulletin, published by Perkin-Elmer & Co., which describes a chromatograph and mechanistic formation of pyrolysis products of phenolic resin around 900°C.

Ouchi and Honda[41] in a comprehensive study of vacuum pyrolysis of phenolformaldehyde resins propose a mechanism of thermal degradation and carbonisation. Megson[42] has examined distillates from pyrolysis of phenolics in vacuo. Wolfs, Krevelen and Waterman[43] studied resin pyrolysis in an inert atmosphere. Friedman[44] reports compositions and average molecular weights of the various degradation gases from glass and nylon-reinforced phenolic resin pyrolysed in an arc image furnace under high vacuum.

The kinetics of the decomposition process was studied by Heron[33], Madorsky and Straus[25], Schulman and Lochte[38], Friedman[45], Conley and Bieron[29], Conley[31] and Auerbach[46]. It was apparent in these studies that the decomposition reactions taking place during the low temperature (early) stages were different from those taking place during the high temperature (latter) studies.

Jeffreys[47] examined thermal stability of phenolic resins and proposed a mechanism by which they degrade.

Nakamura[48] investigated phenolformaldehyde resole and novolac resins, by differential thermal analysis, in order to elucidate the reaction mechanism of thermal hardening. White and Rust[49] have developed a method to show the effect of temperature, catalyst level, resin advancement and water content on the cure rate of phenolic resole resins by D.T.A. This D.T.A. procedure allows for quantitative measurement of the phenolic resin curing exotherm between 135° and 150°C. Pevzner and co-workers[50] studied phenolformaldehyde novolac resin and PVC and also these substances with an admixture of hexamethylenetetramine. The methods used in these investigations were thermographic and thermomechanical. Popov, Druyan and Varshal[51] investigated the thermo-oxidative degradation of phenolformaldehyde (novolac and resole) resins by thermo-gravimetric and differential thermal analyses. Korshak et al[52] reported thermal and thermo-oxidative processes which take place in phenolformaldehyde oligomers of the novolac type in the 150° - 900°C range. The study involved the use of thermogravimetry and infra-red spectroscopy. Doroshenko, Korshak and Sergeev[53] synthesised thermosetting polymers from α,ω-bis-(p-hydroxy-phenyl)-alkanes, i.e. 1,6-bis-(p-hydroxy-phenyl)-hexane, 1,8-bis-(p-hydroxy-phenyl)-octane, and 1,10-bis-(p-hydroxy-phenyl)-decane, by reacting them with formaldehyde to study the effect of the length of the cross-links on the heat resistance and mechanical properties of the polymers. They used thermo-gravimetric and thermo-mechanical methods for this purpose and compared these properties with those of phenol-formaldehyde resole resin. Anderson[54] investigated fifteen phenolic polymers, using the technique of vacuum thermo-gravimetry to monitor their decomposition over a temperature range of 25° to 920°C. Elemental analyses were also made on each of the unpyrolysed polymers. Pyrolysis results are discussed in relationship to the general chemistry of phenolic polymers. Burns and Orrell[55] used differential thermal analysis and thermo-gravimetric analysis combined with infra-red spectroscopy to examine the mechanisms involved in the curing only of phenolformaldehyde novolac resins with hexamine. It has been shown that the curing reaction is a three-stage process. The first stage is the physical change of melting and subsequent formation of hexamine/resin solutions. The second and third stages were found to be two cross-linking reactions occurring in two successive temperature regions. The presence of absorbed moisture modifies the melting and curing processes.

Learmonth[56] used D.T.A. in conjunction with thermo-gravimetric analysis for the investigation of thermal degradation of phenolic resin-based laminates. It was found that with phenolic laminates the pattern of the thermograms was characteristic of the paper, while with epoxide laminates and melamine they were characteristic of the resin used.

Raskina and Kogan[57] applied Rast's method to observe the changes in molecular weight distribution of a novolac resin during drying.

Severov et al [58] made a study of the change in the fine and porous structure of phenolformaldehyde resin in high-speed short-term high temperature heating. The specimens were heated for 1 minute in a resistance furnace with a graphite heater, in a neutral medium, from 200° to 2900°C.

Ouchi [59] studied structural changes during the pyrolysis of a phenolformaldehyde resole resin by infra-red spectroscopy.

Katović [60] has recently published two papers on resole resins. The first paper deals with the curing of resole-type phenolformaldehyde resins. The second paper discusses kinetics of the formation of a dibenzyl ether linkage during curing of resoles. D.T.A. and infra-red spectroscopy were used as analytical tools.

SUMMARY

Although the chemistry of phenolic resin degradation is quite complex, some points have become clear from the literature survey. They are:-

1. Phenolformaldehyde polycondensates may have three groups, i.e. methylene linkage, free methylol group and dimethylene ether bridge.

2. During thermal scission the C-C bond between CH_2 and the benzene ring is broken. At temperatures above 450°C ring scission, char and CO formation are rapid. The hydrogen atoms directly attached to the benzene nuclei begin to split off in the form of H_2 at higher temperatures (700°C).

3. The methylene unit is the most vulnerable position in the cross-linked structure of phenolic resin.

4. During oxidative degradation - CH_2 - changes to hydroperoxide and then to a carbonyl group, while a methylol group changes to a carboxyl group.

5. Gases, tar and solid carbonaceous residue are the main products of degradation. The liberated gases include, water vapour, CO, CO_2, H_2, CH_4, etc. The primary carbonisation is a partial depolymerisation in which the structural units participate in their entirety in the reaction; during this reaction they either remain in the residue or are found in the tar. The tar consists of aromatic and aliphatic units depending upon the temperature of pyrolysis, and the solid residue

becomes richer in carbon content. The carbonaceous residue changes to graphitic structure at higher temperatures. The solid contains carbon, hydrogen and oxygen, and its formation depends on temperature and C/H ratio.

CHAPTER 11

NATURE OF PHENOLIC RESINS

As early as 1872 Baeyer[61] in Germany observed the reaction between phenol and formaldehyde and characterised the phenol alcohols formed. Baekeland[62] discovered in 1907 that useful mouldings could be made if the final stages of the reaction were carried out under heat and pressure, preferably in the presence of a suitable filler. Since the commercial exploitation of phenolformaldehyde resins, voluminous literature on phenolics is being published. Carswell[63] published a book and Hultzsch[64] published a monograph on phenolics in 1947 and 1950 respectively. Megson[42] in 1958 brought out a very useful book entitled "Phenolic Resin Chemistry". In the early part of the book the author has given a detailed survey of the three major schools of thought (i.e. Zinke school, von Euler school, and Hultzsch school) arose regarding the structure of phenolic resins, later he has discussed the chemistry of phenolic resins syntheses, kinetics, structure and fractionation of resins. Conley and Bieron[29] have reviewed the literature up to 1963.

Since Baekeland's findings, phenolic resins have become one of the most prominent and largely used polymers. There is an extensive literature on chemistry of phenolic resins (Megson) and for the moment it is sufficient to summarise very briefly the main features of resin formation and curing.

The polymers derived from the interaction of phenols and formaldehyde differ from other condensation products, in that polyfunctional phenols can form a variety of isomerides of any particular chain length. Polyfunctional phenols may react with formaldehyde in positions both ortho and para to the hydroxyl group. This not only makes the kinetic studies very difficult, but also makes the chemistry of the reaction very complex and difficult to unravel. The useful form of phenolformaldehyde resins is the hardened, cross-linked type, which is not easy to examine by the conventional analytical techniques. The inherent difficulties of analysing such a material are due to its insoluble, hard and infusible nature.

The nature of the phenol and formaldehyde condensation products depends upon their ratio of phenol to formaldehyde and the catalyst used. There are two types of phenolic resins products formed, e.g. resoles and Novolacs.

Resoles

With a basic catalyst (NaOH or NH_4OH) and a mole ratio of formaldehyde to phenol of greater than one, it is possible to attach methylol group to each reactive position (two ortho and one para). In practice, a mixture of mono-, di- and ter- substituted methylol phenols may be present, i.e. the primary reaction products are phenol alcohols. In the second stage the products differ according to the proportion of formaldehyde and may contain methylene and ether linkages and CH_2OH groups in the various free positions. As the reaction proceeds further the smaller chains are built up containing 5-9 rings joined by $-CH_2-$ and perhaps $-CH_2-O-CH_2-$ bridges. Finally after curing the resin may contain a large number of rings linked by one or more methylene bridges. These resins are called one-stage, as there is enough formaldehyde to produce thermosetting resin.

Novolacs

Novolacs or two-stage resins are obtained by reacting less than one mole of formaldehyde per mole of phenol in the presence of an acid (e.g. HCl or $C_2O_4H_2$) catalyst. The resin is readily soluble in ketones and alcohols. Although there may be some methylol groups formed during the acid catalysed reaction, they are believed to be converted to methylene links at the low pH values used. Novolacs contain 3-9 benzene rings linked by the methylene bridges.

In order to cure or set the novolac resin it is necessary to supply more of methylene linkages. This is usually done through the use of hexamethylenetetramine or a cyclic formal. The second addition of methylene bridges to form a thermosetting resin gives rise to the common name "two-stage" resin. During the curing process the hexamine breaks down to liberate ammonia and may act as a catalyst in cross-linking.

$$N_4(CH_2)_6 + 6H_2O \rightleftharpoons 6H_2CO + 4NH_3$$

The reaction is very complex.[42] It is believed to incorporate dibenzylamine bridges which decompose on heating with the final result being methylene bridges.

A simplified account of the present knowledge of the phenolics chemistry is given below.

(a) Stage 1: Formation of phenol alcohols in the presence of acid or base catalyst.

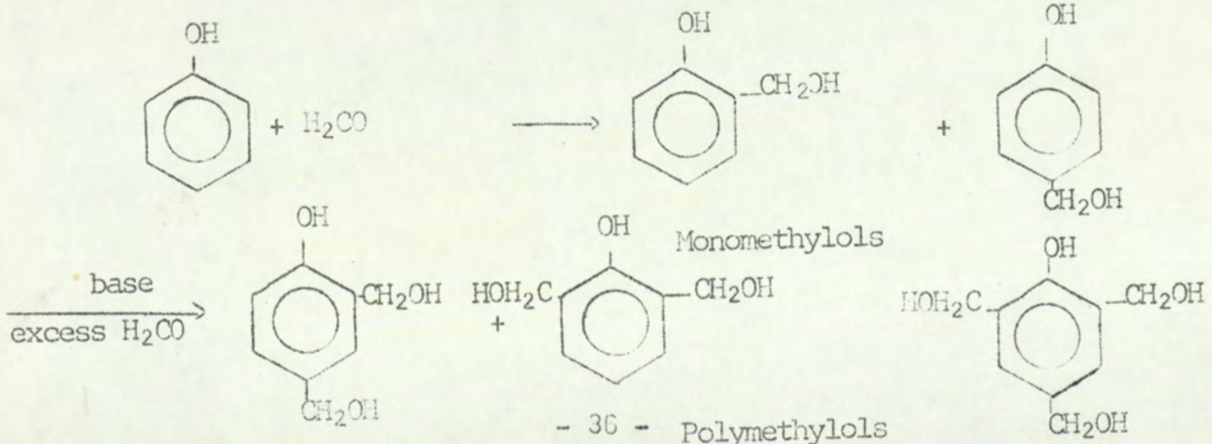

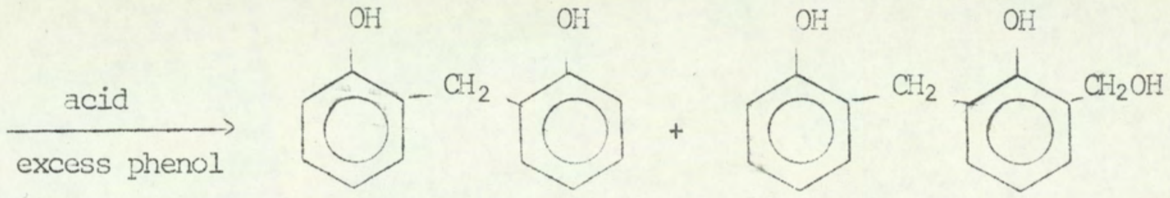

Diphenylmethanes

(b) Stage 2: Condensation of phenol alcohols

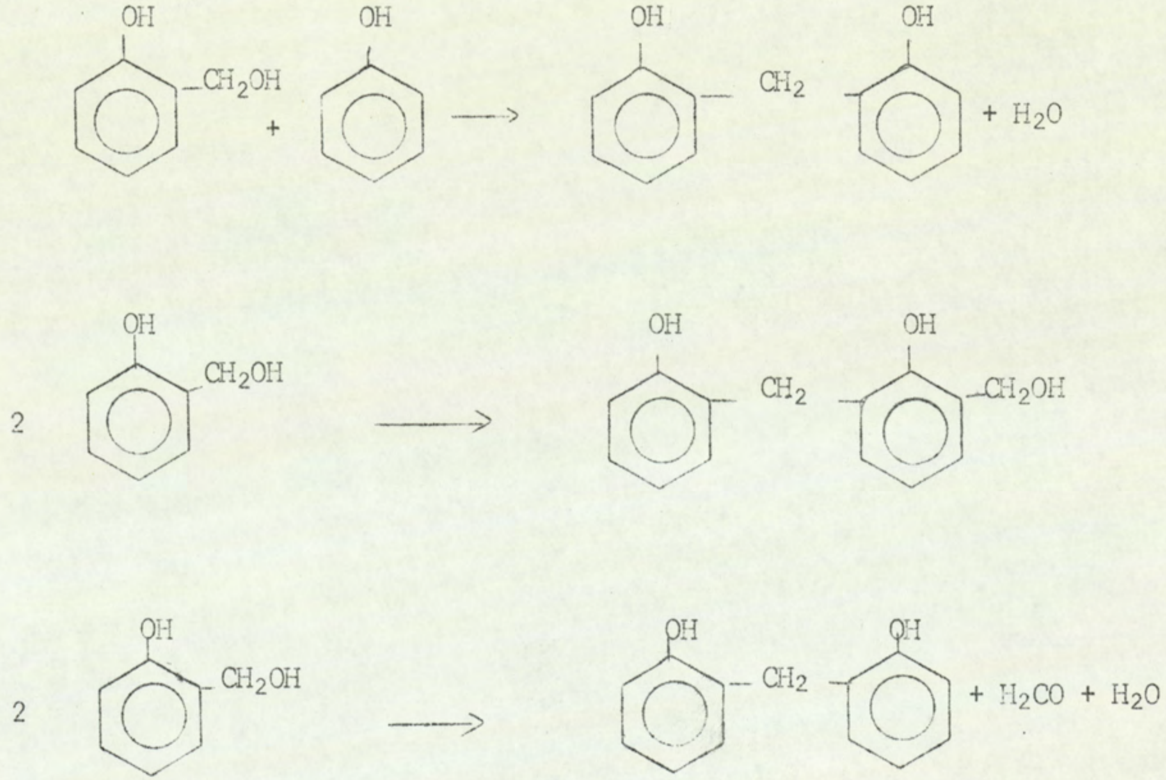

Methylene bridge

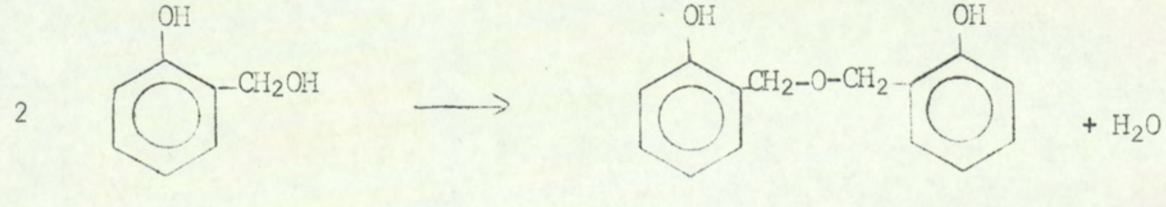

Ether linkages

In general with acid catalysts and excess phenol the products are diphenylmethane derivatives, while with alkalies they are polymethylol phenols, which may contain several rings linked by methylene bridges.

(c) Stage 3: Network formation.

Resole resins having polymethylol groups will cross-link readily, without further addition of formaldehyde, under the action of heat alone (or acid catalyst). Novolac resins need the addition of formaldehyde and alkali - usually in the form of hexamine, which contains both formaldehyde and ammonia or cyclic formals.

With the novolacs possibly a nitrogen atom may enter the bridge, but probably comes out again in the later stages of curing.

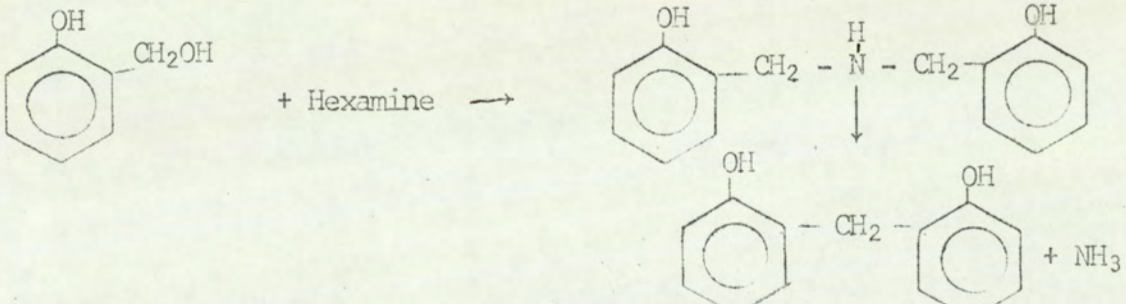

Besides affecting the amount of branching in a phenol resin (via the number of methylol groups introduced) the catalyst may also influence the location of methylene bridges between rings. It is now generally accepted that acid catalyst tends to favour the formation of p,p' linkages, although o, o' or o, p' linkages may also be formed. Obviously when another phenol ring adds to the growing chain it must add to the o-position, and probably with the p-position of the ring being added. Thus the structure of the basic chain is complex

It was shown by Bender[65] that selective catalysts, such as Zn, Al or Mg oxides force the linkage in the ortho position, producing a fast-curing resin of more than 50% 2,2' content. The conditions involved in the production of varying percentages of 2,2' content involved careful control of reaction conditions, i.e. catalyst, temperature,pH, ratio of reactants, and reaction time. He extended the work to show that the two main factors of phenolic resin structure which influenced hexa hardening rate were chain length and the position of the hydroxyl on the ring.

Fraser et al[65a] showed that for the formation of high-ortho resins with a fast rate of curing, the following conditions were necessary:

(1) A molar excess of phenol.

(2) The apparent pH of the reaction mixture should lie between 4 and 7.

(3) The presence of bivalent metal cations such as Mn^{++}, Zn^{++}, Cd^{++}, Mg^{++}, Co^{++}, Ca^{++} and Ba^{++}, which are arranged in decreasing order of usefulness.

More recently Bradley and Dietzler at Dow Chemical Co., California, showed that monovalent alkali metal hydroxides when present in small amounts are also strongly ortho directing in a non-polar solvent such as perchloroethylene, CCl_4, toluene and the like.

Heslinga and Schors[66] report a method of curing phenolic novolac resins by means of cyclic formals under the catalytic influence of strong acids. They propose availability of two cross-linking components per molecule of cyclic formal. In the case of 1,3-dioxane compounds they formulate the reaction scheme shown in equations :-

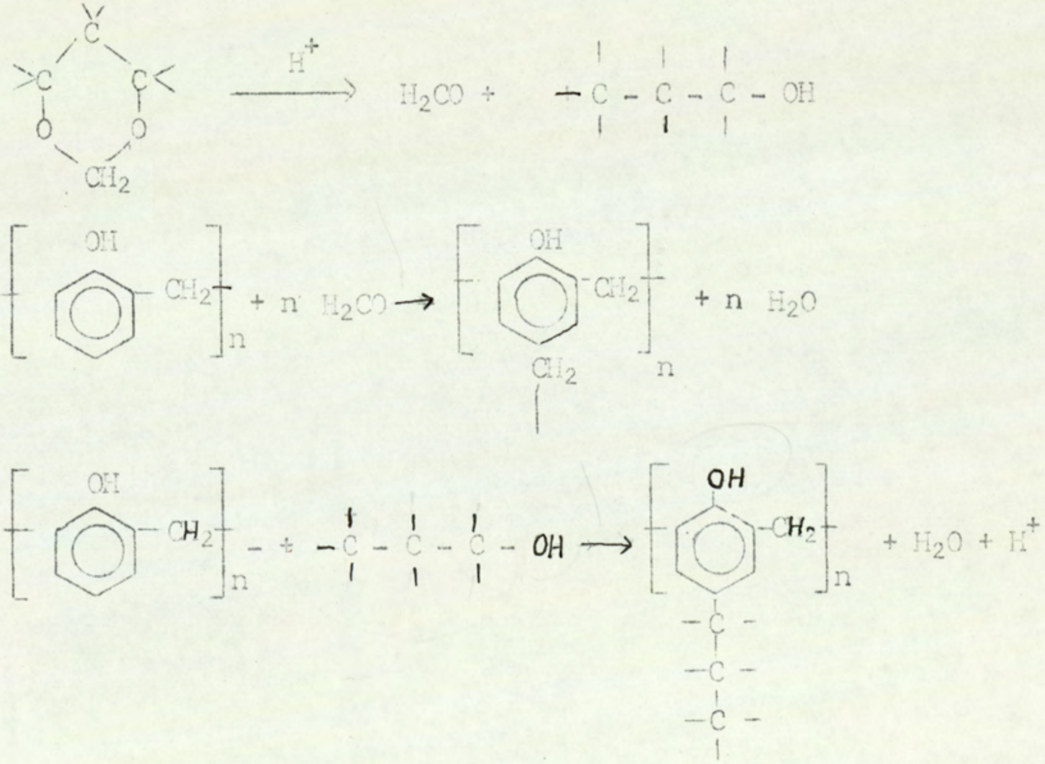

Chemistry of Curing

Curing of phenolic resins is dependent on temperature, and as stated above, upon the presence of excess formaldehyde and alkaline conditions (phenolic resins cured under acidic conditions appear to have a different mechanism). The primary reactions in the range up to 170°C are:

(a) Where a methylol group reacts by the elimination of water with the o- or p- ring hydrogen of another ring to form a methylene bridge.

(b) Where two methylol groups react to form an ether link.

(c) Formaldehyde may be freed by the reversal of the methylol formation reaction,

(d) A bridge may be formed containing nitrogen.

These reactions are of course strictly analogous to the ones met with in the resin formation. Also by analogy it is possible for an ether bridge to split off formaldehyde to give a methylene bridge.

The second phase of the purely thermal reaction of the phenolic resin system starts around 160-70°C but may become extensive at about 200°C. Many of the reactions in this range arise from further reactions of dibenzyl ethers and unreacted methylol groups. These reactions are frequently accompanied by a decrease in the hydroxyl content and a decrease in the molecular weight of the resin, although this may increase again later.

During this same stage the evolution of more than one mole of water, and less than one mole of formaldehyde has been observed by several observers. This has been explained only moderately well in various ways, including further reaction of the free formaldehydes and one other possibility must be mentioned namely ether formation between phenolic hydroxyl groups. Megson[42] has isolated xanthene and various homologues of xanthene from the products obtained by pyrolysis of phenolic resins perhaps formed in this way.

CRITERIA OF THERMAL STABILITY OF POLYMERIC MATERIALS

There are a number of factors that can influence the heat stability of polymeric materials . These include bond strength, activation energies of scission reactions, melting or softening points, crystallinity, the presence of low molecular weight volatile products, "weak links", presence of groups which are readily affected by heat, cross-linking, etc. A proper assessment of the thermal stability of polymers will, therefore, entail a systematic investigation of the above factors.

Since the term "thermal stability" still remains vague even in specialised literature, therefore different investigators have devised relative thermal stability indices. Madorsky[23] suggested that relative heat stability for polymers, which vaporise almost completely below 600°C, can be established by heating under identical conditions and comparing the amount of vaporisation that occurs in a vacuum pyrolysis for 30 minutes at various temperatures.

Another method suggested comparison of temperature[23] (T_h) at which 50% weight of a given polymer is vaporised under standard conditions of pyrolysis. However various polymers, e.g. poly(vinylchloride), phenolic resins, develop cross-linking during pyrolysis and do not vaporise completely. Therefore, the T_h temperature cannot be satisfactorily used to measure the relative thermal stability of these polymers. Madorsky proposed that thermal stability of carbon-chain polymers may be better defined as their tendency to yield a more or less carbonised residue.

Besides these methods some thermo-chemical procedures have been employed to evaluate thermal stability.

The values of the energy of activation (E_o) obtained for different polymers vary according to their thermal stability in a general acceptable manner. A correlation between E_o and thermal stability of a polymer is probably always quite involved. In some polymers, thermal degradation proceeds by two or more reactions which run either concurrently or consecutively. Then the activation energy is presumed to afford an overall picture of the pyrolysis energetics and rate of degradation. It probably involves energies associated with diffusion process, bond ruptures, volatilisation, oxidation or reduction, etc. Any correlation presented in terms of E_o is at best semi-quantitative and should not be used for the determination of precise activation energies.

CHAPTER 111

Experimental Methods

Studies on thermal degradation of organic polymers aims at finding:

(a) The relative thermal stability.

(b) The qualitative and quantitative composition of degradation products as a function of temperature and pressure.

(c) The kinetics and activation energies of the chemical reactions occurring in the process of degradation.

Madorsky has reviewed in detail the equipment and experimental procedures in his book "Thermal Degradation of Organic Polymers". The apparatus used by Madorsky for pyrolysis of polymers at high temperatures is shown in Fig.4.

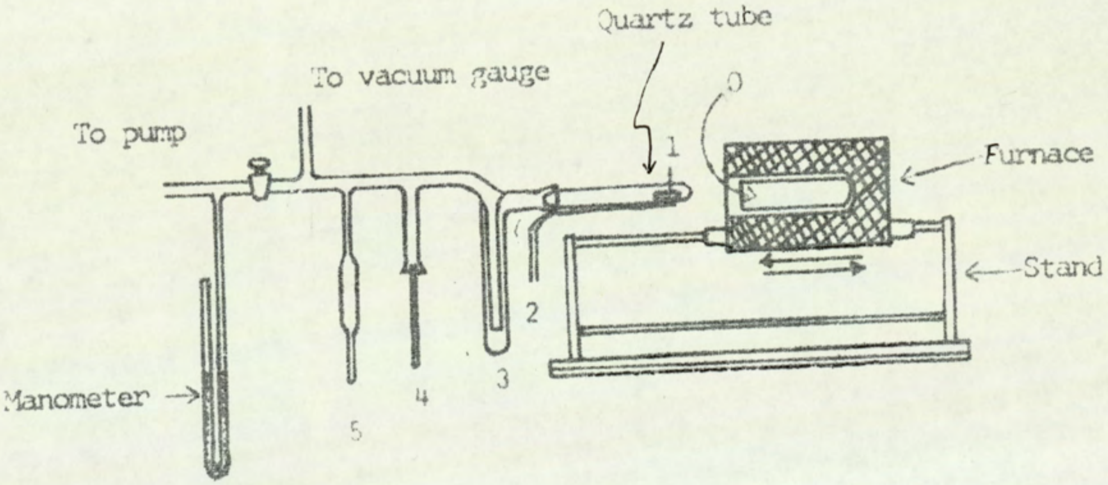

Fig. 4. Equipment for the pyrolysis of polymers at high temperature

0. Stainless steel cylindrical cup
1. Platinum cylindrical cup
2. Platinum-platinum rhodium thermocouple
3. **Liquid nitrogen trap**

4.)
) Sample collecting tubes
5.)

Madorsky *(loc cit)* has reported activation energies for degradation of a number of polymers which vary from 30-73 kcal/mole.

THERMO-ANALYTICAL TECHNIQUES

(a) Differential Thermal Analysis (D.T.A.).

(b) Thermo-gravimetric Analysis (T.G.A.).

(c) Pyrolysis and Identification of Fragments.

Ordinary chemical methods of analysis are impracticable for studying the pyrolysis of highly cross-linked polymers, since such materials are extremely infusible, insoluble and non-volatile. Therefore techniques like differential thermal analysis, thermo-gravimetric analysis and pyrolysis are being used more and more for this purpose.

In the pyrolysis of polymers many complex reactions occur simul-taneously and each reaction has a characteristic activation temperature (corresponding to E_o). By using dynamic tests, i.e. where temperature rises steadily, it is generally possible to separate the reactions in time so that each step has a characteristic plot of reaction rate against temperature (time) (providing the activation temperature of reaction is sufficiently separated and concurrent reactions are isolated). But mass/energy transfer and many other variables make interpretation of thermoanalytical data difficult.

(a) Differential Thermal Analysis

Detailed description of equipment and techniques are not mentioned here, since there is an abundance of literature on the subject [67-76].

Briefly, the reactive substance to be studied is placed in a sample cell and an inert substance is placed in a reference cell. The inert substance is chosen so that its heat capacity and thermal conductivity approximate to that of the reactive material. Both cells are then immersed in a heat bath, and the reaction is initiated by supplying heat to the bath at a predetermined rate in such a way that the temperature of the reference cell, T_r, increases linearly with time. In the absence of reaction, the sample temperature, T, will also increase linearly and equals T_r. When the reaction commences in the sample cell, the heat liberated or absorbed causes T to change from T_r. This difference, $\Delta T = T - T_r$, is recorded by means of a differential thermocouple. The actual reference temperature T_r, is simultaneously recorded. The resulting curve is called a thermogram or a thermal spectrum, from which information on the temperature, heat and rate of transformation can be derived. There are over a dozen of variants on the process, and a variety of commercial equipment is available in the market. However, the main advantage of differential thermal analysis (D.T.A.) over conventional calorimetry is that it is simple, rapid and subject to continuous recording.

As D.T.A. directly measures the heat-energy change occurring in a substance, it is theoretically possible to detect and measure any physical transition and chemical reaction that is accompanied by a thermal-energy change. But the differential thermometric information can be misleading when the endothermic breaking of and the exothermic forming of bonds occur simultaneously in the pyrolysis of substances. For instance, if, at a given temperature, the heats of endothermic reactions were exactly equal to the heats of exothermic ones, a differential thermometric peak would be absent. This would lead to false conclusions that no thermal decomposition has occurred. Changes in specific heat and thermal conductivity of a polymer during pyrolysis also complicate the differential thermometric picture, especially when a quantitative information is desired.

(b) Thermogravimetric Analysis

The history of development of T.G.A. and a review of its applications have been presented by Duval[77] in his book "Inorganic Thermogravimetric Analysis". Newkirk[78] has discussed the effects of different variants on T.G.A.. Murphy,[79] Ke,[80] Kissinger and Newman,[81] Manley[82], Millane[83] and Double,[84] have reviewed applications of thermoanalytical techniques.

Interest in thermogravimetry has increased recently because of the commercial availability of automatic, reliable and continuously recording thermo-balances. This technique measures the change in weight as a result of chemical reactions (decomposition) in a sample on heating, either isothermally or during a programmed heating rate. Since T.G.A. measures losses of weight during pyrolysis rather than heat changes, it is not subject to the above mentioned complications, and should therefore give a more reliable quantitative estimate of the relative thermal stabilities of different polymers.

(c) Pyrolysis and identification of fragments

The development of D.T.A. and T.G.A. led to pyrolysis, collection and identification of the products evolved in successive decomposition reactions. There are several different ways reported in literature for this technique[22,25,34]. The gases and other fragments can be identified by mass spectrography, gas chromatography or IR spectroscopy. However without resorting to analysis of the combustion products, the thermal stability could be identified with the relative proportion of three fragments - volatile products, liquids and char or solid residue.

Complementary nature of T.G.A. and D.T.A.

Despite the shortcomings of differential thermogravimetry as a tool for studying the pyrolysis of polymers, it can sometimes be very useful in revealing, or in clarifying, certain mechanisms of thermal degradation. For instance, it has been shown by D.T.A. that isomerisation of residual epoxy groups in certain epoxide polymers plays an important part in the decomposition mechanism. It is, therefore, necessary that differential thermogravimetry be used to obtain qualitative information on the pyrolysis of polymers, especially highly cross-linked ones, and T.G.A. be used as a quantitative adjunct.

T.G.A. and D.T.A. are complementary techniques in that the information obtained by the application of one approach is often enhanced by the application of the other method. The range of phenomena measurable in the course of a D.T.A. is much larger than in a T.G.A. determination. Thus, during T.G.A. pure fusion reactions, crystalline transitions, glass transitions, crystallisations and solid-solid reactions with no volatile products would not be indicated because they engender no change in weight of the sample. However, the use of T.G.A. frequently allows one to ascribe with some exactness the stoichiometry involved in chemical changes, whereas during D.T.A., these changes are indicated merely by an exothermal or endothermal departure from the base line.

Study of thermal degradation of high polymers can best be completed or corroborated by such techniques as T.G.A. or derivative T.G.A., which measures the weight loss as a function of temperature, and gas chromatography and/or mass spectrometry and/or IR spectroscopy, which identify and measure the decomposition products. Pyrolysis is a complex reaction, during which various other reactions, both endothermic bond rupture, volatilisation, etc. and exothermic bond reforming can occur simultaneously. In such a case, the thermogram shows only the net heat effect and may not give complete information on all individual events.

Knowledge of the nature and amount of the degradation products would complement the data obtained by D.T.A.

DIFFERENTIAL THERMAL ANALYSIS

Theoretical

There is a great deal of literature on theoretical and practical studies of differential thermal analysis of inorganic, organic and polymeric materials.

Kissinger[85] developed an equation that makes possible the determination of the activation energy for a simple decomposition reaction of the type,

$$\text{solid}_1 \rightarrow \text{solid}_2 + \text{gas} .$$

Activation energy can be calculated regardless of the reaction order by making differential thermal analysis patterns at a number of heating rates. Thus

$$\frac{d\,(\ln \phi/T_m{}^2)}{d\,(1/T_m)} = -\,E/R \qquad (1)$$

where T_m = Peak Temperature, $^\circ$k

A plot of $\ln \phi/T_m^2$ versus $1/T_m$ should give a straight line, the slope of which is $-E/R$.

Borchardt and Daniels[86] derived equations, which relate the shape of the differential thermal analysis curve to the kinetics of the reaction giving rise to the curve. For certain reactions the use of these equations allows the order of the reaction, the frequency factor, the activation energy and heat of the reaction to be determined in a single rapid measurement.

It is assumed that the heat evolved in a small time interval is directly proportional to the number of moles reacting during that time:-

$$dH = \frac{KA}{X_o} \, dx \qquad (2)$$

where dH = Heat of reaction

K = Coefficient of heat transfer

A = Total area under D.T.A. curve

X_o = Initial number of moles of reactant

dx = Number of moles reacted.

The rate constant of a reaction of the order of 'n' with respect to one component is :-

$$k = \left[\frac{KAv}{X_o}\right]^{n-1} \frac{C_p \frac{d\Delta T}{dt} + K\Delta T}{\left[K(A-a) - C_p\Delta T\right]^n} \qquad (3)$$

where C_p = Heat capacity

v = volume

a = Area under curve at temperature T(time)

For the case of reaction between multicomponents such as :-

$$lL + mM + \ldots\ldots\ldots\ldots \longrightarrow \text{Products}$$

the reaction rate is given by equation:

$$k = \frac{\left[\frac{KAv}{L_o}\right]^{l + m - 1}\left[C_p \frac{d\Delta T}{dt} + K\Delta T\right]}{\left[K(A-a) - C_p\Delta T\right]^{l}\left[K(\frac{M_o}{L_o}) A - \frac{m}{l} a) - C_p\Delta T\right]^{m}} \qquad (4)$$

where L_o and M_o are the initial number of moles of L and M. The plot of of ln k versus 1/T (activation energy plot) would yield a straight line if the correct value for the order of reaction has been assumed. The correct plot of ln k against 1/T permits the calculation of E and frequency factor Z.

Reich[87] quite recently developed equations for obtaining activation energy from D.T.A. traces, without prior knowledge of reaction order. The equations are:

$$\ln\left[(a-a_i)/A\right] \approx -E/_{RT} + \ln Z\,\Delta T W_o^{\,n-1}/\phi \tag{5}$$

and

$$\ln\left[(a-a_i)/A\right] \approx -E/_{RT} + \ln Z\,\Delta T/\phi \tag{6}$$

From equations (5) and (6) it can be seen that the plot of $\ln\left(\frac{\Delta a}{A}\right)$ or $\ln(\Delta a)$ versus 1/T affords a linear relationship whose slope will yield the value of E.

The same author[88] developed still more equations whereby E, n, and Z may be obtained directly from D.T.A. traces, thus

$$E/R = T^2\Delta T/\breve{a}\,\ln(A/\breve{a}) \qquad \text{for } n = 1 \tag{7}$$

and

$$E/R = \left[(1-n)\,T^2\Delta T/A_T\right] \Big/ (\breve{a}_T/A_T)^n \left[1-(\breve{a}_T/A_T)^{1-n}\right] \tag{8}$$

for $n \neq 1$

where $\breve{a}_T = \int_{T_i}^{\infty} \Delta T dT - \int_{T_i}^{T} \Delta T dT$, $\qquad A_T = \int_{T_i}^{\infty} \Delta T dT$

and ΔT = Height of the D.T.A. curve

After the value of n has been estimated (the method is given in this paper) a value of E may be calculated by means of equation (7) or (8).

Reich[89] presented various expressions for estimating kinetic parameters during pyrolysis from D.T.A. traces. These equations are applied to polytetrafluoroethylene, polyethylene, polypropylene, polystyrene, isotactic poly(propyleneoxide) and poly(methylmethacrylate), The results obtained are compared with reported values, and merits and demerits of the various methods are given.

Another expression is applied to degradation of polyethylene by Reich[90] whereby both E and n may be directly obtained from differential thermograms.

$$\log \left[\frac{(\Delta T_1/A_{T_1})}{(\Delta T_2/A_{T_2})}\right] = - E/_{2\cdot 3R} \left[\frac{(1/_{T_1''} - 1/_{T_1}) \log (\tilde{a}_{T_1}/\tilde{a}_{T_2})}{\log (\tilde{a}_{T_1}/\tilde{a}_{T_1}')}\right] + \log \frac{(\phi)^2}{(\phi)_1} + n \log \left(\frac{A_{T_2}}{A_{T_1}}\right) \qquad (9)$$

where '1' and '2' indicate D.T.A. traces for the same material at two different heating rates.

A very recent method which employs the linearisation of D.T.A. traces is presented by Reich[91], for the estimation of kinetic parameters during polymer degradation. By this method two D.T.A. curves are used and it is not necessary to measure areas prior to evaluating activation energy and the reaction order. The method is applied to polyethylene, polypropylene and polystyrene.

It can readily be seen that a variety of methods exist for kinetic analyses of thermal analysis data, and we shall return to this later, where appropriate.

THERMOGRAVIMETRIC ANALYSIS

Theoretical

The application of thermogravimetric analysis to the investigation of kinetics of thermal degradation is discussed here.

Freeman and Carroll[92] developed equations for irreversible reactions, which may be used to calculate energy of activation and order of reaction from thermogravimetric and volumetric curves. Considering a reaction, in the liquid or the solid states, where one of the products is volatile all other substances being in the condensed state, the equation is derived for n and E. For reaction of this type,

$$a\,A \;=\; b\,B \;+\; c\,C_{(g)}$$

the equation is :-

$$\frac{E}{RT^2}\;\frac{dT}{d\ln X} \;=\; \frac{d\ln(-dx/dt)}{d\ln X} - n\,. \qquad (10)$$

It is apparent that plot of $\frac{dT}{T\,d\log X}$ versus $\frac{d\log(-dX/dt)}{d\log X}$ should result in a straight line with slope of $E/_{2\cdot 3R}$ and intercept of $-n$.

Anderson[93] developed two thermogravimetric methods to show whether rate of weight loss varies with the extent of pyrolysis of polymer. The first of these methods involves obtaining the activation energy, the order of decomposition and the frequency factor by solving three equations simultaneously. The data for these equations are obtained by performing three thermogravimetric experiments at three constant heating rates. The second method is based on the compound interest law. It involves cycling the polymer between 25°C and a fixed higher temperature.

A non-isothermal kinetic treatment is developed by Smith[94] to characterise two principal pyrolysis parameters:

1. Integral procedural decomposition temperature (T_p)
2. Procedural activation energy (E_p)

It is shown that

$$k = \frac{R}{(W_o - x_i)} \qquad (11)$$

where R = Slope of the thermogram at temperature T_i,

x_i = Weight loss at temperature T_i .

The reaction rate-coefficient is determined at each of the temperatures T_1 , T_2 ....and its logarithm is plotted against 1/T. If the assumption of a simple reaction order is correct, a straight line of slope E_p is obtained.

Horowitz and Metzger[95] have developed new mathematical relationships to interpret thermogravimetric traces and to determine kinetic parameters of pyrolysis reactions, thus

$$\ln \ln \left(\frac{Wo}{W}\right) = \frac{E\theta}{RT_s^{\,2}} \qquad (12)$$

and

$$\ln \left(\frac{Wo}{W}\right) = -\frac{Z\,RT_s^{\,2}}{\phi\;E} \exp\left[-\frac{E}{RT_s}\left(1 - \frac{\theta}{T_s}\right)\right] \qquad (13)$$

where a reference temperature T_s is defined such that at T_s

$$\left(\frac{W}{Wo}\right) = \frac{1}{e}$$

and θ is defined such that

$$\theta = T - T_s .$$

Thus a plot of $\ln \ln\left(\frac{Wo}{W}\right)$ against θ should give a straight line whose slope is $E/_{RT_s^2}$, for any single-reaction pyrolysis which gives only gaseous products. The frequency factor, Z, could be evaluated from equation (13).

These workers[96] produced another equation by slightly revising and modifying the derivations developed by van Krevelen et al[97].

$$\ln \ln \left(\frac{Wo}{W}\right) = \left[\frac{E}{RT_s} + 1\right] \ln \frac{T}{T_s} = \left[\frac{E}{RT_s} + 1\right] \ln \left(1 + \frac{\theta}{T_s}\right) \quad (14)$$

Plot of $\ln \ln (\frac{Wo}{W})$ versus $\ln\left(\frac{T}{T_s}\right)$ or $\ln (1 + \frac{\theta}{T_s})$ should give a straight line with a slope $(\frac{E}{RT_s} + 1)$. Thus E could be calculated.

Ingraham and Marrier[98] developed a simplified method for the determination of the activation energy of a heterogeneous reaction having linear kinetics, thus

$$\log \left(\frac{dw}{dT}\right) = \log T - \log \phi + \log C - \frac{E}{2\cdot 303RT} \quad (15)$$

where C is constant.

The activation energy is calculable from the slope of a graph of $\left[\log (\frac{dw}{dT}) - \log T + \log\phi\right]$ versus $1/_T$.

Reich[99] derived the equation

$$E = \frac{2\cdot 303R \log \left[\frac{(\phi)_2}{(\phi)_1} \left(\frac{T_1}{T_2}\right)^2\right]}{(1/_{T_1} - 1/_{T_2})}, \quad (16)$$

to rapidly estimate activation energy from two thermograms obtained at two different heating rates.

Coats and Redfern[100] produced an equation for an initial survey of the kinetics of a particular system of the type:

$$\text{solid}_1 \rightarrow \text{solid}_2 + \text{gas}$$

$$\ln \left(\frac{x}{T^2}\right) = \ln (ZR/\phi.E)\left(1 - \frac{2RT}{E}\right) - (E/_{RT}) \cdot \qquad (17)$$

Thus a plot of $\ln \left(\frac{x}{T^2}\right)$ against $1/_T$ for low values of x, or where n = o should be a straight line with a slope of $-E/_R$.

Reich, Lee and Levi[101] have described a procedure for obtaining kinetic parameters in the degradation of high polymers and the necessary experimental procedure is outlined. They have employed various expressions in estimating kinetic parameters of Teflon 7 thermal degradation.

Reich[102] described a novel procedure for the estimation of E and Z without recourse to the thermogram slopes. For first order kinetics, which polymer degradation usually follows, the following equation may be written

$$\ln \left[\ln \left(\frac{W_i}{W}\right)\right] = -\frac{E}{RT} + \ln \left[\frac{Z\Delta T}{\phi}\right] \qquad (18)$$

when n = o, the relationship becomes

$$\ln (W_i - W) = -\frac{E}{RT} + \ln \left(\frac{Z\Delta T}{\phi}\right) \qquad (19)$$

where ΔT = constant = $(T - T_i)$, and W_i and W = weights of the active material remaining, at temperatures, T_i and T respectively.

Flynn and Wall[103] give a quick and simple method for determining activation energies from weight loss versus temperature data at several heating rates, thus

$$E \cong -4{\cdot}35\ d \log\ (\phi)/d\left(\frac{1}{T}\right) \cdot \qquad (20)$$

This method for determining the activation energy from T.G.A. plots involves only the reading of the temperature at a constant weight loss from several integral thermograms at different heating rates. From the slope of log (ϕ) versus $1/_T$ the activation energy may be calculated.

These workers[104] have recently published a paper giving a method for determining initial kinetic parameters, whenever precise low-conversion data are available.

$$n = \frac{d \log (dx/dt)}{d \log (1 - x)} \tag{21}$$

and

$$E = - R\left[d \ln x_i/d(1/_{T_i})\right] \tag{22}$$

where x_i is fractional weight loss at temperature T_i.

Reich[105] gave a novel and comparatively simple procedure for estimating values of kinetic parameters from thermogravimetric traces. The expressions are:-

$$E/R = S/\left[W_c \ln (Wo,c/W_c)\right] \qquad \text{For } n = 1 \tag{23}$$

and

$$E/R = S(1 - n)/W_c{}^n(Wo,c^{(1-n)} - W_c{}^{(1-n)}) \qquad \text{For } n \neq 1 \tag{24}$$

where $S = d\,Wc/d(1/_T)$

$Wc = W - W_R$

$Wo,c = W_o - W_R$

W = Weight fraction of material remaining ,

W_R = Weight fraction of inactive material after pyrolysis .

Levi, Reich and Lee[106] produced the following equations for determining E, Z and n from T.G.A. traces.

$$\log \left(\frac{dW}{dT}\right) = \frac{E}{R}\left[\left(\frac{W_m}{T_m{}^2 R_m}\right) \log W - \frac{1}{2\cdot 303T}\right] + \log Z \qquad (25)$$

and

$$n = \left(\frac{W_m}{T_m{}^2 R_m}\right) E/R \qquad \text{for } n>o \qquad (26)$$

where

W_m = Weight remaining)
)
T_m = Temperature, ^{o}k) All at the maximum rate
)
R_m = Slope of the thermogram)

The activation energy is calculated from the slope of the line obtained by plotting log(dw/dT) against $\left[\left(\frac{W_m}{T_m{}^2 R_m}\right) \log W - \frac{1}{2\cdot 303T}\right]$, and Z from its intercept. n can then be calculated from equation (26).

Doyle[71] has briefly described systematic errors (residual weight, temperature, time, rate of weight change, heating rate, etc.) which limit the accuracy of thermogravimetric data. He has developed some useful rate equations and their integrals applicable in thermogravimetric analysis calculations. Most of the published work on kinetic analysis of thermogravimetric data deals with various ways of using the Arrhenius equation:

$$k = Z \exp \left(\frac{-E}{RT}\right) . \qquad (27)$$

Doyle has discussed in detail its applications in different forms.

Plan of Experimental Work

Resin used

Most work was done on a commercial novolac R19370.

Some comparative experiments were carried out with two other resins

RW52487
RW54859

Also some experiments were carried out with a high temperature resole DV19162 and commercial compounds

RPD110 **-novolac + asbestos fibre**
RPD150 **-resole + asbestos fibre**
RPD154 **-resole + polyamide + asbestos fibre**

DTA and TGA analyses were to be done separately using the Dupont 900 Thermoanalyser under conditions given in appropriate schedule.

Study of curing variables

- Hexa content
- Curing time
- Curing temperature

Study of analytical variables

- Rate of heating
- Particle size
- Atmosphere

Study of effect of additives

- Metals
- Lewis Acids
- Oxides
- Asbestos and other fibres
- Carbon
- Polymers
- Carbohydrates
- TX fibre

Isothermal Thermogravimetric studies were made on a commercial novolac R19370 in air/self-generated atmosphere.

Temperatures: 320°, 360°, 460°, 555° and 670°C

Study of effect of addenda

- Metals
- Sodium metaborate
- Penta sodium triphosphate
- Lewis Acids
- Oxides
- Ammonium dihydrogen orthophosphate

CHAPTER 1v

PREPARATION OF PHENOLIC RESIN SAMPLES

All samples were heat treated in an atmosphere of air.

1. Novolac

Thermal treatment of phenolformaldehyde novolac resin

Commercial phenolformaldehyde novolac resin (R19370) was ground to pass through a 100 mesh B.S. sieve and samples were heated to 100°, 136°, 146°, 166°, 178°, 204° and 222°C in air for 1½ hours. They were numbered PFA, PFB, PFC, PFD, PFE, PFF and PFG respectively. After cooling in a desiccator they were each ground and sieved through a 100 mesh B.S. sieve. All the samples were friable.

2. Curing the novolac resin with hexamethylenetetramine

100 mesh novolac and finely powdered hexamethylenetetramine were mixed thoroughly in different ratios and were named PFH I through PFH XVI. The weight percentage compositions of each sample are reported in Table 1.

TABLE 1

Percentage compositions of phenolformaldehyde novolac resin and hexamethylenetetramine.

Sample	Phenolformaldehyde resin %	Hexamethylenetetramine %
PFH I	83·0	17·0
PFH II	"	"
PFH III	"	"
PFH IV	"	"
PFH V	"	"
PFH VI	"	"
PFH VII	95·0	5·0
PFH VIII	90·0	10·0
PFH IX	76·0	24·0
PFH X	70·0	30·0
PFH XI	60·0	40·0
PFH XII	50·0	50·0
PFH XIII	90·0	10·0
PFH XIV	"	"
PFH XV	"	"
PFH XVI	"	"

The samples PFH I to PFH V were cured at 128°C for 1 hour, 2 hours, 3 1/3 hours, $3\frac{3}{4}$ hours and 18 1/8 hours respectively. The other seven samples PFH VI to PFH XII were heated at 150°C for 4 hours and 38 minutes. The remaining four samples PFH XIII to PFH XVI were cured at 150°C for $\frac{1}{2}$ hour, 1 hour 2 hours and 3 hours respectively. After cooling them in a desiccator they were ground using an iron pestle and mortar and passed through a 100 mesh B.S. sieve.

3. Sulphur addition

Curing of phenolformaldehyde novolac resin with hexamethylenetetramine in the presence of sulphur.

Three samples, namely PFS, PFHS I and PFHS II were made according to the weight percentage compositions given in Table 2 below.

TABLE 2

Percentage compositions of sulphur containing phenolic resins.

Sample	Phenolformaldehyde resin %	Hexamethylene-tetramine %	Sulphur %
PFS	95·0	-	5·0
PFHS I	90·0	5·0	5·0
PFHS II	85·0	10·0	5·0

All these samples were heated for 5 1/6 hours at 150°C. They were cooled in a desiccator, powdered and sieved through 100 mesh B.S. sieve as usual.

4. Composite phenolics

Asbestos and inorganic additives.

Curing of phenolformaldehyde novolac resin with hexamethylenetetramine in the presence of asbestos and inorganic additives.

Sixteen samples of composite phenolic resin containing phenolformaldehyde, hexamethylenetetramine, asbestos and inorganic additives were prepared. The inorganic additives are glass fibre, $Al(OH)_3$ sodium metaborate, sodium phosphate, boric acid, lead chloride and silica.

They were mixed in a ball mill. The names and composition of the composite materials are shown below in Table 3.

TABLE 3

Percentage composition of the composite materials.

Sample	Novolac resin %	Hexamine %	Asbestos %	Inorganic Additives %
PFHA I	45•0	5•0	50•0	--
PFHA II	45•0	5•0	50•0	--
PFHGF	45•0	5•0	--	50•0
PFHAGF	45•0	5•0	25•0	25•0
PFH $Al(OH)_3$	75•0	8•33	--	16•67
PFHA $Al(OH)_3$	57•7	6•41	23•07	12•82
PFH Sm	75•0	8•33	--	16•67
PFHA Sm	56•25	6•25	25•0	12•5
PFH S	75•0	8•33	--	16•67
PFH ASP	56•25	6•25	25•0	12•5
PFH B	75•0	8•33	--	16•67
PFH AB	57•0	6•3	24•0	12•7
PFH LC	75•0	8•33	--	16•67
PFH ALC	56•25	6•25	25•0	12•5
PFH Si	75•0	8•33	--	16•67
PFH ASi	56•25	6•25	25•0	12•5

PFHA I and PFHA II were cured at 148°-154°C for 1 1/3 hours in a press-moulding machine under a pressure of 12 tons and 50 tons per square inch respectively. The remaining samples of the composite materials were heated at 148°- 154°C for 1 hour under a pressure of

12 tons per square inch, in a press moulding machine. They were cooled in a desiccator.

These samples were fairly hard to grind, so they were first cut down to a small size by an iron file. Then they were ground in an iron mortar and passed through a 60 mesh B.S. sieve.

5. Lewis acids addition

Hardening of phenolformaldehyde novolac resin with hexamethylenetetramine in the presence of Lewis acids.

In every case 85% of phenolformaldehyde novolac resin, 10% of hexamethylenetetramine, and 5% of Lewis acid - $AlCl_3 6H_2O$, $FeCl_3$(anhydrous) and $ZnCl_2$, were mixed together thoroughly. After heating them for 1 hour at 156°C , they were cooled in a desiccator. These samples were reduced in size, as usual, to be passed through a 52 mesh B.S. sieve. They were named PFH-$AlCl_3$, PFH-$FeCl_3$, and PFH $AlCl_3$.

6. Mineral oxides addition

Cross-linking of phenolic novolac resin with hexamethylenetetramine in presence of mineral oxides.

In each sample 85% of phenolformaldehyde novolac resin, 10% of hexamethylenetetramine and 5% of powdered oxide - HgO, MnO_2, Sb_2O_3, SiO_2 and ZnO were mixed together completely and treated as (5). These samples were named PFH-HgO, PFH-MnO_2, PFH-Sb_2O_3, PFH-SiO_2 and PFH-ZnO .

7. Metal addition

Hardening of phenolformaldehyde novolac resin with hexamethylenetetramine in the presence of powdered metals.

In each sample 85% of novolac resin, 10% of hexamethylenetetramine and 5% of powdered metal - Al, Cu, Mg, Pb and Zn were mixed together intimately and treated as (5). These samples were named PFH-Al, PFH-Cu, PFH-Mg, PFH-Pb and PFH-Zn.

8. Carbon addition

Curing of phenolformaldehyde resin with hexamethylenetetramine in the presence of carbons.

In each case 85% of phenolic resin, 10% of hexamethylenetetramine and 5% carbon-C(graphite), C_0 (carbon fibre, $\frac{1}{8}$"), C_1 (No.1), C_2 (No.2) C_3 (No.3), C_4 (No.4), C_5 (No.5), C_6 (No.6), C_7 (No.7) and C_8 (No.8) were mixed thoroughly. The samples were named PFH-C, PFH-C_0, PFH-C_1, PFH-C_2, PFH-C_3, PFH-C_4, PFH-C_5, PFH-C_6, PFH-C_7 and PFH-C_8. The sample PFH-C_9 contained 80% of resin, 10% of hexamethylenetetramine, and 10% of carbon C_8 (No.8). They were treated as (5).

9. Furfuryl alcohol and organic polymers addition

Curing of phenolformaldehyde novolac resin with hexamethylenetetramine in the presence of furfuryl alcohol and organic polymers.

In each case 85% of phenolic resin, 10% of hexamethylenetetramine and 5% of furfuryl alcohol, polyvinyl acetate, polyvinyl alcohol, polyacrylonitril polyvinyl chloride, polystyrene, nylon 66 (0·18" diameter bristles, $\frac{1}{8}$" size cellulose acetate cobutyrate and carboxy methyl cellulose were mixed thoroughly. All these samples were heated for 1 hour at 150°C. After cooling in a desiccator, they were powdered, as usual, and passed through a 52 mesh B.S. sieve. These samples were named PFH-Fur, PFH-PVAcet, PFH-PCAlC, PFH-PAcry, PFH-PVC, PFH-PSty, PFH-N66, PFH-C.Acet.Co. But and PFH-CMC.

10. Refrasil and TX fibre addition

Curing of phenolformaldehyde novolac with hexamethylenetetramine in the presence of Refrasil fibre and TX fibre.

In each sample 85% of phenolic resin, 10% of hexamethylenetetramine and 5% of Refrasil fibre (52 mesh B.S.) and TX fibre (52 mesh B.S.) were mixed completely and treated as (9). They were called PFH-Ref. and PFH-TX respectively.

11. Carbohydrates addition

Curing of Phenolformaldehyde novolac resin with hexamethylenetetramine in the presence of carbohydrates.

In each sample 85% phenolic resin, 10% of hexamethylenetetramine and 5% of carbohydrate - glucose, sucrose and starch were mixed completely and treated as (9). They were named PFH-Glu, PFH-Suc and PFH-Sta respectively.

12. Resole - DV19162

Curing of phenolformaldehyde resole resin with and without hexamethylenetetramine.

The names and percentage compositions of samples prepared from phenolformaldehyde resole resin and hexamethylenetetramine are shown in Table 4 below.

TABLE 4

Names and percentage composition of samples.

Sample	Phenolic resole %	Hexamethylenetetramine %
PFR	100·0	--
$PFRH_1$	99·0	1·0
$PFRH_2$	98·0	2·0
$PFRH_3$	97·0	3·0
$PFRH_4$	96·0	4·0
$PFRH_5$	95·0	5·0

These samples were heated for 1 hour at 150°C. After cooling, they were ground and passed through a 52 mesh B.S. sieve.

13. Novolacs RW52487 and RW54859

Cross-linking of phenolformaldehyde novolac resins - RW52487 and RW 54859, with hexamethylenetetramine

The novolac resins RW52487 and RW54859 were heated for 1 hour at 150°C. They remained highly viscous liquids at this temperature. On cooling, they solidified to a friable mass, which was ground and passed through a 52 mesh B.S. sieve.

Samples A_1, B_1, C_1 and D_1 were prepared from these resins and hexamethylenetetramine. The percentage compositions of these samples are given in table 5 below.

TABLE 5

Percentage compositions of samples A_1, B_1, C_1 and D_1.

Sample	RW52487 %	RW54859 %	Hexamethylenetetramine %
A_1	90•0	----	10•0
B_1	95•0	----	5•0
C_1	----	90•0	10•0
D_1	----	95•0	5•0

All these samples were treated as (9).

EXPERIMENTAL

Differential Thermal Analysis

EQUIPMENT: Du Pont 900 Thermoanalyser. (See Fig. 4a, 4b.)

CONDITIONS:

1. The equipment was calibrated occasionally with benzoic acid.
2. The corrected peak temperstures are given in Tables.
3. Correction for non-linearity of C/A thermocouple - tables provided with the instrument.
4. Pure samples without diluent were used.

EXPERIMENTAL CONDITION A

Standard cell	(500°C Cat.No. 900270)
Sensitivity	0·5°C per inch of ordinate
Temperature scale	50°C per inch of abscissa
Thermocouple	C/A Cat.No. 900329
Reference	Alumina
Sample Tube	2 mm diameter
Weight	4 - 6 mg.
Packing	Tight

EXPERIMENTAL CONDITION B

Intermediate cell	(1000°C Cat.No.900160)
Sample tube	4 mm diameter, with porcelain sleeves
Weight	18-24 mg.
Other variables	As Condition A.

SCHEDULE A

Effect of variations in analytical procedure

Table	Fig.	φ, °C/ min	Gas flow scfh	Atmosphere	Samples	Condition	Variable
6	6a 6b	30 50	1	N_2 flow	PFA, PFC, PFD, PFE, PFF	A	Linear rate of heating to 500°C
7	7a 7b 7c	20, 30, 40, 50, 60.	1	N_2 flow Air flow	PFB PFG	A	"
8	8a 8b 8c	10,20,30 40,50,60, 70,90,100,	1	Air flow	PFG	B	Linear rate of heating to 850°C (Loose packing)
9	9a 9b	30	1, 2, 3½, 4.	Air flow N_2 flow CO_2 flow O_2 flow	PFG	B	"
10	10a 10b	30	Vacuum 1",5",10", 15", 20", 25", 30".	Vacuum (Purged with N_2)	PFG	B	"
10a	-	-	-	-	-	-	List of mean peak temperatures.

Resin used novolac R19370 heat treated in air - not crosslinked.

SCHEDULE B

Effect of variations in the resin

Table	Fig.	φ, °C/ min.	Gas flow scf h	Atmosphere	Sample	Condition	Variables
11a	11a	30	2	N_2 flow	PFH I-V	B	17% hexamine 100 mesh B.S.
11b	11b	30	2	"	PFH XIII-XVI	B	10% hexamine 100 mesh B.S.
12	12a 12b	30	2	"	PFH VI-XII (except IX)	B	Different concentrations of hexamine Table I 100 mesh B.S.
13	13	10,20,30, 40,50.	2	"	PFH VIII	B	100 mesh B.S.
14	14a 14b	30	2	"	PFH IX	B	Different mesh sizes.
15	15	30	2	"	PFH I,II, IV,V.	B	Loose packing 100 mesh B.S.
16	16a 16b	30	2	"	Novolac A_1, B_1, C_1, D_1.		Composition Table 5 Novolac RW5248 and RW54859. 52 mesh B.S.
17	17	30	2	"	PFR, $PFRH_1$ $PFRH_2$, $PFRH_3$.	B	Composition Table 4 Resole DV19162 52 mesh B.S.

Resin used is generally novolac R19370. Heat treated or cross-linked in air.

SCHEDULE C

Effect of additives to the resin R19370.

Table	Fig.	ϕ, ^{o}C/min	Gas flow scf h	Atmosphere	Sample	Condition	Variables
18	18	30	2	N_2 flow	PFS, PFHS I, PFHS II.	B	Composition Table 2 100 mesh B.S.
19	19a 19b 19c	30	2	"	Asbestos, PFHA I, PFHA II, PFHB, PFHAB, PFHSm, PFHASm, PFHSP, PFHSAP, PFHGF, PFHAGF, PFHAl(OH)$_3$, PFHAAl(OH)$_3$.		Composition Table 3, 60 mesh B.S.

Resin used novolac R19370. Cross-linked in presence of additives in atmosphere of air.

RESULTS IN TABULAR FORM

Effect of variations in analytical procedure

The peak temperatures are taken as the points of intersection of the tangents drawn to both sides of the peaks.

TABLES, 6a and 6b

Peak Temperatures, °C.

	Table 6a			Table 6b			
Sample	A	B	C	A	B	C	H
PFA (100°)	57·0	91·0	159·0	59·0	-	148·0	419·0
PFC (146°)	57·0	-	155·0	61·0	94·0	177·0	417·0
PFD (166°)	57·0	-	155·0	61·0	99·0	159·0	419·0
PFE (178°)	57·0	-	155·0	61·0	-	164·0	420·0
PFF (204°)	62·0	-	152·0	64·0	110·0	169·0	419·0

Heating time 1½ hours.

Notes: 1. Heating temperatures are shown in parentheses.

2. 2 mm diameter tube, 100 mesh, N_2 flow.

3. Peak B is present only for PFA. Fig. 6a.

4. Peak B is missing for PFA and PFE. Fig. 6b.

5. All peaks are endothermic, Figs. 6a and 6b.

6. Fig. 6a, ϕ = 30°C/min. Fig. 6b, ϕ = 50°C/min.

7. These samples contained no hexamine.

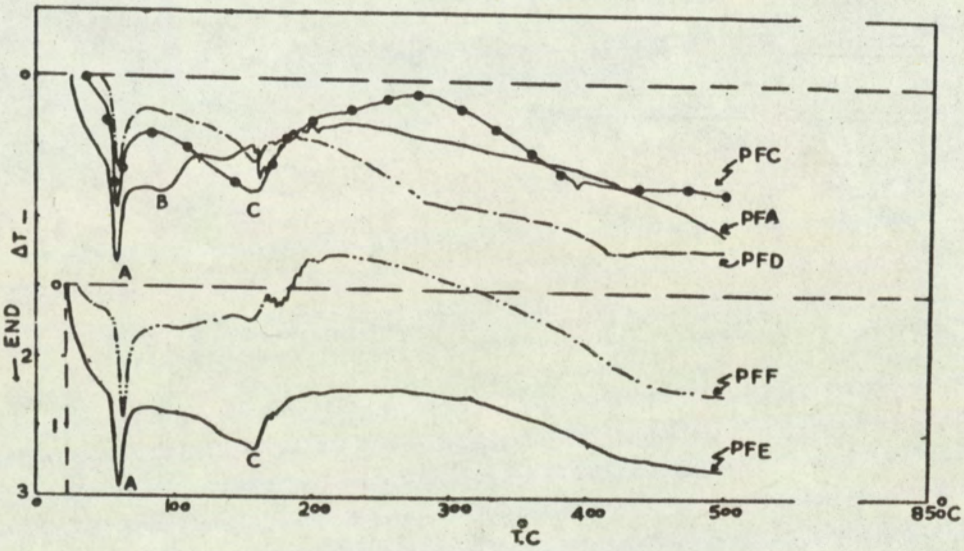

Fig.6a. DTA Thermograms of the phenolic novolac resin R19370 showing effects for curing temperature for 30°C/min

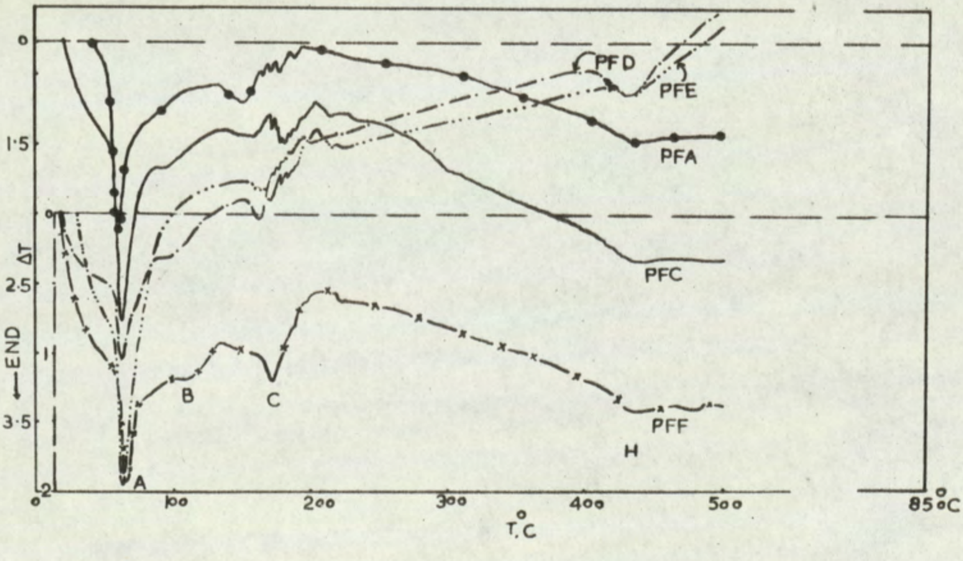

Fig.6b. DTA Thermograms of the phenolic novolac resin R19370 showing effects for curing temperature for 50°C/min

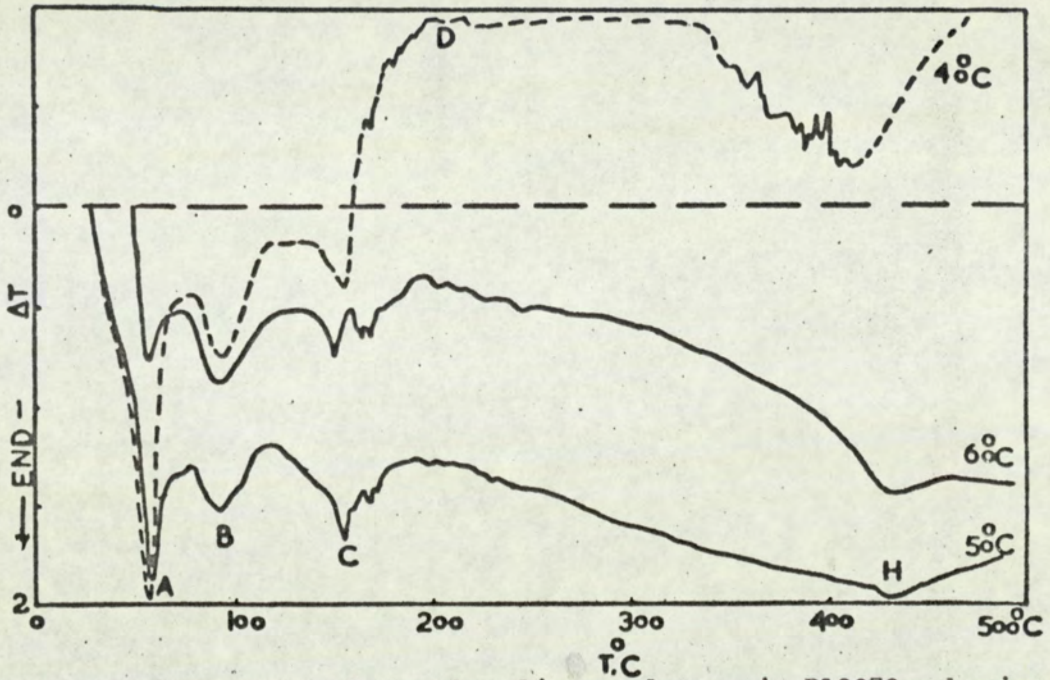

Fig.7a. DTA Thermograms of the phenolic novolac resin R19370, showing the effects of heating rates in N_2 atmosphere (Sample PFB)

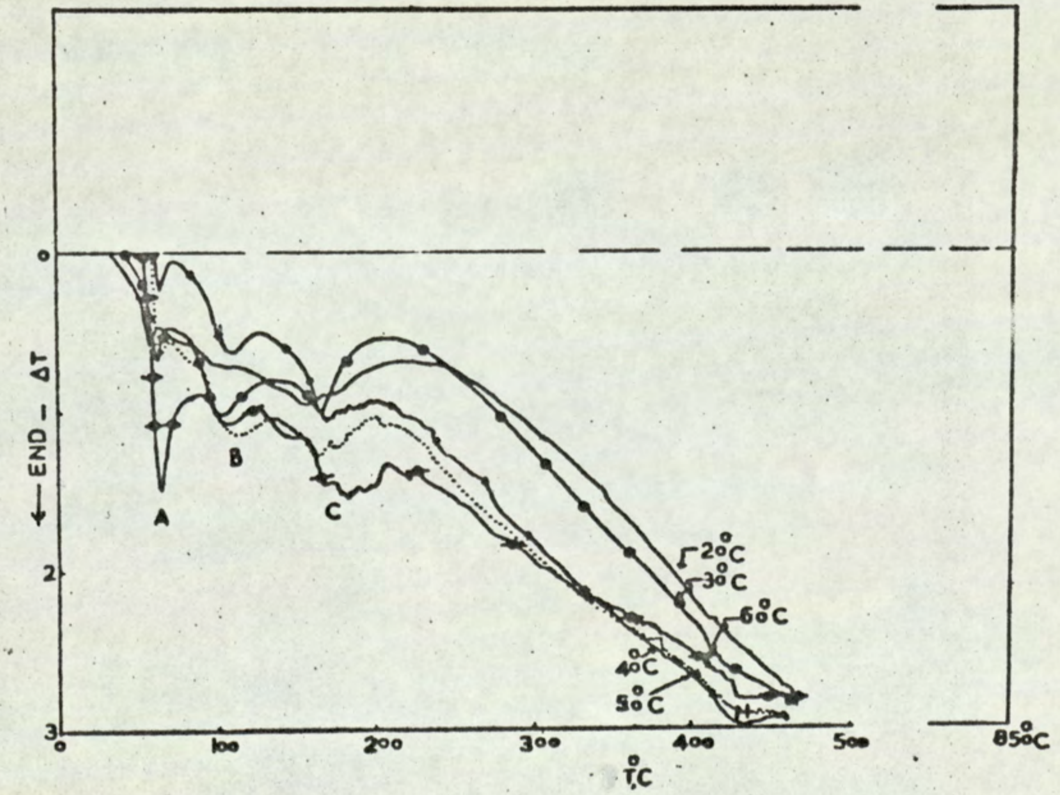

Fig.7b. DTA Thermograms of the phenolic novolac resin R19370, showing the effects of heating rates in air atmosphere (Sample PFG)

Table 7a

Peak temperatures, °C

ϕ, °C/min	A	B	C	D	H
40·0	56·0	91·0	152·0	173·0-334·0	402·0
50·0	57·0	91·0	152·0	-	419·0
60·0	57·0	92·0	151·0	-	419·0

Notes:

1. 2 mm diameter tube, 100 mesh, N_2 flow.
2. Peak D is a broad exothermic for sample PFB with heating rate 40°C/min only. Fig. 7a.
3. These samples contained no hexamine.

Tables 7b and 7c

Peak Temperatures, °C

	Table 7b				Table 7c			
ϕ, °C/min	A	B	C	H	A	B	C	H
20·0	57·0	95·0	157·0	–	–	–	–	–
30·0	60·0	98·0	162·0	–	60·0	102·0	159·0	418·0
40·0	61·0	102·0	163·0	416·0	60·0	104·0	164·0	414·0
50·0	62·0	102·0	160·0	416·0	61·0	100·0	157·0	416·0
60·0	62·0	103·0	163·0	417·0	61·0	109·0	157·0	416·0

Notes:

1. 2 mm diameter tube, 100 mesh.
2. Peak H missing for heating rates 20 and 30 C/min.
3. Air flow Table 7b. Fig. 7b.
4. N_2 flow Table 7c. Fig. 7c.
5. These samples contained no hexamine.

Table 8

Peak Temperatures, °C

ϕ, °C/min	A	B	C	D	E	F	H
10·0	56·0	98·0	154·5	184·5	320·0	370·0	405·0
20·0	57·0	104·5	158·0	186·0	323·0	375·0	419·0
30·0	61·5	114·0	161·5	197·0	328·0	380·0	426·0
40·0	61·0	109·0	162·0	214·5	-	362·0	430·0
50·0	64·0	105·0	169·0	232·0	338·0	368·0	430·0
60·0	64·0	109·0	158·0	214·0	335·0	370·0	429·0
70·0	64·0	122·0	159·5	187·0	325·0	392·0	440·0
90·0	69·0	122·0	171·0	224·0	331·0	382·0	443·0
100·0	69·0	109·0	167·0	225·0	335·0	388·0	443·0

Notes:

1. Air flow,
2. Seven main peaks selected - others inconsistent. Figs. 8a, 8b and 8c.
3. Peak D is exothermic.
4. Results are used to plot heating rates against peak temperature, Fig.8d.
5. Results are used to calculate activation energies, Fig.8e.
6. Peaks are very consistent.
7. These samples contained no hexamine.

Table 9

Peak Temperatures, °C

Gas	Flow scfh	A	B	C	D	E	H
Air	1	63·0	105·0	171·0	206·0	299·0	415·0
"	2	64·0	107·0	173·0	212·0	301·0	414·0
"	$3\frac{1}{2}$	63·0	105·0	174·0	206·0	300·0	415·0
"	4	62·0	113·0	165·0	204·0	303·0	414·0
N_2	1	59·0	102·0	155·0	187·0	-	421·0
CO_2	1	57·0	100·0	144·0	167·0-368·0	-	414·0
O_2	1	61·0	109·0	161·0	206·0	288·0	422·0

Notes:

1. Peaks are very complex. Figs. 9a and 9b.
2. Six main peaks A, B, C, D, E and H are selected.
3. Peak D is exothermic.
4. Peak E is absent in N_2 and CO_2 atmospheres, Fig. 9b.
5. Broad Peak D (of Table 7a) is present in CO_2 atmosphere.
6. These samples contained no hexamine.

Table 10

Peak Temperatures, °C

Vacuum (inches)	A	B	C	D	E	F	H
1·0	69·0	125·0	-	147·0	338·0	398·0	423·0
5·0	64·0	105·0	-	155·0	353·0	400·0	423·0
10·0	67·0	127·0	-	162·0	353·0	400·0	438·0
15·0	64·0	105·0	-	182·0	329·0	393·0	417·0
20·0	62·0	107·0	142·0	177·0	331·0	391·0	421·0
25·0	63·0	109·0	155·0	187·0	326·0	391·0	447·0
30·0	65·0	109·0	151·0	217·0	339·0	393·0	427·0

Notes:

1. Peak distribution is complex especially in range 220-450°C Figs. 10a and 10b.
2. Seven main peaks are selected, A, B, C, D, E, F and H.
3. Peak D is exothermic.
4. Peak C is missing at 1", 5", 10" and 15".
5. These samples contained no hexamine.

DISCUSSION

Table 10a

List of mean peak temperatures from Tables 6-10 of DTA

Peak	Mean Temperature, °C 2 mm dia. tube	Temperature °C	Mean Temperature, °C 4 mm dia. tube	Temperature range, °C	Exothermic/ Endothermic
A	59·1	56·0-64·0	62·6	56·0-69·0	Endo
B	97·4	91·0-110·0	108·5	98·0-127·0	"
C	158·0	148·0-177·0	159·7	142·0-174·0	"
D	-	173·0-334·0	196·2	147·0-232·0	Exo
E	-	-	315·3	288·0-339·0	Endo
F	-	-	385·7	362·0-400·0	"
H	41 ·0	402·0-420·0	422·5	405·0-443·0	"

Table 11a

Peak temperatures, °C

Sample	B	C	D	L (doublet)
PFH I (1)	145·0	-	-	530·0, 532·0
PFH II (2)	157·0	-	285·0	530·0, 532·0
PFH III (3)	164·0	-	280·0	530·0, 532·0
PFH IV (4)	165·0	211·0	287·0	530·0, 532·0
PFH V $(18\frac{1}{2})$	171·0	-	272·0	530·0, 532·0

Notes:

1. Effect of curing time.
2. Curing time in hours is given in parentheses.
3. Peak C is shown by sample PFH IV.
4. Peak D is exothermic. Fig. 11a.
5. Peak D is missing for sample PFH I.
6. Peaks B and D are quite consistent.
7. Peak L is very consistent doublet.
8. Curing temperature 128°C, 100 mesh, N_2 flow.
9. **From here all samples contained no hexamine.**

Table 11b

Peak Temperatures, °C

Sample		B	C	D	L
PFH XIII	($\frac{1}{2}$)	152·0	-	236·0	532·0
PFH XIV	(1)	164·0	-	236·0	532·0
PFH XV	(2)	150·0	189·0	241·0	532·0
PFH XVI	(3)	155·0	197·0	248·0	532·0

Notes:

1. Effect of curing time.
2. Curing time in hours is given in parentheses.
3. Peak C is missing for samples PFH XIII and XIV.
4. Three peaks B, D and L are very consistent.
5. Peak D is exothermic. Fig. 11b.
6. Curing temperature 150°C, 100 mesh, N_2 flow.

Table 12

Peak temperatures, °C

Sample	B	C	J	D	H	L (doublet)
PFH VI	-	202·0	-	278·0	-	530·0, 532·0
PFH VII	125·0	180·0	-	225·0	414·0	530·0, 532·0
PFH VIII	-	197·0	-	236·0	-	530·0, 532·0
PFH X	139·0	195·0	271·0	300·0	-	- 532·0
PFH XI	-	198·0	274·0	310·0	-	530·0, 532·0
PFH XII	137·0	200·0	278·0	316·0	-	530·0, 532·0

Notes:

1. Effect of hexamine concentration, Table 1 .
2. Cured at 150°C for 4½ hours.
3. Peak B is missing for samples PFH VI, VIII and XI.
4. Peak J is shown by samples PFH X, XI and XII.
5. Peak H is shown by sample PFH VII.
6. Single peak L is shown by sample PFH X.
7. Peak D is exothermic. Figs. 12a and 12b.
8. N_2 flow, 100 mesh.

Table 12

Peak temperatures, °C

Sample	B	C	J	D	H	L (doublet)
PFH VI	-	202·0	-	278·0	-	530·0, 532·0
PFH VII	125·0	180·0	-	225·0	414·0	530·0, 532·0
PFH VIII	-	197·0	-	236·0	-	530·0, 532·0
PFH X	139·0	195·0	271·0	300·0	-	- 532·0
PFH XI	-	198·0	274·0	310·0	-	530·0, 532·0
PFH XII	137·0	200·0	278·0	316·0	-	530·0, 532·0

Notes:

1. Effect of hexamine concentration, Table 1.
2. Cured at 150°C for 4½ hours.
3. Peak B is missing for samples PFH VI, VIII and XI.
4. Peak J is shown by samples PFH X, XI and XII.
5. Peak H is shown by sample PFH VII.
6. Single peak L is shown by sample PFH X.
7. Peak D is exothermic. Figs. 12a and 12b.
8. N_2 flow, 100 mesh.

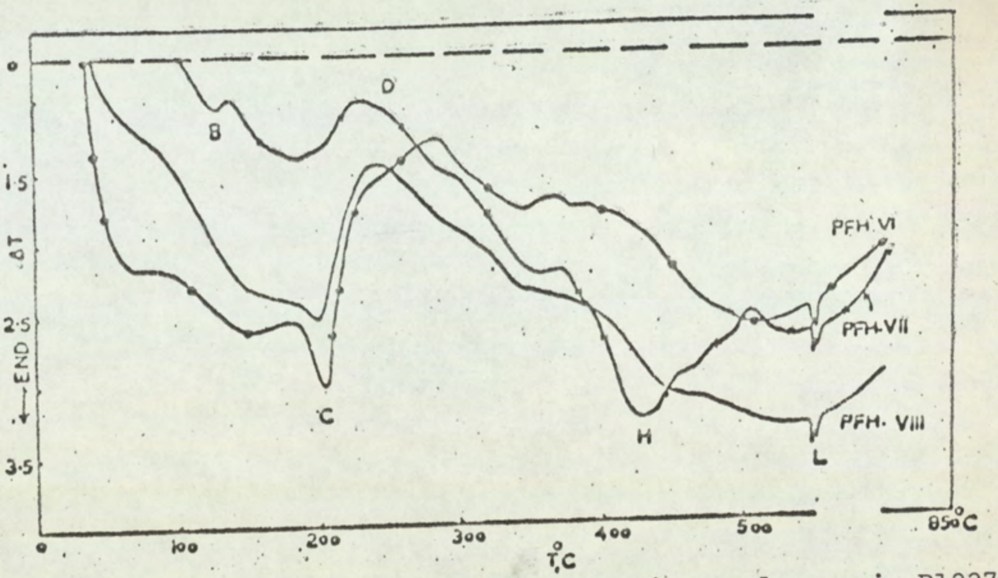

Fig.12a. DTA thermograms of the phenolic novolac resin R19370
Effect of hexamine concentration

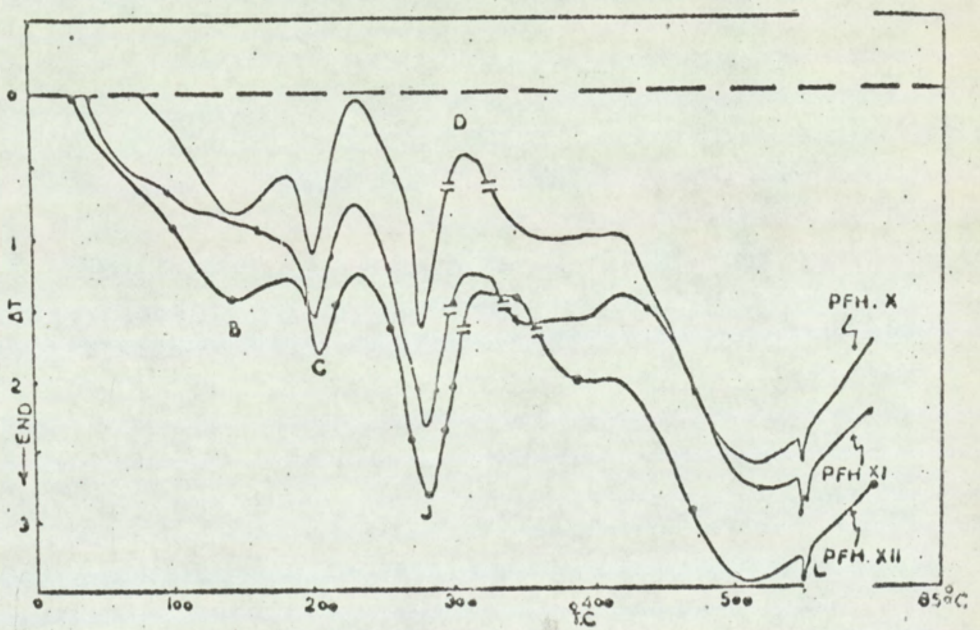

Fig.12b. DTA thermograms of the phenolic novolac resin R19370.
Effect of hexamine concentration.

Table 13

Peak temperatures, °C

ϕ, °C/min	C valley	D	L valley
10	147·0 - 197·0	-	-
20	147·0 - 197·0	-	419·0 - 522·0
30	147·0 - 197·0	236·0	429·0 - 532·0
40	150·0 - 197·0	251·0	443·0 - 532·0
50	161·0 - 197·0	254·0	446·0

Notes:

1. Effect of heating rates. Fig.13.
2. Sample PFH VIII, 100 mesh, N_2 flow.
3. Peaks C and L are broad endothermic.
4. Peak D is exothermic.
5. Broad endothermic L is missing for heating rate 10°C/min.

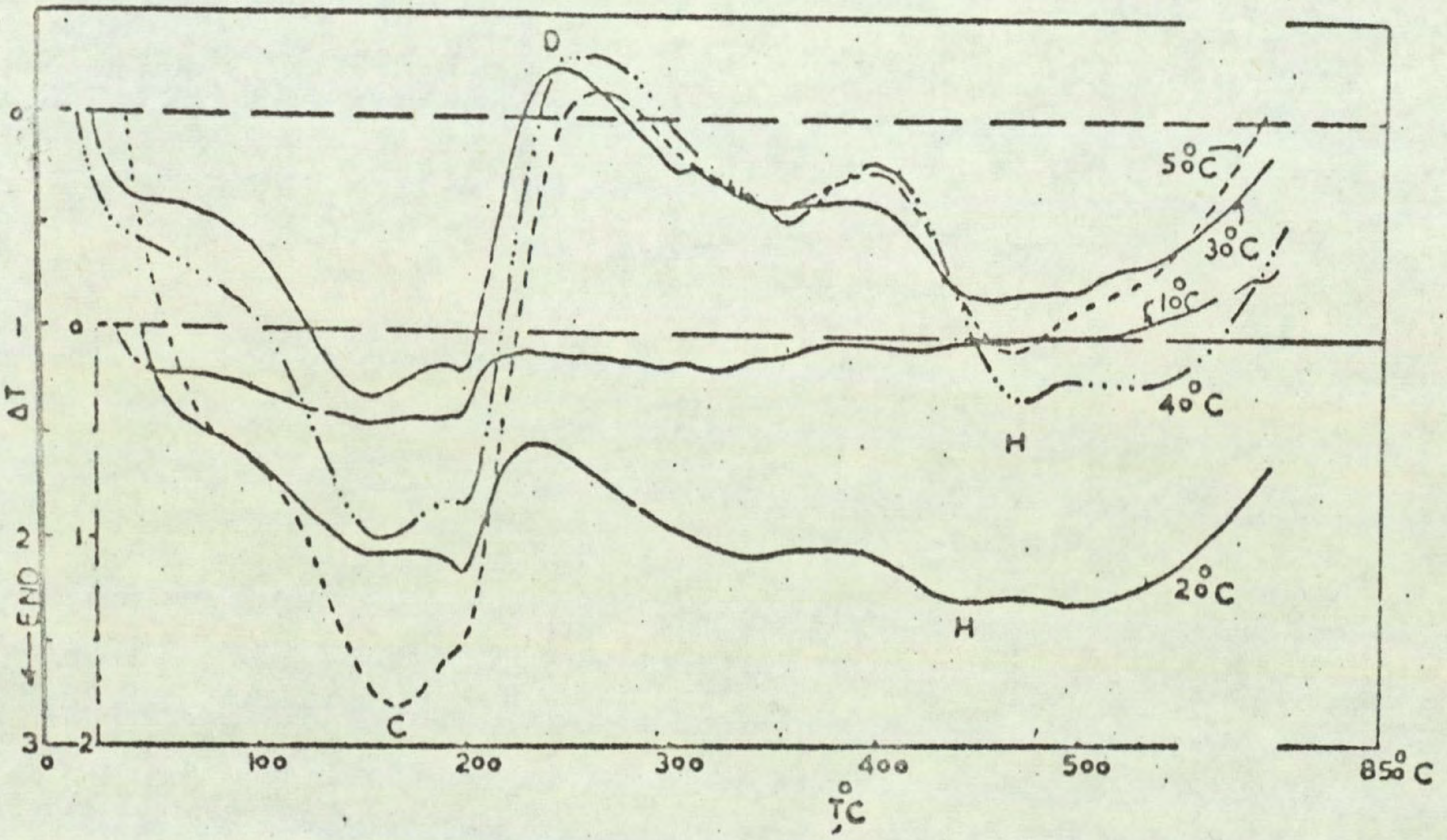

Fig.13. DTA curves of the phenolic resin sample PFH VIII. Effect of heating rates.

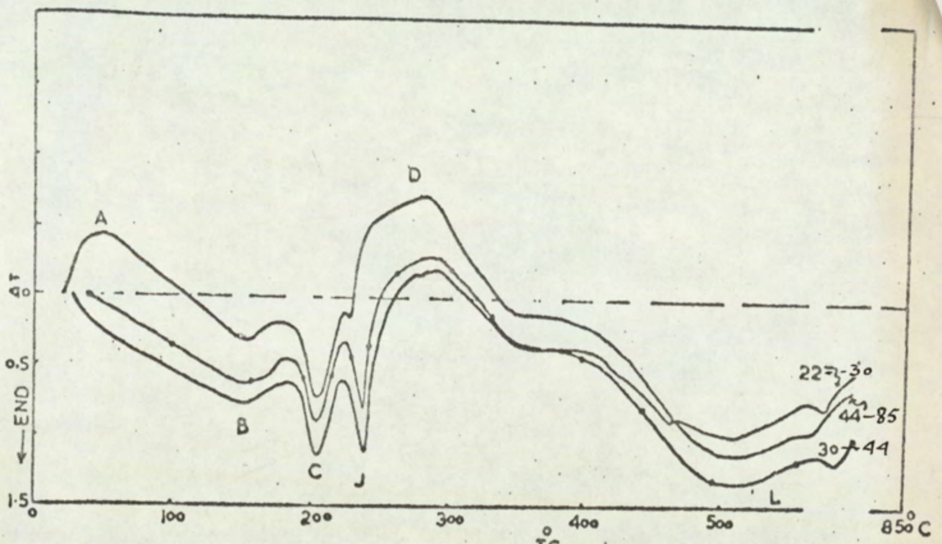

Fig.14a. DTA Thermograms of the phenolic resin sample PFH IX
Effect of grain size.

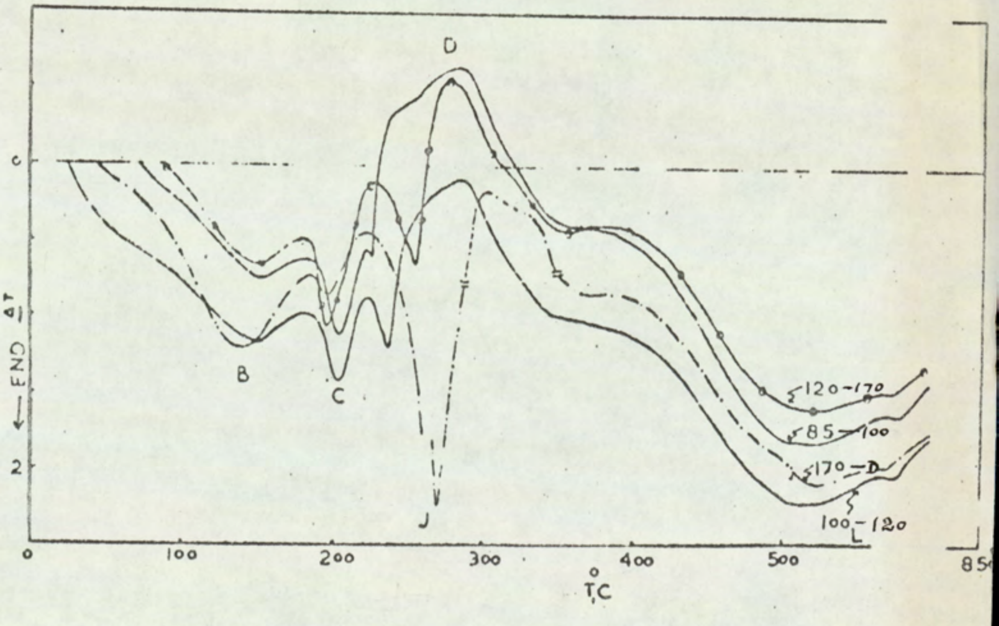

Fig.14b. DTA Thermograms of the phenolic resin sample PFH I
Effect of grain size.

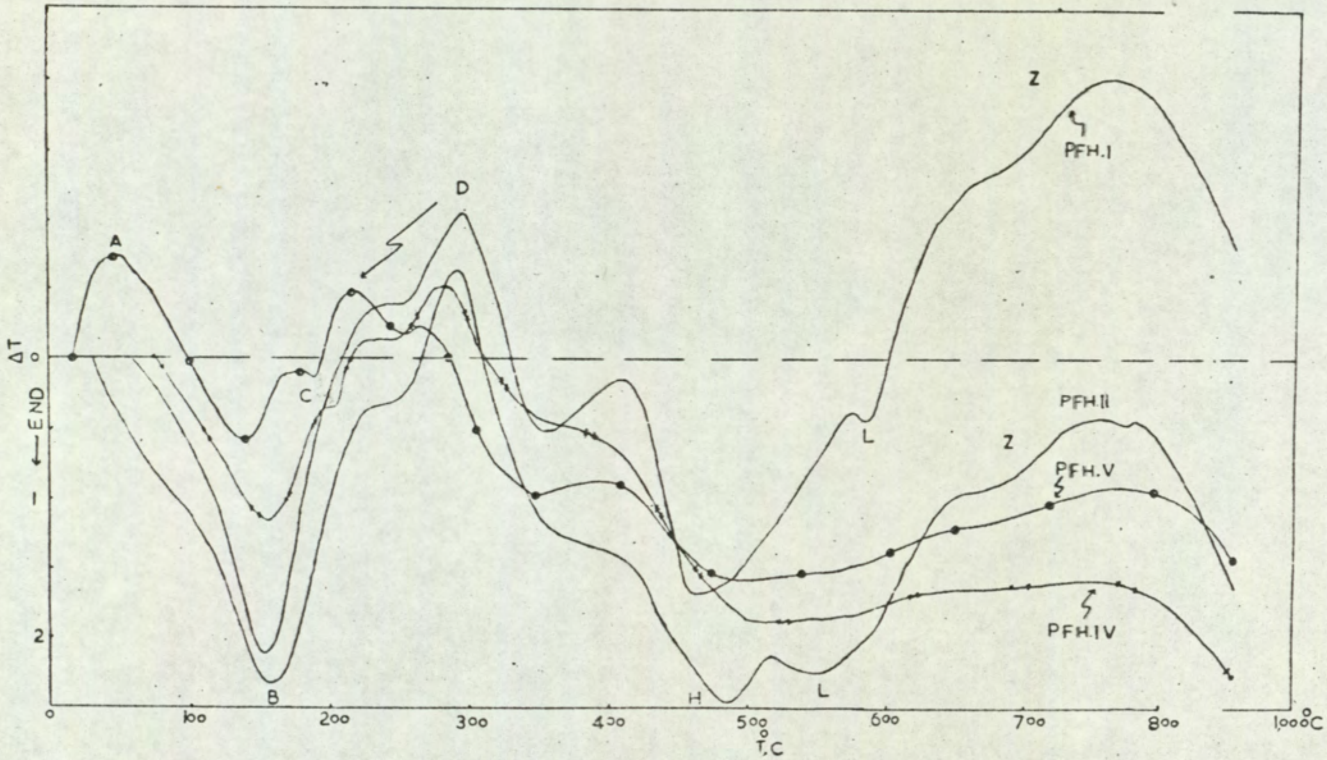

Fig.15. DTA Thermograms of the phenolic resin
Effect of loose packing

Table 14

Peak temperatures, °C

Grist (mesh B.S.)	A	B	C	J	D	L valley
22-30	-	147·0	202·0	234·0	273·0	494·0 - 555·0
30-44	-	147·0	200·0	229·0	271·0	485·0 - 558·0
44-85	43·0	149·0	201·0	224·0	266·0	485·0 - 551·0
85-100	-	147·0	200·0	221·0	256·0	485·0 - 558·0
100-120	-	147·0	200·0	232·0	271·0	485·0 - 557·0
120-170	-	147·0	187·0	249·0	271·0	485·0 - 555·0
170-dust	-	134·0	186·0	265·0	282·0	504·0 - 551·0

Notes:

1. Effect of particle size.
2. Sample PFH IX, N_2 flow.
3. Exothermic peak A is shown only by particle size 44-85 B.S.
4. Five peaks B, C, J, D and L are very consistent. Figs. 14a and 14b.
5. Peak D is exothermic.

Table 15

Peak temperatures, °C

Sample	A	B	C	D	H	L	Z
PFH I	-	152·0	-	291·0	443·0	566·0	607·0 - 759·0
PFH II	-	152·0	-	286·0	470·0	532·0	616·0 - 759·0
PFH IV	-	152·0	202·0	278·5	-	-	-
PFH V	43·0	135·0	185·0	210·0	-	-	-

Notes:

1. Effect of loose packing.
2. 100 mesh, N_2 flow.
3. Exothermic peak A (of Table 14) is shown only by sample PFH V.
4. Two peaks B and D are very consistent. Fig.15.
5. Peaks D and Z are exothermic.
6. Peak C is missing for samples PFH I and II.
7. Peaks H, L and Z are missing for samples PFH IV and V.

Table 16

Peak temperatures, °C

Sample	A	B	B'	C	D	F
RW52487	76·0	129·0	–	182·0	217·0	381·0
A_1(10)	40·0	–	–	180·0	–	383·0
B_1(5)	66·0	–	–	157·0	–	381·0
RW54859	42·0	93·0	–	162·0	187·0	376·0
C_1(10)	61·0	120·0	148·0	–	–	400·0
D_1(5)	59·0	–	152·0	–	–	381·0

Notes: 1. Effect of hexamine concentration. Concentration of hexamine is given is parentheses.

2. 52 mesh, N_2 flow.

3 Peak A and F are very consistent for all samples. Figs.16a and 16b.

4. Peaks B' and D are exothermic.

5. Peak B is missing for samples A_1, B_1 and D_1.

6. Exothermic peak B' is shown by samples C_1 and D_1 and endothermic peak C is missing for them.

7. Exothermic peak D is shown by novolac RW52487 and RW54859.

Table 17

Peak temperatures, °C

Samples	A	B	C	D	H	Z
PFR	54·0	129·0	251·0	-	391·0	593·0 - 759·0
$PFRH_1$	40·0	127·0	-	236·0	391·0	612·0 - 773·0
$PFRH_2$	30·0	117·0	-	251·0	419·0	612·0 - 771·0
$PFRH_3$	28·0	117·0	-	251·0	414·0	612·0 - 776·0

Notes:

1. Effect of hexamine. Table 4.
2. 52 mesh, N_2 flow.
3. Five peaks are very consistent for all samples, except peak D is missing for PFR. Fig.17.
4. Peaks D and Z are exothermic.
5. Peak C is present only for sample PFR.

<u>Table 17a</u>

Resins used	Ref.	Peak Temperatures, °C								
	108	60-70	-	-	-	168-180	-	-	-	-
	48	60	125	-	-	185	-	-	-	-
		70	125	150 Exo	-	180	-	-	-	-
Novolac alone (A)	51	60	120	150 Exo	-	170	330	-	-	>500 Exo)
" (B)	"	60	110 Exo	140	-	-	200-295	-	460	>500 Exo)
Novolac + 10% hexa (B)	"	60	-	140	155 Exo	-	175-385	-	435	>500 Exo
Resole (C)	"	55	120 Exo	140	-	-	285	-	>425 Exo	-
Novolac	50	70	130	-	-	-	-	-	-	-
Novolac + hexa	"	80	-	150 Exo	-	-	-	-	-	-
Cured phenolic	107	52 Exo	-	-	-	175	220	265	440	580-670 Exo
Novolac alone (A)	〃	41,62	-	-	190 Exo	-	-	-	-	-
Novolac + hexamine (A)	55	20-100	-	-	100-180	-	180-230 Exo	-	250-400	
(D)	60	-	-	-	156 Exo	-	-	-	-	-
(D)	"	-	-	148 Exo	156 Exo 164 Exo	-	210 Exo 234 Exo	-	-	-
Cured resole (E)	49	-	-	135-150 Exo	-	-	-	-	-	-

Table 17a (contd)

Resins used	Ref	Peak Temperatures, °C								
Uncured resole (E)	Table 8	-	110	-	-	-	-	-	-	-
Uncured novolac (air) (C)	Table 9	61.5	114	-	161.5	197 Exo	-	328	380	426
Uncured Novolac (N_2) (C)	"	59	102	-	155	187 Exo	-	-	-	421
Uncured novolac (CO_2) (C)	Table 9	57	100	144	-	-	167-368 Exo	-	-	414
Cured novolac (N_2) (C)	Table 11a	-	-	-	157 157	- -	285 Exo	-	-	530, 532
Cured novolac (N_2) (C)	Table 11b	-	-	150	-	189	241 Exo	-	-	530
Cured novolac (N_2) (C)	Table 16	40	-	-	-	180	-	-	383	-
Cured resole (N_2) (C)	Table 17	54	129	-	-	-	257	-	391	593-761

Exothermic peaks are indicated by Exo. The other peaks are endothermic.

(A) = 10°C/min, (B) = 20°C/min, (C) = 30°C/min, (D) = 5°C/min,

(E) = 5·6°C/min, (A_1) = 100°C/min.

Table 18

Peak temperatures, °C

Sample	A	B	C	D	E_1	E	L
PFS	66•0	170•0	203•0	227•0	266•0	280•0	541•0
PFHS I	-	-	192•0	-	263•0	-	535•0
PFHS II	-	-	198•0	-	256•0	-	534•0

Notes:

1. Effect of sulphur. Table 2.
2. 100 mesh, N_2 flow.
3. Seven peaks are shown by sample PFS. Fig. 18.
4. Three peaks C, E_1 and L are very consistent for all samples and other four peaks A, B, D and E are absent from PFHS I and PFHS II
5. Peak D is exothermic.

Table 19

Peak temperatures, °C

Sample	A	B	C	D	E	H	Z	S	O
Asbestos	-	122·0	-	-	-	-	-	714·0	821·0
PFHA I	50·0	129·0	-	271·0	-	443·0	-	696·0	820·0
PFHA II	50·0	132·0	-	270·0	-	452·0	-	696·0	820·0
PFHB	35·0	142·0	-	-	328·	-	643·0– 745·0	-	-
PFHAB	35·0	135·0	-	-	-	-	-	694·0	820·0
PFHSm	40·0	162·0	243·0	-	-	-	602·0– 770·0	-	-
PFHASm	33·0	132·0	-	-	-	-	697·0– 769·0	-	-
PFHSP	42·0	142·0	222·0	-	-	-	612·0– 780·0	-	-
PFHASP	45·0	131·0	215·0	-	-	-	-	685·0	817·0
PFHGF	38·0	131·0	-	252·0	-	-	616·0– 788·0	-	-
PFHAGF	48·0	129·0	-	252·0	-	-	-	690·0	829·0
PFHAl(OH)$_3$	42·0	139.0	219·0	251·0 °C	329·0	-	597.0– 745·0	-	-
PFHAAl(OH)$_3$	33.0	127·0	-	-	327·0	-	-	687·0	831·0

Table 19 (contd)

Notes:

1. Effect of additives, Table 3.
2. 60 mesh, N_2 flow.
3. Endothermic peaks B and S, and exothermic peak 0 are shown by asbestos.
4. Endothermic peaks A and B are very consistent for all samples. Figs. 19a, 19b, and 19c.
5. Peak C is present for samples PFHSm, PFHSP, PFHASP and PFHAl(OH)$_3$.
6. Exothermic peak D is present for samples PFHA I, II, PFHGF and PFHAGF.
7. Endothermic peak C' (instead of exothermic peak D) is shown by sample PFHAl(OH)$_3$.
8. Endothermic peak E is shown by samples PFHB, PFHAl(OH)$_3$ and PFHAAl(OH)$_3$.
9. Endothermic peak H is shown by samplees PFHA I and II.
10. Broad exothermic peak Z is shown by PFHB, PFHSm, PFHASm, PFHSP, PFHGF and PFHAl(OH)$_3$.
11. Endothermic peak S is shown by samples PFHA I and II, PFHAB, PFHASP, PFHAGF and PFHAAl(OH)$_3$.
12. Exothermic peak 0 is shown by samples PFHA I, II, PFHAB, PFHASP, PFHAGF and PFHAAl(OH)$_3$.

DISCUSSION

The Table 10a summarises the number of peaks, mean peak temperatures, temperature range and the nature of the peaks, obtained with 2 mm and 4 mm diameter tubes. The difference in the patterns of the thermograms (Figs.6a-8c) indicates that the thermal behaviour of the uncured resin is partly influenced by the variations in the analytical procedure and is partly characteristic of the resin. In the case of 2mm diameter tube no signal is shown for the changes, in the resin, in the region of 200-400°C, but three signals in that range are given by the 4mm diameter sample tube. The exothermic peak D is shown in one case for the 2mm diameter tube (173·0-334·0°C, Fig. 7a). The endothermic peaks A, B, C and H are seen to be independent of the variation in the analytical procedure. It is chemical and physical changes in the sample, probably resulting in variation of the mass/energy transfer in the range of 200·0-400·0°C, that balance the exothermic and endothermic heat changes involved (in 2mm diameter tube) and suppress the appearance of peaks D, E and F.

It is seen from the Table 10a that the peaks in 4mm diameter tube occur at slightly higher temperatures than the corresponding peaks in the 2mm diameter tube. The difference in the peak temperatures may be explained as follows :-

(a) The differential thermocouple placed in th 4mm diameter tube is covered by a porcelain tube (to keep it vertical and in the centre of the tube) which restricts the diffusion of the gaseous products. Thus the pressure of the gases is increased and the subsequent reactions occur at higher temperatures.

(b) The quantity of the resin may affect the heat transfer to the thermocouple.

(c) The physical and chemical reactions change the structure of the resin and so results in a change in thermal diffusivity.

Effect of heating rates

It is seen in Table 8 that the peaks mainly shift to higher temperatures as the heating rate is increased from 10° to 100°C/min. The peak temperature increases as the heating rate is increased in agreement with the current views[73] but in opposition to those of Nakamura[48]. The shifts in the peaks with temperatures are quite normal and can be explained by:

(a) high heat flux with increased temperature, and

(b) the van't Hoff expression

$$\frac{d\ln P}{dT} = \frac{\Delta H}{RT^2} \tag{28}$$

The higher the heating rate, the less gas will diffuse out before reaction becomes very rapid. The fact that the initially released gas does not have time to diffuse out means that the concentration of the gas can increase to some particular level with less total decomposition. Thus the gases that are given off tend to inhibit further decomposition resulting in higher peak (decomposition) temperature. This statement is substantiated by a plot of heating rates, °C/min. versus T_m °K, Fig. 8d. In the thermoanalytical study of kaolinite Kissinger* examined the effect

---

* through Garn[73]

of heating rate on peak temperature and found variations of 100°C.

Effects of analytical variables

(a) Heating rates (Table 8)

(b) N_2 flow and different gases (Table 9)

(c) Vacuum (Table 10)

The effect of heating rate on peak shift has been discussed earlier. Here it will be dealt with vis-a-vis effects of (b) and (c) on the peaks. The average peak temperatures obtained under above conditions are shown in Table 10b.

Table 10b

Average peak Temperatures, °C

Variable	A	B	C	D	E	F	H
ϕ	62•8	110•0	162•2	207•0	329•0	376•3	429•4
N_2 flow and other gases	61•3	106•0	163•3	203•5	298•2	-	416•4
Vacuum	64•8	112•4	149•3	175•3	338•1	395•1	428•0

It is apparent from the Table 10b that the peaks are highly consistent and the peak temperatures are reasonably in agreement except that peak F is missing in the presence of N_2 and other gases. The corresponding thermograms in Figs. 8a, 8b and 8c, 9a and 9b and 10a and 10b follow the same general pattern during the resin transformations and appear to be independent of the analytical variables listed above. This characteristic feature of the DTA curves could be explained as follows:-

1. All the samples (PFA-PFG) of the phenolic resin (R 19370) form oligomers in the same range of molecular weight distribution, irrespective of the heating temperature. The phenolic oligomers may consist of mainly linear and possibly some branched or slightly cross-linked molecules.

2. On heating the resin under conditions (a) and (b) the volatile products of degradation start coming out of the decomposition zone and the dynamic gases (air, N_2 and CO_2) have no access to the sample.

3. The sample tube is sealed from these gases.

4. The effect of the vacuum is contrary to expectations, i.e. the decrease in peak temperatures is not proportional to the vacuum. The transformation temperatures seem to be least affected by vacuum and surprisingly they are consistent. This odd behaviour resulted due to early sealing of the sample tube with carbonised resin.

Thus in each case it appears that the resin decomposed in the self-generated atmosphere and showed consistent peaks.

Drift of base line

It is seen from DTA thermograms that the base line drifts continuously. This makes it difficult, sometimes, to decide whether the reaction is exothermic or endothermic. This is seen to be the inherent limitation of the DTA measurements. Under steady heating conditions with no reaction, the observed temperature difference depends both on the heating rate and on the thermal diffusivity, d, of the material. (d = ratio of thermal conductivity, λ, to the product of specific heat, Cp, and the density, ρ). Arens* derived an expression for the steady state temperature differences,

$$\Delta T = \frac{1}{4} \frac{dT}{dt} r \left(\frac{1}{d'} - \frac{1}{d}\right) \qquad (29)$$

where dT/dt = heating rate,

r = radius of the cavity,

d' = thermal diffusivity of the sample,

and d = thermal diffusivity of the reference.

The underlying problem in achieving a low ΔT and hence a nearly zero base line is that of matching the thermal diffusivity of the reference (or inert) material to that of the specimen. The problem in achieving also a base line drift is that of matching the thermal diffusivity of the specimen to that of the inert material at all temperatures in the range studied. It is clear from the equation (29) for the steady-state temperature difference, that the difference is a direct function of the heating rate, i.e. at higher heating rates the drift will be larger. With a single reference material, this matching is obviously not possible for more than a few fortuitously chosen specimens. Some base line deviation and indeed some drift is to be expected unless a special effort has been made to match the reference to the specimen. (In the absence of such precautions, a base line of nearly zero and which does not drift is prima-facie evidence of a low-sensitivity apparatus).

It is for this reason that a base line is not the same before and after the reaction. Even in crystalline rearrangements, but especially in decomposition reactions, the thermal conductivity and the specific heat of the product will differ from its initial form; in decompositions also the density must change.

---

* through Garn[73]

Effect of variation in the resin pyrolysis conditions

1. Effect of curing with hexamine

The results of the study of the effects of phenolic resin variations on pyrolysis are shown in the Tables 11a-19 and Figs. 11a-19c.

It is seen in the Tables 11a-15 that the resin (R 19370) cured with hexamine does not show peak A (softening point) under various conditions of investigation, thus indicating cross-linking of the resin into a three dimensional structure. The endothermic peak C is missing in the Tables 11a and 11b except for three cases. The endothermic peak H around 422°C is also suppressed in all cases except the samples PFH VIII, Table 12, PFH I and II, Table 15. Some new peaks, e.g. J, L and Z are shown. An exothermic peak A at 43°c appears in two cases, Tables 14 and 15. All other peaks are shifted to higher temperatures.

2. Effect of curing time and temperatures (Table 11a and 11b)

The average peak temperatures of the resin cured with 17% and 10% hexamine for different times are given in Table 11c.

Table 11c

Average peak temperatures, °C

Hexamine concentration	Curing Temperature °C	B	C	D	L (doublet)
17%	128·0	160·4	211·0	281·0	530·0, 532·0
10%	150·0	155·2	193·0	240·0	532·0

The peaks B, C and D, which are mainly due to post-curing, are seen to be at higher temperatures for 17% hexamine content. This shift to higher temperature is undoubtedly caused by further cross-linking of the resin. The general forms of the thermograms are the same and no other significant changes occurred in the DTA curves as a result of wide changes in the time and temperature of cure. Similar results are reported by Heron[33] during derivative thermogravimetric (D.T.G.) study of phenolic resin.

3. Effect of hexamine concentration (Table 12)

There are three main effects of hexamine concentration on pyrolysis of the resin. First, a very strong new endothermic peak J appears for hexamine content of 30%, 40% and 50% at 271·0°, 274·0° and 278·0°C. This endotherm is due to melting, sublimation and dissociation of hexamine. Some pockets of hexamine powder were seen with the naked eyes before grinding the resin. Burns and Orrell[55] have also shown that the hexamine is not soluble in the melt, which leads to the formation of heterogeneously cured resin. They claim to have observed microscopically this type of heterogeneous cure, and extracted unreacted hexamine crystals from closed pores in the samples which were cured for 24 hours at 170°C,

4. Effect of heating rates

On degradation of the resin sample PFH VIII at heating rates 10°, 20°, 30°, 40° and 50°C/min in the flowing N_2 atmosphere two endothermic valleys (overlapping of reactions) C and L, and an exothermic peak D (for 30°, 40° and 50°C/min) are prominent at 147·0 - 197·0°, 419·0 - 532·0° and 236·0 - 254·0°C respectively, Fig. 13, Table 13. At the last three heating rates the peaks become more pronounced, as expected, since more energy changes are involved. The pattern of the thermograms is unchanged. The first valley is caused by overlapping of the post-curing and oxidation reactions and the second valley is mainly due to degradation, oxidation, depolymerisation and carbonisation. The exothermic peak D may be due to new bond-making either in post-curing or oxidation.

5. Effect of varying grist on degradation

Seven samples of resin (PFH IX) of different particle size range were compared. The DTA spectra are shown in Figs.14a and 14b. There is no variation in the general shape of the thermograms except that an exothermic peak A at 43°C, for grist 44-85 B.S., and a very sharp endotherm J, for grist 170-dust, are shown. Here J, too, is a new peak in the range of 221·0 -265·0°C. Peak J is produced by melting, sublimation and dissociation of the excess hexamine (PFH IX contained 24% hexamine) and the peak L shifts to the higher range 485·0 -558·0°C

As the grain size decreases the surface area increases and the sample can be more closely packed, leading to enhanced thermal conductivity. Smith* relates the heat conductivity of a powder to the volume fractions of air and solid. He shows,

$$\lambda = \lambda_1 V_1 + \lambda_2 V_2 \tag{30}$$

where λ = heat conductivity,

V = volume fraction.

1 and 2 stand for air and powdered substance.

---

* through Garn[73]

For ordinary purposes the contribution of air can be neglected (the packing must be carefully controlled as a part of any effort to obtain a zero base line). The peaks should appear at lower temperatures, which is seen to hold for peaks B and C for particle size 170-dust. However, on the contrary, the peaks J, D and L make their appearance at higher temperatures. The increase in peak temperatures is probably caused by a rise in the pressure, which develops due to the sealing of the sample tube by the hardened resin. On heating to a temperature as high as 550°C or thereabouts, the char becomes porous releasing the pressure and so the peak (L) temperature does not rise, Table 14.

6. Effect of packing density

To show the effect of packing density the average peak temperatures are given in Table 11d.

Table 11d

Average peak temperatures, $^{\circ}$C

Packing	Table	A	B	C	D	H	L	Z
Tight	11a	-	160·4	211·0	281·0	-	530·0, 332·0	-
Loose	15	43·0	148·0	193·5	266·4	456·5	549 0	611·5- 759·0

The (spurious) exothermic peak A is similar to the one reported in the Table 14. (We will discuss this later.) The peaks H and Z are missing in tight packing. The sharp doublet at 530·0°and 532·0°C is not shown in loose packing; instead there is a comparatively broad peak L at 549·0°C

The difference in the behaviour of the thermograms depends on the tightness of packing on two grounds.

(a) Packing density affects the heat transfer from the wall of the sample cavity to the thermocouple junction.

(b) It also affects the diffusion of gases in or out in decomposition reactions.

Tight packing is generally preferable because it decreases the thermal gradient by increasing the heat conductivity and is more reproducible (especially in the absence of decomposition and forced passage of gases). Loose packing shows the effect of a long-drawn-out endotherm as the lower thermal conductivity produces a larger temperature lag.

The fortuitous appearance of the exothermic peak A at 43°C is most likely due to the difference in the packing density between the specimen and reference material. A similar exotherm is reported only by Claver[107] for phenolic resin degradation. Arens found severe differences on DTA thermograms of quartz and kaolinite due to differences in tightness of packing of specimen and reference. His results are reported by Garn[73].

PHENOLIC RESINS RW 52487$^+$ and RW 54859$^+$

The specimens RW 52487 and RW 54859 are xylenol-formaldehyde and fast curing high ortho phenolic resins respectively.

The DTA peaks shown by phenolic samples RW 52487, RW 54859, A_1 , B_1, C_1 and D_1 (cured with hexamine) are given in Table 16, Fig. 16a and 16b. The two endothermic peaks H and L are missing but a new exothermic peak B' is shown at 148° and 152°C by the samples C_1 and D_1 respectively. The cured specimens indicated different behaviour on degradation showing that the original resin specimens RW's had different histories and they are also different from the standard novolac resin R 19370. The difference in the thermal behaviour is shown in Table 16c. Figs. 16 ., 10a and 11b.

TABLE 16c

DTA peak temperatures, °C of resins RW 52487, RW 54859, R 19370, A_1, C_1 and PFH XIII (last three samples cured with 10% hexamine)

Resin	Table	A	B	B'*	C	D*	E	F	H	L
RW 52487	16	76·0	129·0	-	182·0	217·0	-	381·0	-	-
RW 54859	16	42·0	93·0	-	162·0	187·0	-	376·0	-	-
R 19370	10a	62·6	108·5	-	159·7	196·2	315·3	385·7	422·5	-
A_1	16	40·0	-	-	180·0	-	-	383·0	-	-
C_1	16	61·0	120·0	148·0	-	-	-	400·0	-	-
PFH XIII	11b	-	152·0	-	-	236·0	-	-	-	532

* exothermic peaks , + i.e. with high proportion of oo' links.

PHENOLIC RESOLE DV 19162

The DTA curves of resole with and without hexamine are shown in Fig. 17. For the simple cured resole endothermic peak C at 251.0°C is present and an exothermic peak D around 250°C is missing. The thermograms produced by the resole samples $PFRH_1$, $PFRH_2$ and $PFRH_3$ containing 1%, 2% and 3% hexamine, are exactly similar in form. The exothermic peak D cannot be due to the melting of unreacted hexamine (as this would of course be endothermic) and a similar peak has been shown by crosslinked novolac resin. Moreover for such samples of novolac, where excess of hexamine was present, a strong endothermic peak J was shown as a melting point of hexamine, Tables 12 and 14. It is probable that about 1% of hexamine (H_2CO) has reacted to crosslink resole in three ways (Megson):-

(1) with nuclear hydrogens,

(2) with phenolic hydroxyls,

(3) with methylene bridges,

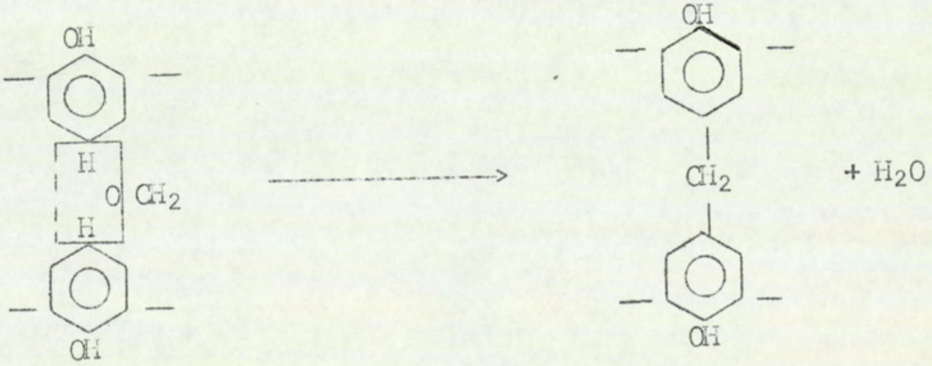

(1)

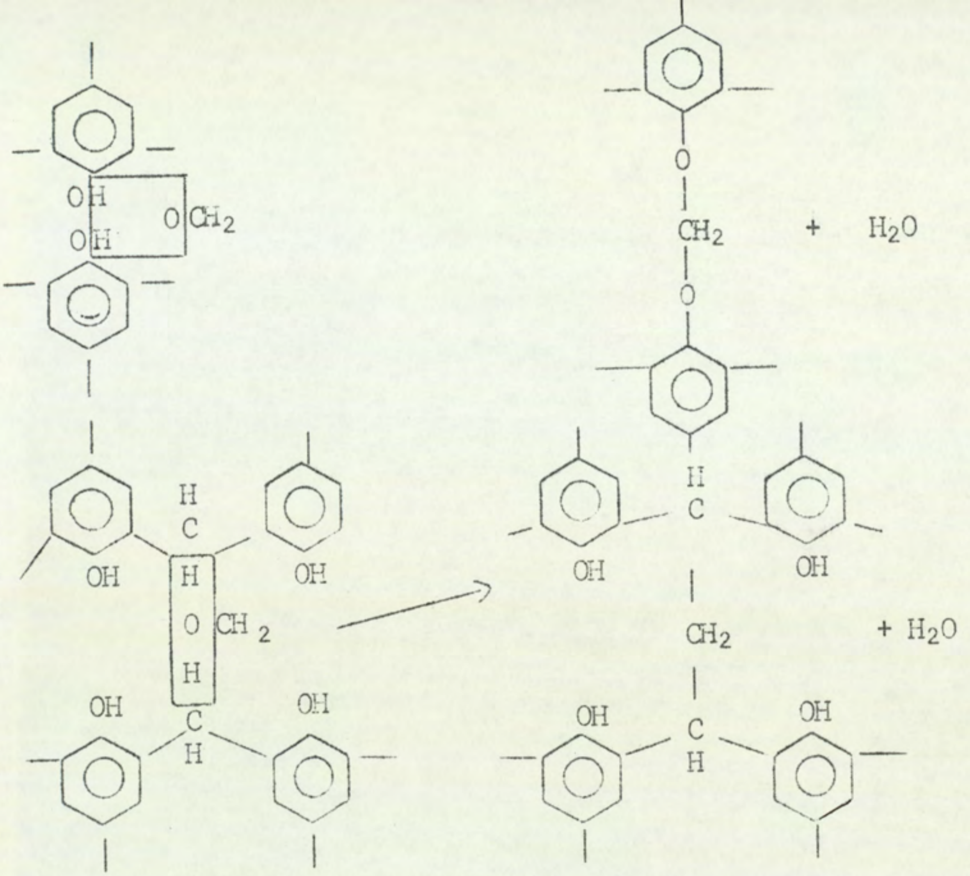

(2)

(3)

or might react on free activated position of ring to give methylol group which could cross-link the resin. Such reactions do not give an entirely satisfactory explanation, mainly because the resole should contain excess formaldehyde (or methylol) group in any case.

The mechanism of further reaction of resoles in the molten state is not very well understood, and we cannot exclude the possibility that the hexamine or ammonia derived from it, is in fact acting as a catalyst for a non-radical process.

The thermograms of resole almost resemble with those of novolac samples PFH I and II (Fig.15) except for peaks A and L. Most likely it indicates that there is no difference in the structures of resole and novolac after curing.

The comparison of the peaks is made with those reported by other investigators in Table 17a.

On inspection of the Table 17a very little agreement is found between the peak temperatures. The difference can be explained by the following variations:

(1) Instrument used for analytical purpose, its sensitivity.

(2) Heating rate.

(3) Atmosphere - static or dynamic - oxidising/reducing.

(4) Sample holder (size, material).

(5) Position of the thermocouple.

(6) Packing density.

(7) Grist.

(8) Degradation is kinetic or diffusion controlled.

(9) Quantity of the sample.

(10) History of the resin - composition, P/F ratio, catalyst, hexamine concentration, curing time, temperature and atmosphere, the degree of cross-linking, the amount of volatile products in the resin, etc.

(11) Sample with or without diluent.

EFFECT OF SULPHUR, CHRYSOTILE ASBESTOS AND INORGANIC ADDITIVES ON RESIN DEGRADATION - PHENOLIC COMPOSITES

The effect of 5% sulphur addition during cross-linking of novolac resin is seen in Table 18 and Fig. 18. The first two endothermic peaks A, B, and the exothermic peak D are suppressed and three endothermic peaks a (192, 198°), (256, 263°) and 534/35° are shown. Sulphur has entered into chemical reaction with resin/products and altered the degradation scheme.

The influence of asbestos and inorganic additives on resin degradation is shown by DTA curves in Figs. 19a, 19b and 19c. The general form of the curves of the samples PFHA I, PFHB, PFHAB, PFHSm, PFHASm, PFHSP, PFHASP, PFHGF, PFHAGF, PFHAl(OH)$_3$ and PFHAAl(OH)$_3$ is markedly different from the curves obtained by cured or uncured resin without additives. The characteristic temperatures of the events occurring during thermo-oxidative degradation are mentioned in Table 19. The first two peaks A (melting point) and B (curing) are invariably given by all the specimens. The peak C is shown by the samples containing sodium metaborate, sodium phosphate and alumina. The peaks D, E and H are produced by the samples having severally asbestos and glass fibre, boric acid and alumina, and asbestos. The peak Z is shown by samples containing inorganic additives (without asbestos) except the sample PFHASm. The last two peaks S and O are shown by all those specimens of resin that contained asbestos except the sample PFHASm. The sample containing alumina gave a small endothermic peak C' at 251°C. Both the samples with alumina, PFHAl(OH)$_3$ and PFHAAl(OH)$_3$, showed very strong endothermic peak E at 328°C due to dehydration of alumina, and a very feeble endotherm at the same temperature is shown by the resin sample having boric acid.

The large endotherm S around 714°C is due to dehydration of chrysotile asbestos and the exotherm near 820°C is caused by transformation of anhydride to forsterite[112] and silica.

The total decomposition of chrysotile asbestos corresponds to

$$2\ (3\ \mathrm{Mgo},\ 2SiO_2,\ 2H_2O) \longrightarrow 3\ Mg_2SiO_4 + SiO_2 + 4H_2O.$$

A small endothermic peak B at 122°C is also shown by asbestos, which is probably due to evaporation of adsorbed moisture.

ENERGY CHANGES

Assuming that the area under any peak is proportional to the reaction responsible for that peak, then the area under the peaks can be arranged in decreasing order, so as to reflect the corresponding order of energy changes.

Table 19d

Energy changes based on peak area

Area under peak	variable	Fig
B>D*	Curing time of novolac	11a and 11b
J>B>C	Hexamine concentration	12b.
C>D*	Heating rate	13
J>D*>B>C	Grain size	14
Z*>B>H>D*	Loose packing	15
Z*>B>D*	Cured resole	17
S>B>O*	Composite	19a and 19b
S≈E>B>O*	Novolac	19c

* exothermic peak

The areas under peaks B, C, D, H and Z (due to cross-linking, oxidation, degradation and char formation, etc.) can be decreased by curing the resin under non-oxidative conditions or in a vacuum. If the resin could be fully cross-linked the peaks due to postcuring will vanish away.

The three bigger endothermic peaks J, E and S can be controlled by adjusting the amount of hexamine, hydrated alumina and chrysotile asbestos respectively.

The apparent heat capacity of chrysotile asbestos from 25° to 140°C as calculated by Rogers[109], is 0·504 kcal/g.

Thermodynamic analysis shows that the reactions between silica (from asbestos or glass) and carbon most likely to occur from the point of view of equilibrium are:

$$SiO_2 + 3C \longrightarrow SiC + 2CO$$

$$\Delta H_{20000}{}^{o}k = 133 \text{ kcal}$$

$$SiO + 2C \longrightarrow Si(l) + 2CO$$

$$\Delta H_{20000}{}^{o}k = 157 \text{ kcal}$$

$$SiO_2 + C \longrightarrow SiO(g) + CO$$

$$\Delta H_{20000}{}^{o}k = 147 \text{ kcal}.$$

Beecher and Rosenweig[8] studied the kinetics of these reactions from 1350 to 1700°C by measuring the pressure of CO. They used an Arrhenius analysis and found the activation energy to be 92 kcal/mole. The reactions between carbon and silica absorb heat to the extent of about 4 kcal per gram of carbon consumed. Thus the process is an important heat sink.

Table 19e gives representative bond energies in kcal/mole to show the order of stability.

Table 19e

Bond energies[113,114], kcal/mole

H-H	104	Si-C	89
O-O	30	C-N	49-82
O-H	118	C-F	94-119
C-C	85	Si-Si	53
C-Cl	81	Si-Cl	91
C-O	86	Si-O	108
C-H	99	Si-H	76

CONCLUSIONS

1. The novolac resin R 19370 is changed to oligomers on heating. These oligomers showed four endothermic peaks in the 2mm diameter tube and six endothermic peaks and one exothermic peak in the 4 mm diameter tube (see Table 10a).

2. The first peak at ca.60°C is due to melting of the resin. All the other peaks are caused by post-curing[+], thermal and oxidative degradation and carbonisation. These peaks, in general, may be correlated tentatively by common knowledge of the reactions of the polymer.

3. On curing the resin with the hexamine the melting point is eliminated and some new peaks are produced. In some cases endothermic valleys are shown due to overlapping of the reactions (See Tables 13 and 14)

4. On increasing the heating rate the peaks shift to higher temperatures.

5. Packing density affects the DTA thermograms.

6. Areas under the DTA peaks are consistent but the peaks are affected by hexamine concentration (Fig.12).

7. Cured and uncured novolac specimens (RWS) show a different DTA pattern (Fig.16) from the standard novolac R 19370 (Figs.11a and 12). This shows differences in the structures of the resins.

8. The resole DV 19162 gives different form of thermograms (Fig.17) than novolac as expected.

9. The DTA spectra are highly influenced by chrysotile asbestos and other

---

[+] i.e. elimination reactions

inorganic additives above about 300°C (Figs. 19a, 19b and 19c). The dehydration of asbestos shows a strong endothermic peak at ca.714°C and a small exothermic peak at 821°C. The dehydration of alumina also gives a marked endotherm at 328°C.

CHAPTER V

CORRELATION OF THE PEAKS WITH VARIOUS REACTIONS

The chemistry of phenolic resin degradation is quite complex to understand clearly, because of the competitive and consecutive reactions, e.g. post-curing, oxidative degradation, thermal fragmentation, oxidation/reduction, carbonisation, etc. In the present studies an attempt is made to correlate differential thermogram peaks with the main reactions of resin degradation. For the purpose of correlation we would mainly rely on the studies of Megson, Ouchi and Honda, Heron, Shulman and Lochte, Madorsky and Conley et al.

It may be found comparatively easy to correlate the first few peaks with the most probable reactions, but for the later peaks it is really difficult to associate them with specific reactions. These difficulties arise from:

(1) The complex nature of the resin.

(2) The problem of knowing where and when a particular product is formed, i.e. whether it is produced in the solid, liquid or gaseous phase.

(3) The question of the sequence of departure of the products from the reaction zone/s.

(4) Changes in the basic mechanism of pyrolysis.

(5) Participation of secondary or "cracking" reactions.

All the differential thermograms of heat treated (uncured) and cured resin show the same general form in their own class, except for some minor variations. The thermal spectra are divided into two main parts for discussion.

(a) Low temperature region (40 - 420°C).

(b) High temperature region (420 - 850°C).

Peak A

The peak A around 60°C is due to the softening point of the resin. The melting point of the resin is eliminated on cross-linking the resin with hexamine.

Peaks B, C, D and H (below ~ 420°C)

The peaks B and C in the range of about 140- 200°C are produced by further cross-linking of the resin. The main reactions are believed to be due to the formation of methylene ether and methylene bridges.+ On raising the temperature to about 250°C formaldehyde is given off. The reactions are illustrated below:

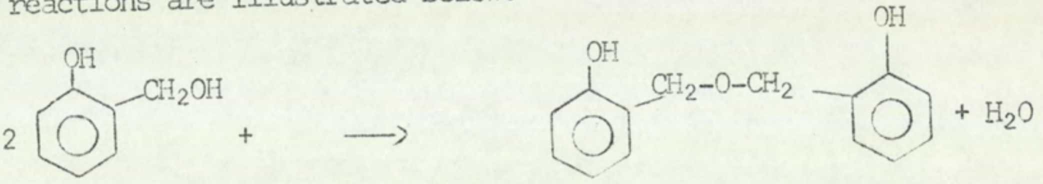

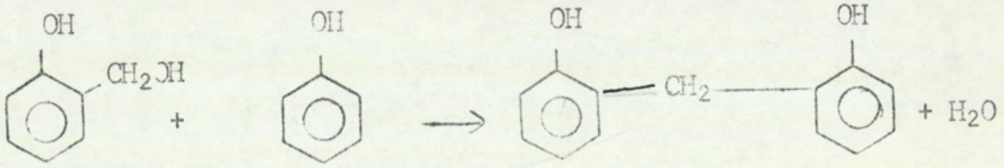

+ "and possibly elimination of H_2O and HCHO."

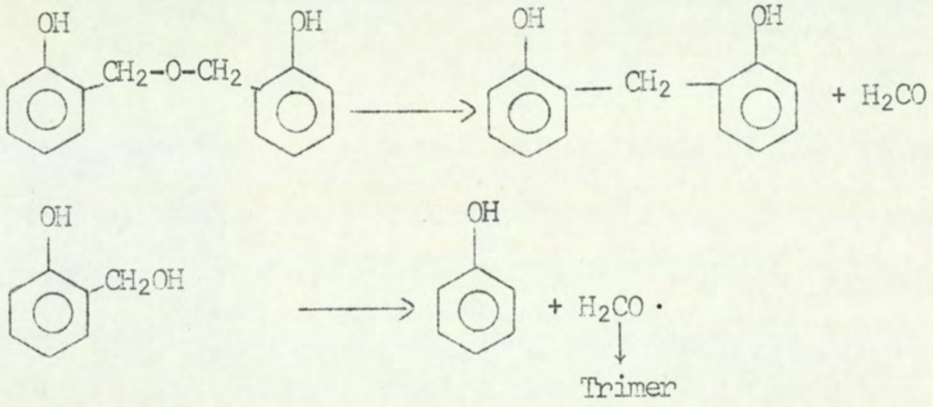

It has been found (Megson) that hexamine reacts with phenolic novolac resins to form bis- and tris-hydroxybenzyl amines or polynuclear derivatives of similar structures. Phenols with free ortho positions appear to form the secondary amines more readily and those with free para positions show a tendency to form more of the tertiary amines. All these amine linkages appear to be unstable at high temperatures and change to other linkages on heating. If the amount of nitrogen is limited the rings are coupled by the methylene bridges and in excess of N_2 azomethine linkages may form. The latter may decompose to xanthene, methyl phenols and methylamines. The products with azomethine groups are bright yellow and may be responsible for the colour of hexamine cured novolacs at moderate temperatures.

The other possibility is the formation of quinone methides due to thermal decomposition of the hydroxybenzylamines. The highly reactive (postulated intermediate) quinone methide gives complex condensed rings of red or brown colour.

Briefly, to explain the reaction of hexamine with novolac the following principal reactions are postulated:

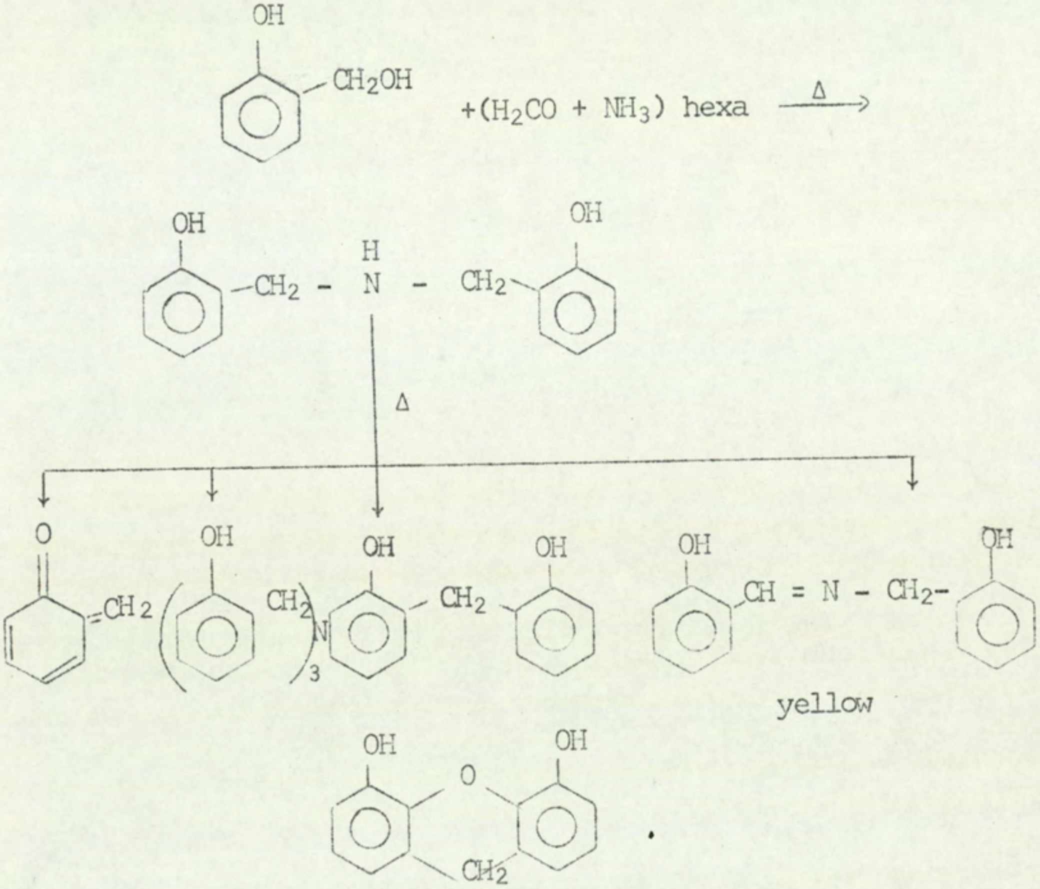

Xanthene

The exothermic peak D around 250°C is most probably due to oxidation of methylene bridges and methylol groups and further curing , thus

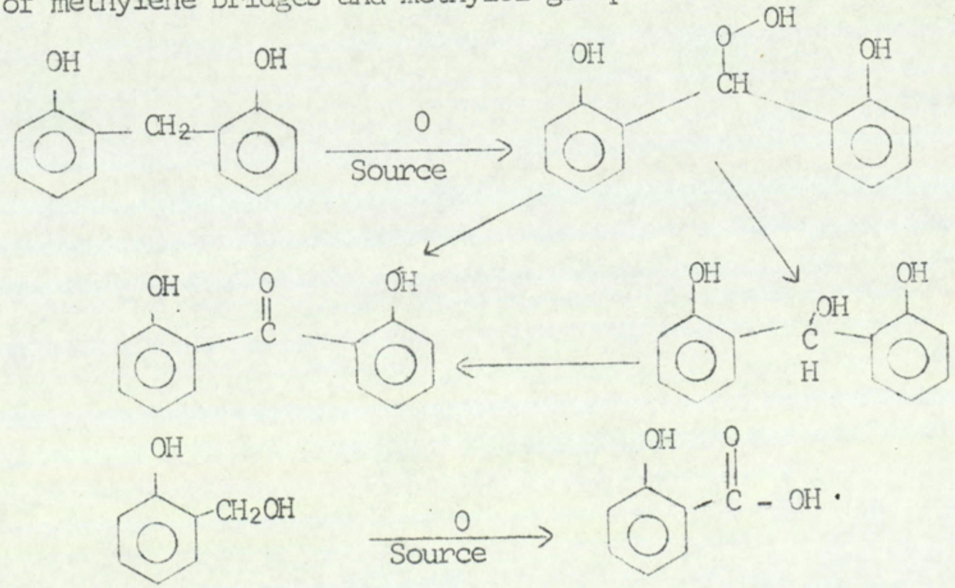

The methylene bridges in phenolics have been found to be highly susceptible to oxidation and is oxidised to the keto group fairly rapidly at temperatures as low as 150°C. The oxidation rate increases further around 400°C (Conley). Lady et al [110] in the study of polybenzyl and diphenylmethane postulated a mechanism for oxidation of methylene linkages activated by adjacent rings and this was later substantiated by Conley[111] during oxidative degradation of polybenzyl. The methylene linkage may be oxidised by moisture[63] at comparatively high temperature, thus

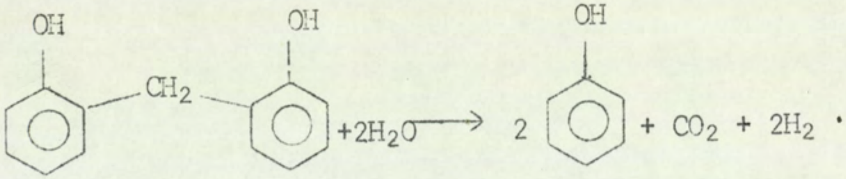

(H$_2$ could react to give phenols

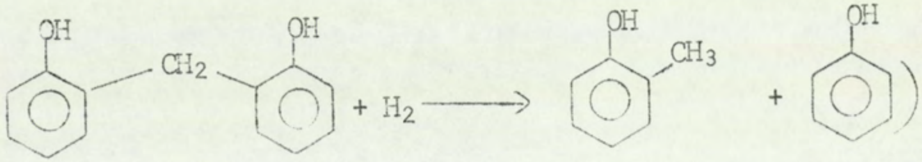

Thus methylene linkage is the weakest bond in phenolic resin.

The endothermic peak 'H' around 400°C may be due to dehydration reaction between phenolic hydroxyl groups/and hydroxyl groups and methylene bridges[59].

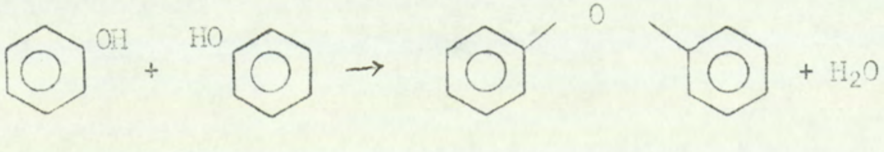

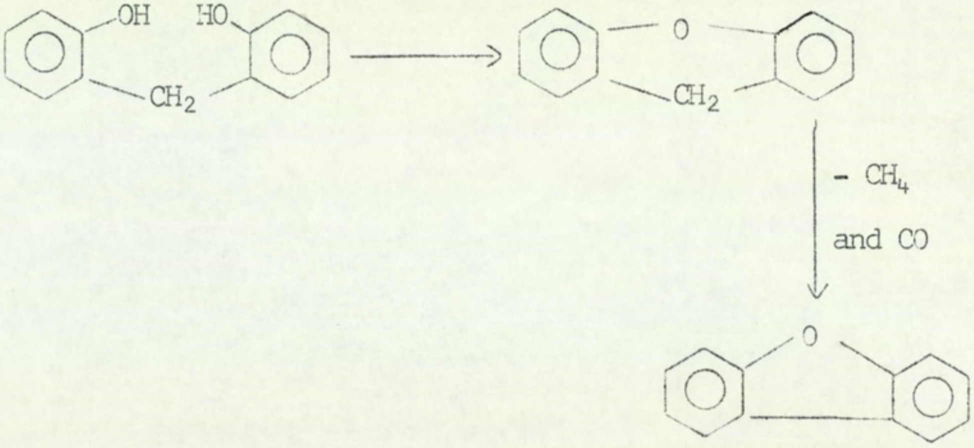

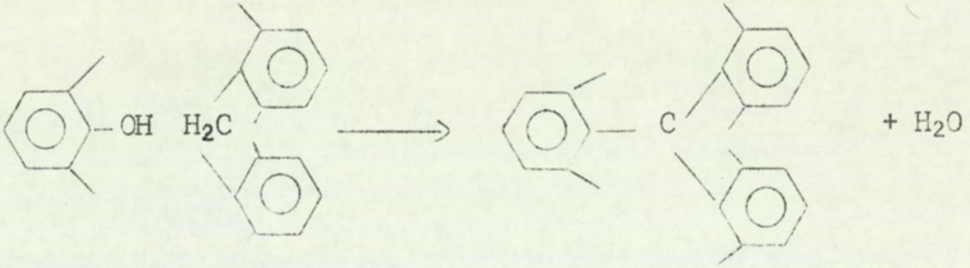

Jackson and Conley *(loc cit)* have not been able to find evidence in favour of the mechanism originally proposed by Ouchi and Honda *(loc cit)* and recently confirmed by the spectrometric studies of resin by Ouchi *(loc cit)*. Megson *(loc cit)* supports the idea of Redfern that there is some evidence in favour of the participation of the hydroxyl groups.

6. Peaks L and Z (500 - 780°C)

Most of the (oxidative degradation) thermal fragmentation, distillation of volatile degradation products, free radical reactions, oxidation/reduction, carbonisation, graphitisation, ring scission, etc. occur in the temperature region of 400°-780°C. The overall effect of all these reactions is observed in a consistent broad exothermic peak Z in the range of 600°- 775°C.

Thermal oxidative processes lead to CO, CO_2, benzaldehyde, benzene and toluene (schemes I to III proposed by Conley and co-workers), while thermal fragmentation reactions account for formation of phenol, and phenolic homologues(Scheme II).

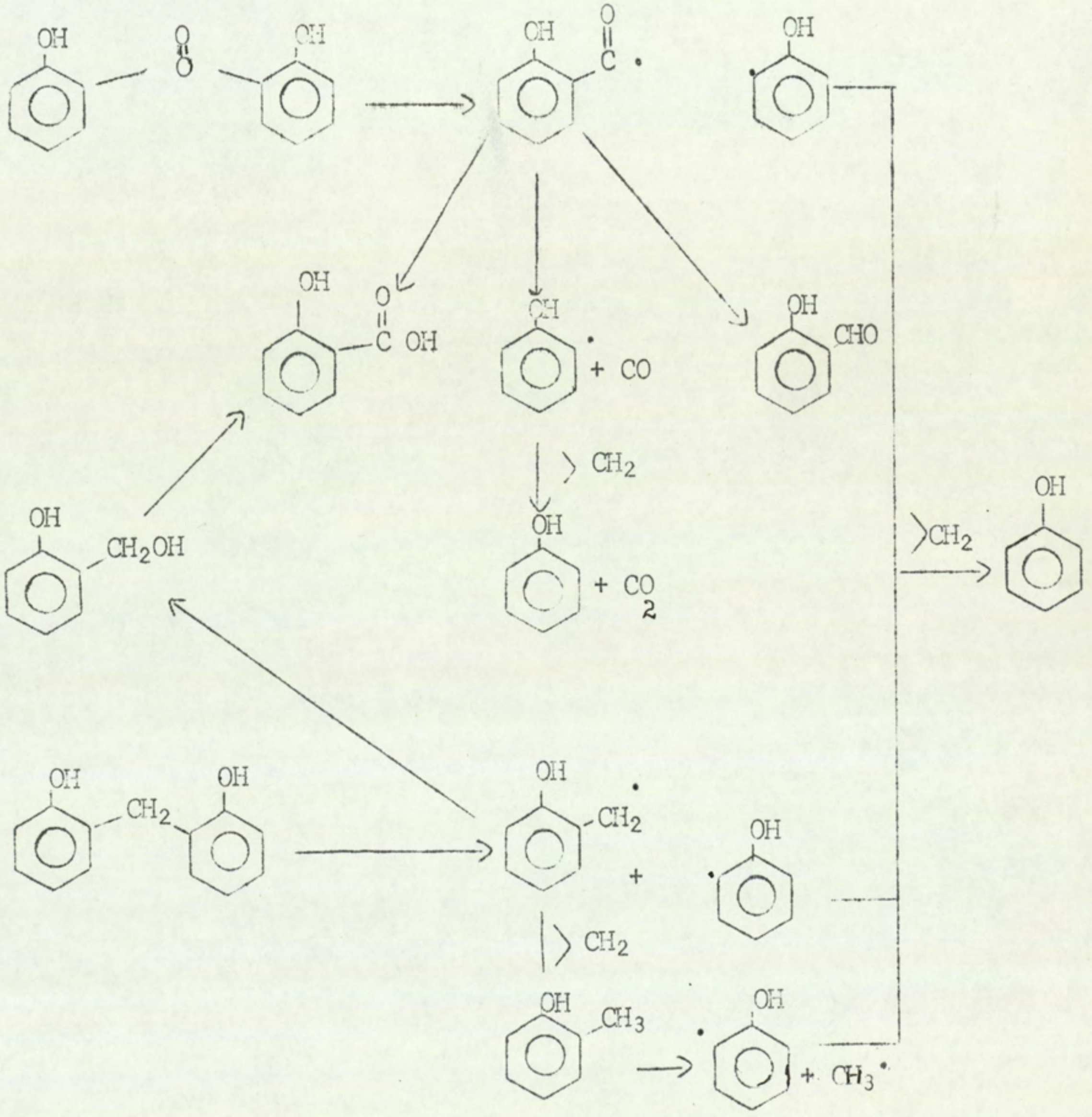

I

II

$$\dot{C}H_3 + \xrightarrow{\rangle CH_2} CH_4 + \rangle \dot{C}H$$

III

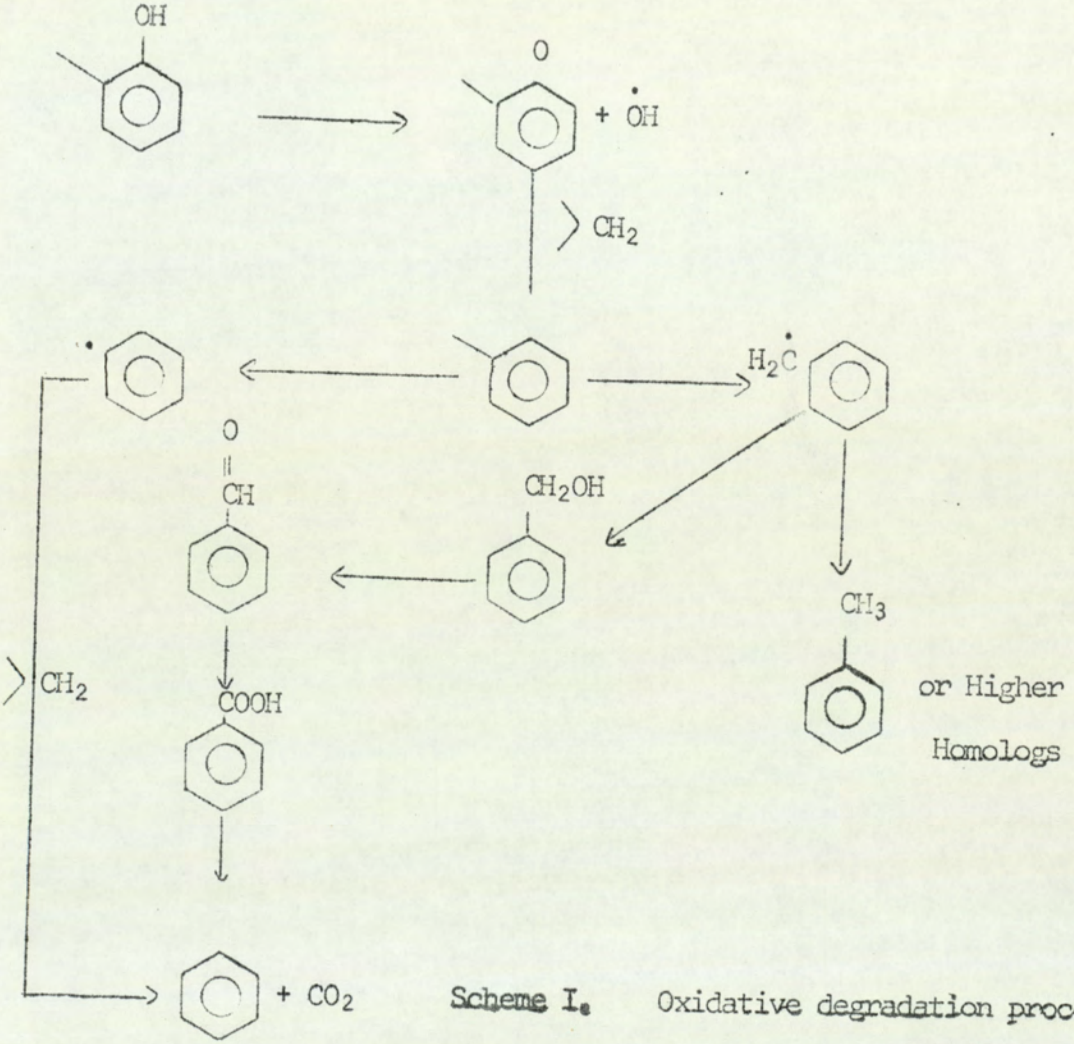

Scheme I. Oxidative degradation processes
Scheme II. Fragmentation reactions
Scheme III. Formation of benzenoid species

Char Formation

(In the following pages different views on char formation are mentioned. The actual char formation is not substantiated by Conley et al or any one else but are likely (or unlikely) hypotheses.)

A reaction scheme accounting for the decomposition products of phenolics and for char formation has been proposed by Jackson and Conley which is substantiated by Schulman and Lochte[38] in their mass spectrometric thermal analysis of phenolformaldehyde. This scheme is not in agreement with the one advanced by Ouchi and Honda. At temperature above 600°C CO formation accompanies char forming reaction, through quinone type intermediate, as summarised below.

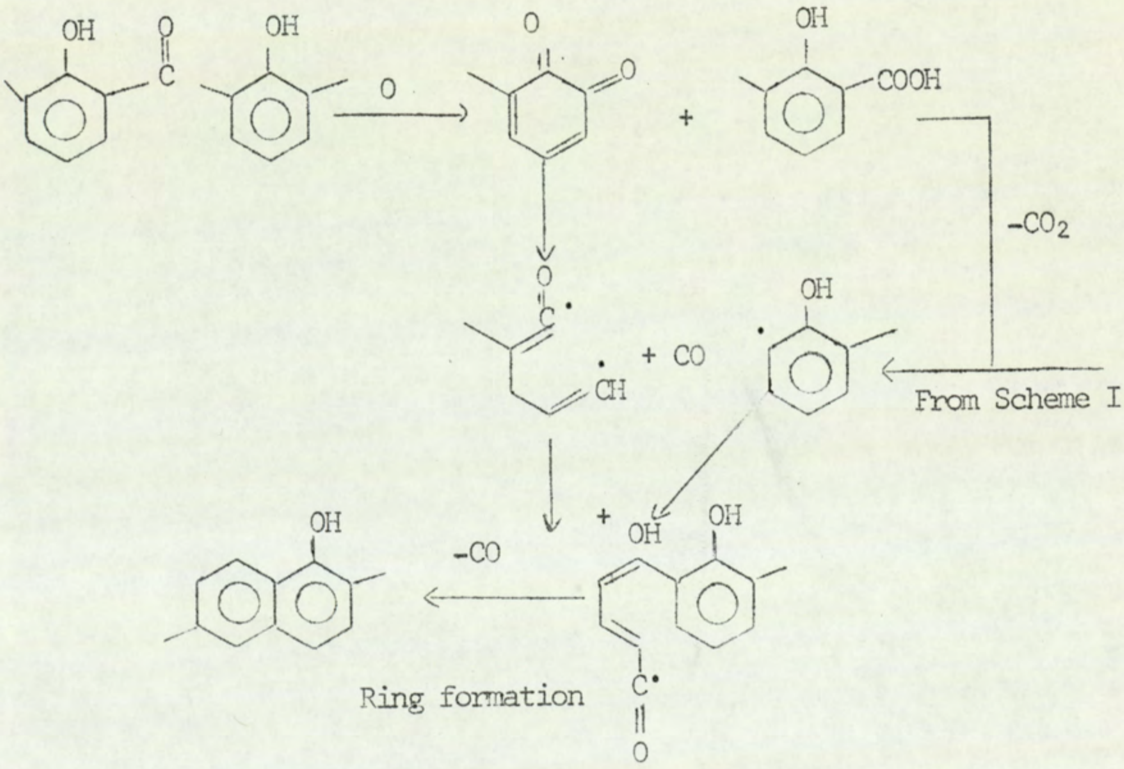

Polyvinyl Chloride

Polyvinyl chloride loses HCl ca 200°C and leaves polyene structures -C=C-C=C-C=C-. Polyene is postulated to undergo inter- and intra-chain cyclisation (a Diels-Alder mechanism) to give tar (which contain aromatic and aliphatic groups) and char (Gilbert and Kipling[115]). C:H ratio of PVC gives high yield of char.

Ouchi and Honda have postulated that the ease of graphitisation of phenolformaldehyde resin depends on the kind of original phenol, in other words, the greater the number of OH or CH_3 radicals the greater is the ease of graphitisation. The following three steps were suggested by them to account for the formation of carbonaceous material from phenolic resin.

In the first stage, the carbonaceous material of the resin contain structures as the products of equation (1) and (2)

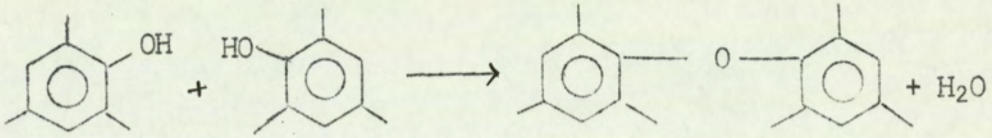

(1)

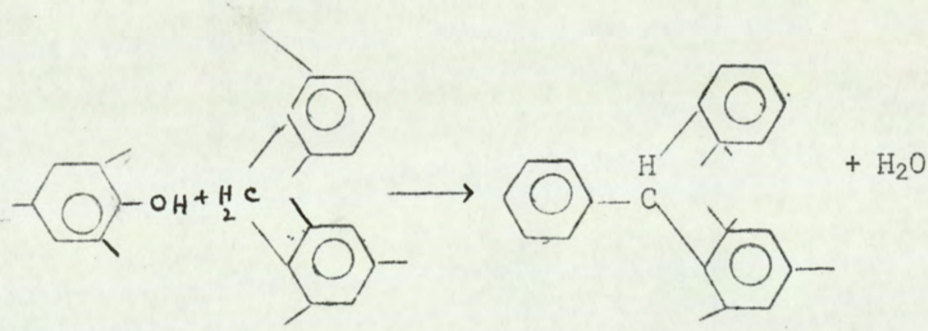

(2)

In the second step the benzene nuclei combine directly with one another as diphenyl by breaking off $-CH_2-$ and -O- bridges. An idealised model of the structure at this stage is given below.

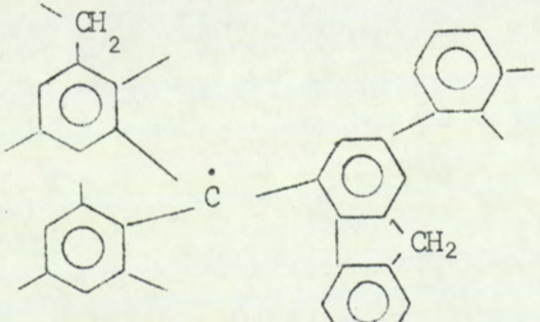

During this stage the decomposition of bridges producing some unpaired electrons and the direct bonding of the benzene nuclei take place simultaneously.

In the third step, the remaining hydrogen atoms are removed and at the same time the size of the aromatic nuclei increases by the partial rearrangement, accompanying the strong three dimensional bonding among them.

Wolfs, Krevelen and Waterman *(loc cit)* suggest that the primary carbonisation is a partial depolymerisation accompanied by disproportionation of the hydrogen in the nethylene bridges; the average number of carbon atoms per monomer unit does not change. Some monomer units become richer in hydrogen and finally get into the tar; others lose this hydrogen and remain in the residue. Basically, the shortage of reactive hydrogen governs the primary carbonisation. The possible mechanism to illustrate this point is shown here.

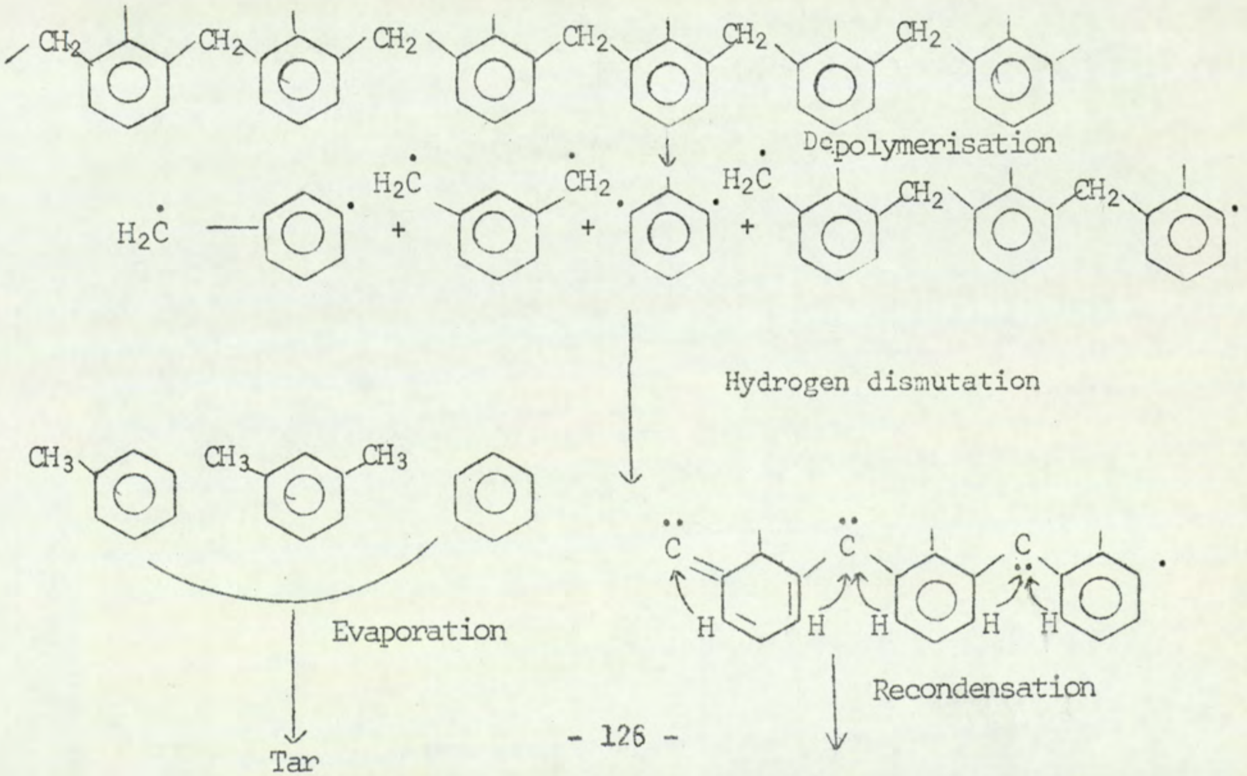

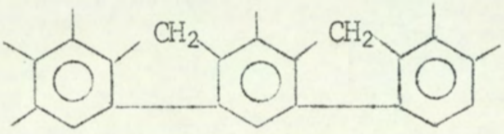

Residue (Semicoke)

Another route for the carbonisation of phenolics may be considered. At high temperature ring-opening and the fragmentation of aromatics are more significant than condensation. However, direct carbonisation of aromatics can take place under some conditions. Most probably it involves condensation reactions to form higher aromatics, concomitant with the loss of hydrogen. Some possible condensation reactions involving phenyl radicals and benzene to yield carbonaceous residue are:

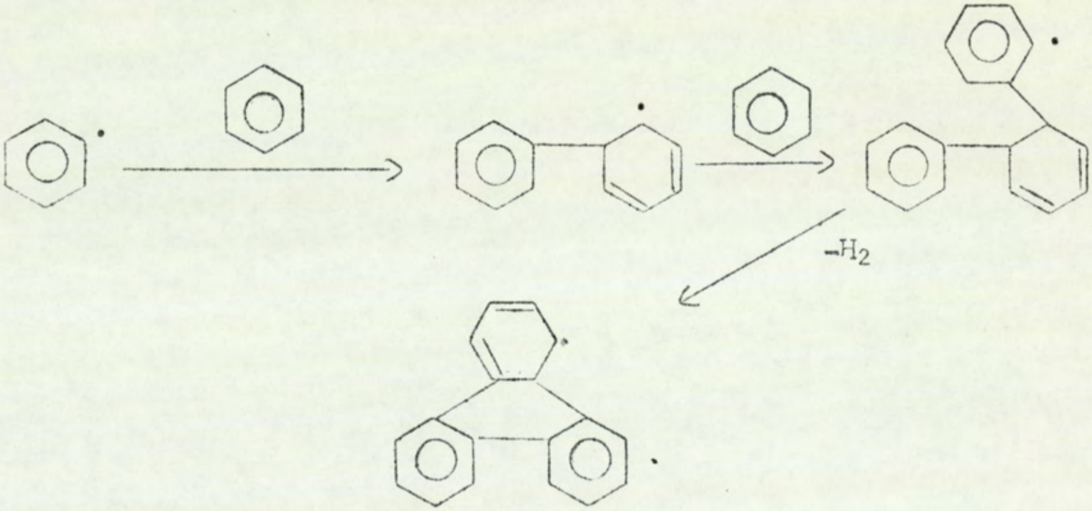

Since aromatic structures are thermodynamically more stable at higher temperatures, cyclisation takes place with the formation of a graphitic network. The distance between graphitic planes, and the development of three-dimensional order, depends on the decomposition temperature.

Resonance energy due to delocalisation of the π electrons indicates the gain in stability. The Table 19f shows the increase in resonance energy (stability) with increase in the number of rings

Table[116] 19f

Compound	Resonance energy (kcal)
Benzene	36·0
Naphthalene	61·0
Anthracene	83·5
Phenanthrene	91·9
Naphthacene	110·0
Benzathracene	111·6
Benzophenanthrene	109·6
Chrysene	116·5
Triphenylene	117·7

Hence graphite-like structure is the most stable one.

Thermal fragmentation of the resin mainly starts around 400 °C by rupturing of the carbon-carbon bonds between the methylene and the aromatic rings (Megson *(loc cit)*), thus

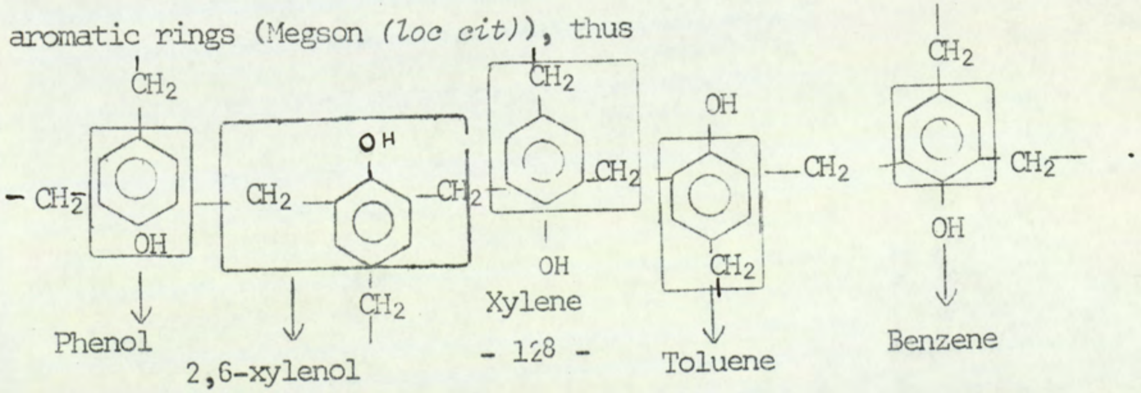

Reference may be made to the work of Ouchi and Honda *(loc cit)*, where they have proposed a mechanism for the production of H_2, CO, CO_2, H_2, CH_4, C_2H_4, etc.

These gases would be formed by the following reactions:

$$-CH_2- + H_2O \rightarrow CO + 2H_2$$

$$-CH_2- + H_2 \rightarrow CH_4$$

$$-CH_2- + O \rightarrow CO + H_2$$

$$-CH_2- + -CH_2- \rightarrow C_2H_4$$

$$-CH_2- + H_2 \rightarrow C_2H_6$$

$$CO + O \rightarrow CO_2 .$$

The production of methane at a lower temperature would be due to the removal of terminal methyl groups which would react as follows at temperatures above 300°C.

$$-CH_3 + \tfrac{1}{2} H_2 \rightarrow CH_4$$

As the temperature rises, the gases formed are heated by radiation and react with one another giving rise to secondary reactions.

400 - 1000°C

1. $CO_2 + C \rightleftharpoons 2\,CO$
2. $C + H_2O \rightleftharpoons CO + H_2$
3. $CH_4 + H_2O \rightleftharpoons CO + 3H_2$

SUMMARY

Uncured phenolic novolacs show similar curves irrespective of heat treatment. Peaks are associated with melting loss of minor constituents and loss of low molecular weight materials.

2. They were used to study the effect of analytical process variables. Heating at 30°C/min in an atmosphere of nitrogen was effective. Activation energies of the main peaks were recorded.

Addition of hexamine, with heating over 120°C gave a simplified curve with three main peaks at ca. 220°C, 280°C, 530°C, 10%hexamine gave stable results, and excess gave a series of peaks identified with physical and chemical changes in the excess hexamine.

Other resins gave varying results, inconclusive, due probably to excessive base line drift.

Sulphur was an effective cross-link but not in presence of hexamine.

The following additives have the results stated.

Asbestos: Strong persistent endxotherm at ca 700°C.

Boric Acid: Endxotherm at 140°C (perhaps due to boric acid).

Alumina: Strong persistent endotherm at 330°C.

Sodium metaborate: Apparent exotherm at 6-800°C.

Sodium phosphate: Sharp endotherm at 220°C.

Glass Fibre: Weak endotherm at 380°C.

(most of these not very significant and apparently not affecting the resin).

7. D.T.A. results were often dubious due to base line drift and the presence of sporadic peaks which may be adventitious (due to instrumentation, etc.)

Characteristic Stages of Degradation

Peak A	Peaks B,C,D.	Peaks H,L.	Peaks Z, etc.
60°C	100-250°C	4-800°C	700-1000°C
Melting	Postcuring	Thermal reforming	Carbonisation
Phase Change	Losses of H_2O and HCHO	Depolymerisation	Loss of residual groups and ring stripping
	Oxidation of $-CH_2-$	Repolymerisation	Dismutation
	Reaction with hexa		Ring fission and condensation
			Graphatisation

EXPERIMENTAL

PROGRAMMED THERMOGRAVIMETRIC ANALYSIS (PTGA)

Studies of Phenolic Resins and Phenolic Composites

EQUIPMENT: Du Pont Thermogravimetric Analyser 950. Fig.5.

N.B.

1. No buoyancy correction is applied.
2. C/A thermocouple is kept just under the Pt boat in every case.

EXPERIMENTAL CONDITION C

Pt boat (Cat.No.950060), scale 1·0 mg per inch (y-axis)

Temperature scale 100 C per inch (x-axis)

Time constant 1 second

C/A thermocouple (Cat.No.900329)

Heating rate 30°C per minute to 1070°C

N_2 flow 2SCFH

SCHEDULE D

Table	Fig.	Samples	Condition	Variable
20a		PFH I - V	C	Curing time, 17% hexamine
20b	20b	PFH XIII-XVI	C	Curing time, 10% hexamine
21		PFH VI - XII (IX)	C	Hexamine
22	22	PFH IX	C	Grain size
23	23	PFH VIII	C	N_2 flow, Air, CO_2 and still atmosphere
24	24	RW54859 RW52487 B_1, C_1, D_1	C	Hexamine
25		PFR-$PFRH_5$	C	Hexamine
26	26	PFS-PFHS II	C	Sulphur
27		PFHC-$PFHC_9$	C	Carbon
28		PFH-gluc, suc, sta	C	Carbohydrates
29		PFH-Fur, PVAcry, PV-Alc PVC, Cell.Bty., CMC, N66, Sty.	C	Furfuryl alcohol and organic polymers.
30	30	PFH-Al, Cu, Mg, Zn.	C	Powdered metals
31	31	PFH-$AlCl_3$, $FeCl_3$, $ZnCl_2$.	C	Lewis Acids
32	32	PFH-HgO, MnO_2 Sb_2O_3, SiO_2 ZnO	C	Mineral Oxides
33	33a 33b 33c	PFH-A I, II, GF. AGF, $Al(OH)_3$, $AAl(OH)_3$, B, AB, Sm, ASm, SP, ASP, LC, AlC, Ref, Si	C	Asbestos and inorganic additives - phenolic composites

Table	Fig.	Samples	Condition	Variables
34	34	TX, PFHTX, RPD-110, 150, 154.	C	TX, Commercial phenolic composites.

RESULTS

The results of PTGA studies are reported in tabular form, i.e. Tables 20a - 34, and in the corresponding figures. (Figures carry the same number corresponding to the Tables.) Generally the % residue at 200°, 400°, 500°, 600°, 850° and 1070°C is given in the Tables. The last column of each table shows the temperature, °C, at which 50% loss of the final loss at 1070°C occurs. In some cases this criterion of heat stability corresponds to stability based on final residue, while in other cases there is scattering of this temperature. This variation in stability temperature is because of the presence of volatile material in the specimens. In the present investigation residue at 1070°C is the measure of heat stability.

Figures are obtained by plotting % residue versus temperature, °C.

Table 20a

Percentage residue at temperatures, °C.

Sample	200	500	850	1070	Temperature at 50% loss, °C.
R19370	-	-	-	32·0	
PFH I (1)	95·4	85·9	57·6	55·6	556·0
PFH II (2)	94·6	84·9	54·4	53·8	552·0
PFH III (3 1/3)	96·6	84·3	54·6	53·2	548·0
PFH IV (3 $\frac{3}{4}$)	94·5	84·3	56·0	53·0	545·0
PFH V (18 $\frac{1}{3}$)	93·6	84·8	55·2	52·4	540·0

Notes:

1. 17% hexamine.
2. Effect of curing time at 128°C. Curing time (hours) is given in parentheses.
3. ~ 37 mg weight used.
4. 100 mesh, ϕ, 30°C/min. N_2 flow.

Table 20b

Percentage residue at temperatures, °C.

Sample	200	500	820	1070	Temperature at 50% loss, °C
PFH XIII (½)	96·4	83·6	56·8	55·4	569·0
PFH XIV (1)	98·0	85·8	55·5	53·7	543·0
PFH XV (2)	97·7	81·8	53·1	52·5	536·0
PFH XVI (3)	97·7	82·7	53·4	52·0	532·0

Notes:

1. 10% hexamine.
2. Effect of curing time at 150°C.
3. Curing time (hours) is given in parentheses.
4. 100 mesh, ϕ, 30°C/min. N_2 flow.
5. $\sim$ 33 mg weight is used.

Table 21

	Percentage residue at temperatures, °C					
Sample	200	400	500	850	1070	Temperature at 50% loss, °C
PFH VII (5)	98·6	93·3	78·3	50·9	49·5	524·0
PFH VIII (10)	98·9	96·0	88·2	57·6	55·9	574·0
PFH VI (17)	98·9	93·0	88·9	58·2	56·6	579·0
PFH X (30)	93·6	78·0	73·8	47·3	46·0	494·0
PFH XI (40)	94·1	72·8	69·1	44·6	43·3	419·0
PFH XII (50)	92·1	56·9	53·3	34·6	33·9	256·0

Notes:

1. ∿ 34 mg weight used·
2. Effect of hexamine on cross-linking at 150°C·
3. Percentage concentration is given in parentheses.
4. 100 mesh, ϕ, 30°C/min. N_2 flow·

Decreasing order in thermal stability:

PFH VI≃PFH VIII>PFH VII>PFH X>PFH XI>PFH XII.

Table 22

Percentage residue at temperatures, °C.

Grist Mesh B.S.	200	400	500	850	1070	Temperature at 50% loss, °C
22-30	98·1	92·4	89·4	60·0	58·3	553·0
30-44	98·2	95·5	87·5	60·0	58·5	551·0
44-85	97·5	94·6	86·3	59·8	59·4	541·0
85-100	97·9	91·6	85·7	60·2	58·7	532·0
100-120	97·8	92·0	87·5	60·1	58·4	560·0
120-170	96·6	88·9	83·2	55·6	54·5	530·0
170-Dust	90·0	77·9	70·3	48·7	47·6	464·0

Notes:

1. PFH IX, ϕ, 30°C/min. N_2 flow.
2. Effect of grist.
3. ∿ 34 mg weight is used.

Table 23

Percentage residue at temperatures, °C

Atmosphere	200	400	500	600	700	800	1070	Temperature at 50% loss °C
N_2 1scfh	98·4	94·0	86·2	-	-	56·9	55·6	554·0
N_2 2scfh	98·9	96·0	88·2	-	-	57·6	55·3	571·0
N_2 3scfh	99·0	93·8	85·0	-	-	56·5	55·2	532·0
N_2 4scfh	99·6	95·8	91·3	-	-	58·2	56·0	597·0
Air 2scfh	98·8	92·3	67·8	-	-	No residue at 800°C		--
CO_2 2scfh	98·6	93·7	85·1	81·1	61·2	55·8	46·9	569·0
Still atm	98·3	94·4	88·9	81·8	75·0	69·5	60·5	590·0

Notes:

1. Effect N_2 flow and different gases.
2. PFH VIII, 100 mesh, ϕ, 30°/C min, Still atm.$>N_2>CO_2$
3. ∼ 32 mg weight is used.

Decreasing order of thermal stability:

still atm $>N_2>CO_2 \gg$ air.

Table 24

Percentage residue at temperatures, °C

Sample	200	400	500	600	700	850	1070	Temperature at 50% loss °C
RW54859	99·0	81·3	44·3	30·0	27·4	26·0	25·2	430·0
B_1(5)	98·4	75·4	54·5	46·4	43·4	40·0	38·7	443·0
RW52487	99·6	74·7	35·2	20·6	18·5	17·3	16·6	421·0
C_1(10)	96·7	89·6	80·4	70·0	60·3	55·6	54·1	524·0
D_1(5)	97·6	83·0	68·8	61·6	49·4	48·2	47·3	496·0

Notes:

1. ∿ 25 mg weight is used.
2. 52 mesh, ϕ, 30°C/min. N_2 flow.
3. Effect of hexamine concentration on RW's.
4. % hexamine is given in parentheses.

   Decreasing order in thermal stability:

   $C_1 > D_1 > B_1 >$ RW54859 > RW52487.

Table 25

Percentage residue at temperatures, °C

Sample	200	400	500	850	1070	Temperature at 50% loss, °C
PFR	92·3	86·6	76·3	53·4	51·2	487·0
$PFRH_1$	93·3	87·4	78·4	53·6	52·3	523·0
$PFRH_2$	94·7	89·6	81·6	54·8	53·6	534·0
$PFRH_3$	95·2	90·2	82·4	57·1	55·5	546·0
$PFRH_4$	95·3	91·6	86·2	58·0	56·5	555·0
$PFRH_5$	95·7	91·8	88·5	60·8	58·7	577·0

Notes:-

1. ~ 26 mg weight is used ·
2. Effect of hexamine ·
3. 52 mesh, ϕ, 30°C/min. N_2 flow ·

Decreasing order in thermal stability:

$PFRH_5 > PFRH_4 > PFRH_3 > PFRH_2 > PFRH_1 > PFR$ ·

Table 26

Percentage residue at temperatures, °C

Sample	200	400	500	600	700	850	1070	Temperature at 50% Loss °C
PFS	99·2	81·4	67·4	57·5	50·3	46·0	45·0	455·0
PFHS I	98·7	88·1	80·3	71·5	61·3	55·1	53·5	526·0
PFHS II	99·0	90·3	83·3	74·5	62·2	56·8	55·5	538·0

Notes:

1. ∿ 40 mg weight is used.
2. Effect of sulphur.
3. 100 mesh, ϕ, 30°C/min, N_2 flow.
   Decreasing order of thermal stability:
   PFHS II>PFHS I>PFS.

Table 27

Percentage residue at temperatures, °C

Sample	200	400	500	850	1070	Temperature at 50% loss °C
PFHC	97·8	93·3	86·3	57·5	56·0	560·0
PFHC_o	95·2	93·9	86·6	56·6	55·0	559·0
PFHC_1	93·3	93·8	88·1	59·6	57·6	568·0
PFHC_2	97·5	93·8	86·6	59·0	57·4	555·0
PFHC_3	96·6	93·6	86·7	59·0	57·4	553·0
PFHC_4	97·1	93·6	85·7	59·2	57·7	543·0
PFHC_5	97·1	93·2	85·6	58·4	57·0	546·0
PFHC_6	97·0	93·5	87·5	59·8	58·0	563·0
PFHC_7	96·3	92·9	86·5	58·3	57·0	548·0
PFHC_8	97·9	93·2	89·1	58·5	56·7	574·0
PFHC_9	97·9	93·7	88·1	58·9	57·2	569·0

Notes:-

1. ∼ 26 mg weight is used.
2. Effect of various types of carbon.
3. 52 mesh, ϕ, 30°C/min, N_2 flow.

Table 28

Percentage residue at temperatures, °C

Sample	200	400	500	850	1070	Temperature at 50% loss °C
PFH-gluc.	98·8	92·6	83·8	54·8	53·4	546·0
PFH-suc.	98·1	89·1	72·8	53·5	51·4	534·0
PFH-sta.	98·8	92·0	84·4	54·4	52·6	558·0

Notes:

1. ~ 25 mg weight is used.
2. 52 mesh, ϕ, 30°C/min, N_2 flow.
3. Effect of carbohydrates.

Table 29

Percentage residue at temperatures, °C

Sample	200	400	500	850	1070	Temperature at 50% loss °C
PFH-Fur	98·7	92·8	80·6	51·2	50·0	541·0
PFH-PVAcry	98·0	91·7	80·7	52·2	50·3	537·0
PFH-PVAlc	98·1	92·0	81·8	52·7	51·1	537·0
PFH-PVC	97·7	90·0	83·8	54·9	52·8	549·0
PFH-Cell Bty	97·9	92·6	83·5	53·2	51·5	553·0
PFH-C.M.Cell.	98·9	91·8	82·9	53·0	51·2	553·0
PFH-N66	97·7	93·1	84·3	52·8	51·5	534·0
PFH-Psty	98·2	93·8	85·9	54·4	52·8	555·0

Notes:

1. ∿ 24 mg weight is used·
2. Effect of furfuryl alcohol and organic polymers·
3. 52 mesh, ϕ, 30°C/min, N_2 flow.

Table 30

Percentage residue at temperatures, °C

Sample	200	400	500	600	700	850	1070	Temperature at 50% loss °C
PFHAl	98·2	93·8	89·2	80·3	67·6	61·7	60·0	579·0
PFHCu	98·2	93·8	88·7	78·6	66·3	60·0	58·8	569·0
PFHMg	98·2	93·7	87·5	77·4	65·6	61·4	60·3	560·0
PFHZn	98·0	93·2	88·8	76·3	66·4	59·7	56·9	560·0

Notes:

1. Effect of powdered metals ·
2. ∿ 30 mg weight is used.
3. 52 mesh, ϕ, 30°C/min, N_2 flow .

Decreasing order of thermal stability:
Mg ≷ Al>Cu>Zn.

Table 31

Sample	Percentage residue at temperatures, °C 200	400	500	600	700	850	1070	Temperature at 50% loss °C
PFH-$AlCl_3$	97·6	88·8	81·2	71·2	59·6	53·4	51·4	541·0
PFH-$FeCl_3$	98·5	92·8	86·7	78·5	71·2	64·8	62·0	556·0
PFH-$ZnCl_2$	98·5	92·4	85·1	78·5	69·3	62·0	59·4	554·0

Notes:

1. Effect of Lewis acids.
2. ∿ 25 mg weight is used.
3. 52 mesh, ϕ, 30°C/min. N_2 flow.

Decreasing order of thermal stability:

$FeCL_3 > ZnCl_2 > AlCl_3$ ·

Table 32

Percentage residue at temperatures, °C

Sample	200	400	500	600	700	850	1070	Temperature at 50% loss °C
PFHHgO	99·0	91·5	82·8	72·3	59·9	53·1	51·4	551·0
PFHMnO_2	99·0	92·6	84·8	76·5	67·5	63·0	61·2	535·0
PFHSb_2O_3	99·3	94·7	89·6	80·2	68·8	61·2	59·3	582·0
PFHSiO_2	99·0	94·1	87·3	86·6	80·7	56·9	55·0	579·0
PFHZnO	99·0	93·8	86·5	78·0	67·8	60·4	57·3	575·0

Notes:

1. Effect of mineral oxides.
2. ~ 27 mg weight is used.
3. 52 mesh, ϕ, 30°C/min. N_2 flow.
   Decreasing order of thermal stability:

   $MnO_2 > Sb_2O_3 > ZnO > Si_2O > HgO$.

Table 33

Percentage residue at temperatures, °C

Sample	200	400	500	600	700	850	1070	Temperature at 50% loss °C
Asbestos	99·8	99·4	98·4	97·6	95·1	86·6	85·7	682·0
PFHA I	98·4	95·2	90·8	85·2	76·3	69·6	68·0	566·0
PFHA II	98·6	95·6	90·6	85·2	77·4	68·9	67·8	565·0
PFHASi	98·8	96·4	93·3	85·9	75·9	70·0	68·2	576·0
PFHAB	93·7	89·7	87·4	85·4	78·5	70·6	67·7	585·0
PFHALC	98·5	96·0	91·5	84·1	77·0	69·5	65·4	575·0
PFHASm	95·4	91·8	86·5	77·3	71·7	66·9	62·2	541·0
PFHASP	98·5	95·3	89·6	81·0	72·5	67·6	61·8	559·0
PFHAAl(OH)$_3$	96·8	89·0	84·6	76·7	65·1	58·4	55·8	541·0
PFHB	96·0	91·7	89·4	85·3	76·9	69·1	65·5	585·0
PFHSm	93·4	86·2	81·0	78·1	70·0	65·5	61·4	477·0
PFHRef	97·8	93·8	88·9	82·0	72·0	60·5	58·6	552·0
PFHSP	98·7	93·0	84·8	75·2	68·0	64·3	58·4	523·0
PFHLC	98·3	93·3	87·4	81·9	71·2	61·2	56·6	590·0
PFHAl(OH)$_3$	96·8	89·0	84·6	76·7	65·1	58·4	55·8	541·0
PFHGF	99·1	96·9	93·4	88·2	80·5	76·2	74·5	569·0
PFHAGF	99·2	97·1	94·6	89·2	80·3	74·3	72·8	587·0

Notes:

1. Effect of asbestos and inorganic additives - phenolic composites.
2. $\sim$ 24 mg weight is used.
3. 60 mesh, ϕ, 30°C/min. N_2 flow.

Table 33

Notes (contd)

Decreasing order of thermal stability

PFHA I = PFHA II

ASi>AB>ALC>ASm≈ASP>AAl$(OH)_3$

B>Sm>Ref≈SP>LC>Al$(OH)_3$

Table 34

Percentage residue at temperatures, °C

Sample	200	400	500	600	700	850	1070	Temperature at 50% loss °C
TX	98·0	92·4	67·4	63·7	62·0	60·8	57·5	442·0
PFHTX	97·7	93·9	86·7	74·8	63·6	58·2	55·4	554·0
RPD110	96·9	94·5	92·0	87·8	82·2	74·6	72·7	600·0
RPD150	98·5	95·3	93·5	89·5	84·4	74·0	72·0	643·0
RPD154	97·4	92·9	80·9	74·3	70·5	63·8	62·8	483·0

Notes:

1. 52 mesh, ϕ, 30°C/min. N_2 flow.
2. ∿ 25 mg weight is used.

Decreasing order of thermal stability:

RPD110≈RPD150>RPD154>PFHTX.

DISCUSSION

The term carbon or char is used for residue of phenolic resin and composite materials.

When a specimen is heated in ambient air or any gas of comparable density, the apparent weight changes with temperature due to displaced gas, and the specimen appears to gain weight as it is heated (Garn). Hence a correction for buoyancy must be made in order to get the exact weight of the residue at any instant. However, in the present investigations no buoyancy correction has been made since we were interested in the relative thermal stabilities. In order to determine the thermal stability, it was of interest to compare the percentage residual weight by TGA at 1070°C, under standard experimental conditions (30°C/min heating rate and N_2 flow 2 scfh). Some investigators use temperature at 50% loss of the ultimate loss, under identical conditions, as a standard of thermal stability.

While thermogravimetry is most widely used for obtaining information on the thermal stability of a polymeric material, we must bear in mind that this dynamic technique is highly dependent on experimental conditions. A strict comparison of thermal stabilities can only be obtained by analysing the samples under identical conditions. This limitation rules out any attempt to compile a meaningful library of thermograms obtained from different sources.

The correlation of polymer structure and thermal stability is of fundamental interest in the development of thermally stable polymers. Although no basic general theory has been devised certain principles have been discussed by various authors as a guide to predict and improve the thermal stability of a polymer.

Generally these principles have been arrived at and tested by preparing a series of compounds of known structures and by actually comparing their thermal stabilities. Dynamic thermogravimetry is ideally suited for such rapid screening and confirming purposes.

When a graph of weight loss or percentage weight loss of polymer is plotted against increasing temperature a sigmoid curve is generally obtained as shown in Fig. 19f (Learmonth[116a]).

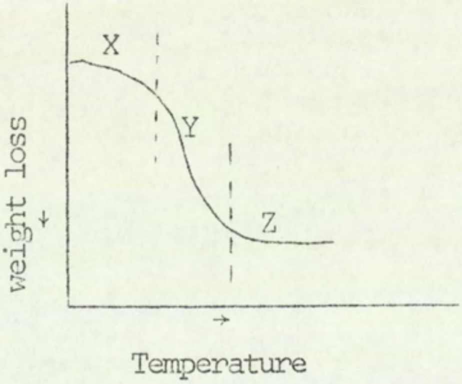

Fig. 19f.

The thermogram can be divided into three parts, i.e. X, Y and Z,

where X is due to small weight loss,

Y is due to rapid weight loss,

and Z is due to asymptotic weight loss.

At low temperatures (20 ∿ 400°C, part X) the weight loss is small for 30°C/min. This loss is consistent with a generalised mechanism for weight loss of phenolic resin which can be depicted as shown below:

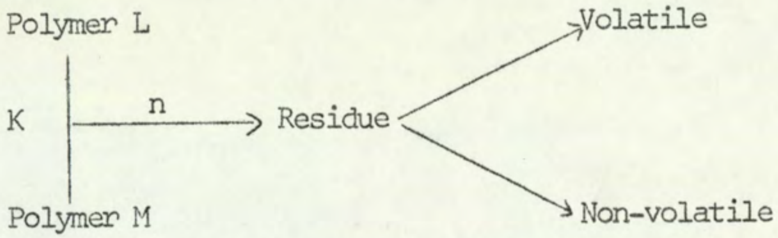

where polymer L is the starting cross-linked resin, polymer M is the post-cured material, n is the number of reaction steps required to give the products (volatile and non-volatile) and determined by the temperature and molecular weight of the polymer, and K is the extended condensation (post-curing). Weight loss at low heating rates would be greater than that observed at higher heating rates if the diffusion of material of high volatility (low molecular weight) is the mechanism controlling the weight loss. At high heating rates, the volatile species would be expected to undergo thermally induced further pyrolysis reactions, (K) since they would not have time to diffuse out of the solid matrix.

In the present investigations weight loss at 30°C/min is more than that at 25°C/min up to about 400°C Fig. 22b. Hence the diffusion of gases is not the mechanism controlling the weight loss.

At high temperatures (400 ∿ 750°C, part Y) more of the residue from polymer L is volatilised as it degrades. Thus part Y of the thermogram indicated catastrophic degradation and reformation stages of the resin. The rapid loss in weight is followed by stabilisation of the residue or very slow rate of break down ca 750°C, part Z.

" Though bond breaking occurs a good deal of the loss must be hydrogen, with consequent lower weight loss per mole".

Effect of curing time

The effect of curing time on the crosslinking and thermal stability of the resin R19370 is shown in Tables 20a and 20b. It appears from the tables that the cross-linking of the resin is complete within half an hour. The thermal stability (% residue and temperature at 50% loss) falls with increasing time. This decreases in heat stability is thought to be due to oxidation of the methylene bonds. 10% of hexamine appears to be a sufficient quantity for novolac cross-linking.

Effect of hexamine

The effect of hexamine concentration on curing and heat stability is shown in Table 21. It is found that a novolac cross-linked with 10% and 17% hexamine gave the maximum amount of carbon. The thermal stability of the resin cured with 5%, 30%, 40% and 50% is less than that of resin cross-linked with 10% and 17%. But it must be remembered that any excess of hexamine over the stoichiometric proportion will simply be lost as HCHO and NH_3 and this will appear as diminished thermal stability. In the sample PFH VII 5% of hexamine appears to be an insufficient quantity for curing, whereas in the samples PFH X, XI and XII there is an excess of hexamine. The very fast degradation of the last three specimens starts at ca.170°, 164° and 154°C respectively. Increase in hexamine concentration decreases the thermal stability by producing excess H_2CO, NH_3 and free radicals etc., which break up the structure of the hardened resin. Heron observed the same effect.

The order of lowering of the heat stability of the specimens PFH's is shown below:

PFH VI ≈ PFH VIII>PFH VII>PFH X>PFH XI>PFH XII.

Effect of grain size

The influence of grain size on the decomposition and heat stability is shown in Fig.22a and Table 22. Grist 22 to 120 mesh B.S. gave the maximum quantity of carbon. The rate of degradation becomes rapid, in the cases of particles of size below 120 mesh B.S. in the initial stages of heating. The decomposition of the specimen of grist 170-dust starts at lower temperature and is very rapid. Thus the heat stability of the resin decreases as the grain size is reduced. This is probably caused by mechanical and oxidative degradation during grinding and increase in the surface area of the resin. Heron and Conley et al have also shown that oxidation is mostly a surface phenomenon. The results of Heron *(loc cit)* showing the effect of particle size on degradation of resin are in close agreement with our findings. Jeffreys[47] also found that the smaller the particle size the greater the weight loss.

In the present case if temperatures at 50% loss (of the ultimate loss) is used as a parameter of thermal stability the results do not correspond to those where residual char is used. This scatter in temperatures is probably due to varying amount of volatile material entrapped in the specimens.

Influence of Gases

The influence of N_2,air and CO_2 flow and still atmosphere on the rate of decomposition of the resin sample PFH VII is shown in Fig.23 and Table 23. Carbon yield at 1070°C in N_2 flow 1-4 scfh is reasonably constant, showing that N_2 flow does not affect the degradation of the resin. In air atmosphere all of the resin is oxidised at ca.800°C. CO_2 markedly reduces the carbon yield at ca 950°C, as expected, on account of the reaction between CO_2 and carbon ,

$$CO_2 + C \rightleftharpoons 2CO.$$

Still atmosphere showed a beneficial effect on heat stability of the resin. The increased pressure of the effluent gases resulted in suppression of volatile products. Thenthey might have deposited carbon on the residue or surface of the platinum boat or modified the scheme of degradation. The amount of carbon is increased from about 55% in N_2 to 60·5% in still atmosphere (atm) at 1070°C.

The decreasing order of relative thermal stability is given below:

$$\text{still atm} > N_2 > CO_2 >> O_2 .$$

Resin RW54859, RW52487, B_1, C_1 and D_1.

The uncured novolac resin samples RW's start decomposing rapidly at about 250°C, whereas the cured samples begin rapid degradation at ca.450°C. The amount of carbonaceous residue at 1070°C of these specimens is less than for the standard cured and uncured novolac resin (R19370). See Table 24a, Fig.24.

Table 24a

% carbon residue at 1070°C

Sample	% residue at 1070°C	Table
RW54859	25·2	24
B_1	38·7	"
RW52487	16·6	"
C_1	54·1	"
D_1	47·3	"
R19370	32·0	20a
PFH VIII	55·9	21

The order of decreasing thermal stability of the uncured and cured resins is shown in the following series respectively,

$R19370 > RW54859 > RW52487$ and $PFH\ VIII > C_1 > D_1 > B_1$ ·

Thus DTA and TGA thermograms and % carbon at 1070°C clearly show the difference between the original resins (discussed under DTA).

Influence of hexamine on resole

The results of TGA studies of resole specimens are recorded in Table 25. The thermal stability increases as the hexamine concentration increases, which is reflected in the quantity of carbon at 1070°C and temperature at 50% loss (explained in DTA section).

The order of decreasing heat stability is as follows:

$PFRH_5 > PFRH_4 > PFRH_3 > PFRH_2 > PFRH_1 > PFR$.

Comparison of carbon yields

Table 25a summarises the work from different sources in order to compare the carbon quantity.

Table 25a

% char from TGA of phenolic resins

Sample	Char %	Temperature °C	Atmosphere	Heating rate °C/min	Investigator(s)
F/p = 1·3	56·5	1000	N_2 flow	5	Kohn[117]
F/p = 2·5	59·0	"	"	"	"
Phenolic	54·0	920	Vac 0·05 mm	3	Anderson[54]
"	41·0	"	"	"	"
Novolac 113 (uncured)	34·65	ca 600	-	20	Popov et al[51]
Novolac + 10% hexamine	45·61	"	-	"	"
Resole	60·0	"	-	"	"
Phenolic (Post-cured)	60·0	850	Argon flow	3·3	Lochte et al[32]
PFH VIII	55·9	1070	N_2 flow	30	Present work Table 21
"	60·5	"	Still atm	"	" Table 23
C_1	54·1	"	N_2 flow	"	" Table 24
R19370 (uncured) i.e. PFC	32·0	"	N_2 flow	10	" Table 24a
PFR	51·2	"	"	30	' Table 25
PFRH 5	58·7	"	"	"	" "

It is clear from the Table 25a that our values of the amount of carbon agree with those reported by other investigators. Thus the quantity of carbon is independent of the analytical variables and the history of the resins. Most probably, all these resins follow the same route of curing, post-curing, degradation and char formation.

Heat absorbing fillers

The heat absorbing fillers chosen were:

1. Sulphur
2. Asbestos
3. Various other organic and inorganic compounds.

These were selected because of

(1) the large amount of heat absorbed during thermal decomposition combined with substantial gas evolution. (To study the energy changes DTA of the phenolic composites is needed.) and

(2) to modify the quality and quantity of the char.

Influence of sulphur

The addition of 5% sulphur in the uncured resin 19370 increased the quantity of carbon from 32% to 45%. Sulphur might have reduced the quantity of the volatile products or have changed the course of degradation as to enhance the amount of carbon or presumably by increasing the degree of cross-linking of the decomposing polymer[118]. The addition of 5% sulphur to the resin plus hexamine before cross-linking showed no effect on the carbonaceous residue, Table 26 (Fig.26). It looks as if sulphur was swept out of the system by hexamine. The order of decreasing thermal stability is as follows:

PFHS II>PFHS I>PFS>PFC.

Effect of carbon, furfuryl alcohol, carbohydrates and organic polymers.

The addition of different types of carbon before curing the resin has not affected materially the quantity of char (Table 27). This appears anomalous and some further work might well be done at some future time. The mixing of carbohydrates, furfuryl alcohol and organic polymers before cross-linking the resin has rather shown adverse effect on char, i.e. the quantity of the carbon has decreased by a few per cent. H_2O, CO, H_2, CO_2 and other volatile products from these materials must have reacted with carbon to give more of CO and CO_2, which is responsible for the decreased quantity of carbon (Tables 27-29).

Influence of powdered metals, Lewis acids and mineral oxides.

Metals

The object of adding metals was to prevent oxidative degradation by producing a reducing environment.

Lewis Acids

These presumably act if the thermal reforming is ionic in nature, and they would actually be expected to assist in ring closures.

Acid catalysts (Lewis type) have been reported[12] to lower the decomposition temperature and change the course of degradation so as to produce a higher proportion of carbonaceous residue.

Mineral oxides

Mineral additions may act on the phenolic resins in two different ways:

(i) in small quantities they may have a catalytic effect,

(ii) in greater quantities they may combine with the resin to give organometallic chelates[119,120].

Tables 30-32 and Figs. 30-32 show the results of thermogravimetric analyses of the various resins. The examination of the different results makes it possible to conclude that the addition of metals, Lewis acids (except $AlCl_3$) and mineral oxides (except HgO) have increased the carbon yield. The decreasing order of the thermal stability is as follows:

(1) Metals $Mg \approx Al > Cu > Zn$.

(2) Lewis Acids $FeCl_3 > ZnCl_2 > AlCl_3$.

(3) Mineral oxides $MnO_2 > Sb_2O_3 > ZnO > SiO_2 > HgO$.

Kohn[121] has reported effect of 5% mineral oxides on thermal stability of the resin. He used the temperature at which pyrolysis started as the index of the heat stability. He found the decreasing order of thermal stability as follows:

$$MnO_2 > ZnO > SiO_2 > HgO > Al_2O_3 > As_2O_3 > CdO > BeO.$$

Kohn's observation is in agreement with the present work.

Influence of asbestos[122] and inorganic additives

Asbestos and inorganic additives were mainly added with a view to produce endothermic changes (i.e. DTA studies) but TGA studies were also made in order to see their effect on the thermal stability of the resin.

The effects of asbestos and inorganic additives on final char are given in Table 33. TGA curves are shown in Figs. 33a, 33b, 33c.

The residue left by the chrysotile asbestos is 85·7%. The phenolic samples PFHAI and II cured under pressure of 12 and 50 tons per square inch respectively, gave 68% char. This indicated that the cross-linking mechanism was independent of change in the pressure applied.

Six specimens of the resin cured with 6·25% hexamine + 25% asbestos + 12·5% inorganic additive (silica, boric acid, lead chloride, sodium metaborate or hydrated alumina) showed decrease in the thermal stability in the following order:

$$\mathrm{ASi>AB>ALC>ASm\approx ASP>AAl(OH)_3}.$$

The other six samples of the resin cured with 8% hexamine plus 17% inorganic fillers (given above) indicated decrease in the thermal stability in the following order:

$$\mathrm{B>Sm>Ref\approx SP>LC>Al(OH)_3}.$$

The other two samples PFHGF and PFHAGF cross-linked with 5% hexamine + 5% glass fibre and 5% hexamine + 25% asbestos + 25% glass fibre showed no appreciable difference in the final residue. The specimen containing asbestos is definitely better ablative material than the sample without asbestos because:

(1) asbestos gives a strong endothermic peak at ca 714°C, and

(2) specific gravity of the asbestos is less than that of the glass fibre.

From the Table 34 it is seen that the TX fibre (magnesia) did not affect the final residue of the phenolic resin.

Three commercial samples RPD110, RPD150 and RPD154 showed the following order of heat stability, (Fig. 34)

RPD110≈RPD150 > RPD154.

These are commercial materials made from chrysotile asbestos and an unknown resin, (but believed very similar to the one we used). It is known that RPD110 and RPD150 differ only in relative proportions of resin and asbestos, while RPD154 contains a proportion of a polyamide such as nylon.

SUMMARY

1. The thermograms from T.G.A. are much less spectacular than from D.T.A., but, being more consistent are more immediately useful.
2. The effects of curing conditions were confirmed. CO_2 was found to have quite a strong oxidising effect.
3. The addition of carbon gave a corresponding increase in the yield of charred residue. Various polymers had little effect.
4. Powdered metals gave a small increase in carbon yield - perhaps not significant.
5. Lewis acids, especially $FeCl_3$ gave a large increase in yield of residue.

6. Mineral Oxides - MnO_2, ZnO, etc. - gave some increase in residue.

7. Asbestos gave a high yield of char, but not when allowance had been made for the inorganic part.

8. Borates, phosphates and alumina affected the yield of carbon to varying degrees in the region 200-400°C and 600-1000°C.

9. A commercial material containing nylon showed the predicted loss between 350-700°C.

CONCLUSIONS

An accurate description of the pyrolysis mechanism is not possible, since it is uncertain whether the degradation products are directly produced from the resin or are formed by post-cracking of large fragments on the platinum boat. However, some simple conclusions may be drawn from the TGA results.

1. The carbon yield is dependent on the concentration of hexamine used in curing the novolac. 10-17% hexamine gave the maximum quantity of carbon. The resole used gave comparable results with 5% added hexamine.

2. The heat stability of the resin reaches a maximum at 10-17% and with higher concentrations of hexamine the loss in pryolysis increases again, but partly due to loss of unreacted hexamine.
3. Finer the particle size greater is the degradation, i.e. degradation temperature is lowered. This is consistent with pyrolysis being a surface phenomenon.
4. The rate of oxidative degradation of phenolic resin increased with increasing oxygen concentration.
5. The small addition of sulphur to uncured novolac resin increases the carbon yield but it does not influence the amount of carbon of cross-linked novolac resin.
6. Added carbon, furfuryl alcohol, carbohydrates and organic polymers do not appear to have much effect on the carbon yield.
7. It is possible to reduce the losses of phenolic resin as a function of temperature by means of additives like,

    (i) powdered metals,
    (ii) Lewis acids,
    and (iii) mineral oxides.

    The most effective additive in each class is Mg(%Al), $FeCl_3$ and MnO_2 respectively, and it is clear that each of these is affecting one stage or other of pyrolysis.
8. Cross-linking and mineral addition to the novolac resin shifts the catastrophic degradation temperature from ca. 250°C (of uncured resin) to ca 400-450°C.

9. Asbestos and inorganic additives show generally increase in the heat stability of the resin.

These basic results suggest that thermal stability of the phenolic resins can be improved by:

1. removing volatile products of curing or post-curing,
2. by fully cross-linking the resin,
3. excluding oxygen and CO_2 from the atmosphere,
4. adding suitable minerals,
5. nature of the resin.

The following observations have been made by Jeffreys:

(1) Substitution of the phenolic nucleus reduces the heat stability.

(2) The longer the length of the substituent chain (up to a certain chain length) the lower is the stability.

(3) Branching of the alkyl substituent leads to decreased stability.

(4) The condensation of phenols with benzaldehyde and furfuraldehyde gives resins with inferior heat stability to those from formaldehyde.

Note: Our criterion of thermal stability is the quantity of carbon produced which may or may not be a complete analysis of the ablative picture. Since in addition to carbon yield the ablation process depends on the following factors:-

1. Structure of the carbon-amorphors or graphite.
2. Hardness and thermal conductivity of the carbon.
3. Orientation of the graphitic layers.
4. Fineness and porosity of the carbon.

5. Endothermic reactions.
6. Quantity and nature of the volatile products.

CHAPTER V11

CALCULATIONS OF ACTIVATION ENERGY BY DTA

For the simple reaction such as $\text{solid}_1 \xrightarrow{\Delta} \text{solid}_2 + \text{gas}\uparrow$ the Kissinger's *(loc cit)* equation

$$d \ln (\phi/T_m^2)/d(1/T_m) = -E/R.$$

is used for the evaluation of activation energies of the chemical transformations occurring at peak temperatures T_m. The above equation is applied to the events occurring at peaks 'B', 'C', 'D', 'F' and 'H' respectively, in order to calculate activation energies. Figs.3a, 3b and 3c. The necessary data obtained by the use of Kissinger's equation is given below in Table 34.

Table 34

Data obtained by the use of Kissinger's method

Peak	ϕ, °C/min	T_m °k	$\log(\phi/T_m^2)$	$T_m^{-1} \times 10^3$ °k	E, kcal/mole
	10	371·0	-9·53	2·69	
	20	377·5	-8·87	2·65	
	30	387·0	-8·52	2·58	
	40	382·0	-8·20	2·62	
B	50	378·0	-7·96	2·64	30·0
	60	382·0	-7·80	2·61	
	70	395·0	-7·71	2·53	
	90	395·0	-7·46	2·53	
	100	382·0	-7·28	2·61	

Peak	ϕ, °C/min	T_m °k	$\log(\phi/T_m^2)$	$T_m^{-1} x 10^3$ °k	E, kcal/mole
	10	427·5	-9·81	2·34	
	20	431·0	-9·14	2·32	
	30	434·5	-8·75	2·30	
	40	435·0	-8·46	2·30	
C	50	442·0	-8·27	2·26	62·0
	60	431·0	-8·04	2·23	
	70	432·5	-7·89	2·31	
	90	444·0	-7·69	2·25	
	100	440·0	-7·57	2·27	
	10	457·5	-9·95	2·18	
	20	461·0	-9·27	2·17	
	30	478·0	-8·94	2·09	
	40	487·5	-8·70	2·05	
D	50	505·0	-8·54	1·98	24·0
	60	487·0	-8·28	2·05	
	70	-	-	-	
	90	497·0	-7·92	2·01	
	100	498·0	-7·81	2·01	

Peak	ϕ, °C/min	T_m °k	$\log(\phi/T_m^2)$	$T_m^{-1}\times10^3$ °k	E, kcal/mole
	10	588•0	-10•45	1•70	
	20	589•0	-9•76	1•69	
	30	597•0	-9•38	1•67	
	40	-	-	-	
E	50	605•0	-8•90	1•65	85•3
	60	602•0	-8•70	1•66	
	70	592•0	-8•52	1•69	
	90	594•0	-8•27	1•68	
	100	604•0	-8•20	1•65	
	10	638•0	-10•65	1•57	
	20	649•0	-9•96	1•54	
	30	646•0	-9•54	1•54	
	40	636•0	-9•22	1•57	
F	50	647•0	-9•03	1•54	36•0
	60	653•0	-8•87	1•53	
	70	665•0	-8•65	1•51	
	90	655•0	-8•50	1•52	
	100	664•0	-8•41	1•50	

Peak	ϕ, °C/min	T_m °k	log($/T_m^2$)	T_m^{-1}x10^3 °k	E, kcal/mole
	10	678·0	-10·74	1·47	
	20	692·0	-10·08	1·44	
	30	694·0	-9·68	1·44	
	40	703·0	-9·42	1·42	
H	50	703·0	-9·20	1·42	64·0
	60	702·0	-9·01	1·42	
	70	713·0	-8·89	1·40	
	90	717·0	-8·65	1·39	
	100	716·0	-8·54	1·39	

A straight line is obtained by a plot of

$$d \ln \left(\frac{\phi}{T_m{}^2}\right) \text{ versus } \frac{1}{T_m}$$

and its slope multiplied by 2·303R gives an activation energy E kcals/mole for each peak. Fig. 8e, P. 78.

Comparison of Activation Energies, E.

Shulman and Lochte *(loc cit)* have investigated the degradation of phenol-formaldehyde polycondensates by mass spectrometric thermal analysis up to 800°C. They have reported values of activation energies for the formation of each product and for degradation of the polymer. These values are compared with those obtained by us in the following Table 35.

Table 35

Shulman and Lochte

Product	Resin D, F/P = 2·00 E, kcal/mole	Resin B, F/P = 2·36 E, kcal/mole
H_2	29	32
CH_4	18	17
H_2O	27	17
CO	28/56	40/45
CH_2O	16	11
CO_2	19	-
C_6H_6	-	-
Toluene	-	28
Phenol	99	57
Cresols	74	48
Xylenols	88	55

Present Work

	Resin R19370, PFG	
Peak	Temperature, °C	E, kcal/mole
B	98·0 - 109·0	30·0
C	154·5 - 167·0	62·0
D*	184·5 - 225·0	24·0
E	315·0 - 331·0	85·3
F	365·0 - 391·0	36·0
H	405·0 - 443·0	64·0

*Exothermic

The values of the energy of activation vary from 16•0 - 99•0 kcal/mole and 11•0 - 57•0 kcal/mole for the resin D and B respectively, whereas our values range from 24 - 85•3 kcal/mole. Conley and Bieron, Madorsky, Friedman, Farmer, Heron and Wilson have reported the overall values of the activation energies, 19•5, 18, 55, 13-20, 15 and 16-35 kcal/mole respectively, for the degradation of phenolic resin.

Activation energies for phenolic decomposition show considerable variations, due to a number of factors. The purity, phenol/formaldehyde ratio, catalyst, degree and mode of cross-linking, oxidative degradation, thermal scission and degradative atmosphere. Variation in experimental techniques and formal treatment of the kinetic data also leads to further discrepancies in the values obtained.

Some more explanation is necessary in order to rationalise the differences in the activation energies obtained by different workers. The thermal degradation of a polymer is generally a many-step process, each step having its own rate and activation energy. The overall rate observed is a function of the rates of the specific steps (controlled, of course, by the slowest step) and the overall activation energy is likewise related to the activation energies of the various individual reactions. A thorough discussion of these points can be found in Wall and Flynn's excellent review* of polymer degradation in which they show (if chain transfer is neglected) that

$$E_{th} = (E_1/2) + E_2 - (E_4/2)$$

---

* Wall, L.A. and Flynn, J.H., Rubber Chem.and Technology, <u>35</u>, 1157 (1962)

where E_{th} = the overall energy of activation for the thermal decompostion,

E_1 = the activation energy for the initiation step (homolytic scission of a carbon-carbon bond),

E_2 = the activation energy for depropagation,

E_3 = the activation energy of chain transfer (neglected, being unimportant),

and E_4 = the activation energy for the chain termination.

In the gas phase E_4 is generally assumed to be zero, but in a viscous condensed medium a value as high as 20 kcal/mole has been reported* for polymethylmethacrylate. It should also be realised that the importance of depropagation is greatest when pyrolysis occurs at relatively low temperatures and the number of homolytic carbon-carbon scissions per given period of time is small. If, however, the pyrolysis is carried out at higher temperatures where a large number of carbon-carbon scissions occur in a given period of time, the contribution of depropagation to overall degradation tends to become negligible.

At higher temperatures one can expect that polymer degradation should tend to occur primarily by random carbon-carbon scission and the role of degradation should become less important. Under these conditions E_{th} approaches either D(R-R) or E, (which is equal to D(R-R) + E_4), depending on what effect radical recombination has on the rate of degradation. D(R-R) is the dissociation energy of the carbon-carbon bond. Since D(R-R) is generally in the range of 60-85 kcal/mole, the activation energies obtained in this study are quite reasonable.

Moreover, these values of activation energies are quite comparable

---

* Simha, R., Wall, L.A. and Bren, J.,. J.Chem.Phys. <u>29</u>, 894 (1958)

with those of Shulman and Lochte obtained for degradation products of phenolic resins. Thus showing that our values of activation energies are due to thermal scission of carbon-carbon bonds, while the low values reported by other workers are for the oxidative degradation of the resin.

CALCULATION OF ACTIVATION ENERGY BY TGA

Gravimetric methods for the determination of rate of degradation at constant or programmed temperatures are satisfactory only for polymers with a very little non-volatile residue. For char-forming polymers, the kinetic calculations must be confined to the first few per cent of weight loss to avoid complications introduced by assumption of an active weight fraction, with an inert char equal at all stages of degradation to the product of residual weight fraction and the active fraction which has reacted. This method cannot apply to phenolic resins with any reliability since the initial weight loss is caused mostly by post-curing rather than general degradation.

Reich equation (16),

$$E = \frac{2 \cdot 303R \log \left| \frac{(\phi)_2}{(\phi)1} \left(\frac{T_1}{T_2} \right)^2 \right|}{(1/T_1 - 1/T_2)}$$

is used to calculate the energy of activation of phenolic resin (PFH XIV) degradation in the temperature range 500-650°C. The temperatures corresponding to the same weight loss on heating rates of 30° and 25°C/min, from Fig.22b, and the energy of activation are given in Table 36.

Table 36

Parameters of the above equation

Weight loss mg	T_2 °k (at 30°C/min)	T_1 °k (at 25°C/min)	E kcal/mole
27·5	813	793	7·65
26·5	841	818	7·59
25·5	863	843	9·68
24·5	888	865	8·76
23·5	908	888	11·10
22·5	929	911	8·66

The mean value of E is 8·90 kcal/mole.

Assuming the weight of final char is constant, we can apply the first order equation to the degradation of the resin.

$$K = \frac{2\cdot 303}{t} \log \frac{\omega_\infty - \omega_o}{\omega_\infty - \omega_t}$$

where K = Rate constant, min^{-1},

t = Time (minutes),

ω_∞ = Final weight of char,

ω_o = Initial weight of the resin,

ω_t = Weight of the residue at any time (t).

Table 37

Kinetic data for the resin PFH XIV in the range
450 - 700°C (30°C/min)

Time minutes	$-(\omega_\infty-\omega_0)$ mg	$-(\omega_\infty-\omega_t)$ mg	K, $\text{min}^{-1}\times10^{-2}$
18	17·85	9·65	2·6
19	17·85	8·55	3·0
20	17·85	7·35	3·7
21	17·85	5·85	4·5

Table 38

Kinetic data for the resin PFH-Al in the range
500 - 680°C (30°C/min)

Time minutes	$-(\omega_\infty-\omega_0)$ mg	$-(\omega_\infty-\omega_t)$	K, $\text{min}^{-1}\times10^{-2}$
17	11·95	8·45	2·0
18	11·95	7·75	2·4
19	11·95	6·85	2·9
20	11·95	6·05	3·0

The values of rate constants are reasonably consistent in both the cases of cross-linked resin and the resin cured in the presence of powdered aluminium metal. Hence the degradation of the resin in the range of 450 - 700°C follows first order reaction kinetics.

Since the different products have quite different activation energies (and are formed in different temperature ranges), the average activation energy is a function of temperature. For polymers with a high **percentage** of residual char, thermogravimetric kinetic techniques are not very satisfactory. The difference between activation energies reported earlier is caused mainly by using different stages of cure as the basis for determining initial weight and phenol formaldehyde ratio.

Shulman and Lochte *(loc cit)* have reported values of the activation energies of the order of 11-16 kcal/mole for H_2CO, 17 kcal/mole for H_2O and 16·7 - 19·5 kcal/mole for low temperature oxidation.

The different energies of activation are obtained for decomposition of resin by DTA and TGA in the present studies. Since the starting material is the same, the question arises as to what causes these differences. There are four distinct possibilities:

1. A change in the basic mechanism of pyrolysis,
2. Participation of the secondary or "cracking" reactions,
3. Major oxidative degradation. ((a) TGA was carried out three months later than DTA, (b) The purging of thermogravimetric equipment was not effective.)
4. Platinum boat might have acted catalytically to change the course of reaction. (This point needs further verification.)

Thus, it is very likely that O_2 is necessary for the reaction to occur at relatively low temperatures and its presence must indeed result in a lower activation energy for a phenolic system. For purely thermal effects higher activation energy will be necessary and it is reasonable to expect a different reaction route.

Not enough is known of the basic mechanism alone to exclude the possibility of change. The formation of degradation products could be the result of free radical formation and oxidative degradation may partly follow ionic process (Madorsky and Levine). However, a change in mechanism would affect the nature of volatile products and of the residue, whereas the participation of cracking would be reflected only in the nature of gases. The smoothness of TGA curves argues against the change in mechanism. But a marked difference in the volatile constituents, observed at 300°, 500°, 800° and 1200°C (Madorsky) suggests an increasing participation of secondary or "cracking" reactions.

In a cross-linked polymeric system the onset and end of pyrolysis are not well defined. The process of thermal degradation is continuous and includes consecutive chemical reactions.

CONCLUSIONS

1. The high values of activation energy indicate thermal scission of C-C bonds, which is followed by free radical mechanism of degradation.
2. The low values of activation energy show oxidative degradation and is presumably partly followed by ionic reactions.
3. It may not be easy to isolate thermal degradation from oxidative degradation.

SUMMARY

It is shown[47] that both substitution of the phenolic nucleus and replacement of H_2CO by benzaldehyde and furfuraldehyde give resins of inferior heat stability as compared to the ordinary phenolformaldehyde resin. Hence, the presence of a methylene bridge is thermally much more stable than a substituted one[123].

There are at least two important reasons for this good thermal stability. First is the extreme stability of methylene bridges in the highly cross-linked network. This in turn is due to resonance stabilisation of the benzyl group. The effect of phenyl groups on the stability of the methyl radical is remarkable. Free benzyl can be represented by five different electronic structures,

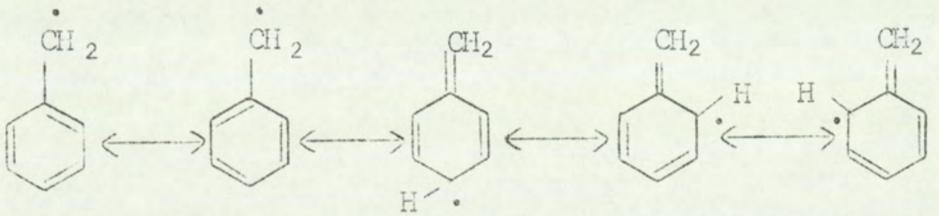

.

Second is the high concentration of benzene rings in the cross-linked network. The phenyl radicals formed by pyrolysis of the resin could coalesce into clusters of benzene rings, which would have high resonance stabilisation energy characteristic of condensed ring systems. Evidently this is also responsible for the large amounts of carbon remaining after pyrolysis. The whole structure is made up of solid covalent bonds.

However, in the phenolic resin the $-CH_2-$ groups are the most labile part of the structure and will be the first point of attack. At elevated temperatures, these are probably, for the most part, eliminated as free radicals. The free radicals combine to form a variety of aliphatic hydrocarbons and olefins. Meanwhile the active sites on the aromatic nuclei could react to form a polyphenyl type structure. Alternatively these methylene radicals will be oxidised to formaldehyde, methanol or formic acid or will be reduced to methane and formaldehyde. If somehow or other the methylene groups are protected from oxidative attack the thermal stability of the resin will improve considerably.

The reinforcement and fillers are important in moulding materials, but the chemistry of the resin is believed to play a major role in affecting the ablation rate. In ablation, the specimen is subjected to high heating rates on the outside surface. At any time, the specimen is undergoing varying degrees of decomposition depending on the rate of heating, time of exposure and distance from the surface. It would not be easy to prescribe a definitive mechanism. In addition to the expenditure of energy in dissociation of the resin, oxidation effects at the surface complicate the energy balance by the exotherm of the combustion process.

CHAPTER V111

TECHNOLOGICAL SIGNIFICANCE OF JOINT D.T A. AND T.G.A. RESULTS

This section provides an opportunity of correlating the results of D.T.A. and T.G.A. discussed above, and assessing them in a more practical way relative to their application as thermal insulators.

1. The experiments made were restricted to a maximal temperature of about 1000°C. It is true that further incease in temperature is not likely to affect the basic reactions occurring in the absence of oxygen, but other reactions may be possible. It has been shown that CO_2 is apparently oxidising over about 600°C, and the effect of temperature is not known. Secondly solid phase reactions of carbon are likely above 1000°C, e.g. with SiO_2 and this also has not been explored. Further extension of this work is essential as temperatures of 2-3000°C are expected in practice.

2. D.T.A., under the conditions used, proved somewhat capricious and results from it need to be interpreted cautiously (See P. 98). However it does provide some clue as to the nature of the reactions occurring and some correlation with T.G.A. is possible - at least for the main peaks.

   T.G.A., on the other hand, proved a more consistent guide to the course of reactions, though even here there are several anomalies. New equipment now available will allow future work to be done using simultaneous D.T.A. and T.G.A. The technique is less sensitive than the D.T.A. and in general only three main peaks could be defined.

3. Investigation of process variables and analytical variables in general was only valuable in that it enabled areas to be defined where the results were not very sensitive to variables. Some anomalies are discussed in later paragraphs.

4. Resins. The same commercial novolac was used generally and only a limited investigation was made of other resins.

A number of points have arisen which suggest further investigation, though the effects may be second order of magnitude.

(a) No investigation was made of the degree of cross-linking achieved, and this may vary as the resin is changed. In particular the addition of hexamine to the high temperature resole, D.V. 19162 showed an appreciable and unexpected increase in carbon yield.

The use of xylenol based novolac appeared to give higher residue after pyrolysis, though the effect of hexa content was not fully investigated.

Some experiments should be made with the American resin CTL91LD which has been described by a number of investigators.

5. Curing Conditions

No evidence was obtained to show that the conditions under which a resin was cured and postcured had much effect on the pyrolyses. This is however an apparent contradiction to a large body of evidence from various sources. There are however several results which show anomalies in the first stage of pyrolysis.

(a) The addition of boric acid or sodium metaborate shows a very large endotherm at about 150°C and there is some indication of this with sodium metaphosphate. This is correlated with a high initial loss in weight but apparently a final high yield of carbon. One might assume therefore that primary curing had been inhibited. However this does not take into account the fact, wellknown empirically, that during of both novolac and resoles is highly exothermic at about 130-170°C (in presence of air). Does this mean that oxidation during curing is the norm? In any case careful investigation of these materials would be useful. Care must be taken to cover the difference liekly to be found in postcuring provided resins, such as we have used, and commercial moulding up to several kilogram in weight.

6. The conditions of analyses show variations of one sort or another, but one point which may well have significance is the effect of CO_2 in the atmosphere. This appears to be inert except over 800°C where it causes severe additional loss of material. Note also the high residue under "still air" conditions.

7. There was some indication from T.G.A., partly correlated with D.T.A. that the thermal reforming stage of pyrolysis could be modified. For example boric acid and sodium metaborate and alumina appeared to show less here, while aluminium trihydrate acclerated them. Boric acid in particular should be investigated further. RPD154 resin showed high losses in this stage but it contains an unknown proportion of a polyamide resin.

8. Though in the discussion the addition of carbon filler is discounted, it is true that it gave a somewhat higher yield of carbon, as would be expected. This may be worth further investigation.

9. The addition of powered metals showed only a small effect, but Lewis Acids - $FeCl_3$ in particular - showed a distinctly increased carbon yield, and this is distinctly worth considering further. A further search for other catalytic materials might also be made.

10. There was some indication that manganese oxide and antimony oxide showed increased char formation, and this agrees with the work of Kohn. However the effect must be small and retention of the oxide in the char has probably occurred. While this could be investigated further, it does not seem a very promising area.

11. D.T.A. showed major effects from the addition of materials known to lose water. Alumium trihydrate gave a sharp and consistent peak at $300^{o}C$ and chrysotile one at 700°C. This is reflected to some degree only in the T.G.A. curves, but an additional aspect will be discussed later. In the thermal reforming stage of pyrolysis alumina showed some effect but this may be unconnected with the endothermic loss of water, which should have been complete previously. The loss of water for chrysotile asbestos seemed to have little effect, and this may be due to the nature of reactions occurring over $700^{o}C$. It will be interesting in the future to add montmorillonite or other clay minerals or zeolites likely to lose water in the range $400\text{-}700^{o}C$. as this might well affect the thermal reforming. At the same time it has been shown by Madorsky and others that losses of fragments are

less at higher temperature and it may be that cooling the reaction at this stage will be ineffective.

12. A number of D.T.A. peaks are anomalous, and cannot be explained. For example, where hexamine is deficient or absent in a novolac compound, there is always a sharp 'H' peak at 400°C (endotherm). This is unexpected, but may be due to an alternative curing mechanism or loss of some major low molecular weight constituent of the resin or fragment. Again, there is an exothermic 'D' peak at 225-300°C, and this is also erratic though nearly always present. It must be admitted that at the moment we cannot be sure that it is truly an exotherm at this point.

The errant behaviour of the base line presents such identification. It is possible that the associated 'C' peak represents bond breaking, and the exotherm 'D' represents ring formation, but it seems unlikely that these two porcesses will be discrete.

The absence of a 'curing' exotherm has already been commented upon.

13. One possibility which was not pursued, but is possibly interesting in view of the results shown above is the use of a chlorinated phenol in the resin. This would lose HCl at some temperature between 200 and 400°C, and though this would cause a large decrease in weight, it will also presumably remove a considerable amount of energy from the system. Such resins have been described from time to time. A chloro-m-cresol might be persuaded to ring close during pyrolysis.

This raises the generally interesting question as to whether the ablative material we are studying may best be modified by obtaining a higher yield and stronger carbon during pyrolysis, or by the provision of large quantities of low molecular weight material such as hydrogen to cool the system down. We are not able to answer this question, but would refer to the paper by C.E. Mauk of Houston Research Inc. and others who have discussed ablation and generally favour carbon formation. Firing trials of materials containing carbon might well settle this point. One point which we might investigate is the use of cardanol or other phenol with a substantial aliphatic element pendant to the network.

5. In this work we have not especially considered the nature of the reactions in pyrolysis, and we are not aware that this has been discussed clearly by others. It has been assumed that free radicals take part largely (Ouchi, Conley) but except for a paper by Neiman (on epoxy resins) there has not been reported any verification of this. This point seems important, and perhaps we may speculate a little upon it.

<u>Stage 1</u>. Completion of curing - Postcuring. $\angle 200^\circ$C

This is likely to be ionic in nature, and it is known that acids and alkalis and some metals affect it. The only possible radical mechanisms would seem to be polymerisation of quinone methide structures, and there is little evidence available for this. This stage should therefore be subject to catalysis by a variety of compounds.

Stage 2. Thermal Reforming 150-450°C

Perhaps this is a radical process initiated by thermal or thermo-oxidative fission and rapidly terminating by formation of aromatic rings (or condensed rings). In this case radicals should be detectable, and perhaps radical donors or acceptors might modify the course of it. The temperature range seems unfavourable however, and complex, phenols such as are present are often used as radical acceptors.

This is the stage, however, whereby the fate of units in the network is decided and further investigation is essential.

Stage 3. Carbonisation

This must undoubtedly involve free radical processes, though the radicals may not be mobile, and this may account for the condensed ring system resulting.

To sum up, it would appear that this investigation has identified the stages of pyrolysis of phenolic resins, especially in presence of active or inactive additaments. It has however raised more questions than it has answered, and some of these seem important and potentially fruitful.

Firstly, before proceeding further it is necessary to have confirmation as to whether or no increased carbon yield can be correlated with good ablation resistance. If it can be then the results indicate several areas from which the investigation can be extended. If this is not so, further efforts will have to be directed to finding systems having higher losses of low molecular weight material (especially hydrogen or water) to remove energy from the system by one of the methods mentioned in the introduction.

Some of the results obtained indicate the value of added materials, but this is conditional to some extent by the technological processes required. It is essential therefore to examine at least empirically the effect of some of the proposals upon compounding and moulding properties of the resins. This can readily be done when some additional equipment is available.

In addition to estimating the ablative properties of the compounds described, it is necessary to obtain some information about other properties such as strength and extensibility in tension, and the thermal conductivity.

ACTIONS:

It is recommended that future work be concentrated on the following items.

(1) Simultaneous D.T.A. and T.G.A. to clear up anomalies shown above.

(2) Use of other types of asbestos - e.g. crocidolite and vary proportions.

(3) Addition of carbon as a filler.

(4) Addition of boric acid and borates and phosphates, including triphenylphosphate.

(5) Investigation of other hydrated minerals.

(6) Further investigation of Lewis Acids.

(7) Investigation of other concentrated catalysts.

(8) Consideration of radical acceptors and donors, e.g. fluorinated additives or stable peroxides or azo compounds.

(9) Use of chlorinated phenols.

Investigation of effect of degree of crosslinking

Reinvestigation of the effect of curing/postcuring cycle including use of cured resin as a filler.

Evaluation of several compounded materials as insulators, by firing trials

- (a) Containing carbon fillers
- (b) Containing other types of asbestos and varying proportions of resin
- (c) With $FeCl_3$ content
- (d) With cured resin as a filler
- (e) Use of resoles - with mix techniques.

PART II

CHAPTER 1X

SYNOPSIS

Samples of novolac resin cured with hexamine have been pyrolysed isothermally at 320, 360, 440, 555°C, alone and also in the presence of metals, metal oxides, and various inorganic salts.

The increase in the rate of weight loss with temperature and decrease with time have been expressed by two different experimental equations.

It was found that overall activation energies were smaller than reported by other workers, but comparable with the values found by programmed T.G.A. Though the existence of different activation energies in the various stages of pyrolysis were confirmed, but more information is required before these are definitive.

The added materials had large effects on the reaction at low temperature, and in general accelerated decomposition, though A.D.O.P. had an extraordinary retarding effect up to about 500°C. In some cases, this may be associated with formation of complexes with the resin or fragments formed by pyrolysis.

INTRODUCTION

During the last two decades some interesting experimental work has been reported in the literature on rates and activation energies of thermal degradation of polymers. Quite recently the use of polymers in rockets, missiles, space satellites, Apollo and Soyuz programmes has stimulated great interest in systematic research on pyrolysis of polymers. Such studies should be of value in at least two ways. They should provide information regarding both the thermal breakdown of polymers under service conditions at high temperatures and the mechanism or mechanisms of thermal degradation. Such information may lead to suggestions for improving thermal stability.

Grassie and Melville[124] measured the vapour pressure of the pyrolysis products of polymethyl methacrylate in vacuum. Jellinek[125] measured the rate of loss in weight of polystyrene, poly-α-methylstyrene and polyethylene in a vacuum. Oaks and Richards[126] studied degradation rate of polyethylene by measuring rate of change in intrinsic viscosity of thermally degraded specimens. Madorsky[127] measured rates of thermal degradation of polystyrene and polyethylene in a vacuum. Madorsky and Straus[25] determined the activation energies and thermal stability of polyesters, epoxy, phenolic and silicone plastics in a vacuum at 360, 500, 800 and 1200°C.

Besides this the literature survey showed that fairly large body of work has been done on programmed thermogravimetric analysis[73,77,79] of polymeric and non-polymeric materials. But relatively very little work has been carried out on isothermal thermogravimetric analysis. Therefore, we were tempted to study compounded and uncompounded phenolic resin by the latter technique and compare the effects of isothermal conditions on thermal stability and activation energy of degradation of the resin samples. Moreover, the present investigations were made in air/self-generated atmosphere of pyrolysis of the resin. These conditions are nearer to those met in the rocket motor, no doubt here the temperature conditions are mild as compared with those of high temperatures prevailing in the rocket motor. It was hoped to obtain some useful information about the relative importance of the various stages of pyrolysis occurring at different temperatures.

Preparation of the Resin Samples

Table OC

The resin specimen number and composition

Specimen Number	Composition		
	Resin, %	Hexa. %	Additive, %
1C	90.0	10.0	-
2C	85.0	10.0	5.0 Cu grit
3C	85.0	10.0	5.0 Mg grit
4C	85.0	10.0	5.0 Al grit
5C	85.0	10.0	5.0 Sm
6C	85.0	10.0	5.0 PSTP
7C	85.0	10.0	5.0 $AlCl_3$ (hydrated)
8C	85.0	10.0	5.0 $FeCl_3$ (anhydrous)
9C	85.0	10.0	5.0 Sb_2O_3
10C	85.0	10.0	5.0 MgO
11C	85.0	10.0	5.0 ADOP
12C	80.0	10.0	10.0 ADOP
13C	75.0	10.0	15.0 ADOP
14C	70.0	10.0	20.0 ADOP
15C	65.0	10.0	25.0 ADOP
16C	60.0	10.0	30.0 ADOP
17C	50.0	10.0	40.0 ADOP
18C	40.0	10.0	50.0 ADOP
19C	30.0	10.0	60.0 ADOP
20C	20.0	10.0	70.0 ADOP
21C	10.0	10.0	80.0 ADOP
22C	-	-	100.0 ADOP

Sm = Sodium metaborate

PSTP = Penta sodium triphosphate

ADOP = Ammonium dihydrogen orthophosphate

The commercial phenolic resin, R19370, hexa and the different additives were mixed properly and cross-linked in air at 150°C. The resin specimen number and composition at curing time and temperature of 1 hour and 150°C respectively are shown in Table OC.

The samples number 18C - 22C were viscuous and mucky at thetop and could not be ground. So they were further cured at 200°C for one hour in air. Then all the samples were ground with iron pestle and mortar and passed through a 100 mesh B.S. sieve.

Isothermal Thermogravimetric Analysis (ITGA)

Studies of Compounded and Uncompounded Phenolic Resin

Conditions of study

1	Grist	100 B.S. mesh - dust
2	Atmosphere	Air/self-generated (i.e. pyrolysis products)
3	Isothermal temperatures, °C	320, 360, 460, 555 and 670
4	Time of study	40 minutes
5	Thermocouple	Chromel/alumel
6	Crucible	10 ml silica
7	Balance	Mettler

Procedure

0.500 g of each specimen were investigated in a 10 ml silica crucible in air/self-generated atmosphere. The samples were levelled in the crucible in the same manner by tapping its bottom against the top of a table. The temperature of the furnace was controlled by a variac and a voltameter combination and it was noted by a chromel/alumel thermocouple in conjunction with a pyrometer. The pyrometer and the thermocouple were calibrated at different temperatures with substances like benzoic acid, $CuSO_4.5H_2O$, sulphur, $Ba(NO_3)_2$ and NaCl. At the termination of each experiment the tip of the thermocouple was placed in the centre of the crucible, held at the same position in the furnace, and the experimental temperature was recorded. The block diagram of the apparatus is shown in Figure OC.

The weight losses of each specimen at 320, 360, 460, 555 and 670°C were observed at different times over a period of 40 minutes.

RESULTS

The results are given in Tables 1C-14C.

Table 1C

Thermal degradation of the resin sample No. 1C at various temperatures.

Heating time, min	320° C		360° C		460° C		555° C	
	Loss of weight		Loss of weight		Loss of weight		Loss of weight	
	Amount, %	Rate, %/min	Amount, %	Rate, %/min	Amount, %	Rate, %/min	Amount,	Rate, %/min
1	2.2	2.20	2.6	2.60	4.2	4.20	8.8	8.80
2	4.0	2.00	5.0	2.50	8.2	4.10	17.2	8.60
3	5.3	1.76	7.0	2.33	11.5	3.83	23.3	7.77
4	7.0	1.75	8.9	2.22	14.8	3.70	28.0	7.00
5	8.7	1.74	11.0	2.20	18.2	3.64	32.4	6.48
6	10.3	1.72	13.1	2.18	21.2	3.53	35.5	5.91
9	13.8	1.53	19.5	2.16	30.0	3.33	44.6	4.95
12	17.0	1.41	25.2	2.10	37.7	3.14	52.1	4.35
15	20.7	1.40	31.2	2.08	45.3	3.02	58.5	3.90
18	24.0	1.33	36.0	2.00	52.3	2.90	65.0	3.61
21	26.5	1.26	41.2	1.96	58.5	2.78	71.4	3.40
24	28.7	1.20	45.0	1.87	65.0	2.71	78.0	3.25
27	31.3	1.16	48.0	1.77	70.2	2.60	84.0	3.11
30	33.0	1.10	49.9	1.66	75.0	2.50	89.5	2.98
33	34.0	1.03	51.1	1.55	79.2	2.40	94.2	2.85
36	35.0	0.95	52.0	1.44	82.2	2.21	97.0	2.69
40	35.6	0.89	53.2	1.33	85.4	2.13	99.4	2.48

Table 2C

Thermal degradation of the resin sample No. 2C at various temperatures.

Heating time, min	320° C		360° C		460° C		555° C	
	Loss of weight		Loss of weight		Loss of weight		Loss of weight	
	Amount, %	Rate, %/min	Amount, %	Rate, %/min	Amount, %	Rate, %/min	Amount, %	Rate, %/min
1	3.0	3.00	4.2	4.20	8.0	8.00	12.0	12.00
2	4.2	2.10	8.0	4.00	13.2	6.60	19.8	9.90
3	6.0	2.00	11.8	3.93	18.0	6.00	27.4	9.13
4	7.0	1.75	15.2	3.80	22.0	5.50	31.4	7.85
5	7.8	1.56	18.5	3.70	26.2	5.24	35.0	7.00
6	8.8	1.43	22.0	3.66	30.0	5.00	38.0	6.33
9	9.8	1.09	32.0	3.55	38.3	4.15	44.8	4.53
12	10.0	0.83	40.3	3.35	47.7	3.97	52.0	4.33
15	10.5	0.70	48.5	3.23	55.0	3.53	58.2	3.88
18	12.0	0.66	55.8	3.10	62.0	3.44	64.2	3.57
21	17.2	0.81	63.0	3.00	68.0	3.24	70.2	3.34
24	23.0	0.96	69.0	2.87	73.8	3.07	76.0	3.17
27	29.2	1.08	74.8	2.77	79.2	2.93	81.0	3.00
30	35.2	1.17	80.0	2.66	85.0	2.83	86.2	2.87
33	41.0	1.24	84.2	2.55	89.8	2.72	90.4	2.74
36	48.0	1.33	88.0	2.44	92.0	2.55	93.0	2.58
40	55.0	1.37	90.0	2.25	93.6	2.34	94.9	2.37

Table 3C

Thermal degradation of the resin sample No. 3C at various temperatures.

Heating time, min	320° C		360° C		460° C		555° C	
	Loss of weight		Loss of weight		Loss of weight		Loss of weight	
	Amount, %	Rate, %/min	Amount, %	Rate, %/min	Amount, %	Rate, %/min	Amount, %	Rate, %/min
1	3.0	3.00	4.6	4.60	6.2	6.20	8.5	8.50
2	5.0	2.50	8.0	4.00	12.0	6.00	16.5	8.25
3	6.6	2.20	11.8	3.93	16.5	5.50	24.0	8.00
4	7.8	1.95	15.0	3.75	20.4	5.10	29.0	7.25
5	9.0	1.80	17.8	3.56	21.6	4.82	32.2	6.44
6	9.9	1.65	20.0	3.33	28.2	4.56	35.0	5.83
9	12.0	1.33	27.0	3.00	36.0	4.00	44.0	4.88
12	13.0	1.08	33.9	2.82	45.0	3.75	51.5	4.29
15	14.2	0.95	40.9	2.72	53.2	3.54	59.0	3.93
18	15.2	0.84	47.8	2.65	60.9	3.38	65.8	3.65
21	16.0	0.80	55.0	2.62	68.0	3.24	72.9	3.47
24	16.6	0.70	60.6	2.52	75.0	3.12	79.8	3.32
27	17.0	0.67	67.0	2.48	81.4	3.02	84.6	3.13
30	17.4	0.58	72.2	2.40	87.2	2.90	89.0	2.96
33	17.8	0.54	77.0	2.33	91.4	2.77	92.8	2.81
36	18.0	0.50	80.8	2.24	93.8	2.60	95.2	2.64
40	18.2	0.46	84.8	2.12	96.1	2.10	97.0	2.42

Table 4C

Thermal degradation of the resin sample No. 4C at various temperatures.

Heating time, min	320° C		360° C		460° C		555° C	
	Loss of weight		Loss of weight		Loss of weight		Loss of weight	
	Amount, %	Rate, %/min	Amount, %	Rate, %/min	Amount, %	Rate, %/min	Amount, %	Rate, %/min
1	3.2	3.20	4.0	4.00	8.3	8.30	15.0	15.00
2	5.7	2.85	7.8	3.90	13.7	6.85	23.5	11.75
3	7.2	2.40	10.6	3.53	17.2	5.73	31.2	10.40
4	9.0	2.25	13.9	3.47	21.0	5.25	34.4	8.60
5	10.3	2.06	16.2	3.24	24.0	4.80	37.8	7.56
6	11.6	1.93	19.0	3.16	26.5	4.42	41.2	6.90
9	14.5	1.61	25.4	2.82	35.4	3.93	49.8	5.53
12	16.0	1.33	32.6	2.72	44.3	3.70	57.8	4.82
15	17.2	1.14	39.2	2.61	52.0	3.47	65.4	4.37
18	18.3	1.02	46.0	2.55	59.6	3.31	72.4	4.02
21	19.2	0.91	52.2	2.50	67.0	3.20	79.2	3.80
24	20.0	0.83	58.4	2.43	74.0	3.08	85.5	3.54
27	20.4	0.75	64.2	2.38	80.5	2.98	90.6	3.36
30	21.0	0.70	69.6	2.32	85.2	2.84	93.2	3.10
33	21.8	0.66	74.0	2.24	88.4	2.68	94.8	2.87
36	22.2	0.61	77.0	2.14	90.6	2.52	96.2	2.70
40	23.2	0.58	80.2	2.00	91.9	2.30	97.2	2.43

Table 5C

Thermal degradation of the resin sample No. 5C at various temperatures

Heating time, min	320° C		360° C		460° C		555° C		670° C	
	Loss of weight		Loss of weight		Loss of weight		Loss of weight		Loss of weight	
	Amount, %	Rate, %/min	Amount, %	Rate, %/min	Amount, %	Rate, %/min	Amount, %	Rate, %/min	Amount, %	Rate, %/min
1	4.5	4.50	5.2	5.20	7.4	7.40	12.0	12.0	-	-
2	8.8	4.40	10.0	5.00	13.2	6.60	23.4	11.70	37.0	18.50
3	13.0	4.33	14.5	4.83	19.4	6.47	32.4	10.80	38.4	12.80
4	17.0	4.25	19.0	4.75	25.5	6.37	37.2	9.30	40.4	10.10
5	21.0	4.20	23.0	4.60	31.2	6.24	41.0	8.20	43.0	8.60
6	24.8	4.13	26.9	4.48	37.0	6.16	44.9	7.48	45.6	7.60
9	33.7	3.74	35.4	3.93	48.3	5.36	53.3	5.92	53.2	5.91
12	41.2	3.43	43.0	3.58	57.0	4.77	61.0	5.10	67.2	5.60
15	48.4	3.23	51.0	3.40	64.8	4.32	68.0	4.53	69.4	4.63
18	55.0	3.05	57.4	3.20	71.3	3.96	75.1	4.17	80.2	4.45
21	60.2	2.90	62.7	2.99	77.0	3.52	80.8	3.85	85.4	4.07
24	64.0	2.70	66.5	2.77	81.5	3.40	85.9	3.57	-	-
27	66.8	2.44	69.0	2.55	84.8	3.14	89.6	3.32	90.2	3.34
30	67.5	2.25	70.6	2.35	88.0	2.93	92.2	3.07	94.8	3.16
33	68.0	2.06	71.2	2.15	89.8	2.90	93.3	2.83	97.8	2.96
36	68.7	1.90	71.7	1.98	90.8	2.52	94.0	2.61	99.0	2.82
40	69.2	1.70	72.0	1.80	92.1	2.30	94.2	2.35	99.8	2.49

Table 6C

Thermal degradation of the resin sample No. 6C at various temperatures.

Heating time, min	320° C		360° C		460° C		555° C	
	Loss of weight		Loss of weight		Loss of weight		Loss of weight	
	Amount, %	Rate, %/min	Amount, %	Rate, %/min	Amount, %	Rate, %/min	Amount, %	Rate, %/min
1	4.8	4.80	7.0	7.00	10.0	10.00	13.0	13.00
2	9.0	4.50	10.1	5.05	16.2	8.10	19.0	9.50
3	11.5	3.83	13.2	4.40	22.0	7.33	28.0	9.33
4	13.6	3.40	15.2	3.80	25.5	6.38	31.9	7.98
5	15.5	3.10	17.0	3.40	29.0	5.80	35.2	7.04
6	17.2	2.86	19.2	3.20	32.0	5.33	38.2	6.37
9	20.7	2.30	23.4	2.60	40.8	4.53	46.5	5.17
12	25.0	2.10	28.4	2.37	49.0	4.08	55.0	4.58
15	29.2	1.94	32.0	2.13	57.3	3.82	62.2	4.15
18	32.6	1.81	34.4	1.91	63.0	3.50	67.2	3.73
21	36.1	1.72	39.0	1.86	72.0	3.43	76.0	3.62
24	39.0	1.62	41.0	1.71	78.5	3.27	81.7	3.40
27	41.0	1.52	42.8	1.58	84.0	3.11	88.0	3.27
30	42.4	1.41	44.2	1.47	88.0	2.93	92.5	3.08
33	43.5	1.32	45.6	1.38	90.6	2.75	95.6	2.90
36	44.5	1.24	46.0	1.28	91.7	2.55	96.3	2.68
40	45.0	1.12	46.6	1.16	92.9	2.32	96.9	2.42

Table 7C

Thermal degradation of the resin sample No. 7C at various temperatures.

Heating time, min	320° C		360° C		460° C		555° C	
	Loss of weight		Loss of weight		Loss of weight		Loss of weight	
	Amount, %	Rate, %/min	Amount, %	Rate, %/min	Amount, %	Rate, %/min	Amount, %	Rate, %/min
1	4.0	4.00	5.0	5.00	6.5	6.50	12.6	12.60
2	6.8	3.40	8.8	4.40	12.5	6.25	24.8	12.40
3	10.0	3.33	11.8	3.93	18.0	6.00	37.0	12.33
4	13.0	3.25	15.0	3.75	22.0	5.50	41.0	10.25
5	15.8	3.16	18.5	3.70	27.2	5.44	44.5	8.90
6	18.5	3.08	22.0	3.66	32.0	5.33	48.5	8.08
9	25.2	2.80	30.5	3.39	41.2	4.58	57.2	6.36
12	32.0	2.67	38.2	3.18	50.5	4.21	65.5	5.46
15	37.5	2.50	44.2	2.95	58.3	3.89	73.0	4.87
18	42.5	2.36	50.2	2.79	66.0	3.67	81.0	4.50
21	47.4	2.26	55.0	2.62	72.3	3.49	88.0	4.19
24	51.0	2.13	58.6	2.44	78.2	3.25	93.8	3.91
27	54.7	2.03	61.7	2.29	83.0	3.08	97.5	3.61
30	57.4	1.91	63.2	2.11	87.8	2.93	98.8	3.29
33	60.0	1.82	64.5	1.92	91.0	2.76	99.0	3.00
36	62.0	1.72	65.0	1.81	93.8	2.61	99.4	2.76
40	63.0	1.60	65.6	1.39	94.9	2.31	99.6	2.49

Table 8C

Thermal degradation of the resin sample No. 8C at various temperatures.

Heating time, min	320° C		360° C		460° C		555° C	
	Loss of weight		Loss of weight		Loss of weight		Loss of weight	
	Amount, %	Rate, %/min	Amount, %	Rate, %/min	Amount, %	Rate, %/min	Amount, %	Rate, %/min
1	5.0	5.00	7.0	7.00	9.0	9.00	18.0	18.00
2	9.4	4.70	12.6	6.30	15.0	7.50	32.0	16.00
3	13.8	4.60	17.5	5.83	21.4	7.13	37.9	12.63
4	18.1	4.52	21.0	5.25	27.2	6.80	42.5	10.62
5	22.0	4.40	24.0	4.80	31.0	6.20	46.0	9.20
6	25.9	4.32	28.3	4.72	35.0	5.83	49.2	8.20
9	33.6	3.73	36.0	4.00	43.0	4.77	57.2	6.35
12	40.0	3.33	42.0	3.50	50.2	4.18	65.0	5.42
15	46.8	3.12	48.8	3.25	56.8	3.79	71.8	4.79
18	53.8	2.99	55.0	3.06	62.6	3.48	79.2	4.40
21	60.0	2.86	62.0	2.95	69.0	3.29	86.0	4.10
24	66.0	2.75	68.2	2.83	74.2	3.09	92.2	3.84
27	71.8	2.69	74.0	2.74	80.0	2.96	97.0	3.44
30	78.0	2.60	79.8	2.66	85.0	2.83	98.0	3.27
33	82.8	2.51	85.0	2.57	90.1	2.73	99.2	3.01
36	87.8	2.43	88.0	2.43	94.0	2.61	99.4	2.76
40	91.2	2.28	92.0	2.30	96.1	2.40	99.6	2.49

Table 9C

Thermal degradation of the resin sample No. 9C at various temperatures.

Heating time, min	320° C		360° C		460° C		555° C	
	Loss of weight		Loss of weight		Loss of weight		Loss of weight	
	Amount, %	Rate, %/min	Amount, %	Rate, %/min	Amount, %	Rate, %/min	Amount, %	Rate, %/min
1	2.8	2.80	3.0	3.00	5.0	5.00	8.4	8.40
2	5.5	2.75	5.9	2.90	9.2	4.60	16.6	8.30
3	7.7	2.57	8.6	2.86	13.5	4.50	24.0	8.00
4	10.0	2.50	11.2	2.80	17.8	4.45	29.5	7.38
5	12.2	2.44	13.5	2.70	21.8	4.36	35.2	7.04
6	14.4	2.40	15.6	2.60	26.0	4.33	39.5	6.58
9	21.2	2.35	22.8	2.53	37.0	4.11	48.3	5.37
12	27.3	2.27	30.0	2.50	46.3	3.86	56.0	4.66
15	33.0	2.20	36.9	2.46	55.0	3.67	64.0	4.27
18	39.2	2.18	43.0	2.39	62.5	3.47	70.0	3.88
21	44.1	2.10	49.0	2.33	69.2	3.29	76.5	3.64
24	49.0	2.04	53.5	2.23	75.5	3.15	82.0	3.42
27	52.7	1.95	57.4	2.13	81.0	3.00	88.0	3.11
30	55.0	1.83	60.2	2.01	86.5	2.88	92.8	3.09
33	56.6	1.72	61.4	1.80	90.0	2.73	95.8	2.90
36	57.4	1.59	62.0	1.72	92.0	2.56	98.4	2.63
40	58.0	1.45	62.2	1.35	93.5	2.34	99.8	2.50

Table 10C

Thermal degradation of the resin sample No. 10C at various temperatures.

Heating time, min	320° C		360° C		460° C		555° C	
	Loss of weight		Loss of weight		Loss of weight		Loss of weight	
	Amount, %	Rate, %/min	Amount, %	Rate, %/min	Amount, %	Rate, %/min	Amount, %	Rate, %/min
1	3.0	3.00	4.0	4.00	6.0	6.00	11.0	11.00
2	5.6	2.80	7.2	3.60	11.0	5.50	21.0	10.50
3	8.0	2.70	10.0	3.33	15.0	5.00	27.5	9.16
4	10.0	2.50	12.5	3.12	19.0	4.75	34.5	8.62
5	12.0	2.40	15.0	3.00	22.0	4.40	38.2	7.64
6	13.7	2.28	17.0	2.83	25.2	4.20	41.0	6.83
9	18.8	2.09	21.6	2.40	34.2	3.80	49.2	5.46
12	23.2	1.93	26.2	2.19	42.5	3.54	57.0	4.75
15	28.0	1.87	30.5	2.03	49.8	3.32	63.8	4.25
18	32.3	1.80	35.0	1.95	56.2	3.12	70.3	3.90
21	36.3	1.73	38.8	1.85	63.0	3.00	77.0	3.66
24	40.2	1.66	43.0	1.80	69.0	2.88	82.8	3.45
27	43.7	1.62	46.2	1.70	74.0	2.74	88.0	3.26
30	46.8	1.56	49.2	1.64	78.5	2.62	92.2	3.07
33	48.6	1.47	51.6	1.56	82.0	2.50	95.3	2.90
36	50.0	1.40	53.2	1.48	83.9	2.33	97.5	2.71
40	51.0	1.27	54.6	1.37	85.9	2.15	98.6	2.46

Table 11C

Thermal degradation of the resin sample No. 11C at various temperatures.

Heating time, min	320° C		360° C		460° C		555° C	
	Loss of weight		Loss of weight		Loss of weight		Loss of weight	
	Amount, %	Rate, %/min	Amount, %	Rate, %/min	Amount, %	Rate, %/min	Amount, %	Rate, %/min
1	4.0	4.00	5.8	5.80	9.8	9.80	12.0	12.00
2	6.5	3.75	8.6	4.30	13.2	6.60	18.0	9.00
3	8.0	2.66	9.6	3.20	16.3	5.43	23.2	7.71
4	8.9	2.22	10.0	2.50	18.5	4.62	27.0	6.75
5	9.4	1.88	10.5	2.10	20.5	4.10	29.5	5.90
6	9.7	1.62	10.8	1.80	22.2	3.70	32.0	5.33
9	10.1	1.12	11.0	1.22	25.2	2.80	38.0	4.22
12	10.4	0.87	11.5	0.96	27.0	2.25	43.8	3.65
15	10.6	0.70	12.0	0.80	28.4	1.90	49.3	3.29
18	10.8	0.60	12.2	0.70	29.4	1.63	55.5	3.10
21	10.9	0.52	12.6	0.60	30.0	1.43	61.5	2.93
24	11.0	0.46	12.8	0.53	31.0	1.30	67.0	2.90
27	11.1	0.41	13.2	0.49	31.2	1.15	72.9	2.74
30	11.2	0.37	13.8	0.46	32.0	1.07	78.5	2.62
33	11.2	0.34	14.0	0.43	32.5	0.96	83.3	2.53
36	11.2	0.31	14.8	0.41	33.0	0.91	89.0	2.49
40	11.2	0.28	15.2	0.38	33.9	0.85	94.2	2.33

Table 13C

Rate of pyrolysis and energy of activation of the resin specimens at zero time for extrapolated values.

Resin sample number	$\frac{1}{T}$ Å x 10^3								E_o	
	1.68		1.58		1.36		1.20		Kcal/mole	
	log R_{XO}-	log R_{YO}	log R_{XO}-	log R_{YO}	log R_{XO}-	log R_{YO}	log R_{XO}-	log R_{YO}	E_{XO}-	E_{YO}
1C	0.400	0.263	0.440	0.363	0.625	0.570	0.970	0.667	7.36	4.60
2C	-	-	0.630	0.585	0.885	0.653	1.080	0.720	6.44	1.84
3C	0.490	0.160	0.685	0.500	0.840	0.662	1.000	0.730	5.32	3.68
4C	0.520	0.210	0.625	0.492	0.975	0.652	1.230	0.810	5.32	3.68
5C	-	0.670	-	0.715	-	0.795	-	0.830	-	1.84
6C	0.720	0.448	0.810	0.500	1.000	0.720	1.110	0.750	3.68	2.76
7C	0.550	0.520	0.750	0.620	0.835	0.740	1.155	0.885	5.32	3.68
8C	0.710	0.570	0.855	0.595	0.930	0.676	1.300	0.860	3.68	3.68
9C	0.460	0.400	0.490	0.435	0.750	0.675	0.970	0.755	4.60	3.68
10C	0.495	0.346	0.610	0.430	0.810	0.690	1.110	0.748	5.98	4.60
11C	0.670	0.080	0.780	0.150	0.840	0.410	1.050	0.610	3.68	5.06

Table 14C

Rate of pyrolysis and energy of activation of the resin specimens at various percentage losses and temperatures.

Resin sample number	*$\frac{1}{T}$ Å x 10^3	6%		10%	
		**log R_t	$\frac{E}{\text{Kcal/mole}}$	log R_t	$\frac{E}{\text{Kcal/mole}}$
11C	1.68	0.4772		0.0706	
	1.58	0.7782		0.4559	
	1.36	0.9331		1.0000	
	1.20	1.0792	7.36	1.1249	9.20

		20%		30%		40%		50%		60%	
		log R_t	$\frac{E}{\text{Kcal/mole}}$	log R_t	$\frac{E}{\text{Kcal/mole}}$	log R_t	$\frac{E}{\text{Kcal/mole}}$	log R_t	$\frac{E}{\text{Kcal/mole}}$	log R_t	$\frac{E}{\text{Kcal/mole}}$
1C	1.68	0.1472		0.0748		-		-		-	
	1.58	0.3349		0.3157		0.2956		0.2219		-	
	1.36	0.5413		0.5229		0.4966		0.4686		-	-
	1.20	0.9031	8.28	0.8239	8.11	0.7270	7.00	0.6576	7.40	-	-
2C	1.68	-		-		-		-		-	
	1.58	0.5808		0.5606		0.5320		0.5087		-	
	1.36	0.7569		0.6989		0.6131		0.5851		-	
	1.20	1.0000	4.73	0.9330	4.60	0.7570	4.60	0.6576	2.01	-	-
3C	1.68	-		-		-		-		-	
	1.58	0.5228		0.4559		0.4333		0.4202		0.4026	
	1.36	0.6989		0.6320		0.5914		0.5539		0.5302	
	1.20	0.9031	5.52	0.8239	5.52	0.7270	3.70	0.6383	3.22	0.5879	2.76

4C	1.68	0.0882		-		-		-		-	
	1.58	0.4259		0.4357		0.4118		0.3980		0.3846	
	1.36	0.7270		0.6320		0.5809		0.5452		0.5170	
	1.20	1.1249	<u>6.90</u>	1.0000	<u>6.90</u>	0.8617	<u>6.20</u>	0.7448	<u>7.36</u>	0.6643	<u>6.00</u>
5C	1.68	0.6243		0.5878		0.5414		0.5087		0.4560	
	1.58	0.6726		0.6320		0.5707		0.5376		0.4882	
	1.36	0.8239		0.8004		0.7728		0.7213		0.6643	
	1.20	1.1249	<u>6.62</u>	1.0792	<u>6.20</u>	0.9254	<u>4.60</u>	0.8097	<u>3.70</u>	0.7175	<u>3.70</u>
6C	1.68	0.3716		0.2798		0.1956		-		-	
	1.58	0.4717		0.3468		0.2499		-		-	
	1.36	0.8617		0.7569		0.6727		-		-	
	1.20	1.0000	<u>6.44</u>	0.9330	<u>6.42</u>	0.7892	<u>6.00</u>	-		-	
7C	1.68	0.4717		0.4357		0.3846		0.3373		0.2597	
	1.58	0.5606		0.5351		0.4882		0.4686		0.3759	
	1.36	0.7569		0.7364		0.6727		0.6364		0.5879	
	1.20	1.1249	<u>7.36</u>	1.0792	<u>7.36</u>	1.0281	<u>7.36</u>	0.8881	<u>5.60</u>	0.7782	<u>5.52</u>
8C	1.68	0.6478		0.6020		0.5229		0.4815		0.4560	
	1.58	0.6989		0.6642		0.5607		0.5087		0.4717	
	1.36	0.8601		0.7995		0.7128		0.6198		0.5542	
	1.20	1.2041	<u>6.44</u>	1.1761	<u>6.44</u>	1.0902	<u>6.44</u>	0.8861	<u>5.52</u>	0.7676	<u>4.60</u>
9C	1.68	0.3468		0.3468		0.3349		0.3098		-	
	1.58	0.4117		0.3979		0.3846		0.3615		-	
	1.36	0.6243		0.6168		0.6021		0.5851		-	
	1.20	0.9031	<u>6.44</u>	0.8750	<u>6.44</u>	0.8062	<u>5.52</u>	0.7213	<u>4.60</u>	-	
10C	1.68	0.3010		0.2596		0.2219		0.1427		-	
	1.58	0.4559		0.3157		0.2646		0.2076		-	
	1.36	0.6726		0.6020		0.5607		0.5229		-	
	1.20	1.0000	<u>7.36</u>	0.9330	<u>7.36</u>	0.6617	<u>7.36</u>	0.7329	<u>7.36</u>	-	

---

* T °A = t° C + 273

** Rates are calculated from the graphs between percentage weight loss and time (i.e. percentage weight loss/time, minutes)

E = Activation energy

DISCUSSION

The percentage weight losses and the rates (percentage weight loss/ minutes) of losses of each phenolic resin sample are calculated at different times at the isothermal temperatures of 320, 360, 460, 555 and 670°C. The results of the calculations are shown in the Tables 1C-11C. In the typical Figures 1C-5C cumulative losses of weight at various temperatures, expressed in per cent of the original weight of the samples are plotted as a function of time. At a glance it would appear that (i) the percentage weight loss increases gradually with time at a constant temperature, (ii) the higher the temperature the greater is the amount of the resin decomposed at any given time, (iii) the rate of decomposition decreases slowly with time (except in the case of the resin sample No.2C at 320°C), and (iv) the rate of decomposition increases as the temperature is raised. In the case of sample No.2C at 320°C the rate of degradation first decreases up to about 18 minutes and then the rate increases. (This point would be discussed later.) The careful observation will reveal that almost all the resin samples give similar results and plots when treated similarly.

The initial rate of pyrolysis is higher for the first couple of minutes, then it slows down and becomes uniform and towards the end of the experiment the rate further decreases. It is obvious from the results that the degradation follows exponential decay, which could be represented by an equation,

$$R_t = Ae^{-Bt}$$

where R_t is the rate of degradation, A and B are the constants and t is the time at any moment of degradation. On plotting log R_t against t, one should get a straight line. The intercept at the ordinate will give the constant A = R_o (rate at zero time) and slope is equal to -B/2.303.

On plotting log R_t versus time one gets two straight lines x and y intersecting at Z almost in all the cases, Figure 6C. The resin sample No. 5C is an exception as it gives straight lines at 320 and 360°C. Each of the straight lines in the graph indicates that the degradation follows a different exponential decay.

The following equations in Table 12C have been developed for the y part of the degradation curves.

TABLE 12C

The exponential equations of degradation of the phenolic resin samples at different temperatures.

Sample Number	Temperature, °C	Exponential Equation, R_t =
1C	320	$1.832\ e^{-0.0189t}$
	360	$2.307\ e^{-0.0077t}$
	460	$3.715\ e^{-0.0125t}$
	555	$4.645\ e^{-0.0138t}$
2C	320	-
	360	$3.846\ e^{-0.0138t}$
	460	$4.498\ e^{-0.0184t}$
	555	$5.248\ e^{-0.0184t}$

TABLE 12C (contd)

Sample Number	Temperature, $^{\circ}C$	Exponential Equation, R_t =
3C	320	$1.514\ e^{-0.0293t}$
	360	$3.162\ e^{-0.0087t}$
	460	$4.592\ e^{-0.0167t}$
	555	$5.370\ e^{-0.0184t}$
4C	320	$1.622\ e^{-0.0269t}$
	360	$3.105\ e^{-0.0094t}$
	460	$4.487\ e^{-0.0164t}$
	555	$6.457\ e^{-0.0251t}$
5C	320	$4.677\ e^{-0.0251t}$
	360	$5.188\ e^{-0.0276t}$
	460	$6.237\ e^{-0.0263t}$
	555	$6.761\ e^{-0.0269t}$
	760	$6.998\ e^{-0.0287t}$
6C	320	$2.805\ e^{-0.0230t}$
	360	$3.162\ e^{-0.0276t}$
	460	$5.433\ e^{-0.0205t}$
	555	$5.623\ e^{-0.0230t}$
7C	320	$3.311\ e^{-0.0167t}$
	360	$4.169\ e^{-0.0230t}$
	460	$5.495\ e^{-0.0204t}$
	555	$7.674\ e^{-0.0307t}$

TABLE 12C (contd)

Sample Number	Temperature, ^{o}C	Exponential Equation, R_t =
8C	320	$3.715\ e^{-0.0115t}$
	360	$3.936\ e^{-0.0138t}$
	460	$4.742\ e^{-0.0184t}$
	555	$7.244\ e^{-0.0276t}$
9C	320	$2.512\ e^{-0.0092t}$
	360	$2.723\ e^{-0.0083t}$
	460	$4.732\ e^{-0.0173t}$
	555	$5.689\ e^{-0.0230t}$
10C	320	$2.218\ e^{-0.0138t}$
	360	$2.692\ e^{-0.0184t}$
	460	$4.898\ e^{-0.0230t}$
	555	$5.598\ e^{-0.0184t}$
11C	320	$1.202\ e^{-0.0409t}$
	360	$1.413\ e^{-0.0184t}$
	460	$2.570\ e^{-0.0288t}$
	555	$4.074\ e^{-0.0136t}$

X and Y parts of the straight lines have been extrapolated back to zero time to get R_{XO}- and R_{YO} (i.e. rates of degradation at zero time for two composite degradation processes), Figure 6C. The values of log R_{XO}- and log R_{YO} are shown in Table 13C. Also it should be noted that the fraction of the original concentration of the resin remaining at any time, t, is given by the equation:

$$\frac{R_t}{R_{t=o}} = e^{-Bt}$$

One is justified in using the rates of weight losses by degradation at different temperatures for the purpose of calculating activation energies only when the residues corresponding to the rates used have the same average molecular weights and the same distributions. These conditions are met at theoretically zero degradation where the same material is used at different temperatures.

The reason for initial high rates and the breaks at Z in the rate curves is not apparent from this work. The partial explanation may be found in the fact that the reaction mechanisms of degradation would be different for X and Y parts of the curves. At first as the resin specimen attains the equilibrium temperature most of the adsorbed moisture and volatile products, especially of low molecular weight, are driven out and the oxidation would be rapid. As the air atmosphere is replaced by the degradation products the influence of the atmospheric oxygen is diluted. Moreover the volatile products of the pyrolysis would leave the surface of the resin immediately and the degradation products from the lower part of the resin may diffuse out somewhat slowly at a uniform rate. When most of the reactions like oxidation/reduction, dehydration/hydrolysis, bond formation, ring rupture , etc., are nearly over the rate of carbonisation/ graphitisation would be increased. The free-radicals and ions produced during the pyrolysis would further increase the complexity of the degradation. As the pyrolysis advances further the molecular weight and the nature of the phenolic resin changes continuously, which effects the heat capacity, thermal conductivity, diffusion and nature of the volatile products, heat and mass transfer, etc.

Most of the possible reactions during degradation of the phenolic resin have been discussed in Part I of the thesis, pp. 116-129. Although it may not be quite easy to isolate different reactions but it would be of interest to collect and analyse the volatile products and the residue as well in order to attempt to visualise the mechanism of degradation and secondary polymerisation (carbonisation).

Energy of Activation

The activiation energy is calculated by applying Madorsky's[25,127] method, one may also use methods of Jellinek[128] and Atherton[129] by using average rates from the seemingly straight parts of the curves in Figures 1C-5C. Using the Arrhenius equation

$$k = A e^{-E/RT}$$

in the form

$$-E = 2.303 R \frac{d(\log k)}{d(1/T)}$$

the logarithms R_t are plotted against the inverse of absolute temperature to obtain the activation energy, see Figure 7C. The slopes of the straight lines thus obtained give activation energies. The activation energies for 6% and 10% weight losses of the resin sample No. 11C and of the other specimens, No.1C-10C, at 20, 30, 40, 50 and 60% weight losses are calculated and given in Table 14C. The resin sample No. 1C (without any additive) has higher activation energy and is thus thermally more stable except the sample No. 11C. The rate losses for the purpose of such calculations were obtained by drawing the horizontal lines from these percentage weight losses. The rates were calculated at the points where the horizontal lines intersected the graphs between weight losses and time, Figures 1C-5C. Logarithms of these rates are given in Table 14C.

The activation energies at theoretically zero time of degradation are similarly obtained by plotting log R_{XO}-/R_{YO} against 1/T, Figure 8C. The values of the activation energies, E_o, at the zero rate (i.e. zero time) of thermal degradation are given in Table 13C.

Summary of the results of variation of activation energies is given in Table 15C.

TABLE 15C

The activation energies of thermal degradation of the resin sample No. 1C-11C

Sample Number	Degradation, %	Energy of activation K cal/mole
1C-11C	0.0	1.84 - 7.36
11C	6-10	7.36 - 9.20
1C-10C	20-60	2.01 - 8.28

It is apparent from the activation energies, that the resin specimen (No.11C) containing ADOP is thermally more stable.

The values of activation energies of the degradation of the phenolic resin samples obtained by the isothermal thermogravimetric method are smaller than those reported in Part I of the thesis, pp.171-2 (DTA) and pp. 176, 178 (TGA) but they are comparable in magnitude with the latter values. The causes of variation may be found in the history of the resin, different mechanism of degradation under different experimental conditions and various techniques of analysis used by different workers. The apparently probable causes of the different values of activation energy have been discussed on pp.172, 178. The various additives further lower the activation energy of the phenolic resin degradation and thus affect the thermal stability of the resin adversely.

The degradation rates and the activation energies based on these values should not be considered as referring to any particular reaction taking place in the process of the thermal degradation, but should be looked upon as pointed out by Simha , Simha, Wall and Blatz , and Simha and Wall as composite values referring to several reaction mechanisms such as initiation, propagation, oxidation, ring rupture, carbonisation, etc. The question of order of reaction involved in thermal degradation of polymers is of great interest since it may throw light on the mechanism of degradation. Actually one cannot speak of any given order of reaction when several reactions are involved simultaneously.

However, it is not quite easy to find out order of reaction in the present study when the degradation of resin involves many complex reactions, though it has been shown by the programmed thermogravimetric method (p.177) that the overall degradation of the resin obeys a first order reaction.

Effect of Additives

(a) Metals. The powdered Cu, Mg and Al metals were added to provide the reducing atmosphere and also to observe their catalytic effect on the resin degradation. At 320°C for 15 minutes the degradation behaviour in each case (samples No. 2C, 3C and 4C) appears to follow a similar mechanism of thermal degradation. During the subsequent period the specimen containing Cu (sample No.2C) differs in the scheme of pyrolysis by rapidly decomposing, from the other two samples (samples Nos. 3C and 4C), which decompose identically, slowly and uniformly. At 360, 460 and 555°C all the three samples degrade in the same manner giving similar curves on plotting percentage weight loss against time, Figures 2C and 3C.

(b) Metal Halides andOxides. The degradation pattern followed by the resin specimens having metal halides ($AlCl_3$, sample No.7C; and $FeCl_3$, sample No.8C); Sb_2O_3 (sample No.9C) and MgO (sample No.10C) is almost similar in character, Figure 4C. The thermal degradation of the resin is accelerated in the presence of Lewis acids Sb_2O_3 and MgO .

(c) Sodium metaborate and Penta-sodium triphosphate. The catalytic effect of S_mB and PSTP on the degradation of the resin appears to be similar to that of metals (except at 320°C) metal halides and oxides. The graphs obtained on plotting percentage weight loss versus time are similar in nature and resemble, Figure 4C.

The effect of metals, metal halides, metal oxides, SmB and PSTP may partly be explained by considering that they would have entered into a complex formation with the resin. (It requires further work.) The copper complex being less stable starts decomposing rapidly after about 18 minutes at 320°C, Figure 2C. Mg and Al metal complexes show similar stability at 320°C, Figure 3C. At 360, 460 and 555°C all these complexes probably degrade in the same fashion, Figures 2C-3C. Hultzsch[130], and Hultzsch and Hesse[131] have shown that chelate complexes are formed immediately during the phenol formaldehyde condensation or subsequent reactions between reactive groups and metal oxides, metal oxide hydrates, metal salts or metal halides. The metal co-ordinates with the oxygen centres in the resin to form chelate complexes of types shown below:

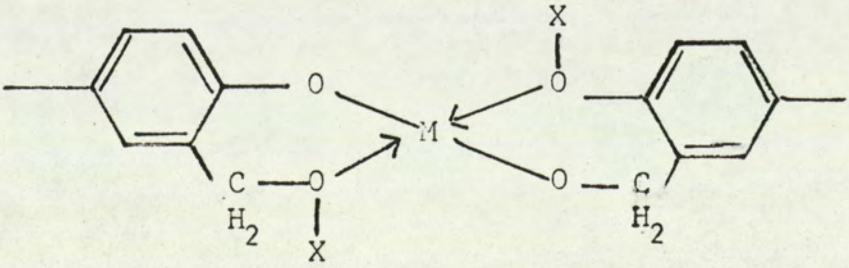

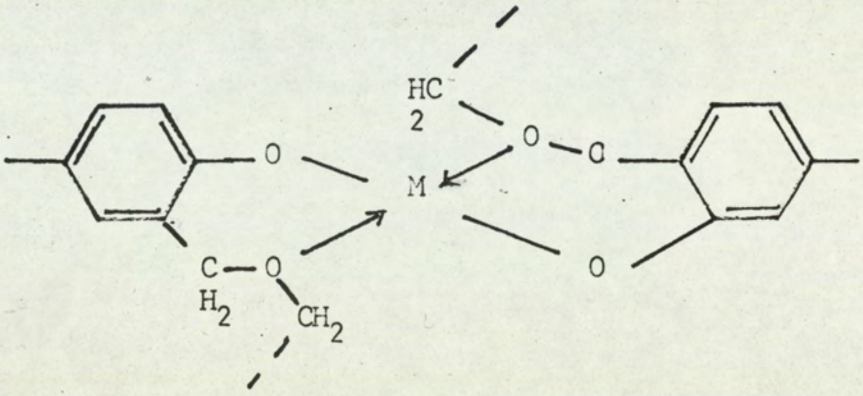

where M = Cu, Mg, Al

X = H or

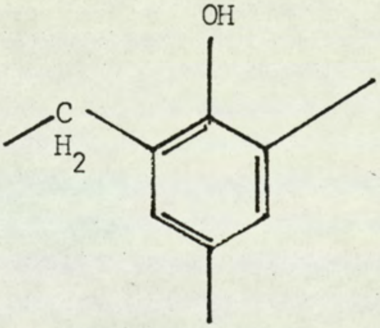

The chelate formation represents an interesting mode of a molecule enlargement related to chelate or co-ordination polymers.

Most probably the metaborate and triphosphate also form some type of complexes with the resin which are not so stable and decompose on heating. (Further work is necessary to elucidate the nature of the complexes.)

(d) ADOP. The effect of ADOP on the thermal stability of the resin is very interesting, 5% addition of ADOP in the resin shows a considerable increase in its thermal stability below 555°C, Figure 5C.

The influence of ADOP concentration on the thermal stability of the resin has been studied.

It is observed that the resin becomes more stable when 40% of ADOP is present in the system. At other concentrations of ADOP the resin is less stable (samples No. 11C-22C). Probably 40% of ADOP is a proper ratio to give a more stable complex with the resin. (This also requires further work to verify the nature of the complex.)

The Effect of Additives on the *Thermal Stability of the Resin

In order to know the effect of additives on the thermal stability of the resin the percentage weight losses at the 40th minute of the degradation of the samples are shown in Table 16C at 320, 360, 460, 555 and 670°C.

---

*Since the experimental conditions of PTGA and ITGA are widely different, the thermal stabilities of resin samples cannot be compared.

TABLE 16C

Percentage weight loss at the 40th minute in the air/self-generated atmosphere at 320, 360, 460, 555 and 670°C.

Sample Number	Composition, %	320°	360°	460°	555°	670°
1C	90 R + 10H	35.6	53.2	85.4.	99.4	-
2C	85R + 10H + 5Cu grit	55.0	90.0	93.6	94.9	-
3C	85R + 10H + 5Mg grit	18.2	84.8	96.1	97.0	-
4C	85R + 10H + 5Al grit	23.2	80.2	91.9	97.2	-
5C	85R + 10H + 5Sm	69.2	72.0	92.1	94.2	-
6C	85R + 10H + 5PSTP	45.0	46.6	92.9	96.9	-
7C	85R + 10H + 5$AlCl_3$	63.0	65.6	94.9	99.6	-
8C	85R + 10H + 5$FeCl_3$	91.2	92.0	96.1	99.6	-
9C	85R + 10H + 5Sb_2O_3	58.0	62.2	93.5	99.8	-
10C	85R + 10H + 5MgO	51.0	54.2	85.9	98.6	-
11C	85R + 10H + 5ADOP	11.2	15.2	33.9	94.2	99.8
12C	80R + 10H + 10ADOP	-	-	-	-	98.8
13C	75R + 10H + 15ADOP	-	-	-	-	98.8
14C	70R + 10H + 20ADOP	-	-	-	-	98.6
15C	65R + 10H + 25ADOP	-	-	-	-	89.0
16C	60R + 10H + 30ADOP	-	-	-	-	88.6
17C	50R + 10H + 40ADOP	-	-	-	-	71.4
18C	40R + 10H + 50ADOP	-	-	-	-	90.0
19C	30R + 10H + 60ADOP	-	-	-	-	92.4
20C	20R + 10H + 70ADOP	-	-	-	-	94.0
21C	10R + 10H + 80ADOP	-	-	-	-	95.2
22C	100 ADOP	-	-	-	-	97.6

R = Resin H = Hexa

The results obtained in the present investigations show that the thermal stabilities of the samples Nos. 1C and 10C are comparable at 360, 460 and 555°C. In all the other cases sample No.1C (without any additive) is more stable below 555°C, except the samples Nos. 3C and 4C at 320°C and the sample No. 6C at 360°C. Thus indicating unhealthy effect of different additives on the thermal stability of the resin. At about 555°C there is not much difference in the thermal stabilities of all these samples.

The sample No.11C is significantly more stable below 555°C than all the other samples. Therefore we were encouraged to study the effect of addition of ADOP on the thermal stability of the resin. The percentage weight losses at 670°C are given in the Table 5C. A plot of percentage weight loss versus temperature gives a curve like the letter V with shoulders as shown in Figure 9C. The lowest point A of the valley is given by the sample containing 40% of ADOP in the resin. Thus the sample having 40% of ADOP is more stable than all the other samples at 670°C. When ADOP is blended with the resin in the proper ratio (40%) its thermal stability increases considerably even at comparatively higher temperature. This is probably due to the formation of polyphosphate[132,133]/phosphorus entering into the carbonisation of the resin on pyrolysis (i.e. some sort of stable complex with the resin is formed).

There are at least two reasons for the poor stability of the resin samples containing additives except the ADOP. One of these is the catalytic effect on degradation of the resin. The other is probably the formation of complexes with the resin, which are unstable at high temperatures. Although the methylene bridges are the weakest points in the crosslinked network of phenolic resin (sample No.1C) but the high concentration of the benzene rings in the crosslinked network bestows greater thermal stability on the resin. The phenyl radicals produced by pyrolysis of the polymer could coalesce into clusters of benzene rings, which would have the high resonance stabilisation energy characteristic of condensed ring systems.

GENERAL

The work described in Part II has shown conclusively that isothermal pyrolysis measurements are required in studying the ablative properties of phenolic resins, to supplement the indications given by DTA and TGA.

It is only necessary to cite the extraordinary effects of the materials added, viz: copper, magnesium, aluminium chloride and ammonium dihydrogen ortho phosphate as shown by plots of loss in weight against time at the same temperature. See Figs. IO C-I to IO C-4.

The TGA thermograms shown in Part I clearly indicate that three stages of reaction occur.

at <c.350°C c.350-700°C and >700°C respectively

Accordingly, with isothermal results at different temperatures it should be possible to calculate separate activation energies for the three zones of pyrolysis. These are shown inferentially in Tables 14C and 15C but the results are not clear enough for useful application to the problem of ablative behaviour. Thus the results at 320°C fall in zone 1 and while we do not yet have enough results to calculate accurate activation energies it is immediately obvious that in this region $AlCl_3$ (and presumably other Lewis Acids) accelerate reaction considerably. This is the region of completion of crosslinking and removal of unused methylol groups, and the effect of Lewis Acids on this process is not unexpected. Copper appears to accelerate reaction after an initial induction period while both Mg and ADOP slow it down markedly.

The results at 360°C must be decidedly in the second reaction zone where polymer reforming is taking place with formation of volatile fragments and a condensed ring structure, and here both $AlCl_3$ and Mg have some increasing effect on the loss in weight, while ADOP still markedly inhibits it. The set of results at 460°C should be in the centre of the same zone, and results are of the same type as at 360°C if due allowance is made for the increased rate of reaction due to temperature.

At 555°C all samples gave rather similar results and there is little indication for the reason for this - possibly loss of ADOP.

It is plain that the experiments described in Part II are highly important and time must be found to carry them further. In particular, for a number of reasons, the results are not quite comparable with those in Part I, because the atmosphere around the samples is not quite inert and the effect of this has not been rigorously established.

SUMMARY

The present investigations on thermal degradation of the phenolic resin samples show that pyrolysis increases with time and temperature. The rate of decomposition decreases gradually with time, but the rate of decomposition increases as the temperature is increased. Almost all the resin samples give similar results and graphs when treated in the same manner. The degradation follows high rate of oxidative degradation and pyrolysis in the initial stages, then there is a break which is followed by a uniform and slow rate of pyrolysis. Thus each of the two degradation rates follows a different exponential equation. Activation energies at different percentage weight losses have been calculated and reported. The values of activation energies are, in general, comparable with those found by programmed TGA but are smaller than the values reported by other workers and found in the present DTA studies. Metals (Cu, Mg and Al), metal halides ($AlCl_3$ and Fe Cl_3), metal oxides (Sb_2O_3 and MgO), sodium metaborate, and pentasodium triphosphate adversely affect the thermal stability of the phenolic resin. Ammonium dihydrogen-ortho-phosphate enhances the thermal stability of the resin.

Fig.4a

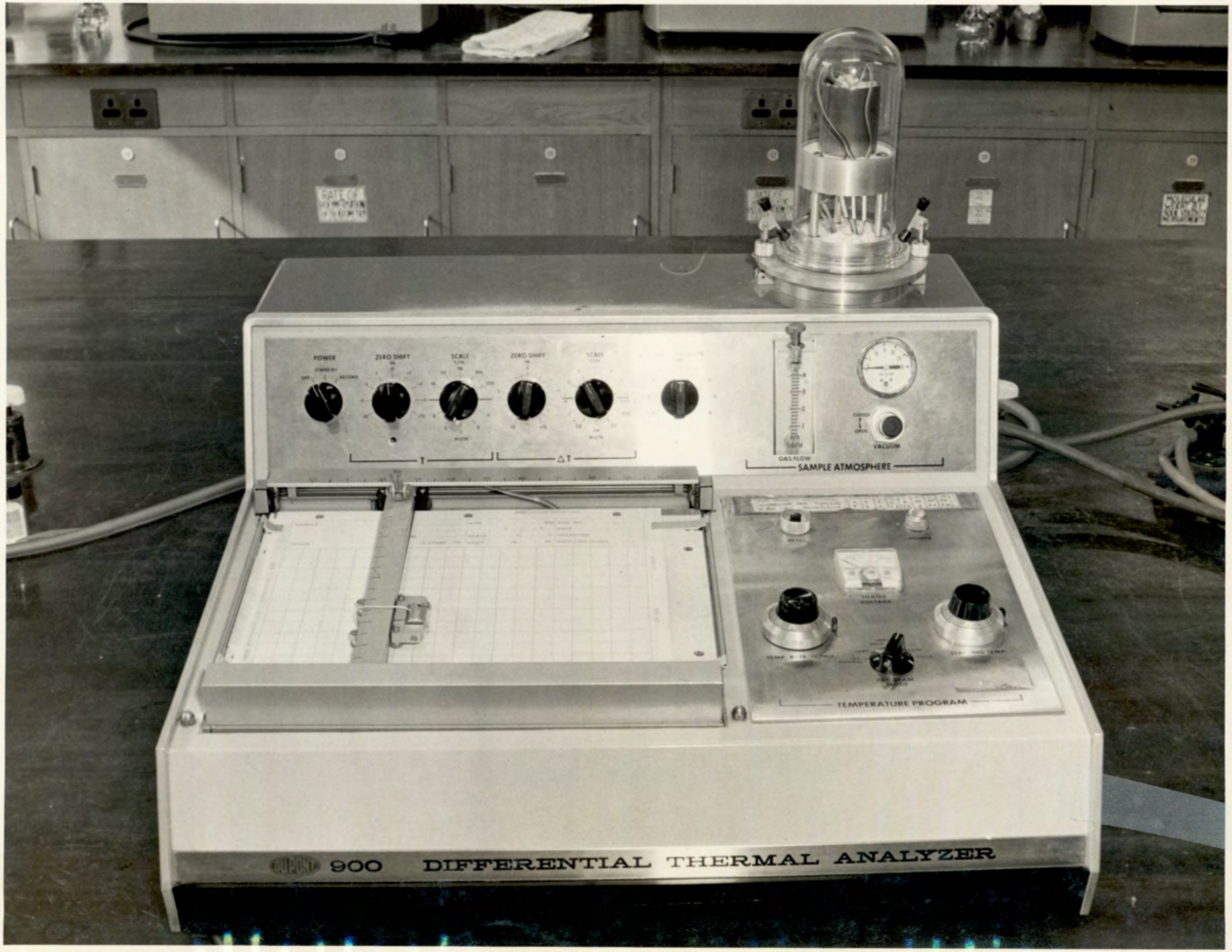
POWER
ZERO SHIFT
SCALE
ZERO SHIFT
SCALE
T
ΔT
GAS FLOW
VACUUM
SAMPLE ATMOSPHERE
RESET
POWER
HEATER VOLTAGE
STARTING TEMP
TEMPERATURE PROGRAM
DU PONT 900 DIFFERENTIAL THERMAL ANALYZER

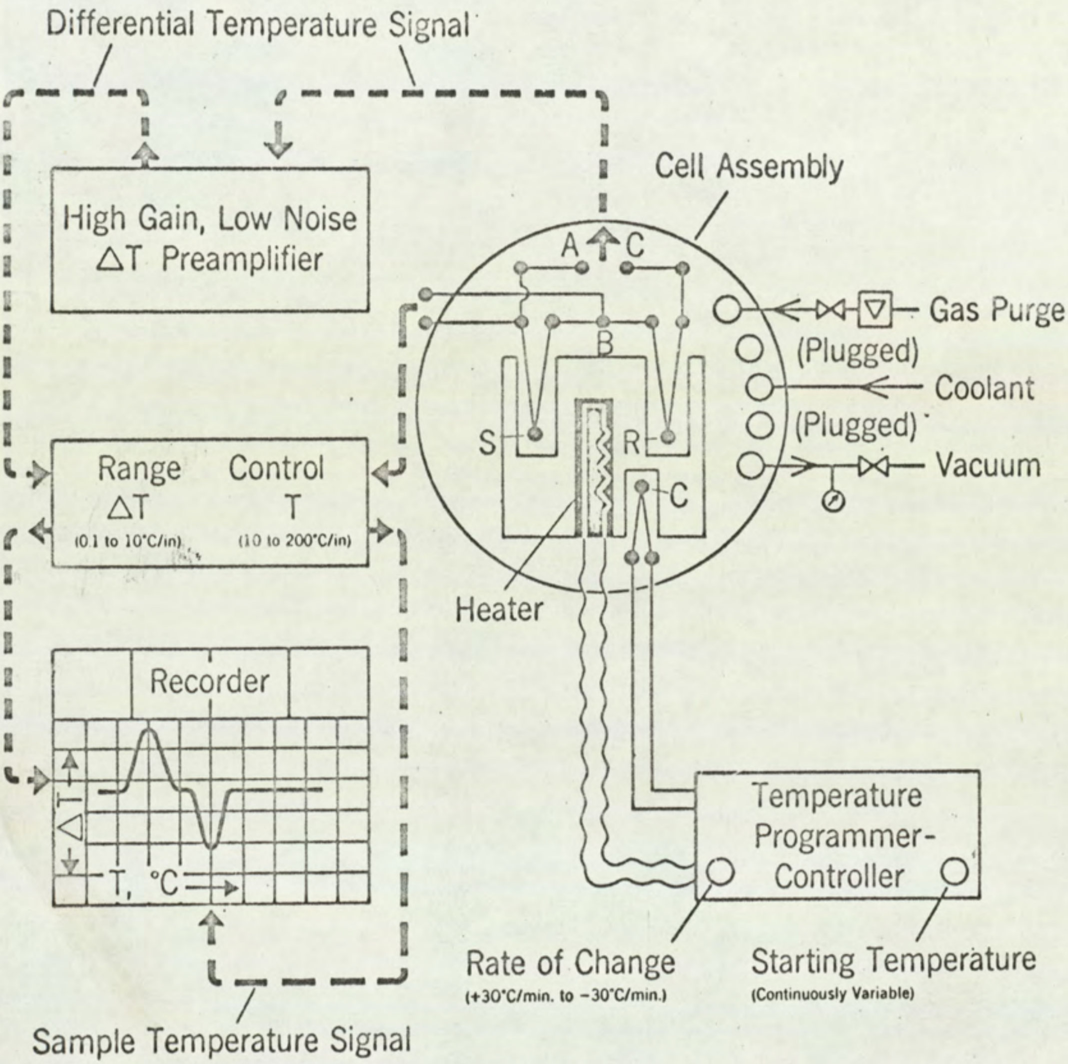

FIGURE 4b. ANALYZER SYSTEM

The DuPont(900) system is shown diagrammatically in Figs. 4a and 4b. S and R are thermocouples immersed in sample and reference material respectively. The difference in temperature, ΔT, is given by the EMF across the points A-C. The sample temperature, T, is indicated by the potential across the points A-B. The unit includes a heating block, a programme devise, a heater, a preamplifier and a recorder to plot ΔT as a function of T.

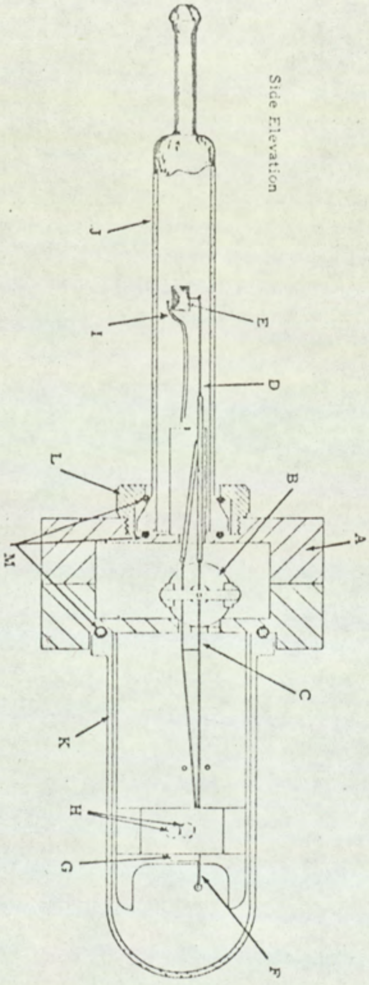

A. Balance Housing
B. Taut-Band meter movement
C. Rear Beam
D. Quartz Rod-Hot member (Removable)
E. Sample Boat
F. Counter-Weight Arm
G. Signal Flag
H. Photo-voltaic cells
I. Sample thermocouple
J. Quartz Furnace Tube
K. Pyrex envelope (cold)
L. Furnace Tube Retainer
M. O rings
N. Lamp Housing
O. Balance Track Guides
P. Purge Gas Inlat

Fig. 5.

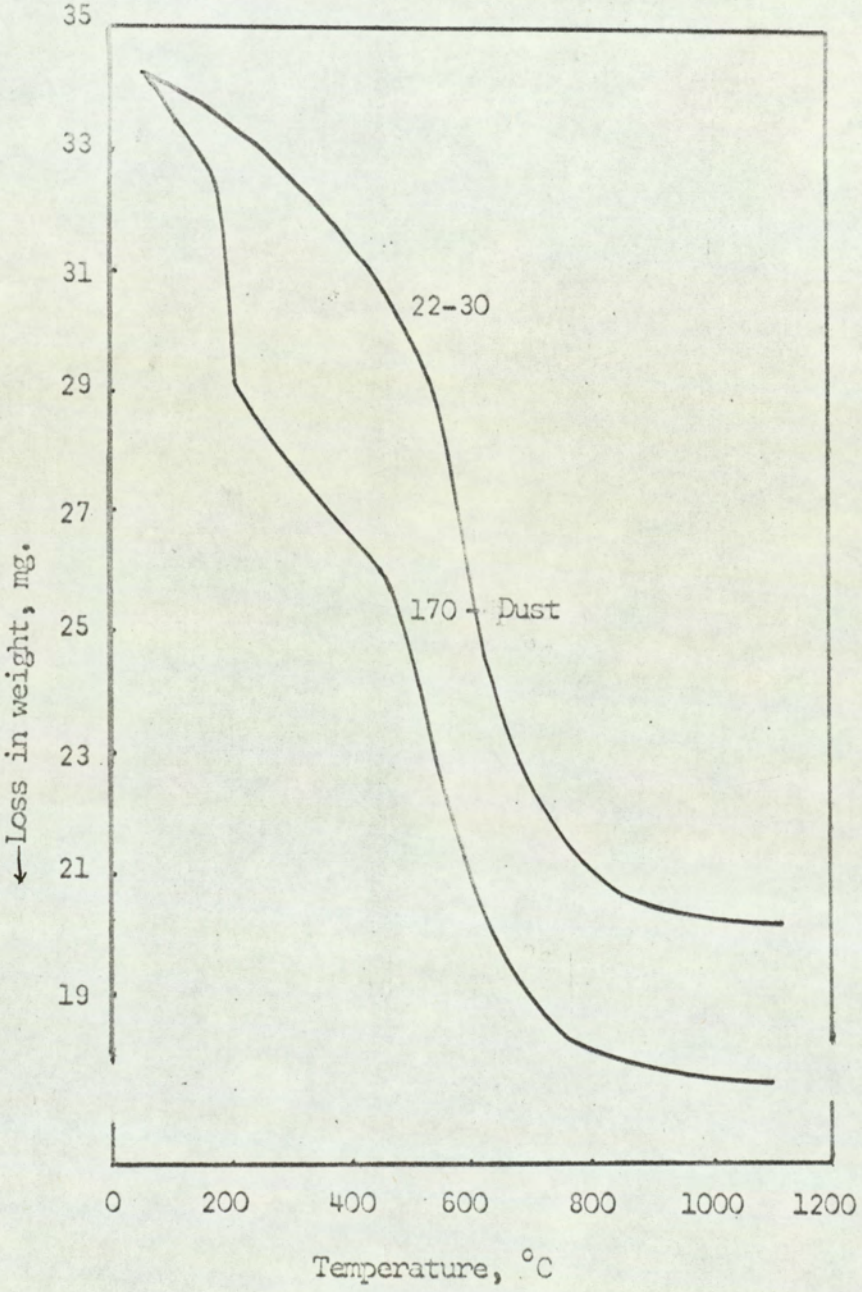

Fig.22 a. TGA Thermograms - Effect of grain size.

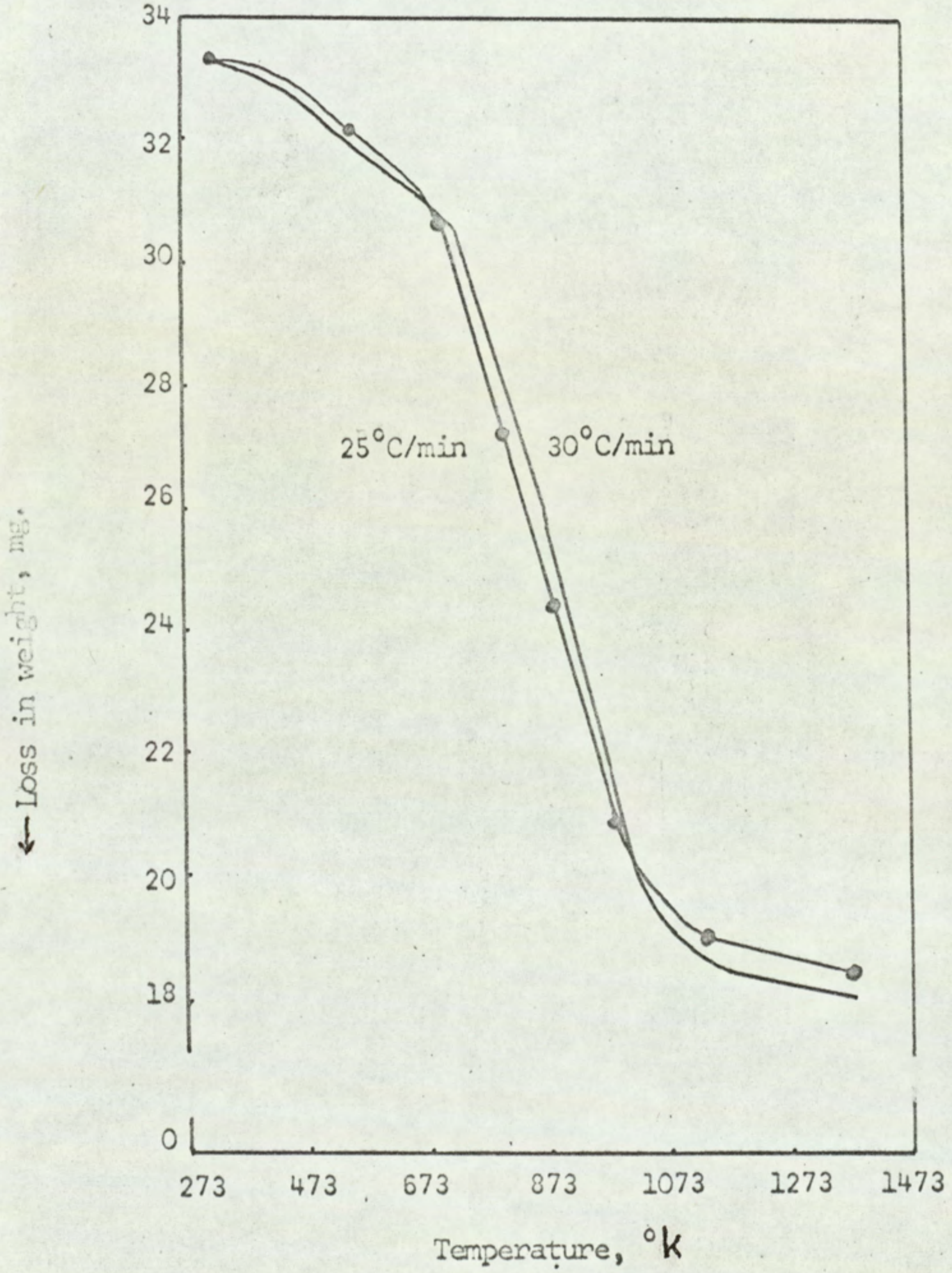

Fig.22b. TGA Thermograms

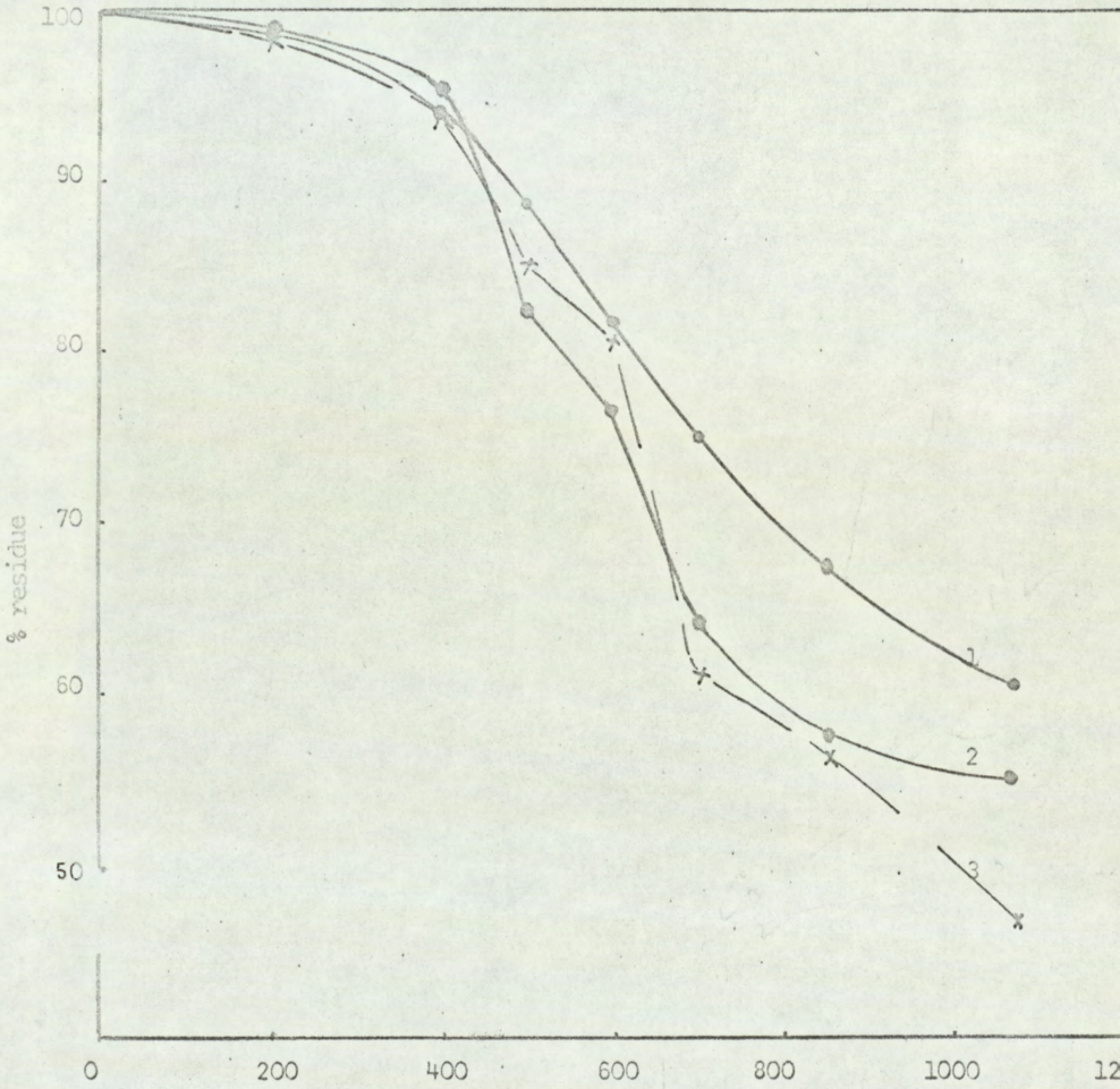

Temperature, °C

Fig. 23 . TGA Thermograms

1. Still Air
2. N_2
3. CO_2

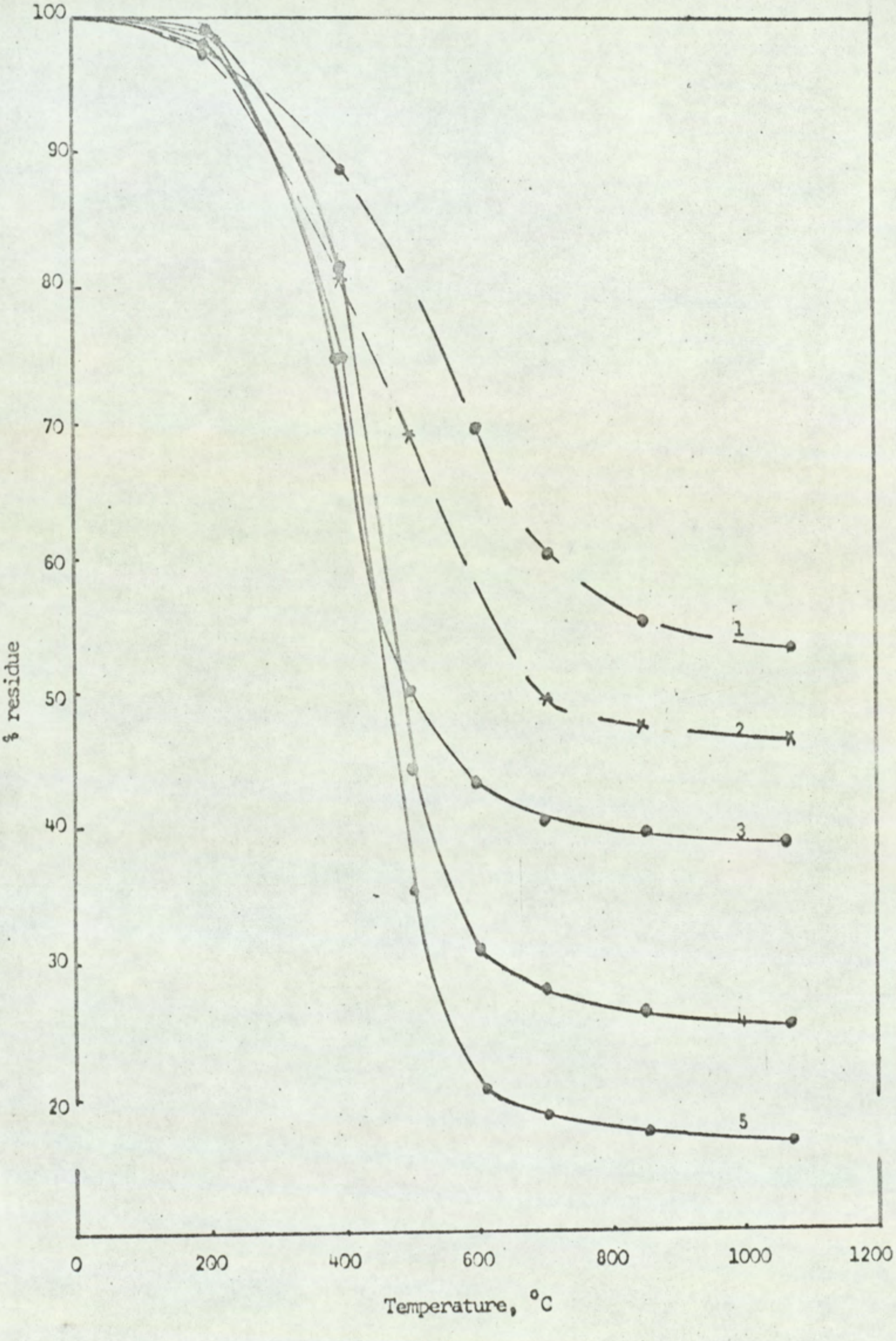

Fig. 24. TGA Thermograms

1. C1
2. D1
3. B1
4. RW54859
5. RW52487

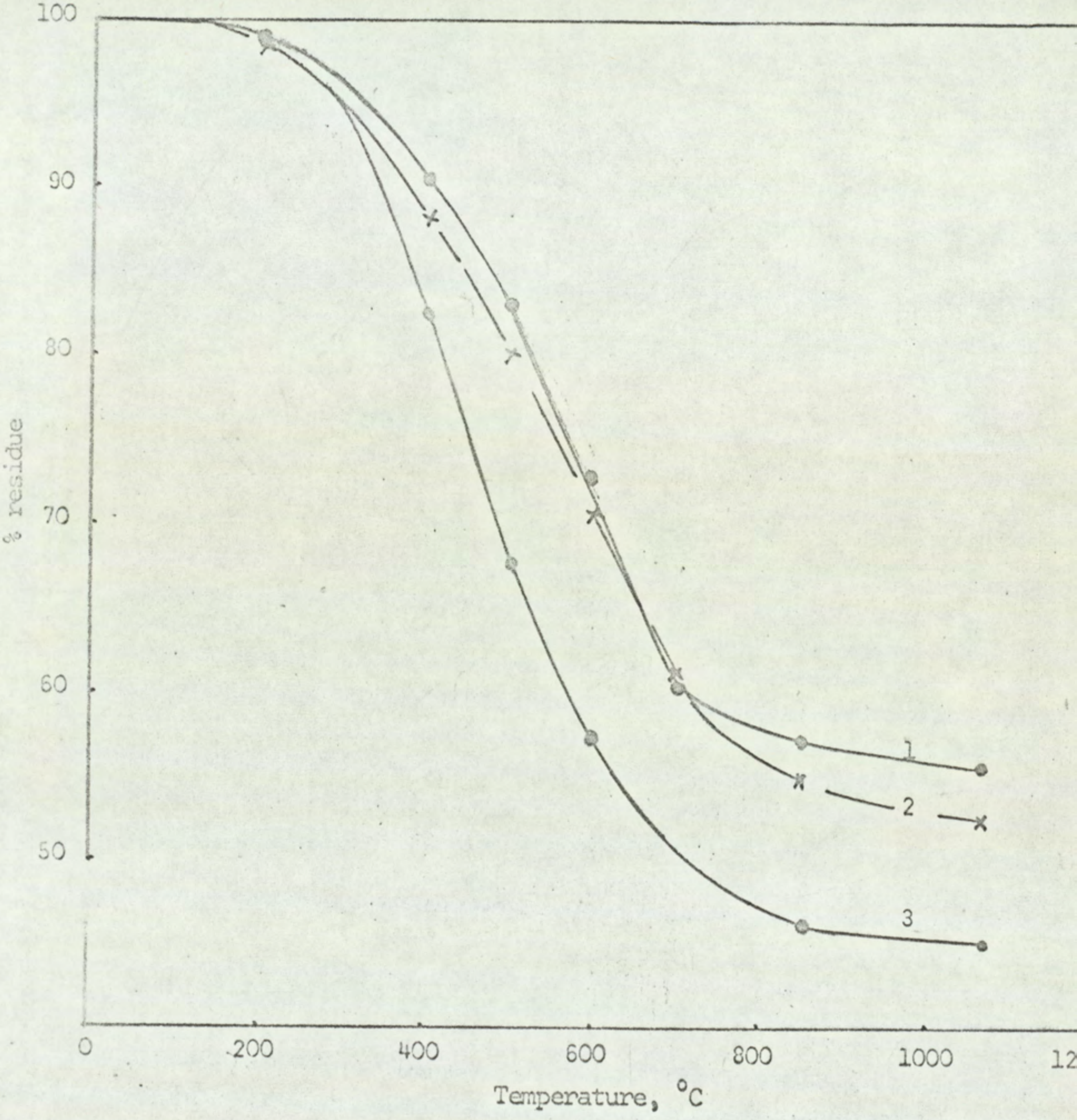

Fig. 26. TGA Thermograms

1. PFHS II
2. PFHS I
3. PFHS

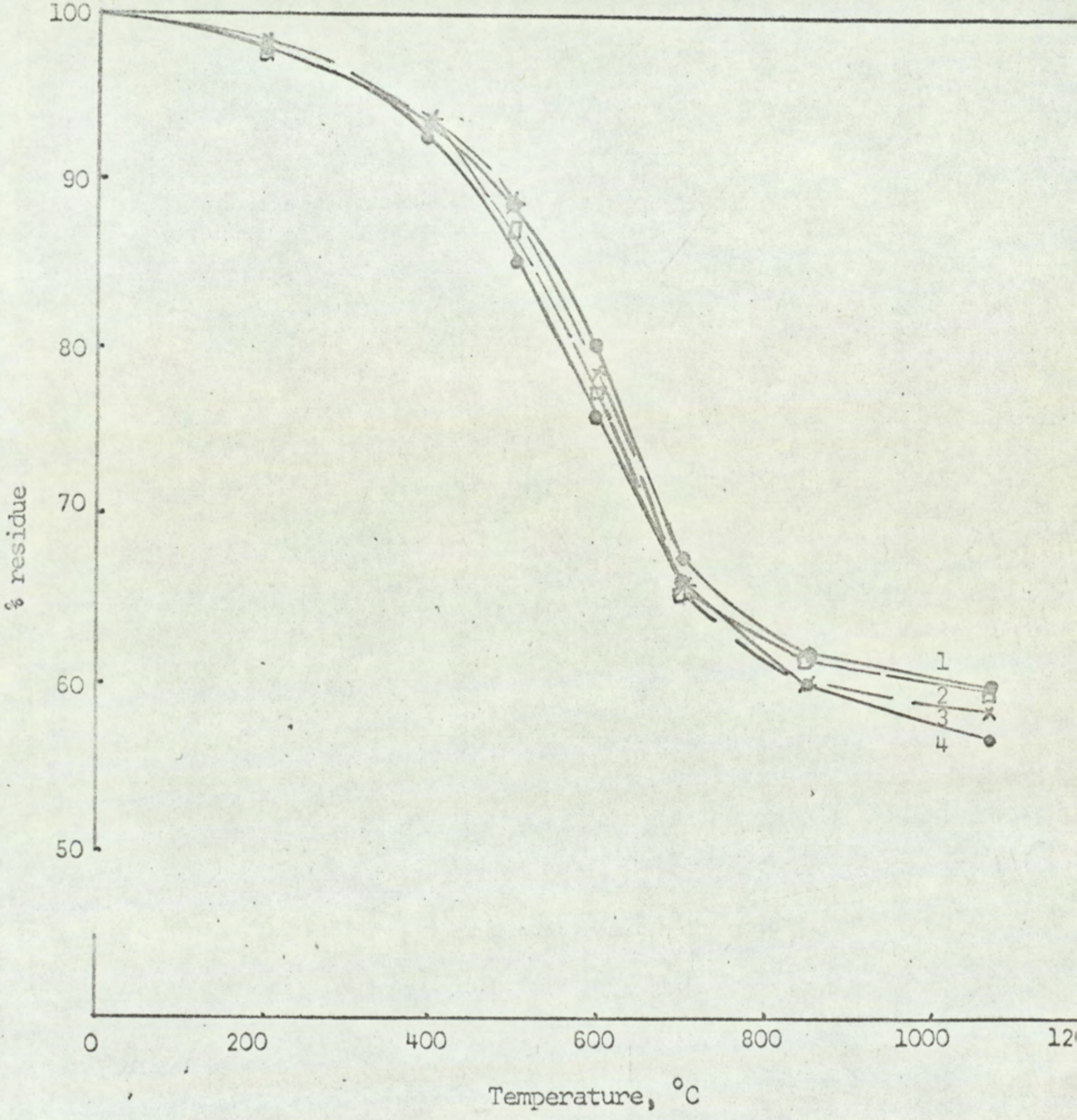

Fig. 30. TGA Thermograms

1. PFHMg
2. PFHAl
3. PFHCu
4. PFHZn

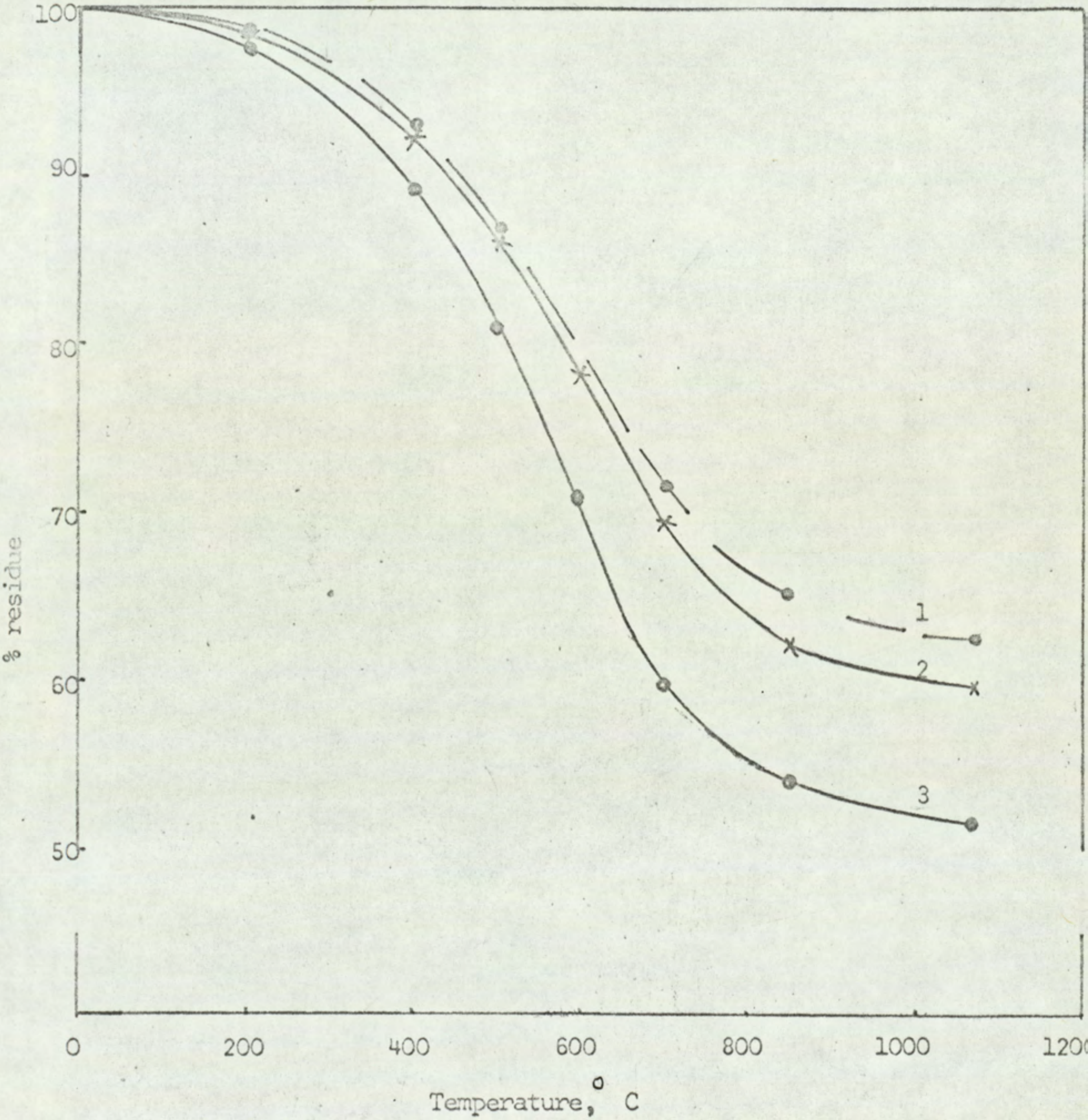

Fig. 31. TGA Thermograms

1. $PFHFeCl_3$
2. $PFHZnCl_2$
3. $PFHAlCl_3$

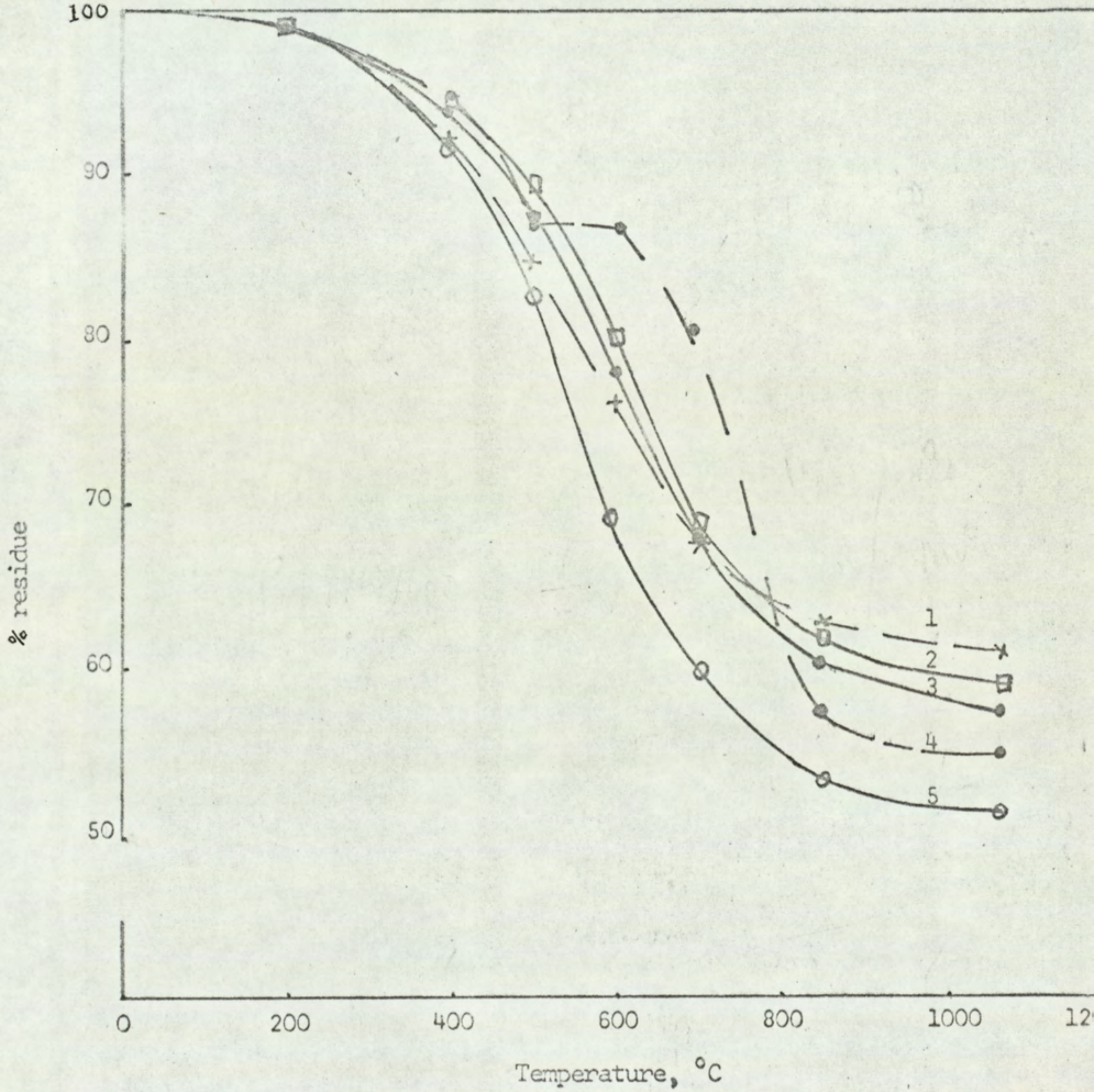

Fig. 32. TGA Thermograms

1. $PFHMnO_2$
2. $PFHSb_2O_3$
3. PFHZnO
4. $PFHSiO_2$
5. PFHHgO

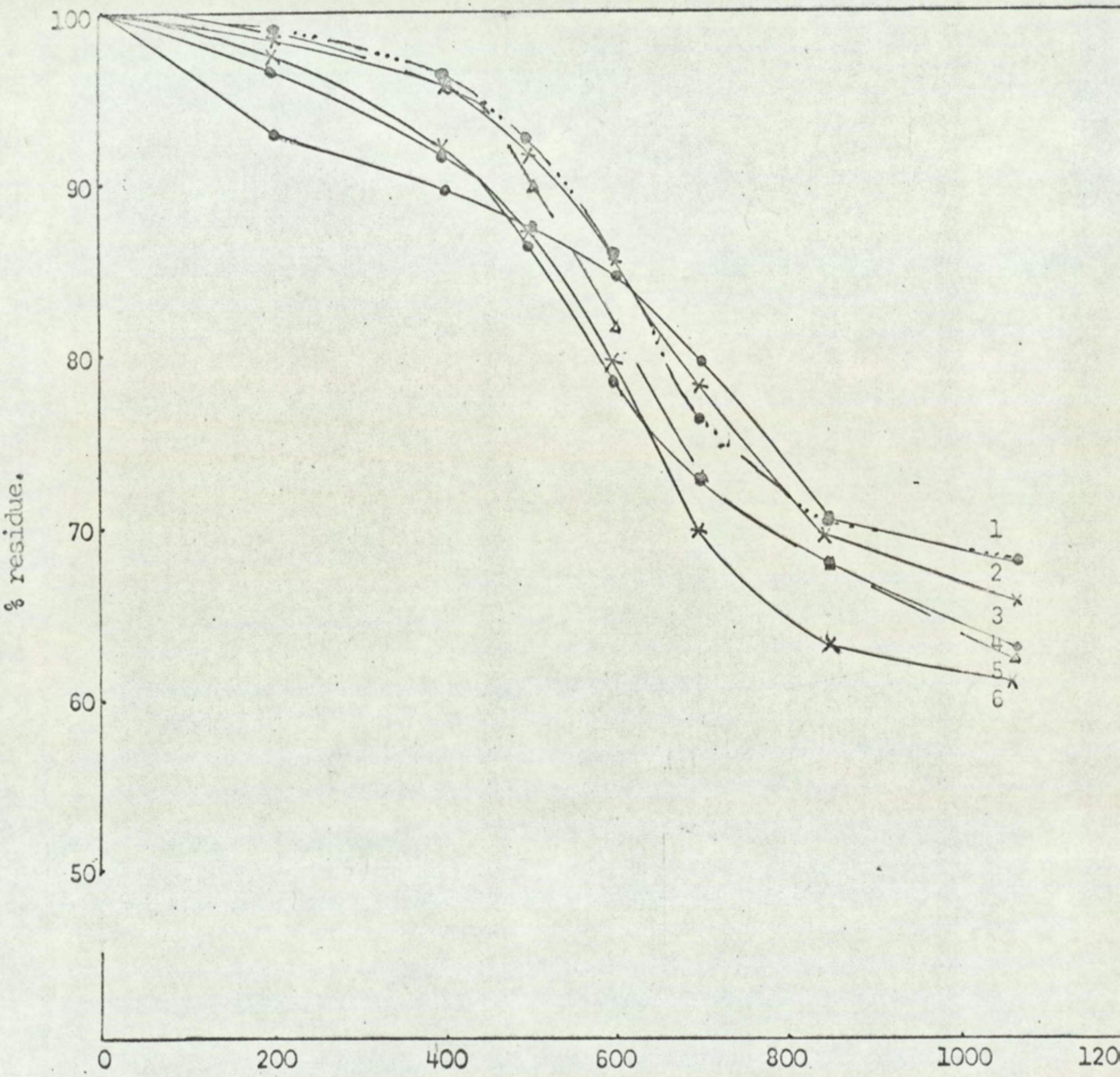

Fig. 33a. TGA Thermograms

1. PFHSi
2. PFHAB
3. PFHALC
4. PFHASm
5. PFHASP
6. PFHAAl(OH)$_3$

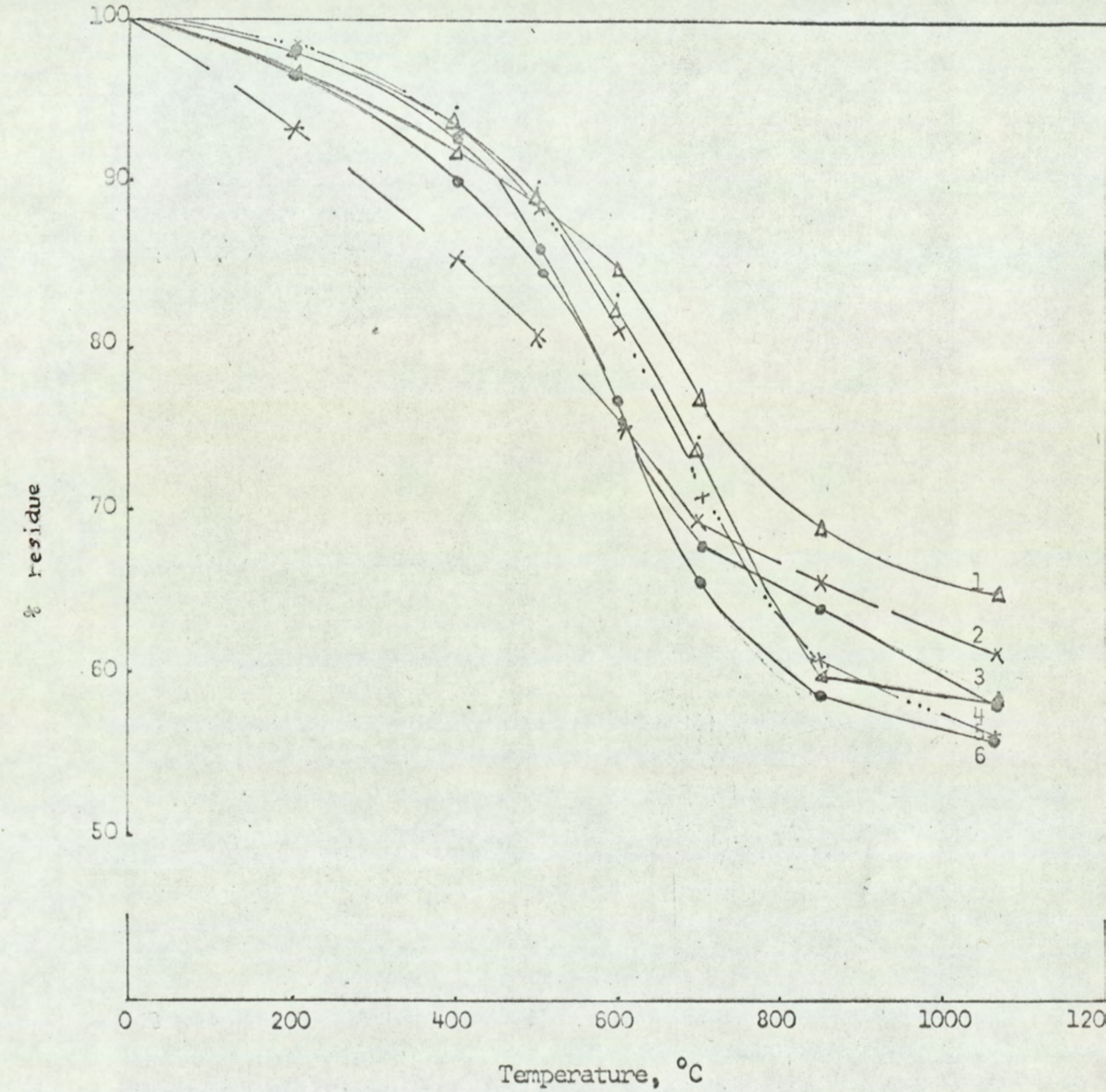

Fig. 33b. TGA Thermograms

1. PFHB
2. PFHSm
3. PFHRef
4. PFHSP
5. PFHLC
6. PFHAl(OH)$_3$

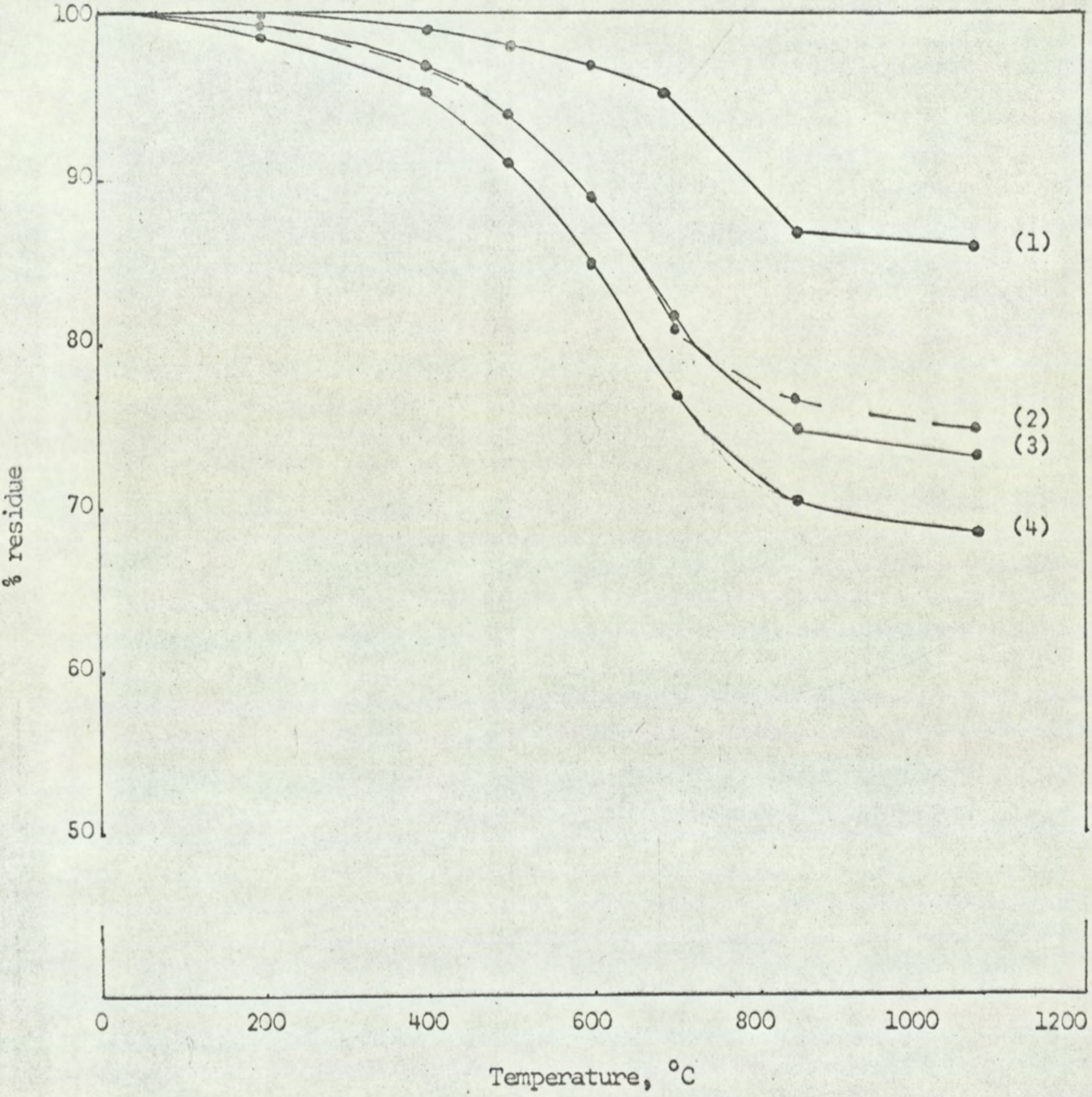

Fig. 33c TGA Thermograms

1. Asbestos
2. PFHG
3. PFHAG
4. PFHAI

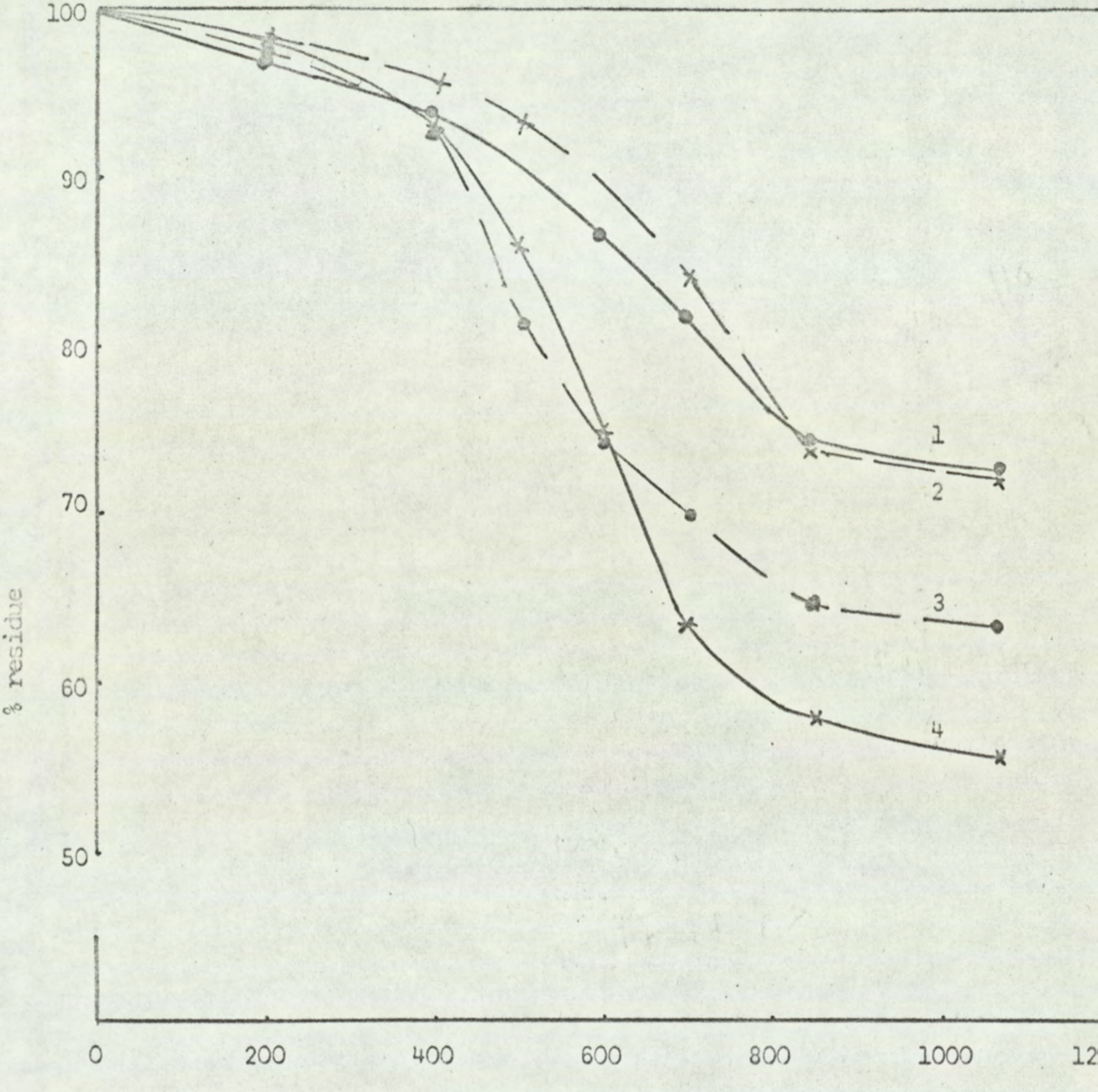

Fig. 34. TGA Thermograms

1. RPD110
2. RPD150
3. RPD154
4. PFHTX

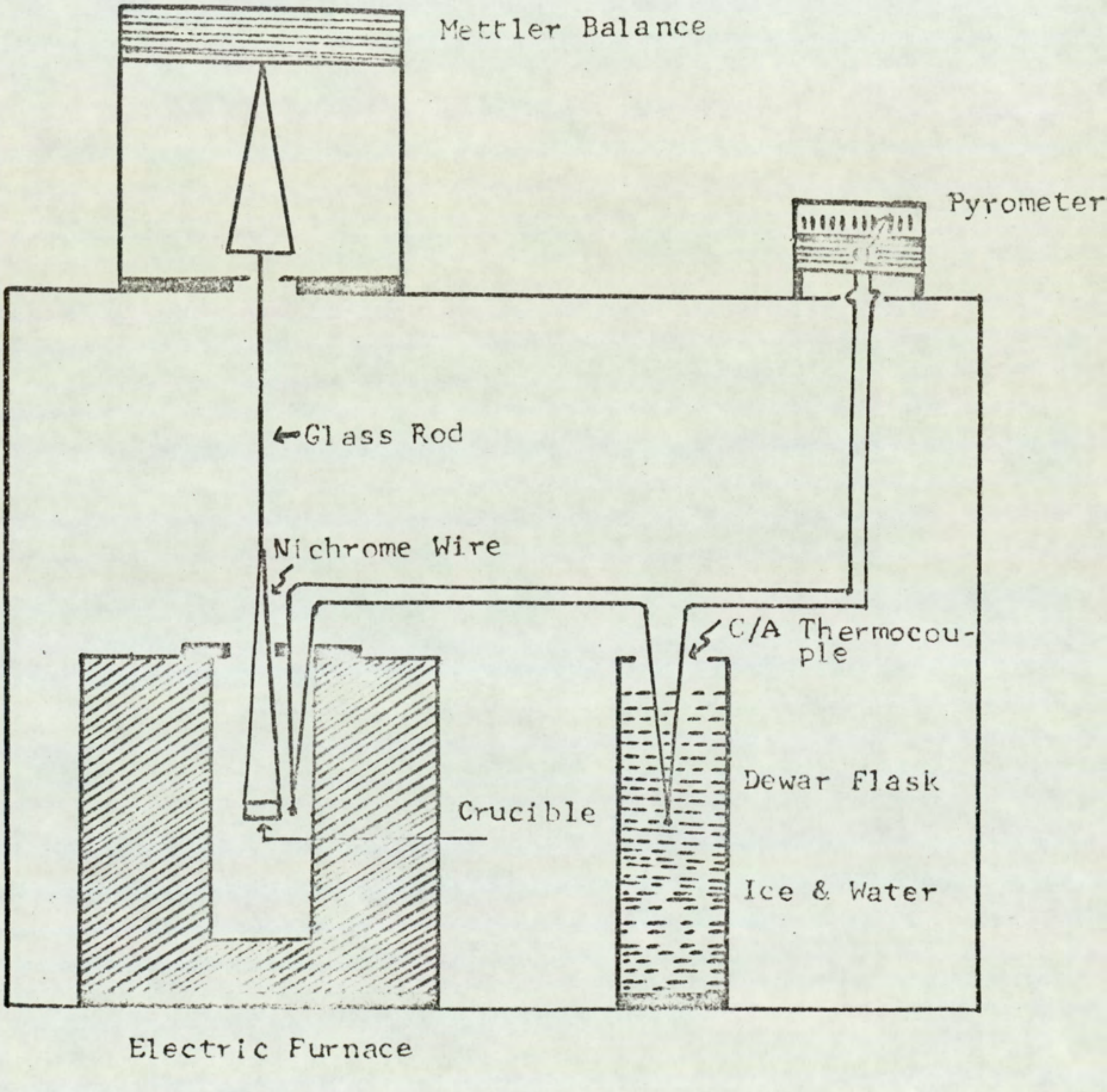

Fig. OC Block diagram of the apparatus

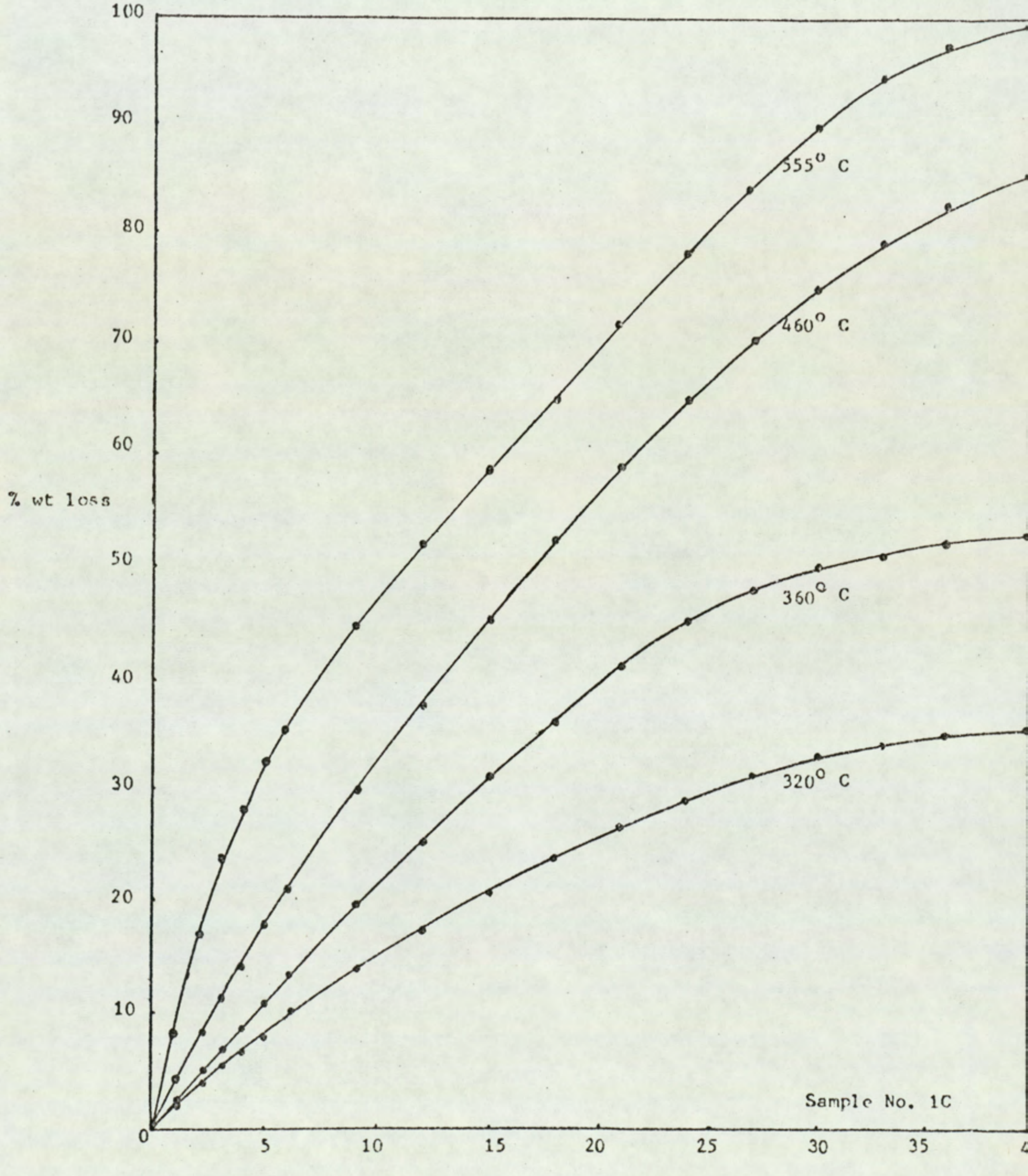

Fig. 1C . Percentage weight loss versus time.

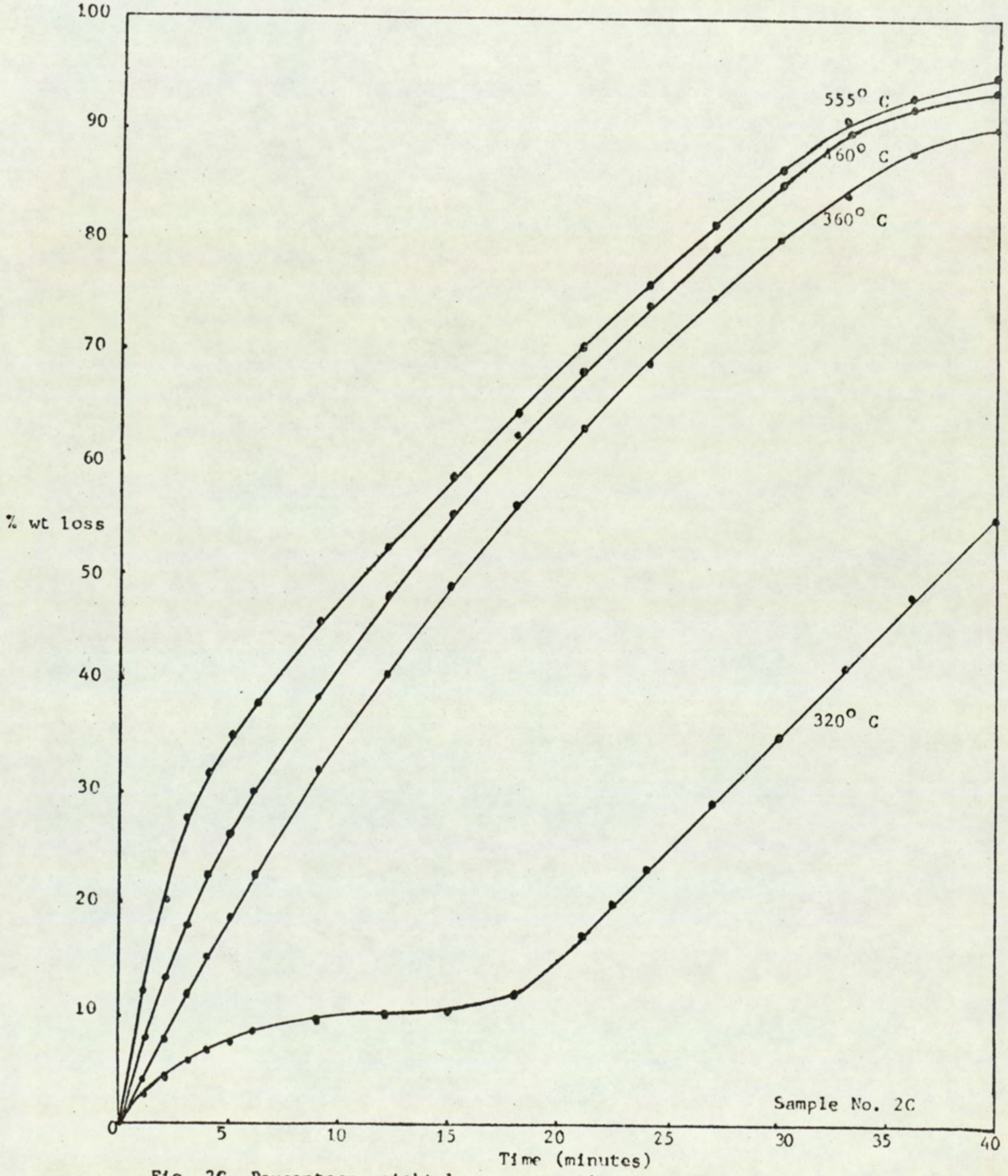

Fig. 2C Percgntage weight loss versus time

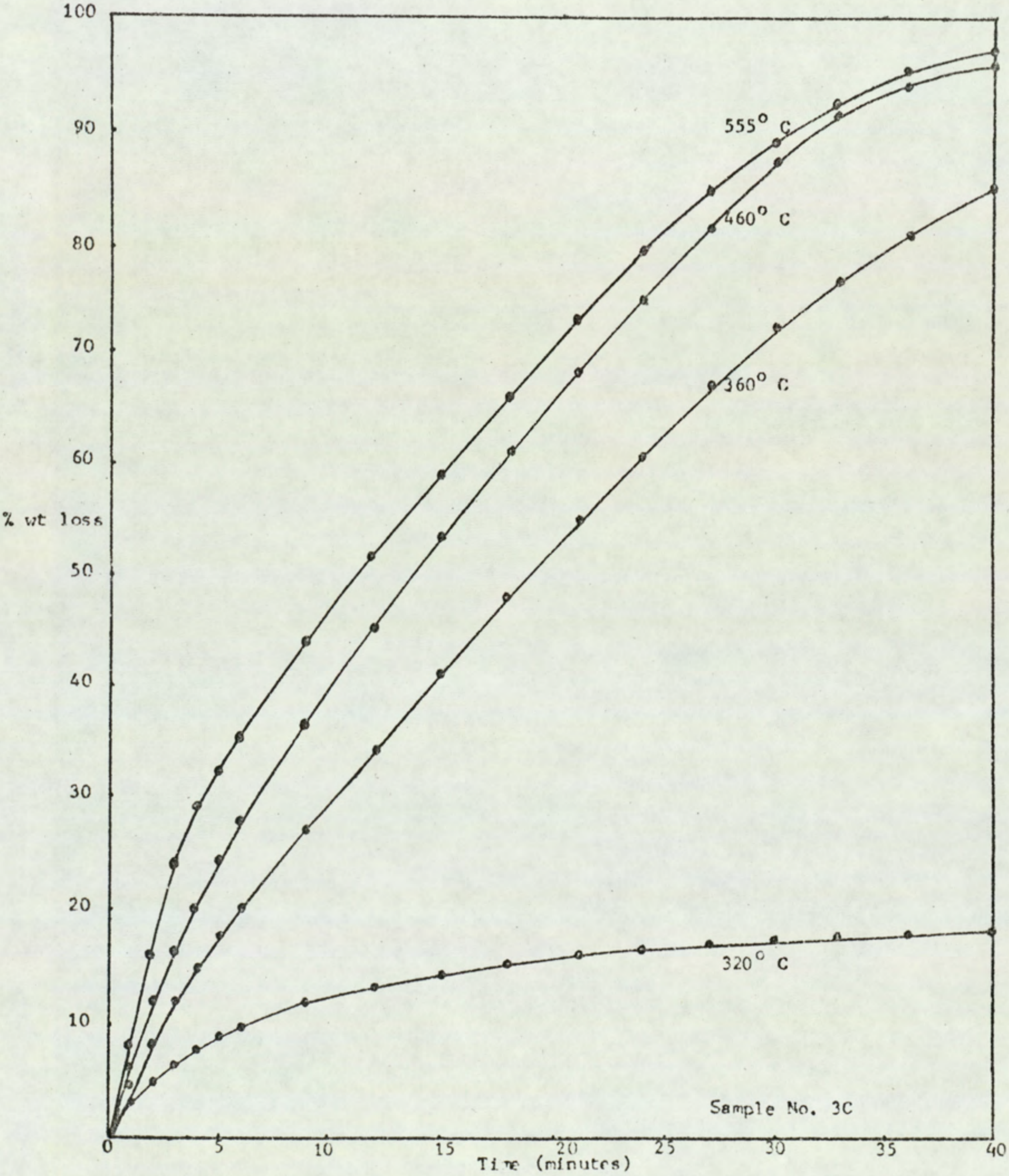

Fig. 3C Percentage weight loss versus time

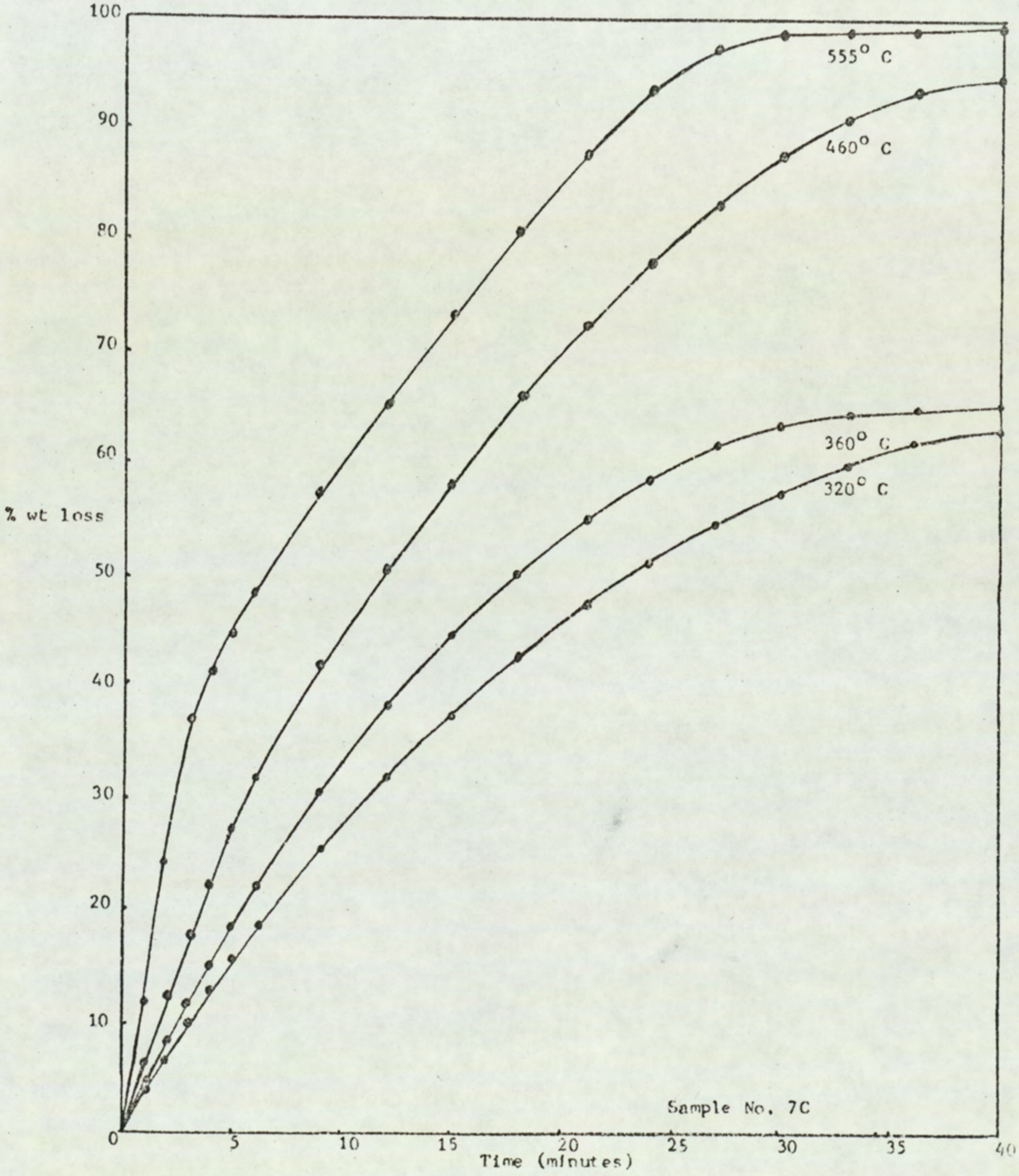

Fig. 4C Percentage weight loss versus time

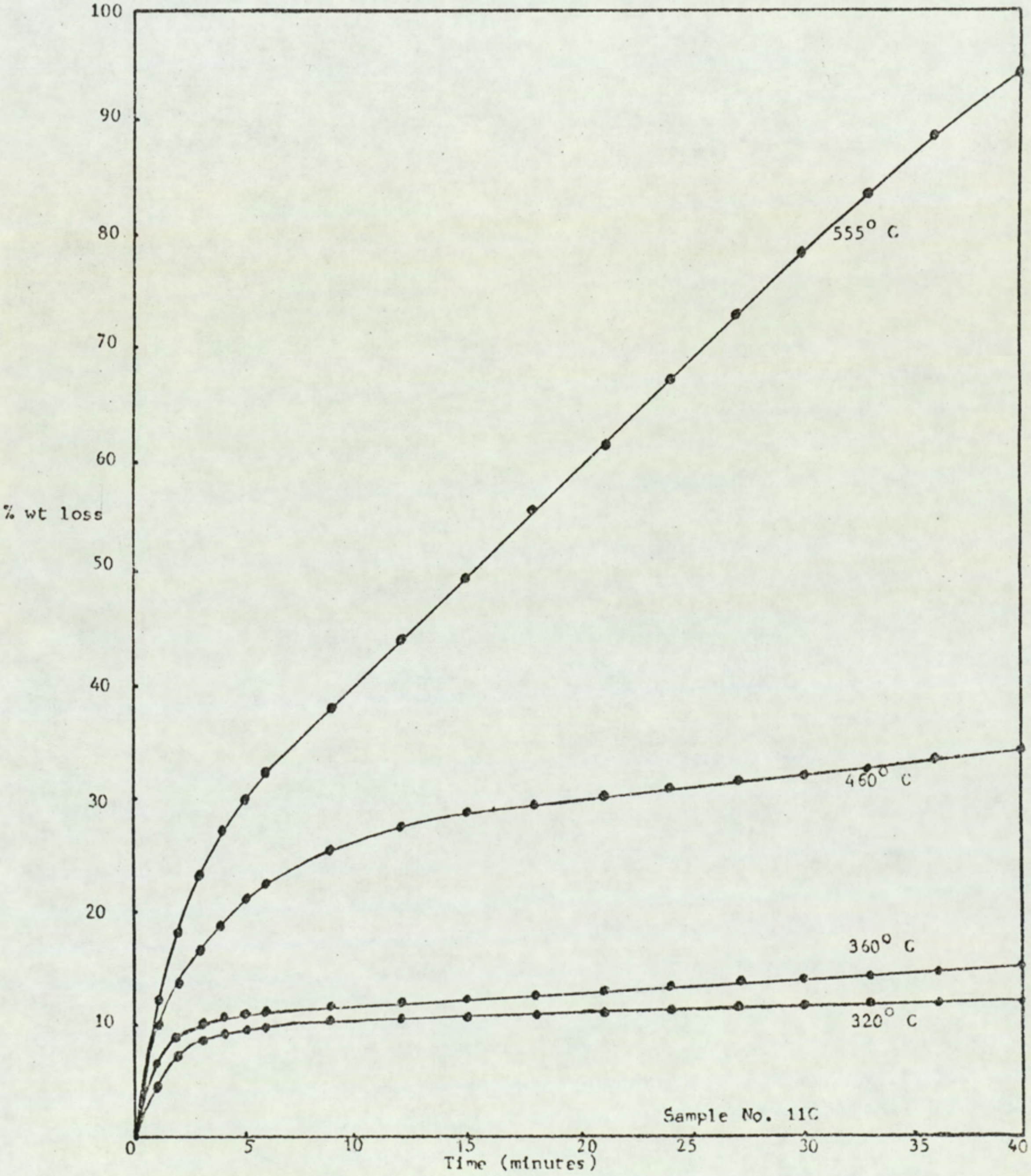

Fig. 5C Percentage weight loss versus time.

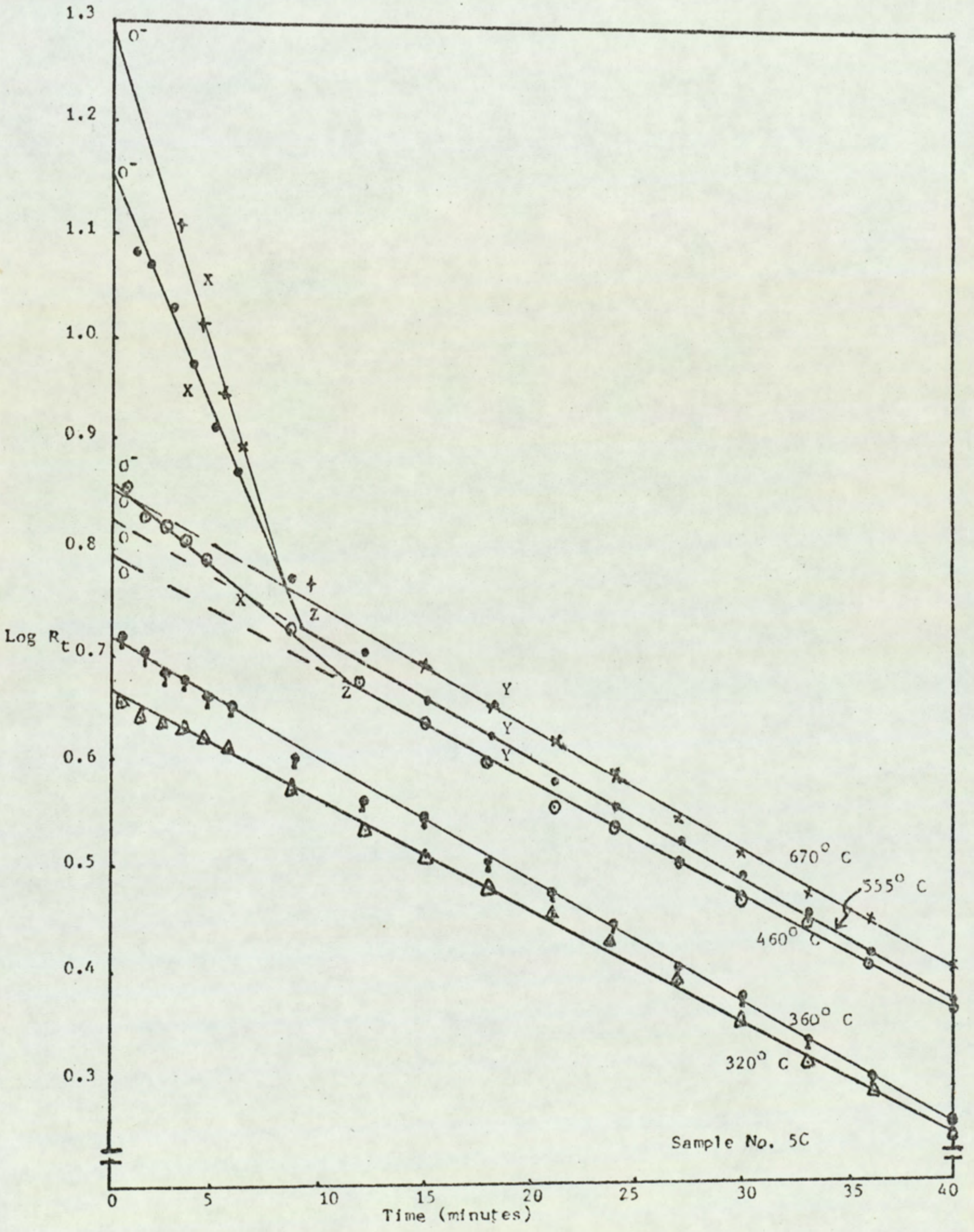

Fig. 6C Log rate versus time

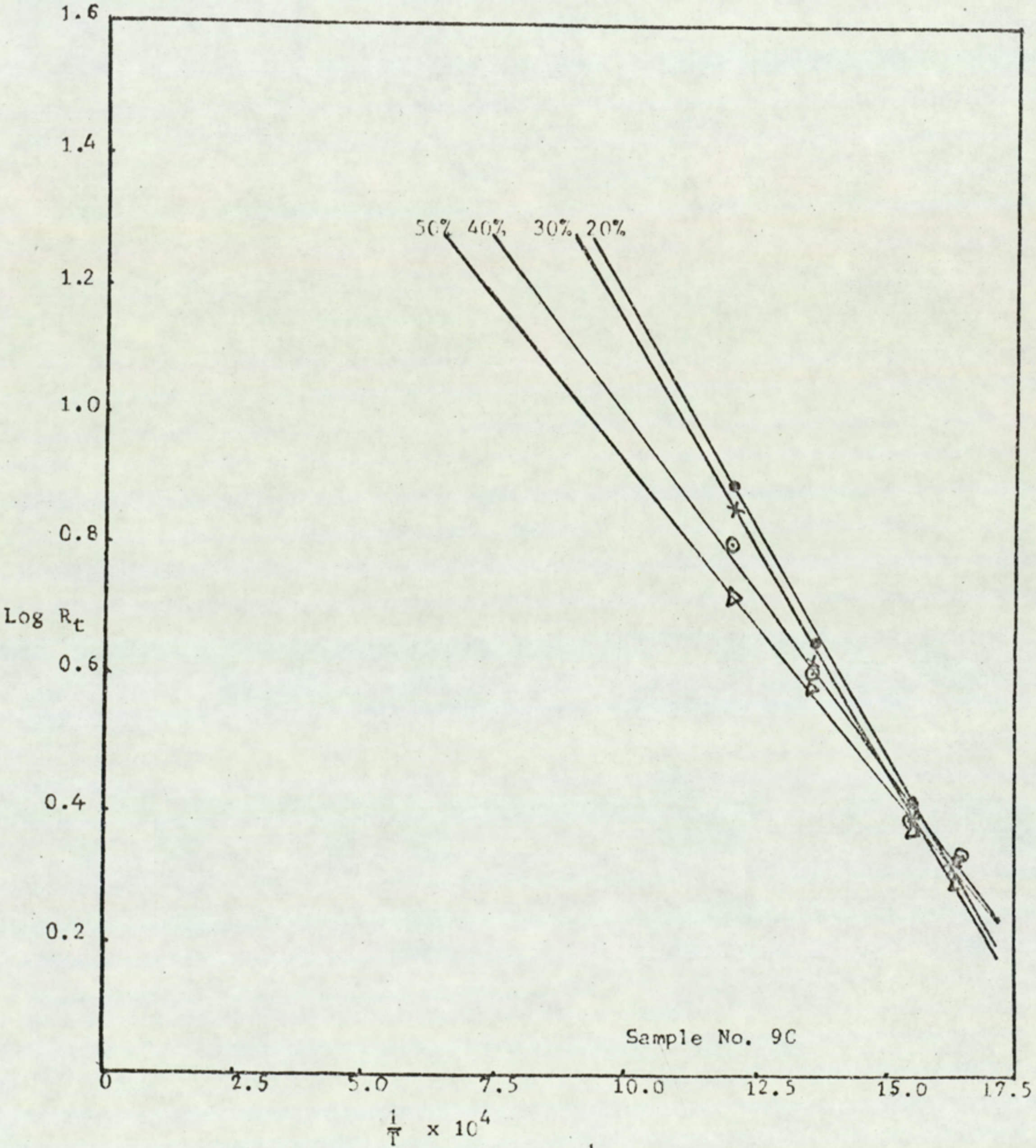

Fig. 7C Log rate versus $\frac{1}{T}$

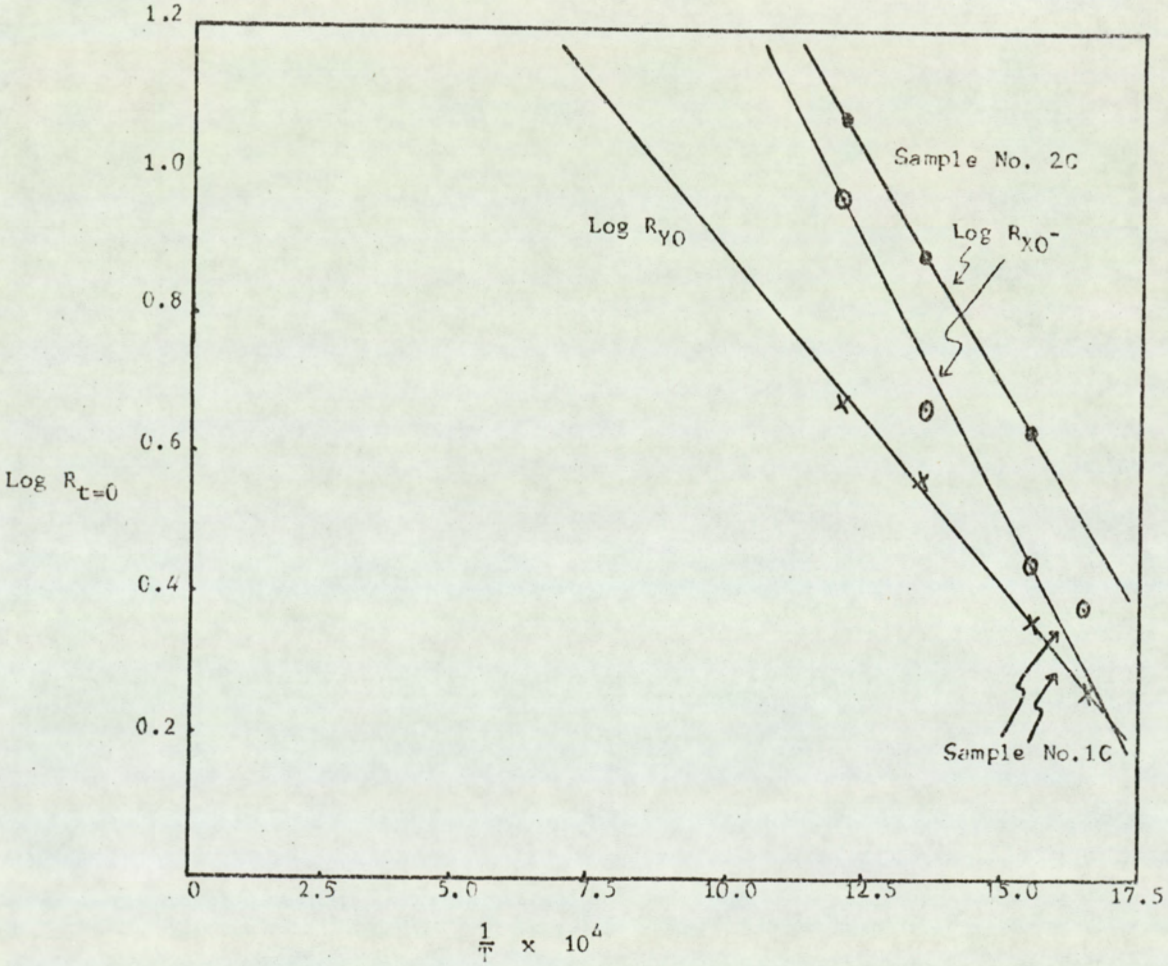

Fig. 8C Log rate versus $\frac{1}{T}$

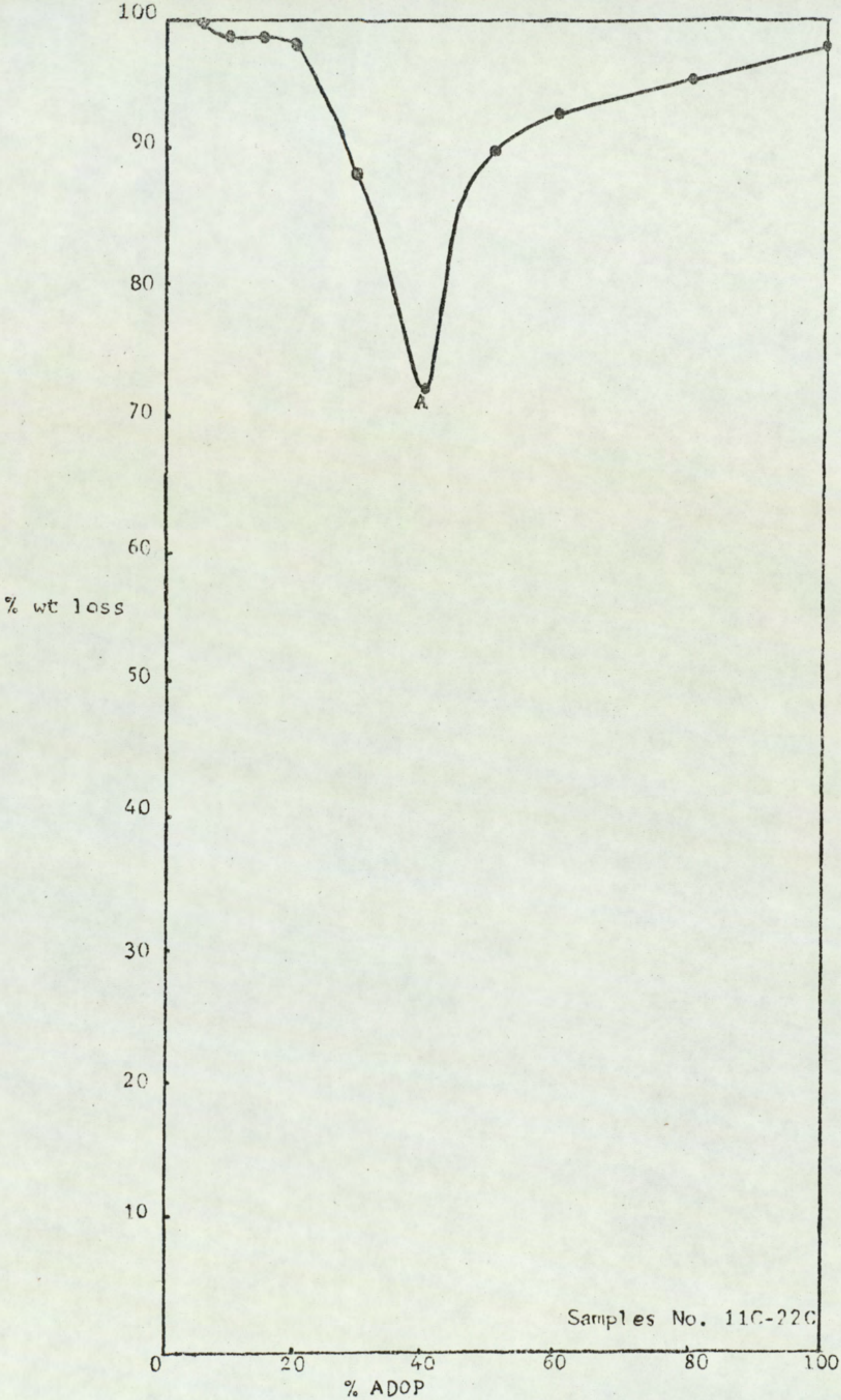

Fig. 9C Percentage weight loss versus % ADOP

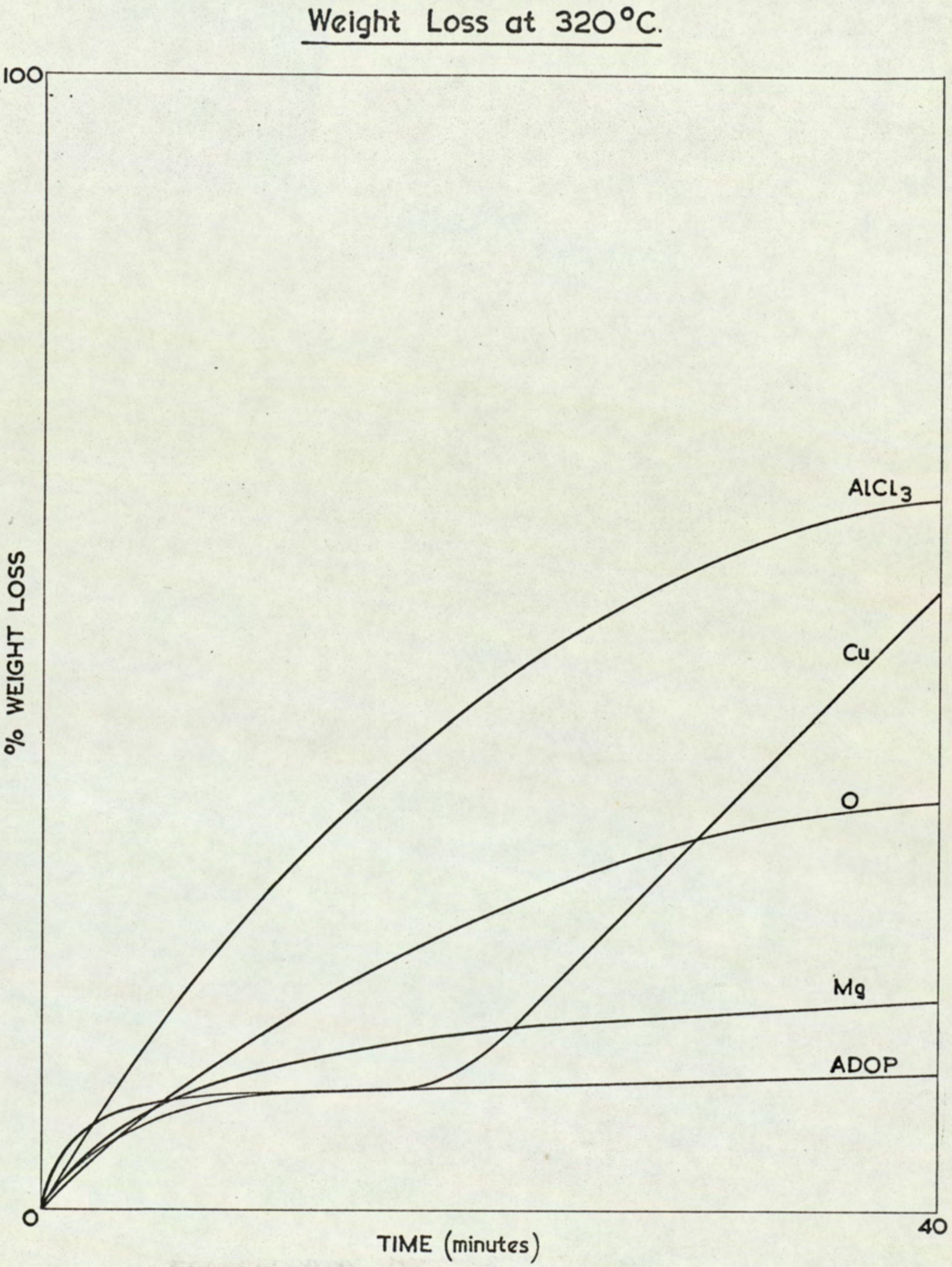

Fig. 10 C-1 Percentage weight loss against time.

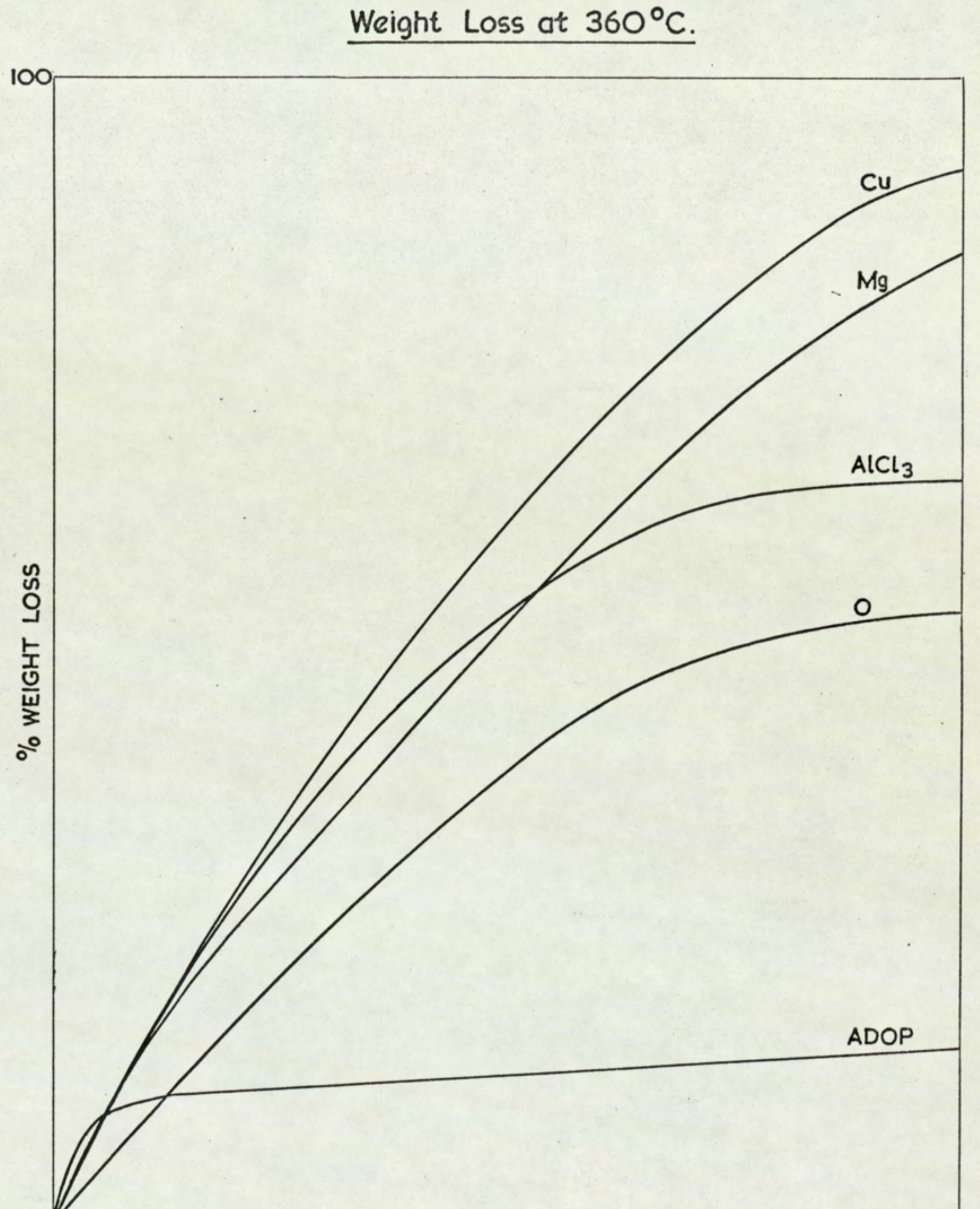

Fig. I0 C-2 Percentage weight loss against time.

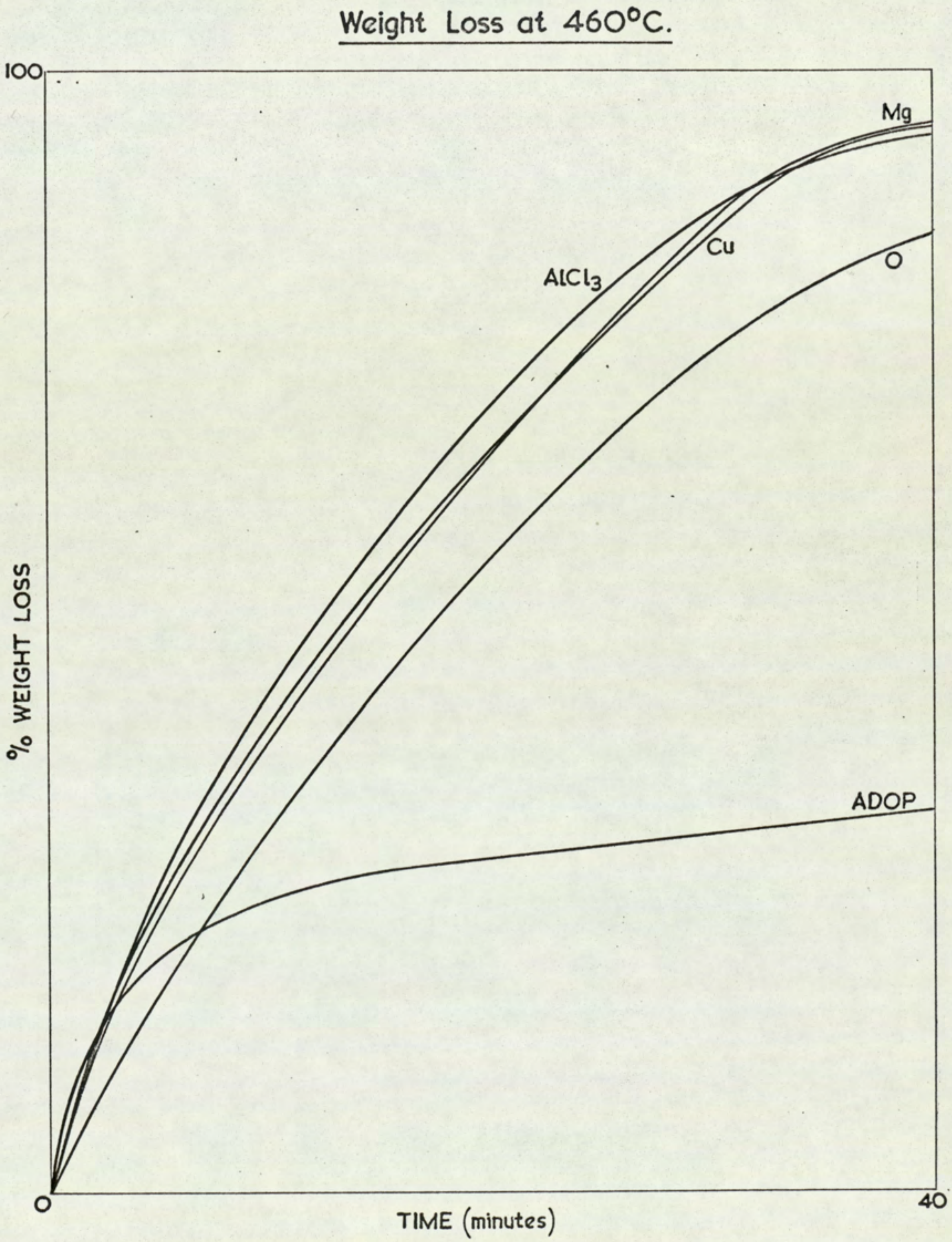

Fig. IO C-3 Percentage weight loss against time.

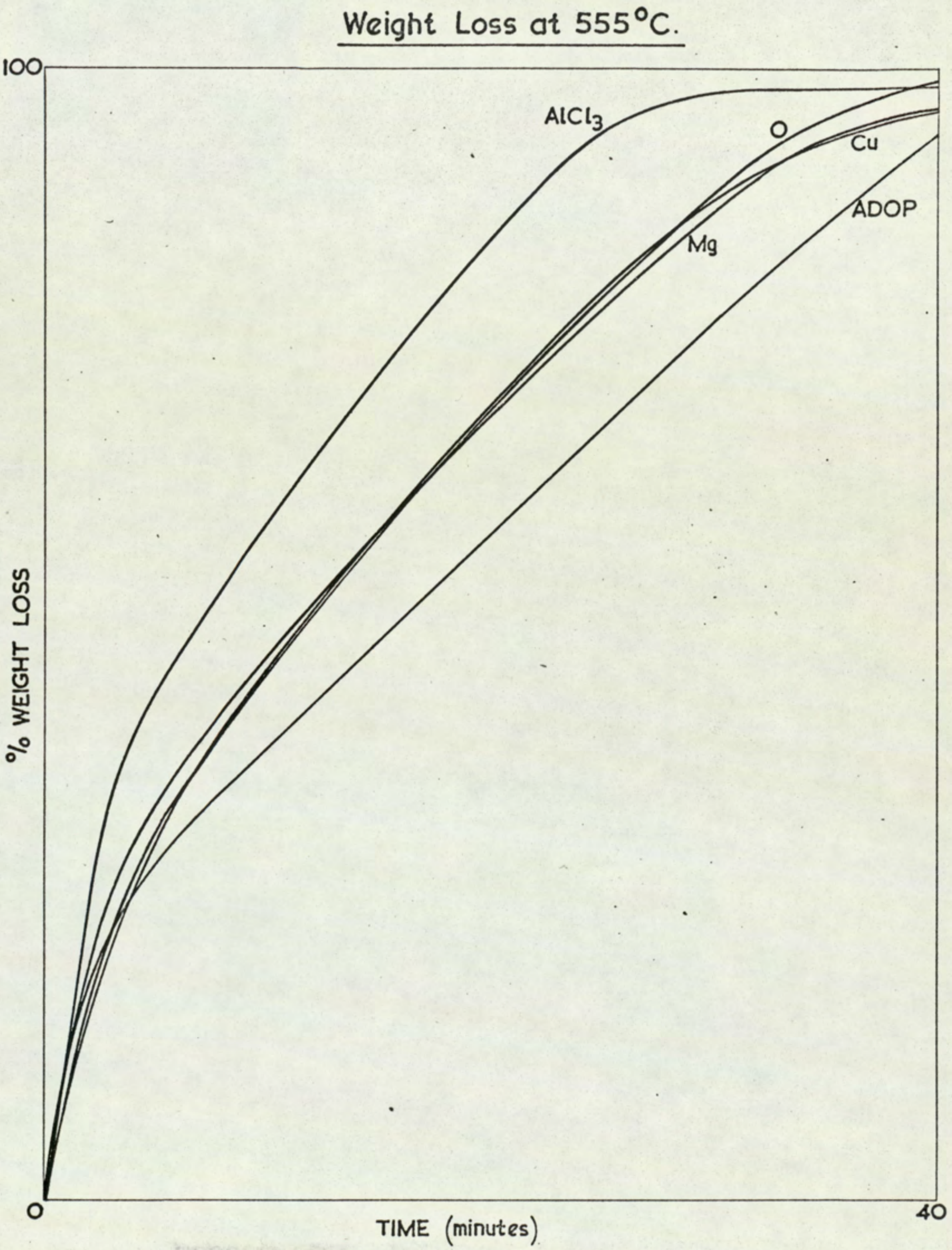

Fig. IO C-4 Percentage weight loss against time.

REFERENCES

1. Hourt, W.C., Ind.Eng.Chem., 52, 761 (1960).

2. Wilson, A.W., Brit.Plastics, 33 , 352 (1960).

3. Schmidt, D.L., Mod. Plastics, 38, 131 (1960).

4. Schmidt, D.L., Ibid., 38, 147 (1960).

5. Bashford, V.G., Chem. and Ind., p.224, February 5th, (1966),

6. Steverding, B., and Nieberlein, V.A., Chem.Eng., 72, 163 (1965).

7. Madorsky, S.L., S.P.E.Journal, 17, 665 (1961).

8. Beecher, N. and Rosensweig, R.E., A.R.S.Journal, p.532, April (1961).

9. Gilchrist, E.M., Brit.Plastics, 33, 359 (1960).

10. Gruntfest, I.J., Chem.Eng. p.134, June 1st (1959).

11. Kennedy, A.J., New Scientist, 226, 670 (1961),
Sci.Journal, p.38, August (1965).

12. Thompson, G.V.E., and Gatland, K.W., "Materials in Space Technology", Iliffe Books Ltd. (London) (1963), p.177.

13. Cariscione, J.M., Volk, H.F., and Smith, A.W., A.I.A.A.Journal, 4, 1791 (1966).

14. Winslow, F.H., Baker, W.O., Pope, N.R., and Matreyek J.Poly.Sci., 16, 101 (1965).

15. Grassie, N., "The Chemistry of High Polymer Degradation Processes", Butterworths (1955), p.25.

16a. Simha, R., and Wall, L.A., J.Phys.Chem. 56, 707 (1952).

16b. Simha, R., Wall, L.A. and Blatz, P.J., J.Poly.Sci., 5, 615.(1950).

17. Grassie, N., Trans. Faraday Soc., 48, 379 (1952).

18. Gilbert, J.B., and Kipling, J.J., Fuel, 41, 249 (1962).

19. Gilbert, J.B., Kipling, J.J., McEnaney, B., and Sherwood, J.N. Polymer, 3, 1 (1962).

20. Madorsky, S.L., Hart, V.E., Straus , S., and Sedlak, V.A., J.Research Nat.Bur.Stds., 51, 327 (1953).

21. Berkowitz-Mattuck, J.B. and Noguchi, T., J.App.Poly.Sci., 7, 709 (1963).

22. Holmes, F.R., and Shaw, C.J.G., J.App.Chem., 11, 210 (1961).

23. Madorsky, S.L., "Thermal Degradation of Organic Polymers" Interscience, John Wiley, (1964), p.238.

24. Learmonth, G.S. and Nabi, G., To be published.

25. Madorsky, S.L., and Straus , S., Mod.Plastics, 38, 134 (1961).

26. Bender, H.L., J.A.C.S., 61, 1812 (1939).

27. Hall, R.W., Chem. and Ind., (London), p.693, July 12th, (1952).

28. Hawkins, E.G.E., J.App.Chem., 6, 131 (1956).

29. Conley, R.T., and Bieron, J.F., J.App.Poly.Sci., 7, 103 (1963).
Ibid., 7, 171 (1963).

30. Jackson, W.M., and Conley, R.T., J.App.Poly.Sci., 8, 2163 (1964).

31. Conley, R.T., J.App.Poly.Sci., 9, 1117 (1965).

32. Lochte, H.W., Strauss, E.L., and Conley, R.T., J.App.Poly.Sci., 9, 2799 (1965).

33. Heron, G.F., Soc.Chem.Ind., Monograph No.13, Macmillan & Co. N.Y. (1961) p.475.

34. Friedman, H.L., J.App.Poly.Sci., 9, 651 (1965).

35. Belinski, C., Recherche Aerospatiale, 54, 28 (1964).

36. Lee, L.H., J.Poly.Sci. Part A, 3, 859 (1965).

37. Lee, L.H., J.App.Poly.Sci., 9, 1981 (1965).

38. Shulman, G.P., and Lochte, H.W., J.App.Poly.Sci. 10, 619 (1966).

39. Zulaica, J. and Guiochon, G., Poly.Letters, 4, 567 (1966).

40. Brauer, G.M., J.Poly.Sci., Part C, 8, 8 (1965).

41. Ouchi, K. and Honda, H., Fuel (London), 38, 429 (1959).

42. Megson, N.J.L., 'Phenolic Resin Chemistry', Butterworths, London, (1958).

43. Wolfs, P.M.J., van Krevelen, D.W., and Waterman, H.I., Fuel (London), 39, 25 (1960).

44. Friedman, H.L., J.App.Poly.Sci., 9, 1005 (1965).

45. Friedman, H.L., J.Poly.Sci., Part C, 6, 183 (1964).

46. Auerbach, I., SC-RR-66-584, November 1966, Sandia Lab., Albuquerque, U.S.A.

47. Jeffreys, K.D., Brit. Plastics, 36, 188 (1963).

48. Nakamura, Y., Kogyo Kagaku Zasshi, 64, 392 (1961).

49. White, R.H. and Rust, T.F., J.App.Poly.Sci., 9, 777 (1965).

50. Pevzner, L.V., Kolodyazhuyi, V.Z., Soviet Plastics, 8, 17 (1966).

51. Popov, V.A., Druyan, I.S., and Varshal, B.G., Soviet Plastics, 5, 19 (1965).

52. Korshak, V.V., Sergeev, V.A., Kozlov, L.V. and Komarova, L.I., Soviet Plastics, 2, 38 (1967).

53. Doroshenko, Y.E., Korshak, V.V. and Sergeev, V.A., Soviet Plastics, 8, 13 (1966).

54. Anderson, H.C., S.P.E. Trans., 2, 202 (1962).

55. Burns, R. and Orrell, E.W., J.Materials Sci., 2, 72 (1967).

56. Learmonth, G.S. and Wilson, T., J.App.Poly.Sci., 8, 2873 (1964).

57. Raskina, A.M. and Kogan, I.N., Soviet Plastics, 3, 49 (1967).

58. Severov, A.A., Gorbacheva, T.B., Lukin, B.V. and Sergeev, V.K., Soviet Plastics, 9, 18 (1965)

59. Ouchi, K., Carbon (London), 4, 59 (1966).

60. Katovic, Z., J.App.Poly.Sci., 11, 85 (1967).
Ibid, 11, 95 (1967).

61. Baeyer, A., Ber.deut.Chem.Ges., 25, 280 (1872).

62. Baekland, L.H., Ind.Eng.Chemi., 1, 149 (1909).

63. Carswell, T.S., 'Phenolplasts', Interscience Publishers, N.Y. and London (1947).

64. Hultzsch, K., Chemie der Phenolharze, Springer-Verlag, Berlin (1950)

65. Bender, H.L., Modern Plastics, 30, 136 (1954), 31, 115 (1954).

65a. Fraser, D.A., Hall, R.W. and Raum, A.L.J., J.App.Chem., 7, 676 (1957).

66. Heslinga, A. and Schors, A. J.App.Poly.Sci., 8, 1933 (1964).

67. Mackenzie, R.C., 'Differential Thermal Investigation of Clays', Min.Soc., London (1957).

68. Smothers, W.J. and Chiang, Y., Handbook of Differential Thermal Analysis, Chemical Publishing Co.Inc. N.Y. (1966).

69. Wedlandt, 'Thermal Methods of Analysis', John Wiley (1964).

70. Redfern, J.P., 'Thermal Analysis', Macmillan & Co.Ltd., (1965).

71. Slade, P.E., Jr. and Jenkins, L.T., 'Techniques and Methods of Polymer Evaluation, Thermal Analysis', Vol.I., Edward Arnold Ltd., London (1966).

72. Macromolecular Reviews, Vol.I. Interscience Publishers (1967) p.173.

73. Garn, P.D., "Thermoanalytical Methods of Investigation",
Academic Press, N.Y., London, (1965).

74. McKenzie, R.C., Analyst, 87, 420 (1962).

75. Chiu, J., App.Poly.Symposia, 2, 25 (1966).

76. Lukasweski, G.M., Laboratory Practice, 14, 1277 (1965).
Ibid., 14, 1399 (1965).
Ibid., 15, 82 (1966).
Ibid., 15, 187 (1966).
Ibid., 15, 302 (1966).
Ibid., 15, 431 (1966).
Ibid., 15, 551 (1966).
Ibid., 15, 664 (1966).
Ibid., 15, 762 (1966).
Ibid., 15, 861 (1966)

77. Duval, C., "Inorganic Thermogravimetric Analysis",
Elsevier, N.Y. (1953).

78. Newkirk, A.E., Anal.Chem., 32, 1558 (1960).

79. Murphy, C.B., Anal.Chem., 30, 867 (1958).
Ibid., 32, 168R (1960).
Ibid., 34, 298R (1962).
Ibid., 36, 347R (1964).
Ibid., 38, 443R (1966).
" ., 40, 380R (1968).

80. Ke, B., "Newer Methods of Polymer Characterization",
Interscience, N.Y., London, (1964), p.347

81. Kissinger, H.E., and Newman, S.B., "Analytical Chemistry of Polymers"
Vol. 12, Pt.2, Interscience, N.Y., London,
(1962) p.159.

82. Manley, T.R., "Techniques of Polymer Science", Soc.Chem.Ind. Monograph, No.17, London, (1963), p.175.

83. Millane, J.J., Plastics, 28, 101 (1963).
29, 81 (1964).

84. Double, J.S., Trans.J.Plastics Inst., p.73 April (1966).

85. Kissinger, H.E., Anal.Chem. 29, 1702 (1957).

86. Borchardt, H.J., and Daniels, F., J.A.C.S., 79, 41 (1957).

87. Reich, L., Poly. Letters, 4, 423 (1966).

88. Reich, L., J.App.Poly.Sci., 10, 465 (1966).

89. Reich, L., Ibid. 10, 813 (1966).

90. Reich, L., Ibid., 10, 1801 (1966).

91. Reich, L., Ibid., 11, 161 (1967).

92. Freeman, E.S. and Carroll, B., J.Phys.Chem., 62, 394 (1958).

93. Anderson, H.C., J.Poly.Sci., Part C, 6, 175 (1964).

94. Smith, D.A., Trans.Inst.Rubber.Ind., 39, T275, (1963).

95. Horwitz, H.H., and Metzger, G., Anal.Chem., 35, 1464 (1963).

96. Horwitz, H.H. and Metzger, G., Presented before the division of Petroleum Chemistry, A.C.S., New York City Meeting, Sept.8-13, (1963).

97. van Krevelan, D.W., van Heerden, C., and Huntjens, F.S., Fuel, 30, 253 (1951).

98. Ingraham, H.C., and Marrir, P., Canadian J.Chem.Eng., 41. 170 (1963).
Ibid., 72, 161 (1964).

99. Reich, L., Poly.Letters, 2, 621 (1964).

100. Coats, A.W., and Redfern, J.P., Poly. Letters, 3, 917 (1965).

101. Reich, L., Lee, H.Y. and Levi, D.W., J.App.Poly.Sci. 9, 351 (1965).

102. Reich, L., Poly.Letters, 3, 231 (1965).

103. Flynn, J.H., and Wall, L.A., Poly.Letters, 4, 323 (1966).

104. Flynn, J.H. and Wall, L.A., Poly.Letters, 5, 191 (1967).

105. Reich, L., J.App.Poly.Sci., 9, 3033 (1965).

106. Reich, L., Lee, H.T. and Levi, D.W., Poly.Eng. and Sci., p.135, July (1965).

107. Claver, G.C. Jr., J.Paint Technology, 38, 69 (1966).

108. Ravich, G.B. and Florova, A.F., Doklady Akad.Nank S.S.S.R., 90, 391 (1953) through Chem.Abst., 47, 9048 (1953).

109. Rogers, K.F., Technical Note No. Chem.1401, August 1962 "The degradation of durestos components at high temperatures".

110. Lady, J.H., Kesse, I. and Adams, R.E., J.App.Poly.Sci., 7, 71 (1960)

111. Conley, R.T., J.App.Poly.Sci., 9, 1107 (1965).

112. Hodgson, A.A., Lecture series (1965) No.4. "Fibrous Silicates" p.38. The Royal Inst.Chem., London.

113. Heslop, R.B. and Robinson, P.L., "Inorganic Chemistry" Elsevier (1963), Chapter 18.

114. Cottrell, T.L., "The Strengths of Chemical Bonds" Butterworths (1958).

115. Gilbert, J.B. and Kipling, J.J., Fuel, 42, 5 (1963).

116. "Proceedings of the Third Conference on Carbon" Pergamon Press (1959) p.7.

116a. Learmonth, G.S., Private communication.

117. Kohn, S., Annales des Mines, X-XI, 1042 (1966).

118. Kipling, J.J., and Shooter, P.J., Carbon, 4, 1 (1966).

119. Levine, H.H., Brit. Plastics, 34, 395 (1961).

120. Hultzsch, K. and Hesse, W., Kunstst. 53, 166(1963).

121. Kohn, S., La. Rech. Aerspot. 96, 39 (1963).

122. Learmonth, G.S., "Laminated Plastics", Leonard Hill Ltd., London, (1951), Chapter 144.

123. Learmonth, G.S. and Searle, D.P., to be published.

124 Grassie, N. and Melville, H.W., Proc. Royal Soc. London, 199, 1(1949).

125. Jellinek, H.H.G., J.Polymer Sci, 4, 13 (1949).

126. Oakes, W.G. and Richards, R.B., J. Chem. Soc. London, 619, 2929 (1949).

127. Madorsky, S.L., J.Polymer Sci. 9. 133 (1949).

128. Jellinek, H.H.G., J.Polymer Sci. 4, 13 (1949).

129. Atherton, A., J.PolymerSci. 5, 378 (1950).

130. Hultzsch, K., Paper read at the ACS symposium at Pittsburgh, Pa. in March (1966).

131. Hultzsch, K. and Hesse, W., Kunststoffe, 53, 170 (1963).

132. Gimblett, F.G.R., "Inorganic Polymer Chemistry", (1963), Butterworths, London, pp. 8, 10, 22, 23, 29-33.

133. Emeleus, H.J. and Aderson, J.S., "Modern Aspects of Inorganic Chemistry", (1962) E.L.B.S., and Routledge and Kegan Paul Limited, London, pp. 336-343.

END